



TECHNISCHE
UNIVERSITÄT
WIEN

Vienna University of Technology

DISSERTATION

Development and application of analytical methods for the determination of fungal bioactive compounds using liquid chromatography – high resolution mass spectrometry

ausgeführt zum Zwecke der Erlangung des akademischen Grades eines Doktors der
technischen Wissenschaften unter der Leitung von

Ao.Univ.Prof. Dr. Rainer Schuhmacher
H97300 Analytikzentrum

Interuniversitäres Department für Agrarbiotechnologie, IFA-Tulln
Universität für Bodenkultur Wien

eingereicht an der Technischen Universität Wien
Fakultät für Technische Chemie

von

Dipl.-Ing. Sylvia Lehner
Matrikelnummer 0325094
Neubaugasse 45
3462 Absdorf

Tulln, am 6.12.2012

Sylvia Lehner

DANKSAGUNG

Allem voran und ganz besonders möchte ich Rainer Schuhmacher danken für die super Betreuung und Unterstützung!!! Für Ideen, Geduld, Ratschläge, und und und... Danke für deine präzise Art, deine Genauigkeit und deine Ausdauer! Und für die eine oder andere Einschulung und Weiterbildung zum Wein verkosten :-)

Vielen, vielen Dank auch besonders an Rudi Krska! Danke für die Möglichkeit am AZ meine Dissertation zu machen! Danke für deinen Input, Anregungen und deinen Fokus aufs Essenzielle!

Danke Marc und Andrea, für euren Einsatz im „Wirkstoffe-Projekt“! Ohne eure Unterstützung wäre vieles nicht möglich gewesen! Danke für eure Bereitschaft mich immer mit Rat und Tat zur Seite zu stehen, mir alles Nötige in der BP zu zeigen und für die Möglichkeit alles Notwendige benutzen zu dürfen!!!

Danke Markus, Sabine, Birgit, Viktor, für eure Unterstützung aus der UT! Und für eure Offenheit neuen Ansätzen gegenüber!

Danke Lea und Irina, für eure Unterstützung bei allem was *Trichoderma* angeht, und besonders bei der Zusammenarbeit beim „Siderophor-Paper“!

Dem gesamten AZ möchte ich ganz besonders und herzlich für die immer freundschaftliche und kollegiale Zusammenarbeit danken!!! Ihr seid wirklich ein super Team und ich möchte mich vor allem für ein sehr, sehr gutes Arbeitsklima bedanken! Danke auch für Unterstützung bei jeder Problemstellung! Ein paar Menschen möchte ich in diesem Zusammenhang noch besonders danken:

Danke Alex, für die Einschulung in alles Wesentliche am AZ, vor allem was das Labor angeht! Für deine Kompetenz und deinen Humor! Und natürlich für 100,000 HPLC-Fraktionierungen!!!!

Danke Renate, für deine kompetente und immer freundliche und hilfsbereite Art! Und für 10,000 Kaffee-Taps ohne die ich meine Diss nie überstanden hätte!!

Danke Wolfgang, vor allem dafür dass du dir die Zeit genommen hast und mir die Messungen auf der GF-AAS ermöglicht hast!!!

Danke Karoline, für dein sorgfältiges Arbeiten und dein Ausdauer beim Kampf mit den Daten!!

Danke, danke, danke, Georg, für die Einschulung auf der Orbitrap, ein offenes Ohr in allen Lebenslagen, Gespräche über Gott und die Welt, für deine eigene Meinung, deine Unterstützungen bei Postern, Publikationen und natürlich Grafiken, eine Million E-Mails und selbstverständlich Schoki ;-)

Danke Nora, für deine Unterstützung!! Fürs Programmieren und natürlich für lustige Loggia-Parties :-)

Danke Christoph, für deine Unterstützung beim Daten auswerten!!! Und für lustige Wuzzl-Runden und deinen trockenen Humor!

Danke Denise, für deine Unterstützung, dein offenes Ohr und für deine quirlige Art die dich manchmal dich selbst überholen lässt!

Danke Kurt, für lustige Kaffeepausen und deine gezielt „provokanten“ Meldungen ;-)

Danke Bernhard, fürs Durchlesen diverser Poster, dein Feedback, deine Kritik, deine Ideen, die Unterstützung mit der Superoberüberdiva, deine Verlässlichkeit! Fürs Wuzzln, feiern, für Kaffee-Pausen, fürs Volleyball spielen.....

Antaaaaaaa!!!! DANKE!!!!!! Wo soll ich da nur anfangen?! Danke für deine erfrischende Art, für deine Lautstärke die durchs ganze IFA hallt, für eine Million Tränen die ich mit und dank dir gelacht habe, fürs Beachen und Wuzzln, für die gemeinsamen Kaffee-Pausen, für deine offene und ehrlich Art..... Danke!

Danke Michi, Hannes, Fru!!! Ohne euch wär ich nie ans IFA gekommen! DANKE!!!

VIELEN, VIELEN, VIELEN DANK, von ganzem Herzen, Paula, Taisha, Carol, Constantin, Saco!!!! Für eure Unterstützung!!! Ohne euch wär gar nichts möglich!!!

Danke Elfi!!!!!!! Danke Thomas!! Vor allem dafür dass ihr immer für mich da seid und mich immer unterstützt habt!!!

TABLE OF CONTENTS

Aims of this Thesis	1
List of Abbreviations	5
Abstract	9
Kurzfassung	13
List of Publications	17
Introduction	21
1 Secondary metabolites in fungi.....	21
1.1 Polyketides	24
1.2 Non-ribosomal peptides.....	26
1.3 Terpenoids	29
2 Liquid chromatography coupled to (tandem) mass spectrometry for the analysis of secondary metabolites	33
2.1 Introduction to liquid chromatography and mass spectrometry	33
2.2 Analytical strategy for the determination of fungal secondary metabolites using LC-HRMS/MS	42
2.3 Development and application of analytical strategies	48
Conclusions and Outlook	51
References.....	55
Original Works.....	63
Curriculum Vitae.....	155

AIMS OF THIS THESIS

“Learn from yesterday, live for today, hope for tomorrow. The important thing is to not stop questioning.”

Albert Einstein

Novel developments in instrumentation technology give rise to new possibilities and hence new insights and achievements for scientific research. Many technological improvements have been achieved in the last decade. Regarding analytical chemistry, a very versatile and frequently employed technique is mass spectrometry. In this respect, instruments have been enhanced regarding their scan speed, sensitivity, resolution as well as their ease of use. A variety of different mass analyzers is available, all of them having specific advantages and limitations. Those include for example triple quadrupole, time-of-flight and a new type of mass analyzer, the Orbitrap, which makes high resolution mass spectrometry (HRMS) affordable to plenty laboratories. These methodologies in conjunction with highly productive liquid chromatography (LC) systems pave the way for novel approaches and hence scientific findings.

Additionally, improvements in electronic data processing, computing power and the possibility to make large amounts of data (e.g. databases) available to the community via the internet led to further advancements of scientific approaches. A paradigm shift in the life sciences towards a holistic understanding of biological systems led to the emergence of the “omics” disciplines (e.g. genomics, transcriptomics, proteomics and metabolomics). Especially metabolomics approaches aim at unraveling significant fundamental principles since it is located at the bottom of the “omics” cascade and portrays the active substances responsible for the resulting phenotype of an organism. Metabolomics approaches require the application of highly sophisticated technologies to fulfill their high demand of studying complex cellular activities and whole metabolic networks. These approaches can basically be divided into targeted analyses, suspects (or targeted) screening approaches and non-targeted screening approaches.

This thesis was carried out in the context of two major intentions: A project entitled “Novel biological active compounds for the development of high-value nutraceuticals and natural plant protectants” and the establishment of a metabolomics platform at the Center for Analytical Chemistry. The aim was to develop different analytical methods for a variety of scientific aspects and questions. The main task was to establish screening strategies and analytical methods for the

detection and characterization of microbial metabolites and antifungal substances. The overall objective was a better understanding of biological interactions like those between different microorganisms or between microorganisms and plants.

Within the project “Novel biological active compounds for the development of high-value nutraceuticals and natural plant protectants”, the goal was to find antagonistic fungi that inhibit the growth of the plant pathogenic fungus *Fusarium graminearum*. The task to be carried out at the Center for Analytical Chemistry was to elucidate the metabolites responsible for biological activity and their corresponding structure. In this respect, the criterion of “biological activity” (inhibiting the growth of *F. graminearum*) of substances had to be fulfilled. The general idea was to employ subsequent steps of activity testing and fractionation/ analytical analysis coupled with differential data analysis (active versus non-active culture supernatants) to narrow down the range of possible metabolites exhibiting activity. This led to the establishment of a workflow in conjunction with the participating project partners. This workflow for screening for biologically active substances of fungal origin is described within this thesis in two poster presentations and a manuscript published in “ALVA Mitteilungen” (paper #1).

Another objective was to explore the potential of targeted and non-targeted screening purposes in metabolomics studies. This was especially important as no accepted guidelines regarding their setup or specific requirements exist among the community to date. Regarding targeted screening approaches, this was achieved by retrospective data analysis of full scan high resolution MS data by applying a positive list of suspect compounds without direct availability of authentic standard compounds. The established method was used to screen for selected fungal metabolites (mycotoxins) in food and feed samples. Additionally, this method was utilized to quantify 20 fungal metabolites for which standard compounds were available. The resulting publication (paper #2) describes the established analytical method and the proof-of-principle of the developed suspects screening.

Another possible strategy in metabolomics analyses is the use of stable isotopes as “anchor” in the search for compounds of interest. A third survey employed an analytical screening approach for iron-containing metabolites (siderophores). The aim was to establish a largely automated non-targeted screening workflow employing specific characteristics of fungal ferri-siderophores present in raw LC-MS data files. Those included the natural iron isotopic pattern, UV/VIS absorption and MS/MS fragment spectra. In this respect, a comprehensive library with to date known siderophores was established. Within this study, three categories of identification/ annotation were distinguished: 1. identification of known siderophores which was supported by the measurement of authentic standard compounds, 2. annotation of known siderophores and 3. characterization of putative novel siderophores based on selected criteria. The developed method and its application to ten wild type *Trichoderma* strains was published in paper #3.

As not much is known about the synthesis of siderophores in *Trichoderma*, it was of interest to further gain information about which genes are responsible for their production. Therefore, the screening method for fungal siderophores was additionally applied to mutant strains of the biocontrol fungus *Trichoderma virens*. These strains showed knockouts in different NRPS genes putatively involved in siderophore biosynthesis. The aim of this study was to evaluate the effects of these knockouts on the metabolites' level. These analyses contributed to a publication in preparation to be submitted to *FEMS Microbiology Letters* (paper #4).

A major challenge in non-targeted metabolomics is the structural elucidation of unknown compounds. A very elegant approach that can facilitate this task is the use of stable isotopic labeling (e.g. by using native and ^{13}C labeled carbon sources). The characteristic isotopic pattern in measurements of a mixture of the native and the labeled culture filtrates show high potential to assist in the structure characterization of these compounds. The manuscript (paper #5), which is in preparation for submission to *Rapid Communications in Mass Spectrometry*, demonstrates the use of stable isotopic labeling (SIL) in the interpretation of tandem MS (MS/MS) spectra. In this respect, native and ^{13}C labeled standard compounds were measured by LC-HRMS/MS. A novel automated software tool was implemented to facilitate and speed up data analysis. This approach enables the determination of the number of carbon atoms of fragment signals in MS/MS spectra and suggests corresponding elemental formulas. Therefore, the established approach exhibits completely new possibilities to facilitate structure elucidation of unknown compounds. The developed automated software program shall be used in future metabolomics studies to facilitate MS/MS interpretation of truly unknown substances.

LIST OF ABBREVIATIONS

ACN	acetonitrile
3ADON	3-acetyldeoxynivalenol
ACP	acyl carrier protein
AFB ₁	aflatoxin B ₁
AFB ₂	aflatoxin B ₂
AFG ₁	aflatoxin G ₁
AFG ₂	aflatoxin G ₂
AFM ₁	aflatoxin M ₁
AGC	automatic gain control
Aib	α -aminoisobutyric acid
APCI	atmospheric pressure chemical ionization
API	atmospheric pressure ionization
APPI	atmospheric pressure photo ionization
AT	acyl transferase domain
C	condensation domain
CAS	Chemical Abstracts Service
C-Mt	C-methylation domains
CI	chemical ionization
CID	collision induced dissociation
Cy	heterocyclization domains
CoA	coenzyme A
DDF	des-diserylglycylferrirhodin
DH	dehydratase domain
DMAPP	dimethylallyl diphosphate
DON	deoxynivalenol
DOXP/ DXP	deoxyxylulose phosphate pathway
E	epimerization domains
EI	electron ionization
EIC	extracted ion chromatogram
EnnB	enniatin B
EnnB ₁	enniatin B ₁
ER	enoyl reductase domain
ESI	electrospray ionization
FA	formic acid
FB ₁	fumonisin B ₁
FB ₂	fumonisin B ₂
FFT	fast Fourier transformation

Determination of fungal bioactive compounds using LC-HRMS

FT	Fourier transformation
FWHM	full width at half maximum
GC	gas chromatography
GF-AAS	graphite furnace atomic absorption spectroscopy
HAc	acetic acid
HCD	higher energy collision dissociation
HPLC	high pressure liquid chromatography
HRMS	high resolution mass spectrometry
HT-2	HT-2 toxin
ICR	ion cyclotron resonance
IUPAC	International Union of Pure and Applied Chemistry
KR	ketoreductase domain
KS	β -ketosynthase domain
LC	liquid chromatography
LCL	lowest calibration level
LOD	limit of detection
LOD _{matrix}	limit of detection in the presence of matrix
LOD _{solvent}	instrument detection limit
LOQ	limit of quantification
LTQ	linear ion trap
QqQ	triple quadrupole
MALDI	matrix-assisted laser desorption/ionization
MeOH	methanol
MEP	methylerythritol phosphate pathway
MPA	mycophenolic acid
MS	mass spectrometry
MS/MS or MS ⁿ	tandem mass spectrometry
m/z	mass-to-charge ratio
MT	methyl transferase domain
NCBI	National Center for Biotechnology Information
NRP	non-ribosomal peptides
NRPS	non-ribosomal peptide synthetase
OTA	ochratoxin A
PCP	peptidyl carrier domain
PKS	polyketide Synthase
ppan	4'-phosphopantetheinyl cofactor
RFC	roquefortine C
RIA	relative isotope abundance
RP	reversed phase
RSD	relative standard deviation
SSE	signal suppression/enhancement
SIL	stable isotopic labeling
S/N	signal-to-noise ratio
SRM	selected reaction monitoring

List of abbreviations

T	thiolation domain
T-2	T-2 toxin
TE	thioesterase domain
TOF	time-of-flight
TUCIM	collection of industrial important microorganisms at Vienna University of Technology
ZON	zearalenone

ABSTRACT

Within this thesis, modern analytical approaches such as HPLC-MS(/MS) were developed and used to study fungal metabolites involved in complex biological interactions as is required for metabolomics studies. Those include targeted analytics, suspects (or targeted) screening approaches and non-targeted screening approaches.

For the elucidation of unknown (novel) bioactive compounds, a bioassay-guided workflow with alternating steps of activity testing and fractionation/analysis was established. To show that the developed workflow is well suited to identify (novel) bioactive metabolites, this workflow was successfully applied to fungal culture supernatants of *Penicillium brevicompactum* and *Myrothecium verrucaria*. The workflow included a database query of the differentially produced metabolites of the unfractionated culture supernatants (active vs. non-active culture filtrates) against a commercial database containing approx. 33,000 fungal and bacterial metabolites. In parallel, culture supernatants were fractionated by HPLC and active fractions analyzed by LC-HRMS. Again, differential analysis of active vs. non-active fractions led to a list of putative active metabolites. By comparison of these two lists, a set of candidates of novel bioactive metabolites was obtained. The workflow has been published in paper #1 and several posters. Applying the workflow to culture broths led, amongst others, to the identification of the substances verrucarin A and mycophenolic acid as bioactive compounds against *Fusarium*. Although these substances are not suited for the direct formulation of novel plant protectants due to their toxicity these results showed the general applicability of the established workflow.

Regarding targeted analytics, a method for the quantification of 20 selected mycotoxins using LC-HRMS was established and selected method performance characteristics such as precision, trueness, limit of detection and matrix effects for regulated mycotoxins were evaluated for the matrix maize. An alternative approach for the estimation of the limit of detection for Orbitrap MS using the signal-to-noise ratio in “full-profile mode” has been proposed and successfully applied. This approach led to detection limits between 8 and 160 ng/g maize. With few exceptions for zearalenone for baby food, ‘bread, pastries and biscuits’ and processed cereal-based food, the LODs obtained were within European Regulation limits for deoxynivalenol, fumonisin B₁ and B₂ and zearalenone. Eight naturally contaminated certified reference materials were used to verify precision and trueness of the developed method for deoxynivalenol, fumonisin B₁, fumonisin B₂, HT-2 toxin, T-2

Determination of fungal bioactive compounds using LC-HRMS

toxin and zearalenone. Additionally, a novel screening approach for 208 fungal metabolites by retrospective data analysis was established. Therefore, a positive list containing the selected metabolites was generated and the full-scan data automatically queried against this list. The screening strategy was based on selected detection and identification criteria including accurate mass, peak intensity and isotopologue ratio. The screening was applied to reference materials and led to the putative detection of 13 further metabolites in addition to the target toxins. This study has been published in the journal *Food Additives and Contaminants: Part A* (paper #2).

Detection and identification of iron-containing metabolites (siderophores) was accomplished by developing a stable isotope-assisted screening workflow. First, a database containing 422 known microbial siderophores and a list of common siderophore neutral losses, typically present in siderophore MS/MS spectra was established. The method was then applied to culture supernatants of ten different *Trichoderma* strains. Those were measured by LC-HRMS and the MS data was automatically screened for the characteristic iron isotopic pattern. The list of obtained putative siderophore-derived MS signals was then queried against the in-house siderophore library. If authentic standard compounds were commercially available, identification was achieved by measurement of these standards (comparison of retention time and MS/MS spectra). If no standard compounds were available or the putative siderophores were not contained in the in-house database, further confidence criteria were applied. Those included, amongst others, the characteristic UV/VIS absorption of fungal siderophores and the presence of characteristic mass increments corresponding to neutral losses in siderophore MS/MS spectra. The study led to the identification of dimerum acid, fusigen, coprogen and ferricrocin. Cis-fusarinine, fusarinine A and B, and des-diserylglycylferrirhodin were annotated (m/z present in in-house library, no commercial standard available). Additionally, at least ten putative novel siderophores of the hydroxamate-type were found. This novel, non-targeted screening approach was published in *Applied and Environmental Microbiology* (paper #3). As siderophores are usually synthesized by non-ribosomal peptide synthases (NRPS), another application of the established workflow was to characterize NRPS-knockout mutants of *Trichoderma virens* regarding their siderophore production. These mutants had knockouts in genes putatively coding for NRPSs involved in siderophore biosynthesis. It was shown that the knockout of the *sidD* gene does not influence the siderophore production pattern. The *sidC* gene seems to be involved in ferricrocin biosynthesis and the *NPS6* gene in the synthesis of almost all siderophores present in *T. virens* (fusarinine A and B, des-diserylglycylferrirhodin, coprogen and six novel siderophores). The results contributed to a draft manuscript which shall be submitted to *FEMS Microbiology Letters* in the near future (paper #4).

The last study (paper #5, in preparation) aimed at facilitating MS/MS interpretation for metabolomics experiments, especially regarding the analysis of unknown compounds. Therefore, stable isotopic labeling (SIL) was applied.

Authentic standard compounds (both native and ^{13}C labeled) were measured with a generic LC-MS/MS method. Manual analysis of the MS/MS spectra was facilitated by the fact that the number of carbon atoms of a fragment ion can be directly derived from the mass shift of the fragment signals of the native and the labeled compound. Additionally, a software tool for the automated analysis of SIL labeled data was developed on the basis of the MS/MS data of the standard compounds. This software helps to determine elemental compositions of fragment signals in MS/MS spectra, which speeds up data analysis and is a first and important step towards structural elucidation of unknowns.

KURZFASSUNG

Im Rahmen dieser Arbeit wurden moderne analytische Methoden wie HPLC-MS(/MS) entwickelt und verwendet um komplexe biologische Interaktionen anhand der involvierten Metaboliten zu untersuchen. Die in der vorliegenden Dissertation verfolgten methodischen Ansätze finden vor allem in Metabolom-Studien Anwendung und umfassen gerichtete quantitative Analysen, Screening-Ansätze nach in den Proben vermuteten Substanzen (gerichtetes Screening) und ungerichtete Screening-Ansätze.

Zur Bestimmung unbekannter (neuartiger) bioaktiver Substanzen wurde ein Bioassay-geleitetes Arbeitsschema entwickelt das abwechselnde Schritte von Aktivitätstests und Fraktionierungen/Analysen umfasste. Die Konzepttauglichkeit hinsichtlich der Anwendbarkeit des entwickelten Arbeitsschemas zur Identifizierung unbekannter (neuartiger) bioaktiver Substanzen wurde anhand fungaler Kulturüberstände von *Penicillium brevicompactum* und *Myrothecium verrucaria* gezeigt. Das Arbeitsschema beinhaltete eine Datenbankabfrage der differentiell produzierten Metaboliten der unfraktionierten Kulturüberstände (aktive gegen nicht-aktive Kulturfiltrate) gegen eine kommerzielle Datenbank mit ca. 33.000 Einträgen fungaler und bakterieller Metaboliten. Parallel dazu wurden Kulturüberstände mittels HPLC fraktioniert und aktive Fraktionen mittels LC-HRMS analysiert. Auch hier führte die differentielle Analyse der aktiven gegen die nicht-aktive Fraktionen zu einer Liste möglicher, gegen *Fusarium* aktiver, Metaboliten. Durch Vergleich der so erhaltenen Ergebnisse mit den Ergebnissen der Datenbankabfrage wurde eine Kandidatenliste neuartiger bioaktiver Metaboliten erhalten. Das Arbeitsschema wurde in paper #1 und mehreren Postern veröffentlicht. Die Anwendung auf gegen *Fusarium* aktive Kulturüberstände umfassten unter anderem die Substanzen Verrucaridin A und Mycophenolsäure. Obwohl diese Verbindungen aufgrund ihrer Toxizität nicht für Formulierungen neuartiger Pflanzenschutzmittel gegen *Fusarium* in Frage kommen, zeigen diese Ergebnisse die generelle Anwendbarkeit des entwickelten Arbeitsschemas.

Darüber hinaus wurde eine Analysenmethode zur Quantifizierung 20 ausgewählter Mykotoxine mittels LC-HRMS entwickelt. Im Rahmen einer In-house Validierung wurden für die gesetzlich geregelten Mykotoxine Präzision, Richtigkeit, Nachweisgrenze und Matrixeffekte für die Matrix Mais ermittelt. Ein alternativer Ansatz zur Bestimmung der Nachweisgrenze in Bezug auf Orbitrap MS unter Verwendung des Signal-Rausch-Verhältnisses im „full-profile Modus“ wurde entwickelt und erfolgreich angewendet. Dieser Ansatz führte zu Nachweisgrenzen

zwischen 8 und 160 ng/g Mais. Mit wenigen Ausnahmen für Zearalenon für Babynahrung, „Brot, Back- und Konditoreiwaren“ und Getreidebeikost lagen die Nachweisgrenzen innerhalb der Grenzwerte der Europäischen Verordnung für Deoxynivalenol, Fumonisin B₁ und B₂ und Zearalenon. Acht natürlich kontaminierte Testmaterialien wurden verwendet um Präzision und Richtigkeit der etablierten Methode für Deoxynivalenol, Fumonisin B₁ und B₂, HT-2 Toxin, T-2 Toxin und Zearalenon zu verifizieren. Zusätzlich wurde ein neuartiger Screening-Ansatz für 208 fungale Metaboliten mittels retrospektiver Datenanalyse vorgestellt. Dazu wurde eine Positivliste der ausgewählten Metaboliten erstellt und die Full-Scan Daten automatisiert nach diesen abgesucht. Diese Screening-Strategie basierte auf ausgewählten Detektions- und Identifikationskriterien, darunter akkurate Masse, Peak-Intensität und Intensitätsverhältnis der isotopologen Signale. Das Screening wurde auf die Testmaterialien angewendet und führte zum positiven Nachweis von 13 Substanzen zusätzlich zu den Ziel-Analyten. Diese Studie wurde im *Journal Food Additives and Contaminants: Part A* (paper #2) veröffentlicht.

Die Detektion und Identifizierung Eisen-haltiger Metaboliten (Siderophore) wurde durch die Entwicklung und Anwendung eines Stabilisotopen-basierten Screening-Arbeitsschemas erreicht. Zuerst wurde eine Datenbank mit 422 bekannten mikrobiellen Siderophoren erstellt und eine Liste gebräuchlicher Masseninkremente, die typisch für Siderophor-MS/MS Spektren sind, erstellt. Diese Methode wurde auf Kulturüberstände von zehn *Trichoderma*-Stämmen angewendet. Diese wurden mittels LC-HRMS gemessen und die MS Daten wurden automatisiert nach dem charakteristischen Eisen-Isotopenmuster abgesucht. Die Liste der erhaltenen, mutmaßlichen Siderophore wurde anschließend gegen die In-house Datenbank abgefragt. Im Falle der Verfügbarkeit kommerzieller authentischer Standardverbindungen konnte die Identifizierung mittels Vergleich der Retentionszeiten und MS/MS-Spektren erfolgen. Falls keine Standardverbindungen verfügbar waren, oder mutmaßliche Siderophore nicht in der In-house Datenbank enthalten waren, wurden zusätzliche Vertrauenskriterien eingesetzt. Diese umfassten unter anderem die charakteristische UV/VIS Absorption fungaler Siderophore und das Vorhandensein charakteristischer Masseninkremente korrespondierend zu Neutralverlusten in Siderophor-MS/MS Spektren. Diese Studie führte zur Identifizierung von Dimerumsäure, Fusigen, Coprogen und Ferricrocin. Cis-fusarinin, Fusarinin A und B und Des-diserylglycylferrirhodin wurden annotiert (*m/z* in der In-house Datenbank enthalten, kein kommerzieller Standard verfügbar). Zusätzlich wurden mindestens zehn neuartige Hydroxamat-Siderophore gefunden. Dieser neuartige ungerichtete Screening-Ansatz wurde in *Applied and Environmental Microbiology* (paper #3) veröffentlicht. Da Siderophore üblicherweise mittels nicht-ribosomaler Peptid Synthetasen (NRPS) synthetisiert werden, wurde in einer weiteren Anwendung das etablierte Arbeitsschema verwendet um NRPS-Knockout Stämme von *Trichoderma virens* hinsichtlich ihrer Siderophor-Produktion zu charakterisieren. Diese Mutanten wiesen Knockouts in Genen auf die vermeintlich in die Siderophore Biosynthese involviert sind. Es konnte gezeigt werden dass der

Knockout des *sidD* Gens das Siderophor-Produktionsmuster nicht beeinflusste. Das *sidC* Gen scheint in die Synthese von Ferricrocin involviert zu sein, während *NPS6* offensichtlich in die Synthese von fast allen von *T. virens* gebildeten Siderophoren involviert ist (Fusarinin A und B, Des-diserylglycylferrirhodin, Coprogen und sechs neuartige Siderophore). Die Ergebnisse trugen zum Entwurf eines Manuskripts bei dass bald bei *FEMS Microbiology Letters* eingereicht werden soll (paper #4).

Die letzte Studie (paper #5, in Vorbereitung) zielte darauf ab die Interpretation von MS/MS Spektren in Metabolomics-Experimenten, speziell im Hinblick auf die Analyse unbekannter Verbindungen zu erleichtern. Daher wurde Stabilisotopen-Markierung verwendet. Authentische Standardverbindungen (natürliche und ^{13}C markiert) wurden mit einer generischen LC-MS/MS Methode gemessen. Die manuelle Auswertung der MS/MS Spektren wurde dadurch erleichtert dass sie Anzahl der Kohlenstoff-Atome der Fragment-Ionen direkt aus dem Massenunterschied der Fragment-Signale der natürlichen und markierten Verbindung abgeleitet werden kann. Zusätzlich wurde eine Software zur automatisierten Analyse Stabilisotopen-markierter Daten auf Basis der MS/MS Daten der Standard-Verbindungen entwickelt. Diese Software hilft bei der Bestimmung der Summenformeln von Fragment-Signalen in MS/MS Spektren. Dies beschleunigt die Datenanalyse und ist ein erster wichtiger Schritt in Richtung Strukturaufklärung unbekannter Verbindungen.

LIST OF PUBLICATIONS

Publications

Paper #1

S.M. Lehner, A. Parich, A. Koutnik, R. Krska, M. Lemmens, R. Schuhmacher. Auf der Suche nach aktiven Metaboliten natürlicher Antagonisten gegen *Fusarium graminearum*. *ALVA Mitteilungen* 8:116-120, 2010. ISSN 1811-7317.

Paper #2 (SCI publication)

S.M. Lehner, N.K.N Neumann, M. Sulyok, R. Krska, M. Lemmens, R. Schuhmacher. Evaluation of LC-high-resolution-FT-Orbitrap MS for the quantification of selected mycotoxins and the simultaneous screening of fungal metabolites in food. *Food Additives and Contaminants: Part A* 28:1457-1468, 2011.

Paper #3 (SCI publication)

S.M. Lehner, N.K.N. Neumann, L. Atanasova, R. Krska, M. Lemmens, I.S. Druzhinina, R. Schuhmacher. Isotope-assisted screening for iron-containing metabolites reveals high diversity of known and unknown siderophores produced by *Trichoderma* spp. *Applied and Environmental Microbiology*, published online ahead of print 12 October 2012, doi:10.1128/AEM.02339-12.

Paper #4, in preparation for submission to FEMS Microbiology Letters

J. Hurley, P.K. Mukherjee, **S.M. Lehner**, R. Schuhmacher, I.S. Druzhinina, R.D. Stipanovic, G. Vittone, and C.M. Kenerley. The siderophores and siderophore biosynthesis genes of *Trichoderma virens*

Paper #5, in preparation for submission to Rapid Communications in Mass Spectrometry

S.M. Lehner*, N.K.N. Neumann*, K. Sedelmaier, M. Lemmens, R. Krska, R. Schuhmacher. Towards structure elucidation of unknown substances: liquid chromatography - tandem mass spectrometry of stable isotopic labelled compounds assists elemental composition determination

* shared first authorship

Oral presentations

S.M. Lehner, A. Parich, R. Schuhmacher, B. Antlinger, S. Frühauf, M. Neureiter, A. Koutnik, R. Krska, M. Lemmens. A bioassay guided approach to identify metabolites in culture filtrates of microorganisms that exhibit activity against *Fusarium graminearum*. 5. ASAC JunganalytikerInnen Forum. September 5-6, 2009. Innsbruck, Austria.

S.M. Lehner, A. Parich, B. Antlinger, S. Frühauf, A. Koutnik, M. Neureiter, R. Krska, R. Schuhmacher. Use of LC-MS in the identification process of new plant protectants against *Fusarium graminearum*. 28th Informal Meeting on Mass Spectrometry. May 2-6, 2010. Kőszeg, Hungary.

S.M. Lehner, N.K.N. Neumann, L. Atanasova, R. Krska, M. Lemmens, I. Druzhinina, R. Schuhmacher. Targeted screening and structure characterization of fungal non-ribosomal peptides (siderophores) using LC-HR-MS/MS on an LTQ Orbitrap XL. MassSpec Forum Vienna. February 21-22, 2012. Vienna, Austria.

S.M. Lehner, N.K.N. Neumann, L. Atanasova, R. Krska, M. Lemmens, I.S. Druzhinina, R. Schuhmacher. LC-HRMS/MS based approach for the screening of microbial iron-containing metabolites (siderophores). 8. JunganalytikerInnen-Forum. June 1-2, 2012. Salzburg, Austria.

Poster presentations

S.M. Lehner, A. Parich, M. Sulyok, R. Schuhmacher, B. Antlinger, S. Frühauf, M. Neureiter, A. Koutnik, R. Krska, M. Lemmens. Detection and characterization of bioactive compounds for the development of natural plant protectants. 27th Informal Meeting on Mass Spectrometry. May 3-6, 2009. Retz, Austria.

S.M. Lehner, A. Parich, M. Sulyok, R. Schuhmacher, B. Antlinger, S. Frühauf, M. Neureiter, A. Koutnik, R. Krska, M. Lemmens. A new approach to identify metabolites in culture broths of microorganisms that exhibit activity against *Fusarium graminearum*. Metabomeeting 2009. July 5-8, 2009. Norwich, UK.

S.M. Lehner, A. Parich, R. Schuhmacher, B. Antlinger, S. Frühauf, M. Neureiter, A. Koutnik, R. Krska, M. Lemmens. A bioassay guided approach to identify metabolites in culture filtrates of microorganisms that exhibit activity against *Fusarium graminearum*. Euroanalysis 2009. September 6-10, 2009. Innsbruck, Austria.

S.M. Lehner, M. Lemmens, R. Krska, R. Schuhmacher. Evaluation of the accuracy of mass and isotopologue ratio measurements using an LTQ Orbitrap XL mass spectrometer in full scan mode. Metabolomics & More. March 10-12, 2010. Munich, Germany.

S.M. Lehner, A. Parich, B. Antlinger, S. Frühauf, A. Koutnik, M. Neureiter, R. Krska, M. Lemmens, R. Schuhmacher. Identification strategy of fungal and bacterial secondary metabolites using accurate mass measurements. *International Metabolomics Austria*. September 2-3, 2010. Vienna, Austria.

S.M. Lehner, A. Parich, A. Koutnik, R. Krska, M. Lemmens, R. Schuhmacher. Auf der Suche nach aktiven Metaboliten natürlicher Antagonisten gegen *Fusarium graminearum*. 13. *MOLD-Meeting* „Ernährungsrisiko Mykotoxine – Vermeidungsstrategien entlang der Lebensmittelkette“. December 2-3, 2010. Linz, Austria.

S.M. Lehner, N.K.N. Neumann, L. Atanasova, R. Krska, M. Lemmens, I. Druzhinina, R. Schuhmacher. Metabolic profiling of iron-containing metabolites secreted by *Trichoderma* using LC-HR-MS/MS. *Metabomeeting 2011*. September 25-28, 2011. Helsinki, Finland.

S.M. Lehner, N.K.N. Neumann, L. Atanasova, R. Krska, M. Lemmens, I.S. Druzhinina, R. Schuhmacher. Targeted screening and structure characterization of iron-containing metabolites (siderophores) from *Trichoderma* spp., *A. alternata* and *A. niger* using LC-HR-MS/MS on an LTQ Orbitrap XL. *IOBC/WPRS Working Group "Biological control of fungal and bacterial plant pathogens"*. June 24-27, 2012. Reims, France.

INTRODUCTION

“Systems biology is where we are moving to. Only, it requires a quite different mindset. It is about putting together rather than taking apart, integration rather than reduction. It starts with what we have learned from the reductionist approach; and then it goes further. It requires that we develop ways of thinking about integration that are as rigorous as our reductionist procedures, but different. This is a major change. It has implications beyond the purely scientific. It means changing our philosophy, in the full sense of the term.”

Denis Noble [1]

“The world as we have created it is a process of our thinking. It cannot be changed without changing our thinking.”

Albert Einstein

1 Secondary metabolites in fungi

To start with a very general overview, the suggestion to distinguish between primary and secondary metabolites has been made by Kössel in 1891. Primary metabolites are metabolites that are involved in anabolism and catabolism – covering the substance classes carbohydrates, lipids, proteins, nucleic acids and their building blocks, such as fatty acids and amino acids. The biochemical pathways for generally synthesizing and modifying these compound classes are largely the same in all organisms [2]. Primary metabolites are required for maintaining basic metabolic functions of biological systems such as respiration, nutrient assimilation, growth and development. They are needed for cell maintenance and proliferation which is why they are produced by every cell of an organism [3].

Secondary metabolites on the contrary are dispensable for sustaining the basic metabolism of an organism. They are structurally highly diverse and each of them is produced only by a limited number of species [4]. They often show bioactivity and are of low molecular weight. Their production is usually restricted to a certain part of the life cycle of a cell or certain environmental conditions [5]. In higher organisms, secondary metabolite production usually occurs only in special, differentiated cells. The functions of these substances or their benefit to an organism often are still unknown. Some of the known purposes are the production of toxic compounds as defense against predators, volatile attractants towards the same or other species, coloring agents to attract or warn other organisms [2] as well as active

compounds that enable symbiotic, opportunistic or parasitic interactions and are involved in signaling [6]. Secondary metabolites can play an important role under distinct environmental conditions, e.g. under iron depletion the production and excretion of iron-chelating agents (siderophores) is essential for covering the organism's demand of iron and sustaining growth [7]. There is a large variety of compounds and basic building units and product diversity is large among different taxonomic groups [5]. Analytical approaches for the determination of secondary metabolites therefore have to cope with this enormous diversity of analytes and with large differences in concentrations among these metabolites. However, the precursors of which secondary metabolites are built from are usually derived from primary metabolism. Due to this possible structural similarities a 'grey area' in the distinction between primary metabolism ("biochemistry") and secondary metabolism ("natural products chemistry") exists [2].

The antibiotics paradigm has dominated experimental approaches concerning the ecological role of secondary metabolites for a long time. A huge number of natural compounds have been purified and their chemical structure determined in the past four decades. The majority of bioassays were developed to assess the potential commercial use of new metabolites instead of addressing their function in natural environments. Achieving innovations in drug development was the main aim of natural products chemistry. At the same time, little effort has been made to unravel the reasons why plants and microbes produce these compounds and to clarify their biological role in nature. Roughly in the 1990s changes in ideas started to take root on both the biologists' and the chemists' side [4]. The trend goes towards holistic approaches such as metabolomics and systems biology, which were in the first years of the 21st century still considered as "emerging fields" [8, 9]. Those approaches aim at unraveling metabolites' functions and the complex interactions between organisms that are taking place in natural environments.

The importance of secondary metabolites regarding their bioactive potential is obvious, yet ambivalent – their suitability to be used for pharmaceutical purposes (e.g. penicillin) as well as the threat they pose towards the health of other organisms (e.g. aflatoxins) has to be acknowledged [10]. They have been of major research interest because of their applicability for the treatment of diseases (e.g. cancer) as well as lead substances for novel therapeutic agents [11]. However, under laboratory cultivation conditions many of the respective genes (or gene clusters) for the production of secondary metabolites are not expressed. It has been hypothesized that this is due to a lack of biological communication partners usually occurring in natural environments and no need for a defense against other interacting organisms. Various attempts are made nowadays to activate the production of these potentially valuable metabolites and hence facilitate natural product discovery [12].

Fungal producers of industrial important secondary metabolites include *Acremonium chrysogenum* (cephalosporin c), *Penicillium chrysogenum* (penicillin) and *Aspergillus* spp. (*A. terreus* produces lovastatin, *A. flavus* produces aspergillol

acid). Besides the production of pharmaceutical drugs, industrial important compounds comprise primary metabolites such as citric acid (produced by *Aspergillus niger*) as well as enzymes (e.g. *T. reesei* for producing cellulases [13]). Another beneficial use of organisms that produce secondary metabolites is e.g. the use of *Trichoderma* spp. as biocontrol agent against fungal phytopathogens and for the enhancement of plant growth. Biocontrol is based on complex cellular interactions and mechanisms such as the competition for nutrients and space (e.g. iron), mycoparasitism (direct attack of one fungus on another) and the stimulation of plant defense mechanisms [14] – all involving secondary metabolites.

Besides the beneficial use of some of these fungi and their metabolites, detrimental effects posed by secondary metabolites also exist. Toxic fungal metabolites such as the mycotoxins produced mainly by *Aspergillus* spp., *Penicillium* spp. and *Fusarium* spp. still are a major problem for food and feed safety today. *Fusarium graminearum* is a highly destructive species and causal agent for *Fusarium* Head Blight (FHB) in small-grain crops. For example, the mycotoxin DON inhibits protein biosynthesis and causes tissue necrosis. Plant infection with these pathogens leads to yield loss and mycotoxin contamination (<http://www.scabusa.org/>, accessed on October 9, 2012). Intoxications with mycotoxins can lead to estrogenic (e.g. zearalenone), gastrointestinal and kidney disorders. They can also induce cancer and mutagenicity. EU legislations aim at protecting humans and animals from mycotoxin consumption and resulting adverse health effects (http://www.efsa.europa.eu/de/topics/topic/mycotoxins.htm#efsa_activities, accessed on October 9, 2012). Regulations or guidelines regarding the maximum tolerated concentrations of many mycotoxins in food and feed exist in more than 100 countries [15], leading to the need for analytical approaches able to monitor their occurrence [16].

Regarding FHB, the aim of the project “Novel biological active compounds for the development of high-value nutraceuticals and natural plant protectants” was to find natural antagonistic microorganisms that exhibit biological activity against *F. graminearum* and to elucidate the structure of these biologically active compounds. Such microorganisms could potentially be used as biocontrol agents. Alternatively, the compounds produced by these organisms could be suitable for the production of novel, natural pesticides.

Secondary metabolites cover a wide range of polarities, structures and molecular masses. They can be separated based on their metabolic origin and hence the large majority comprises the polyketides (and fatty acid-derived compounds), non-ribosomal peptides (and amino acid-derived compounds) and terpenoids. These classes will be further discussed in the following chapters. Very prominent representatives of the polyketides are mycotoxins, which are harmful to vertebrates and other animal groups in low concentrations. Many secondary metabolites, however, are of mixed origin and classification into these classes is

therefore not always possible. For instance, some fungal metabolites can exhibit part polyketide and part amino acid or terpenoid structure. As an example, the aromatic ring of mycophenolic acid is formed from a polyketide while the side chain derives from the mevalonate terpenoid pathway [17]. Other mixed origin secondary metabolites are the alkaloids whose structure usually comprises amino acids in conjunction with building blocks from the acetate, shikimate, or deoxyxylulose phosphate pathway or may even be of terpenoid or steroid origin [2].

1.1 Polyketides

Polyketides are the most abundant fungal secondary metabolites that are synthesized by highly organized multi-enzyme complexes with separate domains. Different domains have different functions, e.g. activation, condensation or reduction. Some domains are optional (e.g. methyl transferase domain). Several domains that achieve one synthetic step (one round of chain elongation and modification) form one module. Fungal polyketides are synthesized by type I polyketide synthases (PKSs). Unlike bacterial type I PKSs, fungal PKSs are limited to one module, which carries out repeated biosynthetic steps. Therefore they are called “iterative PKSs” [5].

PKSs contain similar domain structure as fatty-acid synthases with the main difference between these two substance groups being the reduction of the β -carbon during biosynthesis of fatty acids [5]. In fatty acid synthesis the β -carbon is reduced after each condensation step, leading to full saturation of the products. During polyketide synthesis it is possible that some or all reductive steps after condensation are omitted, resulting in various levels of oxidation in the structure of polyketides [18]. A schematic illustration of the elongation/reduction steps in PKS biosynthesis is shown in Figure 1.

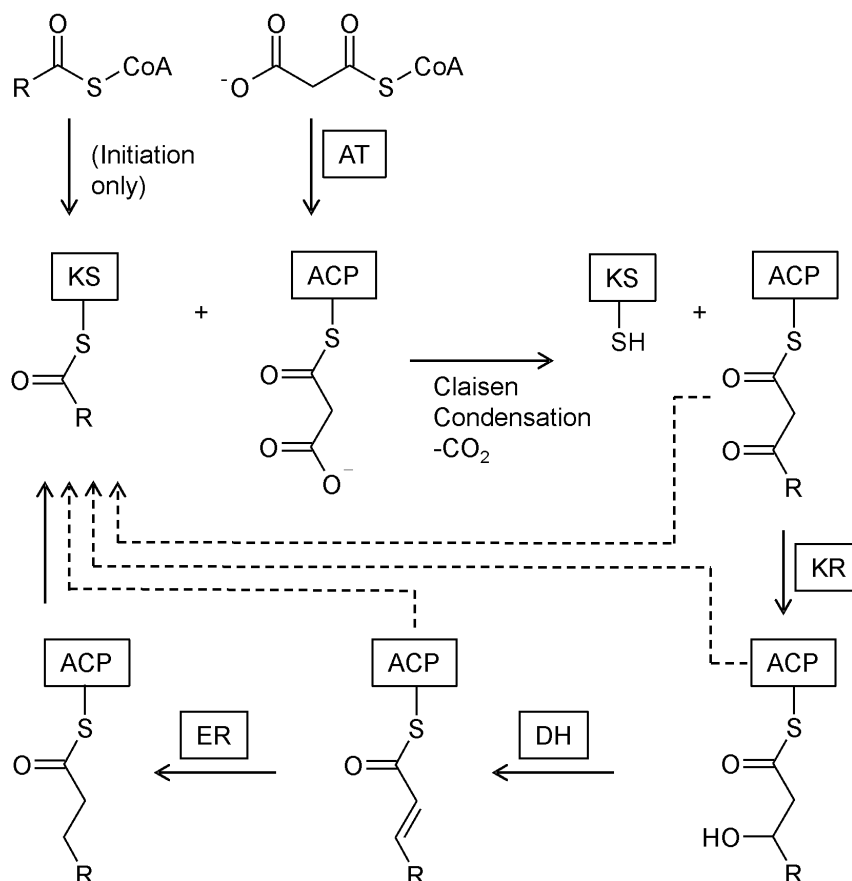


Figure 1 Biosynthesis scheme of one cycle for elongation and reductive processing in fatty acid and polyketide synthesis. Dotted arrows indicate possible pathways for polyketide synthesis, skipping reductive steps; AT...acyl transferase, KS...β-ketosynthase, ACP...acyl carrier protein, KR...ketoreductase, DH...dehydratase, ER...enoyl reductase. Basic building units can be acetyl CoA, malonyl CoA or methylmalonyl CoA; R = -CH₃/ -CH₃COO⁻/ -CH(CH₃)COO⁻. The acyl unit on the ACP is exemplarily depicted as malonyl CoA. Activation of the α-carbon by the carboxyl group makes Claisen condensation more favorable compared to using acetyl CoA (increased acidity of α-hydrogens leading to a more favorable nucleophile for the Claisen reaction) [2].

The poly-1,3-dicarbonyl precursor for PKS synthesis is usually formed from acetyl coenzyme A (acetyl CoA), malonyl CoA or methylmalonyl CoA [19]. In a first step, an acyl starter unit is covalently attached via a thioester bond to the β-ketosynthase (KS) domain. The next acyl unit is bound by an acyl transferase (AT) domain to an acyl carrier protein (ACP), which carries a phosphopantetheinyl arm (ppan). Chain elongation at the ACP is conducted by the KS-domain, which catalyzes the condensation of the acyl units by a decarboxylative Claisen condensation. Modification of the preliminary product by other domains can occur at this stage. Ketoreductase (KR) domains can catalyze the reduction of the β-keto

group to a hydroxyl group, which can then be dehydrated to an alkene by a dehydratase (DH) domain. An enoyl reductase (ER) domain can reduce the alkene to an alkane. Further modifications, e.g. by a methyl transferase domain can also occur. The processed acyl chain is then transferred to the KS-domain and a new acyl unit is attached to the ACP, repeating this condensation/modification cycle. Reaching its final stage, the polyketide is then released from the PKS by a thioesterase domain [18]. The large variety of polyketide structures derives from the number of iteration reactions, reduction reactions, which “extender unit” is used and facultative cyclization of the polyketide chain (in the case of aromatic polyketides). Further diversity is introduced by post-polyketide-synthesis steps [5].

Polyketides are grouped according to the number of acetate units incorporated into their carbon skeleton as tri-, tetra- and pentaketides, etc. Typical representatives for fungal polyketides are significant mycotoxins such as the aflatoxins, fumonisins, ochratoxins, zearalenone and the antifungal agent griseofulvin. In this respect, a quantitative method for the determination of selected mycotoxins in food and feed samples was developed and applied within this thesis. This work was published in *Food Additives and Contaminants: Part A* (paper #2).

1.2 Non-ribosomal peptides

Non-ribosomal peptides (NRPs) are small, bioactive peptides produced by multi-domain, multi-modular enzymes (similar to PKSs) called non-ribosomal peptide synthetases (NRPSs). Those small peptides consist of both, proteinogenic amino acids as well as non-proteinogenic amino acids. One module of an NRPS multienzyme is responsible for the incorporation of one specific amino acid. Its domains are responsible for substrate recognition, activation, binding, modification, elongation and release [20]. An example for NRPS synthesis is given in Figure 2.

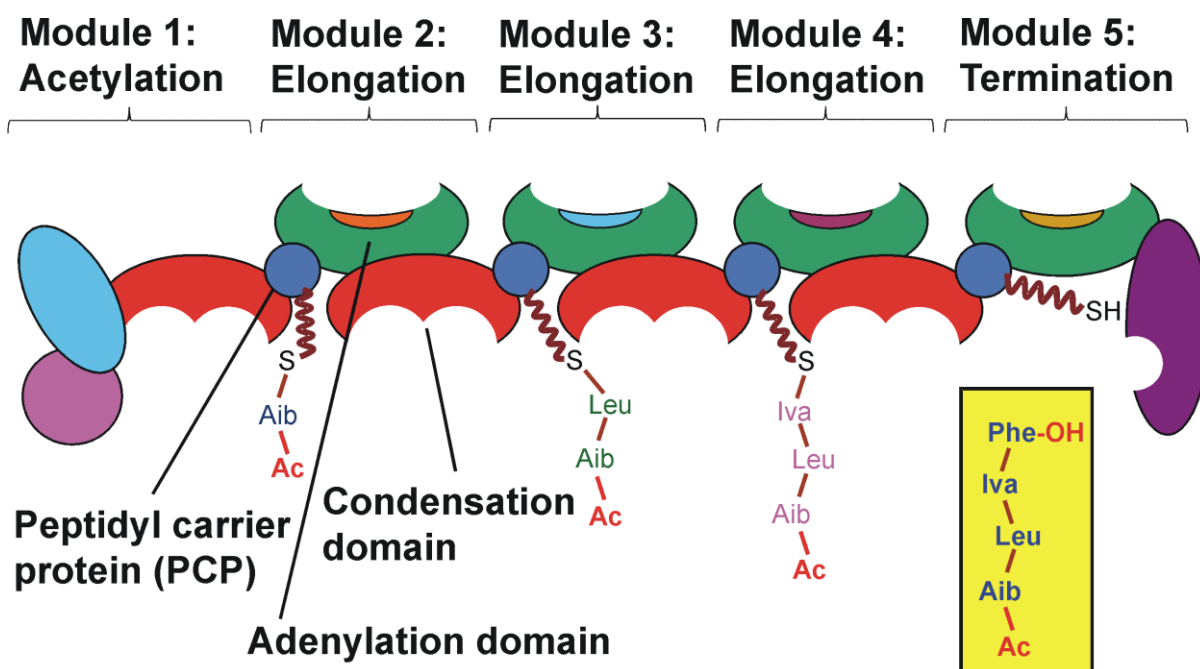


Figure 2 Schematic illustration of the NRPS synthesis of a peptaibol. The multienzyme complex is composed of several modules, responsible for the incorporation of different amino acids. The NRPS synthesis ends by a peptide release via reductive cleavage (courtesy Rainer Schuhmacher).

The first step in NRPS biosynthesis is the adenylation achieved by the adenylation (A) domain that recognizes and selects the substrate amino acid. Activation of the substrate happens in a two-step chemical reaction: First, an amino acid is bound to the adenylation domain and the enzyme catalyzes the aminoacyl adenylate intermediate formation. Then, the activated amino acid is covalently linked via a thioester bond to the 4'-phosphopantetheinyl cofactor (ppan) of the adjacent peptidyl carrier protein (PCP) domain. Crystal structures of different A-domains show low sequence homology but an almost identical fold. They show a channel-like entrance at the substrate-binding site and certain amino acids in specific positions for the interaction with the substrate [20]. The variations of structure and sequence of A-domain binding pockets corresponds to the large diversity of building blocks found in non-ribosomal peptides (NRPs). Contrary to ribosomal protein synthesis, which exhibits very accurate proof reading, NRPSs show less stringent substrate selection [21], leading in some cases to many (micro-heterogeneous) variants of their products.

The second step in NRP synthesis happens at the PCP domain, also known as thiolation domain. The PCP, which shows no autonomous catalytic activity, is responsible for transportation of substrates and elongation intermediates to the catalytic centers [20]. To the side chain of the strictly conserved PCP serine residue a 20 Å long prosthetic ppan moiety is bound which serves as crane for building-block delivery [22]. The combination of the first and second synthesis step is defined as

initiation module since both, the A-domain and the PCP are necessary to activate and covalently bind the first building block for subsequent peptide synthesis. PCPs have a similar function to ACPs from fatty acids and polyketide synthases [20].

After activation and covalent binding of the substrate amino acid to the PCP, stepwise condensation with amino acids bound to downstream PCPs follows by the condensation domain (C) of elongation modules (C-A-PCP). It was shown that C-domains also provide selectivity in non-ribosomal peptide synthesis [23, 24]. C-domains can be replaced by heterocyclization domains, which catalyze peptide elongation as well as heterocyclization [20].

Modifications of the amino acid can occur by editing domains while the intermediate is bound to the PCP. These modifications can increase stability of the NRPS product against proteolytic digestion as well as be important for their folding and hence their biological activity. Those modifications include epimerization (D-isomer of an amino acid), methylation (N-methylation and C-methylation domains), oxidation, reduction and N-formylation [20, 25-29].

Reaching the end of the assembly line, the mature peptide is cleaved from the NRPS machinery by a thioesterase domain, the so-called termination module, which is fused to the C-terminal module. The peptide can be released as linear acid by hydrolysis, as peptidyl amide by aminolysis, or as cyclic product (lactam or lacton) by an intramolecular reaction [20, 30]. Also, reduction of the carboxyl group to an aldehyde or alcohol can occur during release of the product [31]. Post-synthetic modifications, e.g. oxidative cross-linking reactions [32] or glycosylation [33], have also been observed.

Typical representatives of NRPS products are the bioactive linear peptides (peptaibols) with chain lengths from 4-22 amino acids produced by *Trichoderma* spp. Usually they are microheterogenous mixtures of metabolites where certain amino acids in the peptide sequence show certain variability (e.g. leucin/isoleucin) [34]. They contain the non-proteinogenic amino acid α -aminoisobutyric acid (**Aib**), are usually acetylated at their N-terminus and carry an amino alcohol at their C-terminus which is why they are called peptaibols [35]. Concerning the analysis of peptaibols by LC-HRMS the presence of the characteristic mass increment of Aib in tandem MS spectra can be utilized as specific property of these compounds.

Other representatives of NRPS products are siderophores (from Greek, sideros – iron, phorein – to carry sth.). They are produced (and excreted) by microbes and grasses for covering their demand of iron under low iron conditions. Although iron is highly abundant in nature it is oxidized under aqueous, aerobic conditions to ferric oxyhydroxides that exhibit a very low solubility of approx. 1 fg/l (at pH 5) [36, 37]. Siderophores are ferric-iron-chelating agents with a molecular mass of approx. 300-1500 Da. Phytosiderophores belong to the mugineic acids family deriving from the condensation of three S-adenosyl methionine molecules [38]. Fungal siderophores are mainly of the hydroxamate type that are built from the structural unit N⁵-acyl-N⁵-hydroxyornithine [39]. Based on type of acyl group and how

these units are connected they can be further divided into coprogens, ferrichromes and fusarinines. Additionally fungal siderophores seem to play an important role regarding the beneficial role that biocontrol agents (e.g. *Trichoderma*) exhibit. It was shown that fungal mono- and dihydroxamate siderophores increase iron uptake by plants, suggesting an important role in iron acquisition of plants under low iron conditions [40]. For many organisms, not much is known about which NRPS genes are involved in the biosynthesis of specific NRPS products. Within this thesis, a workflow addressing the determination of fungal siderophores using LC-HRMS has been established. Therefore, characteristic properties of fungal ferri-siderophores were used to systematically search for them in LC-HRMS data. These properties included the characteristic UV/VIS absorption, the natural iron isotopic pattern and characteristic mass increments in MS/MS fragment spectra. Some strains from the genus *Trichoderma* can be used as biocontrol agents, which made them particularly interesting for this work. Therefore, this analytical strategy has been applied to ten different wild type *Trichoderma* strains. Additionally, specific NRPS knockout strains of *Trichoderma virens* were investigated regarding the effect of the gene knockouts on the siderophore production. The mutant strains exhibited knockouts in the *sidC*, *sidD* and *NPS6* gene, which are putatively involved in siderophore biosynthesis.

1.3 Terpenoids

Terpenes are formally derived from C_5 isoprene units and are widespread metabolites among fungi and plants. Isoprene is produced naturally but is not involved in the formation of these compounds. The biochemically active isoprene units are the diphosphate (pyrophosphate) esters dimethylallyl diphosphate (DMAPP) and isopentenyl diphosphate (IPP) [2]. Based on the number of isoprene units, hemiterpenes (C_5), monoterpenes (C_{10}), sesquiterpenes (C_{15}), diterpenes (C_{20}), sesterterpenes (C_{25}), triterpenes (C_{30}) and tetraterpenes/carotenoids (C_{40}) are distinguished. The C_5 isoprene units are usually linked head-to-tail. However, since C_{30} and C_{40} terpenoids are based on dimerization of the C_{15} and C_{20} terpenoides, respectively, those building blocks are connected head-to-head [17]. Further modifications include cyclization and rearrangements as is the case e.g. in steroids. Many other natural products comprise terpenoid elements in combination with carbon skeletons from other sources leading to the formation of alkaloids, phenolics and vitamins [2].

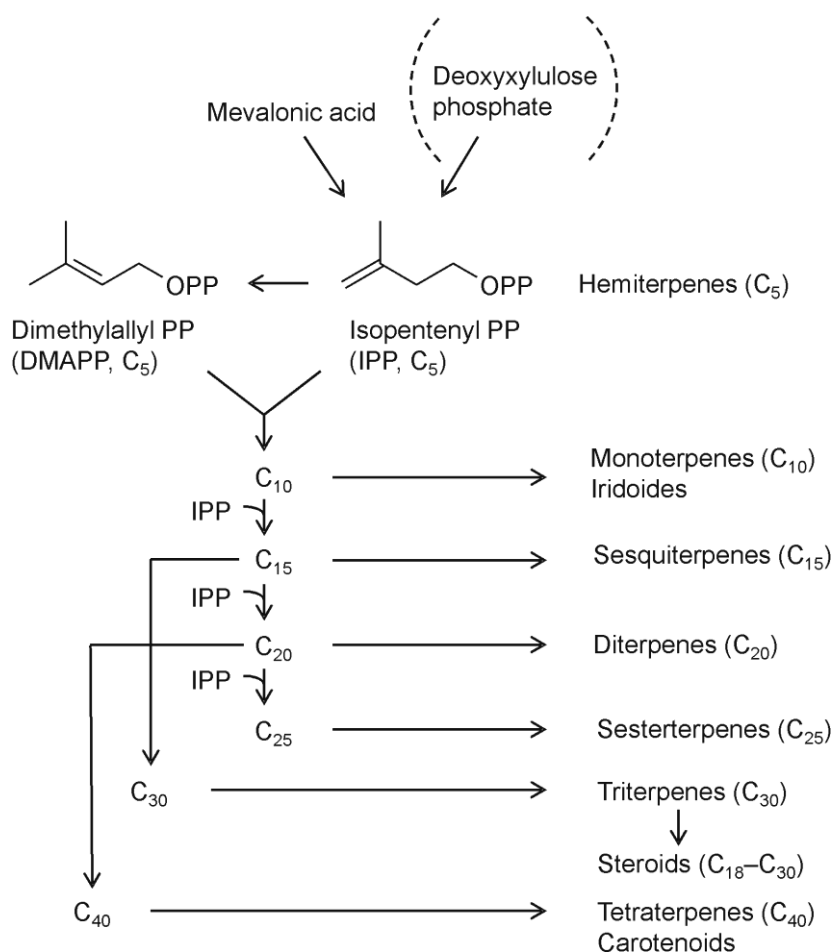


Figure 3 Schematic of the terpene biosynthesis (PP...diphosphate). Formation of IPP via mevalonic acid is the major pathway in fungi.

Two biosynthesis pathways are known: The mevalonate pathway, where the isoprene unit is derived from mevalonic acid, is the major route in fungi and was long time considered to be the only biosynthetic pathway. The non-mevalonate pathway which is also called deoxyxylulose phosphate (DXP or DOXP) pathway or methylerythritol phosphate (MEP) pathway, involves 1-deoxy-D-xylulose 5-phosphate (DXP) and predominates in Streptomyces [17]. Evidences start to be found that this pathway might also be present in fungi [41]. Both pathways produce IPP which, together with its isomer DMAPP, are the basic C₅ unit to be further condensed to bigger structures [42]. The general terpene biosynthesis scheme is shown in Figure 3. The mevalonate pathway starts with acetyl-CoA and acetoacetyl-CoA and forms IPP via mevalonic acid. Its enzymes are present in the cytosol. The non-mevalonate pathway has been associated in plants with the plastids and involves pyruvate and thiamine diphosphate as precursors [43]. Cyclization of the linear diphosphate precursors is achieved by specific cyclases [5]. Biosynthesis of terpenoids usually relies on the presence of a divalent metal ion cofactor (Mg²⁺ (preferably) or Mn²⁺) for activity [43].

Three different prenyltransferases lead to the formation of the linear prenyl diphosphates geranyl diphosphate (GPP, C₁₀), farnesyl diphosphate (FPP, C₁₅) and geranylgeranyl diphosphate (GGPP, C₂₀) [44]. These are the direct precursors for terpene synthesis. The appropriate precursor is ionized to form a carbocation that can then be modified by isomerizations, cyclizations, hydride shifts and/or rearrangements. Termination of the reaction is achieved by deprotonation or water incorporation [45]. It has been shown that single terpene synthases form several different terpenes from a single substrate. For example, the monoterpene synthase sabinene produces mostly sabinene (63%), but also γ -terpinene (21%), terpinolene (7%), limonene (6.5%) and myrcene (2.5%), leading to a typical complex mixture of terpene products [46].

Secondary metabolites show a high structural variability and a high range of natural occurring concentrations. This makes high demands to the analytical approaches employed to tackle them. Their determination is of high interest due to various reasons and concerns ranging from food safety (e.g. mycotoxin contamination) over their beneficial use as producers of bioactive substances (e.g. drugs, enzymes, natural pesticides) to understanding the complex interactions between organisms taking place on a molecular level (e.g. systems biology and metabolomics approaches). In this respect, different analytical strategies are employed. Regarding the monitoring of potentially harmful substances (e.g. in food and feed), so called “multi-methods” have been established that aim at the quantification of a high number of secondary metabolites in one analytical run [47, 48]. On the other hand, targeted as well as non-targeted approaches aim at understanding the context of dynamic interactions in metabolic networks on a systems level. Many metabolomics studies make effort at revealing unexpected or to-date unknown properties of systems [49]. These studies show the highest potential for discovering novel natural compounds. One of the most widely used techniques that is applicable in both respects is liquid chromatography coupled to mass spectrometry, which will be covered in the following chapters.

2 Liquid chromatography coupled to (tandem) mass spectrometry for the analysis of secondary metabolites

“Progress in science depends on new techniques, new discoveries and new ideas, probably in that order.”

Sydney Brenner [50]

2.1 Introduction to liquid chromatography and mass spectrometry

Metabolites are the intermediates and end products of physiological regulatory processes. Their presence can be viewed as the ultimate response of a cell to genetic and environmental variations [9]. In analogy to genomics and other “omics” disciplines, the totality of all metabolites present in an organism is called the metabolome and the corresponding scientific discipline coping with it is called metabolomics. Regarding functional analysis of biological systems (Figure 4) different levels can be distinguished: the study of gene expression (transcriptomics), protein translation (proteomics; including post-translational modifications) and the metabolite network (metabolomics) [51].

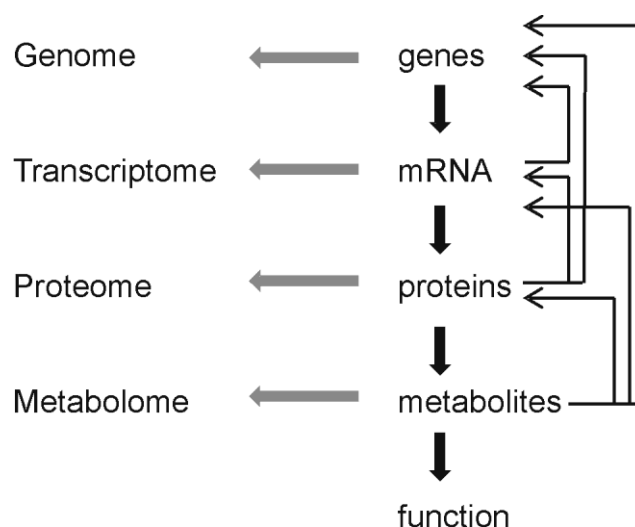


Figure 4 The “omics” cascade. The common flow of information from genes to transcripts to proteins to metabolites to function. Each stage is giving feedback to the previous stages.

Novel “holistic approaches” such as metabolomics aim at the comprehension of whole biological systems – looking at the biochemical changes taking place in living cells during metabolism. In “traditional analytical approaches” the focus lies on certain analytes for which methods are optimized and authentic standard compounds for all analytes are available. “Holistic approaches” aim at covering as much

compounds as possible – e.g. “all” metabolites in the case of metabolomics. Of course, one analytical technique is not able to fulfill this requirement – the application of various analytical techniques is needed to achieve covering as much compounds present in a sample as possible. Also, the need to analyze a diversity of structurally very different components, both known and unknown, at a high dynamic range of concentrations in complex matrices makes the task explicitly difficult. However, a versatile technique that is able to cover a wide range of substances and finds broad application is liquid chromatography coupled to (tandem) mass spectrometry. As this technique has been used throughout this thesis, liquid chromatography and mass spectrometry shall be presented in more detail.

Chromatography (from Greek *chroma* – color, *graphein* – to write) is a separation technique where a mixture of substances in solution (mobile phase) passes a stationary phase and is separated into the different components of the mixture. The mobile phase can either be a gas (gas chromatography, GC) or a liquid (liquid chromatography, LC). In mass spectrometry (MS), the sample is vaporized, ionized and the generated ions are then separated according to their mass-to-charge ratio (m/z). Coupling these two sophisticated techniques gives a separation due to the physicochemical properties of the analytes (according to the mobile and stationary phase) in the first stage and a separation according to the analyte-derived ions in the second stage. Therefore, the generated data shows three dimensions, namely intensity as a function of time (chromatographic dimension) and of m/z (spectrum dimension).

A schematic of a high performance liquid chromatography (HPLC) system is shown in Figure 5. The mobile phase (solvent) is pumped across a sample injector (autosampler) where a liquid sample is introduced into the system. Then the mobile phase passes a column (filled with the stationary phase). There the separation of the analytes present in the sample takes place. The solvent arranges the interaction between the analytes and the stationary phase. This interaction leads to a delayed transport of the analytes through the column (based on the degree of interaction with the stationary phase) leading to characteristic retention times of different substances. Finally, the analytes are detected in a detector (e.g. UV/VIS detector or mass spectrometer) and the data is recorded.

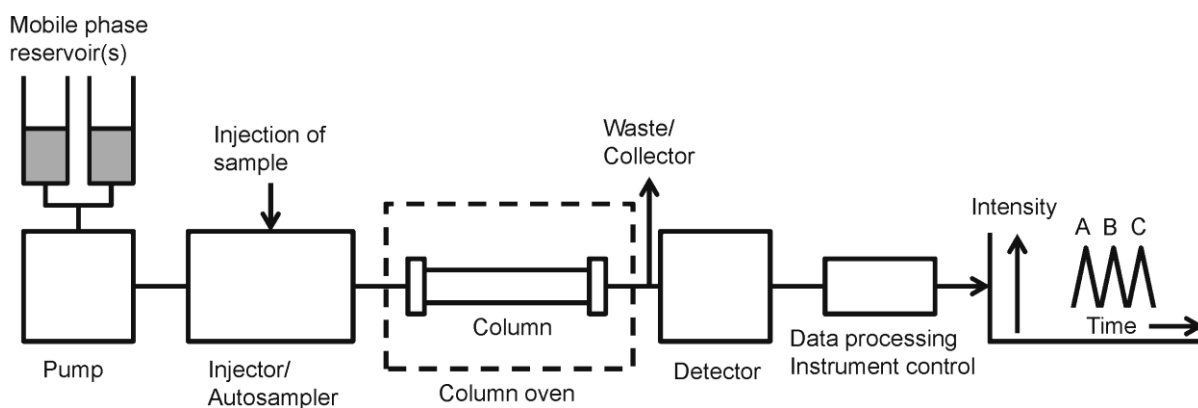


Figure 5 Schematic of an HPLC system

The mobile phase usually consists of water, buffers and/or organic solvents. The term “isocratic” refers to a separation where the composition of the solvent stays the same during the whole chromatographic run. Changing the solvent composition during a separation is called “gradient separation”.

One of the first stationary phases used in column chromatography was silica gel that contains polar hydroxyl groups. Chromatography applying unmodified silica gel as stationary phase is called normal phase (NP) chromatography. Later, the free hydroxyl groups were etherified with functional groups, e.g. alkyl groups (usually C₂ – C₁₈) or aromatic groups. These modifications lead to a reversion of the polarity of the stationary phase compared to NP chromatography - the obtained apolar stationary phases are called reversed phase (RP) materials and find broad applicability. In RP chromatography, hydrophobic interactions between the analyte and the stationary phase occur. The separation of constituents of mixtures usually starts with polar, aqueous solvents as mobile phase; elution is achieved by gradient elution with an increasing proportion of apolar solvent that competes with the analyte for the apolar interaction sites at the stationary phase [52].

Many different detection principles exist that can be employed for the detection of analytes. Very specific detection systems include the measurement of a specific biological activity (e.g. assays for enzymatic reactions). Immunological detection systems employ antibodies. Unspecific detection systems such as measuring the whole protein content of a sample by UV detection (e.g. peptide bond at 206-220 nm, aromatic amino acids at 254 or 280 nm) can also be used. Color reactions (e.g. coomassie blue in Bradford tests) in conjunction with photometric measurements can also be applied [52]. Highly sophisticated detection systems include the use of mass spectrometry, which will be discussed in the following.

A typical mass spectrometer consists of an ion source (where ions are generated from a sample), a mass analyzer (where ions are separated based on their m/z) and an ion detection device (see Figure 6). A mass spectrum is obtained, giving the m/z values of the measured ions against their relative abundances.

Determination of fungal bioactive compounds using LC-HRMS

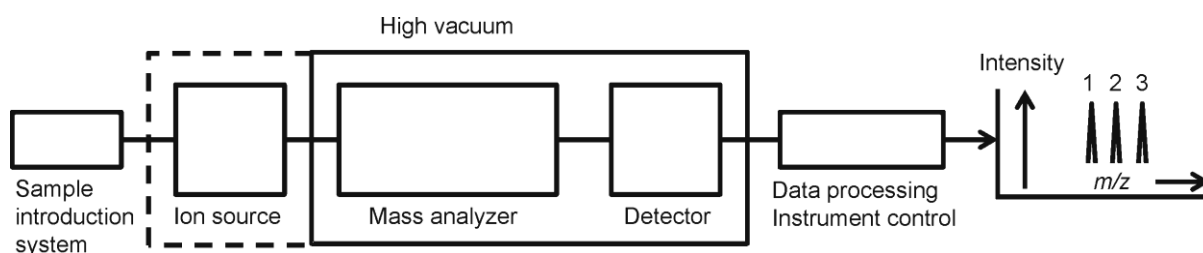


Figure 6 Schematic of a mass spectrometer

Ionization can be achieved either by the uptake or the loss of an electron and various ionization techniques have been developed, e.g. electrospray ionization (ESI), atmospheric pressure chemical ionization (APCI), atmospheric pressure photo ionization (APPI), all of which can be directly coupled to LC). Mass spectrometry requires high vacuum in order for the ions not to collide with gas molecules on their flight through the mass spectrometer. When combined with liquid chromatography, the ionization process takes place at atmospheric pressure (ESI, APCI, APPI), leading to the need to efficiently remove a large excess of LC solvent before the ions reach the high vacuum region of the MS system. To achieve the transfer of the ions into the mass spectrometer towards the high vacuum a high voltage is applied (typically 2-6 kV) in many atmospheric pressure ionization (API) techniques. Inert gas flows (often heated) are applied to support the evaporation of the solvent molecules. To achieve the coupling with API sources differential pumping is applied on one or several stages, each one separated from the others by a skimmer [53]. An overview of the approximate range of application of commonly used mass spectral techniques in metabolomics for selected compound classes is given in Figure 7.

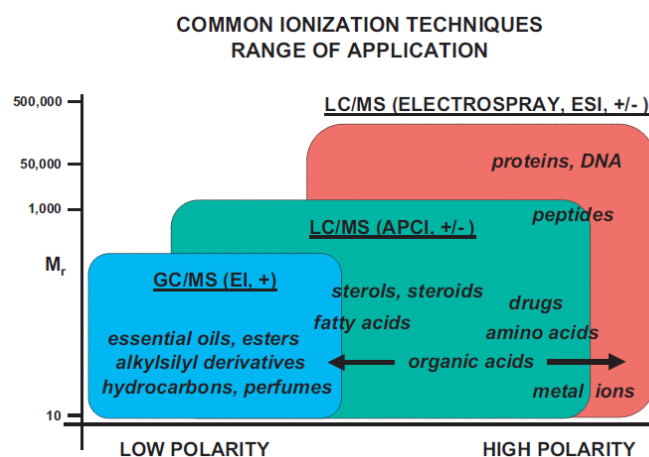


Figure 7 Coverage of compound classes regarding the ionization technique of commonly used GC-MS and LC-MS approaches in metabolomics experiments (reproduced with kind permission from Oxford University Press [54]).

Today, ESI is the most widely used ionization technique in LC-MS [55]. One of its major benefits is that it is directly compatible with liquid chromatography. Additionally, it is the most universal of the known ionization techniques, exhibiting low chemical specificity and at the same time showing very high ionization efficiency [55]. ESI takes place at atmospheric pressure. It is a so-called soft ionization technique and leads to very low fragmentation of the analyte molecules. As this ionization technique was used for this thesis it will be further discussed in the following. A fluid passes through a capillary and is dispersed in many small charged droplets in an electric field. This electric field is obtained by the applied potential difference of 2-6 kV between the capillary and the counter-electrode and leads to a charge accumulation at the liquid surface at the end of the capillary [53]. The liquid protrudes from the capillary tip and forms a Taylor cone. When the Coulombic repulsion of the surface charge is equal to the surface tension of the solution (Rayleigh limit), droplets containing an excess of charge detach from the tip of the Taylor cone. As these droplets move towards the MS interface, charged single ions are generated. Two models have been proposed to describe the ionization process: the ion evaporation model and the charge residue model. The ion evaporation model was originally described by Iribarne and Thomson [56, 57]. It assumes that droplets shrink by solvent evaporation until at a certain point the field strength at the surface is large enough that individual solvated analyte ions are ejected from the droplet. The energy needed to increase the droplet surface is compensated by the gain due to Coulomb repulsion [55]. The charge residue model was originally developed by Dole and co-workers [58]. Highly charged droplets shrink due to solvent evaporation. When the field strength becomes sufficiently large, Coulomb repulsion overcomes surface tension and a Taylor Cone forms locally. From its tip, smaller highly charged droplets are emitted. According to the charge residue model, this process repeats until the droplets generated contain only one analyte ion. After solvent evaporation the analyte ion is released [55].

For the separation of the analyte ions according to m/z , various mass analyzers are applicable: quadrupole, magnetic sector, time-of-flight (TOF), ion trap, ion cyclotron resonance (ICR) and Orbitrap mass analyzers [52].

Ion detectors for mass spectrometry have been reviewed by Koppenaal and co-workers [59]. Nowadays, the most widely used ion detectors are electron multipliers [53]. In this type of ionization device, the entering ions strike a conversion dynode, held at a high potential of opposite polarity to the ions detected, which produces secondary charged particles. For positive ions these particles are electrons and negative ions; for negative ions, the secondary particles are positive ions [60]. These secondary particles then accelerated by a voltage gradient into the electron multiplier where they hit the inner walls with sufficient energy to eject electrons. This leads to an electron cascade, which multiplies the initial incident by at least 10^6 . The resulting electronic current ("analog" counting mode) or alternatively the individual electron pulses (from each single primary ion) are recorded and processed to obtain a mass spectrum [59]. Detection in FT-ICR and Orbitrap MS fundamentally differs

from this principle as the detector consists of a pair of metal plates within the mass analyzer region close to the ion trajectories. The ions perform an oscillation on stable trajectories that induces a current in the outer detector electrode. This image current is recorded and transformed to receive a mass spectrum [53].

Mass spectrometry (MS) has been in development for over a century. Progress over this time has been of great impact for the scientific community [61]. A major recent innovation in type of mass analyzer has been the invention of the Orbitrap analyzer which exhibits high resolving power and was first described in 2000 [62]. It was commercialized as hybrid instrument combining an ion trap with an Orbitrap analyzer (LTQ Orbitrap tandem mass spectrometer) by Thermo Fisher Scientific in 2005 (<http://planetorbitrap.com/history#.UD847CLyC0s>, accessed on August 30, 2012). Its further development and optimization is still in progress [63]. Since Orbitrap MS was used throughout this thesis, this mass analyzer will be discussed further in more detail.

The Orbitrap mass analyzer (shown in Figure 8) consists of a spindle-like central electrode and a barrel-like outer electrode which is split at $z=0$ [62]. Ions are trapped in an electrostatic field and orbit around the inner electrode on stable trajectories. They perform a harmonic oscillation along the z -axis, exhibiting a frequency that is proportional to $(m/z)^{-1/2}$ (Equation 1). This oscillation is recorded by image current detection on the two split halves of the outer electrode and is fast Fourier transformed (FFT) from the time-domain transient into a frequency spectrum. Frequencies are then converted to m/z (according to Equation 1) and thus a mass spectrum is obtained [64, 65].

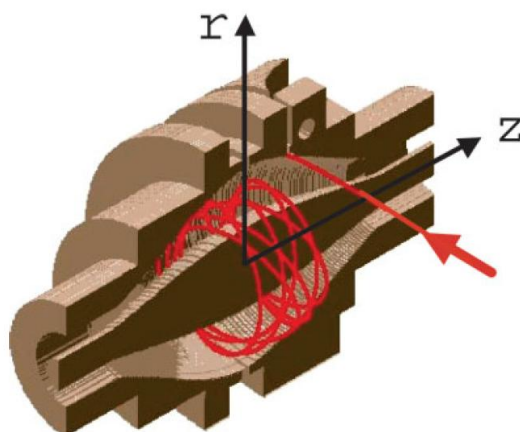


Figure 8 Cross-section of the Orbitrap mass analyzer. Offset from the Orbitrap's equator ($z=0$) and perpendicular to the z -axis (indicated by the red arrow) the ions are injected into the Orbitrap. They begin coherent axial oscillation without the need for any further excitation (reproduced with kind permission from John Wiley & Sons [65], DOI: 10.1002/jms.856, <http://onlinelibrary.wiley.com/doi/10.1002/jms.856/abstract>).

$$\omega = \sqrt{k \cdot \frac{z}{m}}$$

Equation 1

ω ... frequency of axial oscillation [rad/s]

m/z ...mass-to-charge ratio

k ...constant

Major benefits are that the Orbitrap is more compact, less costly and easier to maintain than other high resolution instruments (e.g. FT-ICR) and at the same time shows comparable performance (for relatively short acquisition times ≤ 1.8 sec) [64]. Currently, the latest commercial product (Orbitrap Elite) exhibits a mass resolving power of 240,000 (FWHM) at m/z 400. Using external calibration mass accuracies < 2 ppm are achieved [66].

A schematic of the ion path of the LTQ Orbitrap XL model used in this thesis is shown in Figure 9. Ions are drawn into the ion transfer tube from the ESI nozzle at atmospheric pressure (760 Torr). By a decreasing pressure gradient they enter the tube lens/ skimmer region (1 Torr). The potential of the ion transfer tube is typically set to ± 25 V (positive in positive ionization mode, negative in negative ionization mode) in order to repel ions from the transfer tube and focus them towards the opening of the skimmer. The skimmer is at ground potential and works as vacuum baffle towards the next lower pressure region (10^{-3} Torr). The opening in the skimmer is off-set to the bore of the transfer tube to avoid the passage of neutrals in order to minimize detector noise. The subsequent multipoles focus and transmit the ions from the skimmer to the linear ion trap (LTQ). Neutrals and ions of the opposite polarity are lost in the vacuum. The first and the second multipoles are square quadrupoles. The third and last multipole is an octopole. Several multipoles instead of just one are used to allow for differential pumping and subsequent lower pressure. The multipoles focus the ions by applying radiofrequencies (RF) on opposing poles. Additionally the multipoles keep the ions moving towards the LTQ with differential voltage offsets. While the skimmer is grounded, the first multipole has a voltage offset of approx. 4 V, the second of approx. 7 V and the third of approx. 9 V, all with an opposite polarity of the ions of interest. The first multipole region still contains a considerable amount of gas molecules – slowing the ions down on their way to the LTQ. The inter-multipole lenses, having a charge opposite of the ions of interest, accelerate ions on their way and function as vacuum baffles. The gate lens starts and stops the injection of ions into the LTQ. Ions stored in the LTQ can be detected by the electron multipliers or be moved further through the system into the Orbitrap mass analyzer. Additionally, MS/MS experiments can be carried out in the LTQ. Alternatively, ions can be axially ejected from the LTQ and trapped in the C-trap. MS/MS experiments can be carried out by transferring ions to the HCD cell and returning them to the C-trap. The C-trap is an RF-only quadrupole, bent into a C shape. There the ions are squeezed into a small ion package before being injected into the Orbitrap [60].

LTQ Orbitrap XL

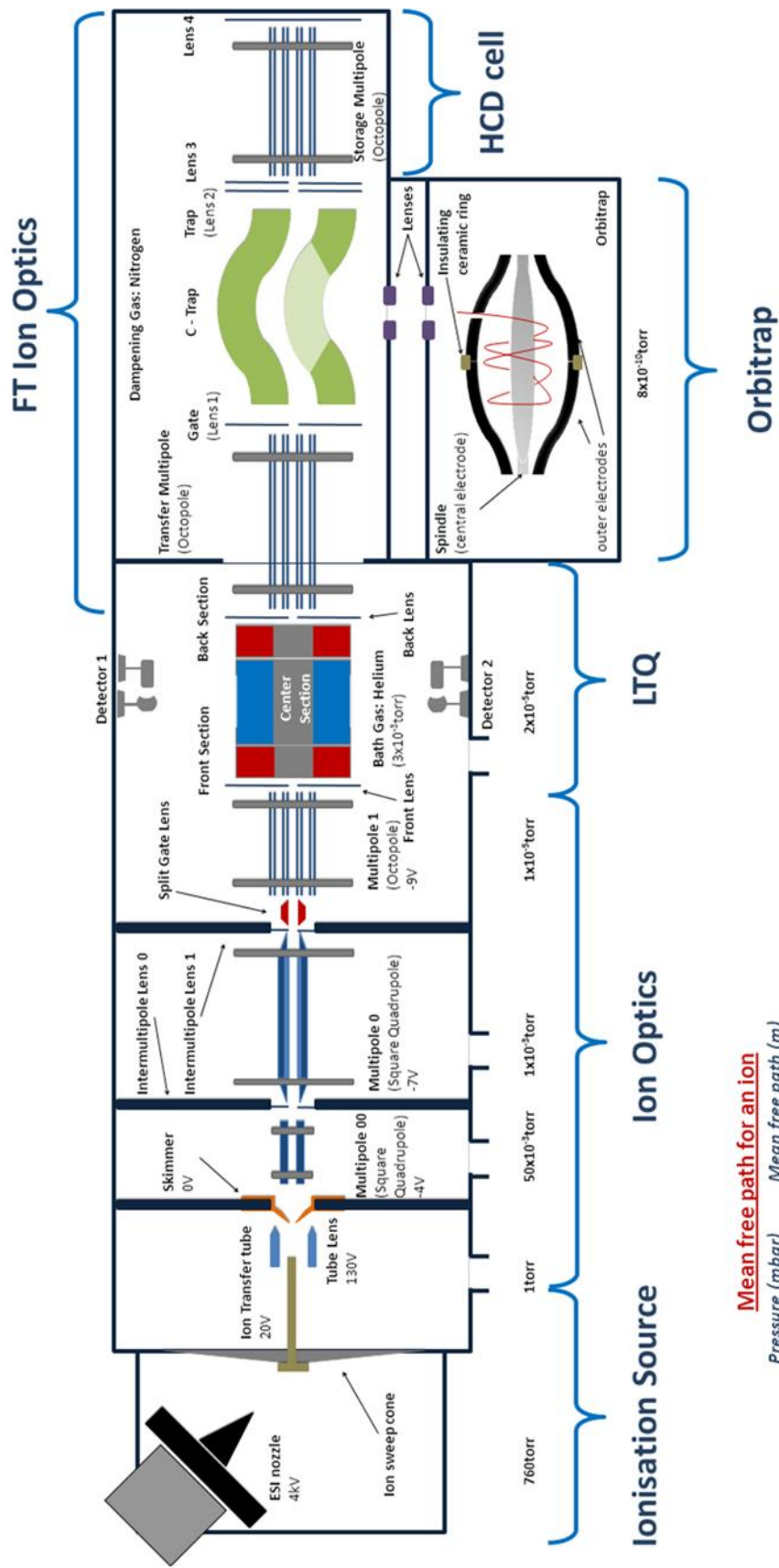


Figure 9 Schematic of the ion path of the LTQ Orbitrap XL (courtesy Bernhard Kluger).

For gaining structural information about an analyte, tandem mass spectrometry (MS/MS or MSⁿ) can be used. Tandem mass spectrometry encompasses at least two stages of mass analysis. In a first step, a precursor mass is isolated and excited to achieve fragmentation. Thus, besides neutral fragments, charged product ions are obtained and are analyzed in a second step. Fragment ions can again be isolated and fragmented in order to gain more exhaustive structural information. Tandem mass spectrometry can either take place “in space” by coupling of two physically distinct instruments or “in time” by performing the appropriate sequence of events in one single ion storage device [53].

In the Orbitrap, different fragmentation techniques are available. The most relevant for this thesis will be discussed in the following:

- Collision induced dissociation (CID): Precursor isolation and fragmentation can take place in the linear ion trap (LTQ). After ion isolation, precursor ion excitation leads to an increase in kinetic energy and hence, ions move faster within the trap. When ions collide with helium gas molecules the kinetic energy is converted into internal vibrational energy within the ions' bonds, increasing with every collision. The increase in vibrational excitation finally either leads to the dissociation of bonds (fragmenting at the weakest bond) or to a rearrangement by an internal reaction, leading to a different mass. Only the precursor ion is activated, leading to fragments that exclusively originate from the precursor ion (not from fragments of the precursor ion). Ions exhibiting a mass that is lower than approx. 1/3 of the precursor mass are not stable in the ion trap (“low mass cutoff”) and cannot be covered with this fragmentation technique.
- Higher energy collision dissociation (HCD): Another possibility is precursor selection in the LTQ and subsequent fragmentation in a special octopole collision cell that is following the curved linear trap (C-trap, see Figure 9). In the collision cell, DC offset voltages are applied in the same way as in quadrupole instruments. The resulting increase in kinetic energy of the ions leads to collision with the gas molecules present in the cell. In HCD, nitrogen is used as collision gas and dissociation occurs after a few collisions between the ions and the gas molecules. MS/MS fragmentation patterns are similar to those obtained from triple quadrupole systems. Fragmentation spectra exhibit a lower mass cutoff (approx. 1/20 of the precursor mass) compared to CID spectra. This configuration operates in a higher collision energy regime compared to a linear ion trap. Successive fragmentation reactions, i.e. fragmentation of the “primary” fragments can occur as the fragments further pick up kinetic energy, leading to more complex MS/MS spectra and complementary information compared to CID MS/MS, especially in the low m/z range [60, 64].

In this respect, both fragmentation techniques were used throughout this thesis - in particular in paper #3 with respect to the siderophore production pattern of ten wild type *Trichoderma* strains and paper #5 (in preparation) regarding MS/MS interpretation of SIL samples.

2.2 Analytical strategy for the determination of fungal secondary metabolites using LC-HRMS/MS

These developments in instrumentation show high potential for novel analytical applications, especially the possibility of retrospective data analysis of full scan high-resolution mass spectra. Besides the (quantitative) target analysis with reference standards, novel methodologies such as targeted (“suspects”) screening approaches without direct need for reference standards and non-targeted screening approaches of unknowns can be distinguished [66]. A schematic is shown in Figure 10. Especially targeted approaches are broadly applicable with respect to the analysis of contaminants e.g. for food and feed safety (e.g. mycotoxins). In this respect, full scan data is searched against a target list. Verification of the results is done by measurements of authentic standard compounds. Retention time and MS/MS fragmentation pattern are compared and need to match with those of the analyte. So-called “suspects screening” approaches open a wide range of possibilities where no direct availability of authentic standard compounds is given. In this case, the full scan data is searched against a list of “suspects”. To gain further certainty, the theoretic isotopic pattern can be compared with the measured isotopic pattern. Further confidence criteria can include the matching of the retention time and the MS/MS spectra with values/spectra from other systems or instrument types or with predicted values/spectra. So-called “non-targeted screening” approaches start with an automated search for reliable features (three dimensional signal comprising a certain m/z value at a certain retention time exhibiting a certain intensity) in the full scan MS data. This way a list of potential MS features of interest is generated. The next steps towards compound characterization include the elucidation of the elemental formulas and the structures of the respective signals. Retention time and MS/MS spectra are considered in the same way as in “suspects screening” approaches. However, no guidelines or specific requirements regarding targeted and non-targeted screening approaches that are agreed upon by the community exist yet.

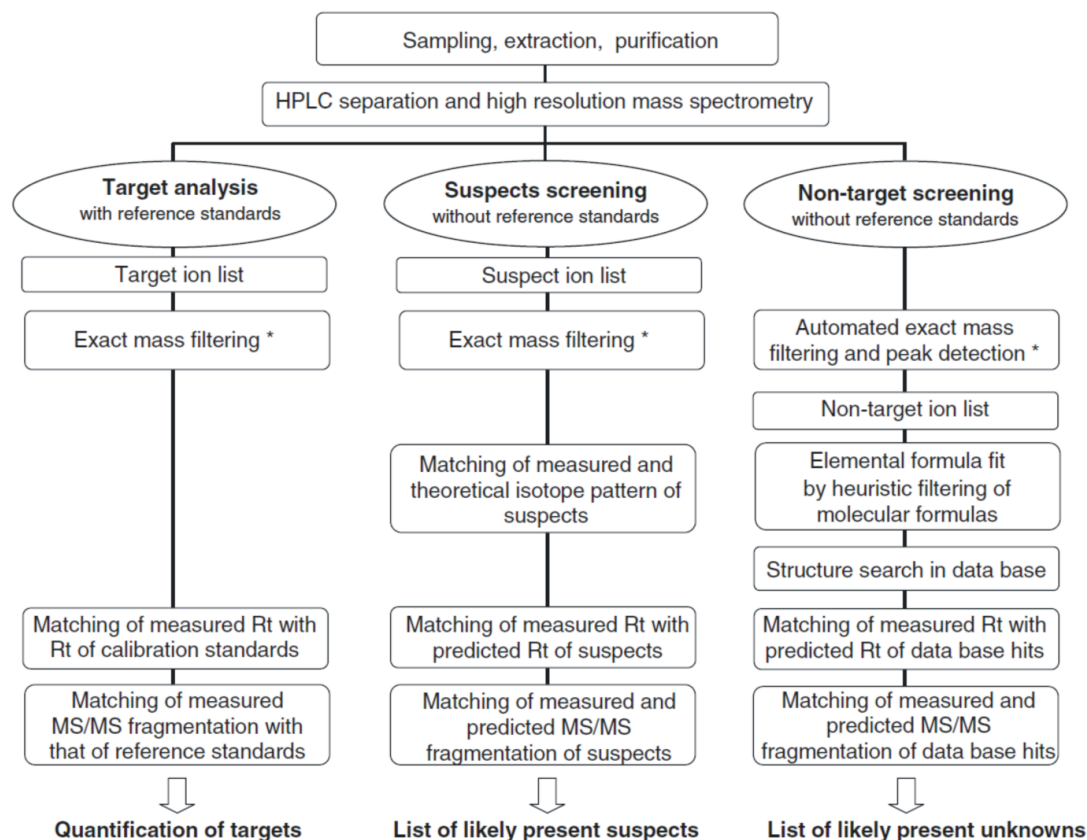


Figure 10 Diagram of different systematic approaches for quantitative target analysis with reference standards, suspects screening without reference standards and non-target screening of unknowns using LC–HRMS/MS. *The m/z range of the extraction window for exact mass filtering is dependent on the resolving power and the mass accuracy of the MS instrument used (reproduced with kind permission from Springer Science and Business Media [66], Fig. 1).

The large amount of information present in high resolution full scan mass spectral data leads to an explicitly complex data evaluation process. Usually for one substance, several signals are present in a mass spectrum, e.g. the protonated molecule (singly charged), in-source fragments (fragments that were generated in the ESI ion source during ionization), isotope peaks (^{13}C , ^{34}S , ^{37}Cl), common adduct ions (e.g. ammonium, sodium, potassium adducts), multiply charged molecules of the protonated molecule and/or adduct ions. Additionally, many artifacts and background ions can be observed in the spectra, e.g. electronic noise (so called “pseudo-ions”) present in Orbitrap MS and multiple plasticizer ions due to sample handling and treatment. An excellent review article on commonly observed background interferences and contaminants has been published by Keller and co-workers [67]. Additionally, a database for background ions has recently been established by Weber and co-workers [68] (<http://www.maconda.bham.ac.uk/>). All these signals need to be discerned for allowing meaningful data evaluation. One application to make use of these inherently present signals is to check mass

accuracy prior to mass spectral measurements. These ions were used in this respect throughout this thesis to test for mass accuracy of the instrument and determine whether mass calibration was necessary (approx. mass deviation ≥ 3 ppm).

2.2.1 Target analysis and method validation

For the unambiguous identification of analytes, the use of authentic standard compounds is an ultimate requirement in mass spectrometry. Criteria for unambiguous identification have been described in recent publications [69-71]. The suggestion of the Metabolomics Standard Initiative (MSI) of the Metabolomics Society, which has been published by Sumner and coworkers [69], is to use at least two independent and orthogonal properties that need to match between the standard and the analyte. Those can include e.g. retention time, accurate mass, tandem MS (MS/MS) or isotope pattern. Sample and standard have to be measured under identical experimental conditions. Quantification of these compounds can be achieved by establishing calibration curves and validation of the used analytical methods.

According to ISO/IEC 17025:2005 validation is the “confirmation by examination and provision of objective evidence that the particular requirements for a specified intended use are fulfilled” [72]. Regarding method validation this can be viewed as defining an analytical requirement and confirming that the performance of an analytical method is consistent with these requirements. The following performance characteristics are usually investigated and documented for verifying that a method is fit for a particular analytical purpose: applicability, selectivity, calibration, trueness, precision, recovery, operating range, limit of quantification, limit of detection, sensitivity and ruggedness. Eventually measurement uncertainty and fitness-for-purpose are also included [73]. All these performance parameters have been covered and discussed in various documents, guides and publications, e.g. Eurachem guides (<http://www.eurachem.org/index.php/publications/guides>), an IUPAC technical report of 2002 [73] or documents from the EU Reference Laboratories (e.g. SANCO/12495/2011, available at http://www.eurl-pesticides.eu/docs/public/tmpl_article.asp?CntID=727&LabID=100&Lang=EN). The general goal of a rigorous method validation is to estimate the uncertainty of measurement, since it is a key indicator of both, fitness for purpose and reliability of results [73].

When coping with real world samples or sample extracts (e.g. maize extract in respect to food and feed analysis), effects reducing or enhancing the analyte signal have to be considered in order to verify accuracy of the results. Extraction efficiency needs to be evaluated and considered. Also, signal suppression/enhancement effects (SSE) have to be taken into account. Those derive from matrix compounds that co-elute with the analyte molecules and alter the ionization process. SSE effects can lead to enhancement or suppression of the analyte signal intensities and therefore result in biased calculated concentrations. These effects need to be

assessed and corrected for in order to obtain reliable results, e.g. to obtain accurate concentration values, to evaluate the limit of detection and to estimate the likelihood of false negative findings. Another issue that has to be critically assessed for obtaining accurate data is the sample preparation procedure, e.g. extraction efficiencies, which has to be carefully evaluated.

For experimentally verifying accuracy (precision and trueness), certified reference materials (CRMs) can be used. Those materials have been characterized by a metrologically valid procedure – one or more specified property values (e.g. concentration of an analyte) are certified and each value is accompanied by an uncertainty at a stated level of confidence [74].

2.2.2 Suspects screening towards compound annotation

If no authentic standard is available, substances can be putatively identified, i.e. annotated, using mass spectrometry based on their accurate mass. Further information present in the mass spectrum can be used to increase confidence in the initial annotation.

The first step is the determination of the identity of the ion species present in a full scan mass spectrum. This can be achieved by observing several characteristic ion species - either in one ionization mode (e.g. the protonated molecule and the sodium adduct in positive ionization mode) or in a combination of the positive and negative ionization mode (e.g. presence of the protonated molecule in positive and the deprotonated molecule in negative ionization mode). Only if the ion species of a signal in a mass spectrum has been assigned, metabolite annotation can be conducted. Annotation (of known compounds) can be achieved by database queries. Specific databases for the organism or the compound type of interest can facilitate this data analysis step. For a target (or “suspects”) screening, the mass spectral data is queried for a pre-defined list of compounds.

A further step towards compound annotation aims at verifying/ elucidating the elemental formula of the detected ions. For masses heavier than 300 Da, even 1 ppm accuracy is not sufficient to obtain only one possible elemental formula for one mass. Kind and Fiehn [75] suggested further heuristic rules for limiting the number of possible elemental formula, e.g. the restriction of element numbers based on the mass of the unknown compound.

Useful information towards determining the elemental composition of a compound present in the full scan spectra is the natural abundance of the stable isotopes of carbon. Since the natural abundance of ^{12}C is 98.9% and that of ^{13}C is 1.1%, the number of carbon atoms present in a molecule can be calculated from the relative intensity heights of the different isotopologue peaks. Characteristic isotope patterns can help to determine the presence of e.g. ^{54}Fe , ^{37}Cl or ^{81}Br . If the resolution of the instrument allows it, additionally the isotopic fine structure can be taken into account for the determination of the presence and number of ^{15}N , ^{18}O

and/or ^{34}S . A paper on the consideration of the isotopic fine structure regarding elemental composition determination has been published by Kaufmann [76].

Another possibility in gaining further evidence for substance annotation (for known compounds) is by comparing experimental tandem MS spectra with tandem MS spectra from different instruments (e.g. if no standard is available in-house) or a spectral library. In an inter-instrument, inter-laboratory study it has been shown that MS/MS spectra similarity can be high among different MS platforms [77]. Available tandem MS libraries include e.g. METLIN [78, 79] (<http://metlin.scripps.edu/>) and MassBank [80] (www.massbank.jp). Obviously, a library with entries appropriate to the sample type (e.g. fungal metabolites in case of fungal samples) should be used to obtain reasonable results. Additionally, the database size plays an important role as only compounds that have been previously measured and added to the library can be verified. Furthermore, an increasing library size increases also the confidence of identification as it demonstrates the uniqueness of its spectrum. A library search should not only yield the most likely compound identity but also a measure of confidence ("score") that it is correct [81]. Also, interpretation regarding structural similarities derived from comparison of MS/MS spectra is highly sophisticated and needs careful validation.

Other computational approaches aim at facilitating this process by predicting MS/MS fragments by *in silico* fragmentation. A commercial software tool called Mass Frontier (HighChem, Ltd., Bratislava, Slovakia, <http://www.highchem.com/>) generates fragments from structure formulas based on a comprehensive set of known reaction mechanisms and library mechanisms (fragmentation rules generated from curated literature data) that supports automated fragmentation prediction. Other freely available software tools apply different strategies. For example, MetFrag [82] (<http://msbi.ipb-halle.de/MetFrag/>) first generates a compound list based on database entries for the precursor mass, generates *in silico* fragments from these structures and then compares the *in silico* fragments with the experimental fragments. Sirius² [83, 84] (<http://bio.informatik.uni-jena.de/sirius2/>) first suggests elemental formula candidates for the precursor mass and the fragments under consideration of the isotope pattern of the precursor and then generates hypothetical fragmentation trees (including dependencies between fragment ions). Comparison of computed trees can then reveal information about (un)known compounds.

Stable isotopic labeling (SIL) can also facilitate compound annotation, but as it is of particular value in non-targeted studies it will be discussed in the following chapter.

2.2.3 Non-targeted screening approaches and to date unknown compounds

Non-targeted screening approaches show the potential to find new, to date unknown substances. However, potentially unknown compounds that cannot be identified or annotated pose the biggest challenge in modern analytical approaches. Nevertheless, the initial elucidation steps are similar to compound annotation. First, the identity of the ion species needs to be identified. The next step is the determination of the elemental formula. Again, heuristic rules [75] as well as natural isotope patterns and fine structures can help in this respect. Similar to compound annotation, comparing experimental tandem MS spectra with those of authentic standard compounds might help in elucidating the structure of unknowns. Again, *in silico* approaches can also facilitate structure elucidation.

Another challenge, especially in non-targeted approaches, is the high amount of background signals in high-resolution MS data. A particularly powerful technique in this respect consists of full *in vivo* stable isotopic labeling of whole organisms, e.g. by ^{13}C or ^{15}N [85-87]. Organisms are cultivated on growth medium, containing either the native or the isotopically labeled substrate. Prior to LC-MS(/MS) measurements, samples of both conditions (e.g. the culture supernatants) are combined. Since a signal derived from metabolism needs to be present in both the unlabeled and the labeled form, both of these need to be present in the raw mass spectral data. Sophisticated data analysis tools can be used to search for and identify these peak pairs automatically [88]. An additional benefit of the stable isotopic labeling (SIL) approach is that the number of atoms of the labeled element present in a molecule can be directly calculated from the m/z difference between the two signals in the mass spectrum. For example, given that a compound contains ten carbon atoms and is singly charged, the difference between the two most intense signals of this compound in a mass spectrum is ten times the mass difference between ^{12}C and ^{13}C ($\Delta m/z$ 1.00335 for $z=1$). This is especially advantageous in case that the relative isotopic abundances of the natural isotopes of the unlabeled compound are determined with poor accuracy and therefore cannot be used to reliably estimate the number of carbon atoms present in a substance – as is the case in Orbitrap MS [89].

The elaborate steps and the chemical knowledge necessary to achieve reliable compound annotation and elemental formula/structure determination of unknowns make it to date not feasible to automate all data analysis steps in metabolomics experiments. On the other hand due to the vast amount of data generated by modern high resolution mass spectrometry, manual inspection of the whole data is not feasible as well. Many software tools using various different approaches aim at facilitating these tasks. Nevertheless, one software tool alone is not able to accomplish all the requirements. Additionally, since most of these software tools tend to be black boxes especially for users that are not familiar with sophisticated bioinformatics and chemometrics approaches, care has to be taken

with the outcome. The results obtained need to be carefully considered and critically assessed regarding their plausibility and true informative value. It has proved useful to verify processed data by going back to the raw data (at least to a certain extent) and verify the computed results, especially since many algorithms and software tools still are under development.

Many metabolomics approaches aim at the holistic report of the conditions of living systems. Therefore, non-targeted approaches play an important role in this respect. In contrast to targeted methods however, no consensus among the metabolomics community exists yet regarding method validation of non-targeted methods. The Metabolomics Standards Initiative (<http://msi-workgroups.sourceforge.net/>) of the Metabolomics Society (<http://www.metabolomicsociety.org/>) published several articles comprising suggestions for minimum reporting standards in metabolomics experiments [69, 90-96].

2.3 Development and application of analytical strategies

The following chapter will give an overview of the analytical strategies that were developed and applied within this thesis. The studies conducted within this thesis made use of a new kind of high resolution mass spectrometer (Orbitrap MS). Full-scan data obtained by high resolution mass spectrometry give the possibility of retrospective data analysis and make novel screening approaches feasible. To date hardly any approaches exist that fully exploit this new possibility. Hence, no consensus among the scientific community regarding suggestions or requirements concerning their implementation exist yet. These facts make this work particularly innovative and therefore this thesis represents a contribution to the community in this respect.

Special screening approaches may require even further criteria than those that were mentioned on the previous pages. Within the project “Novel biological active compounds for the development of high-value nutraceuticals and natural plant protectants” it was an essential prerequisite for a substance to be considered of further interest that this substance exhibited biological activity – meaning the inhibition of the growth of the plant pathogenic fungus *Fusarium graminearum*. Therefore, within this thesis, a special workflow was developed in close collaboration with our project partners and is shown in Figure 11. This workflow included alternating steps of

- activity testing,
- culture supernatant fractionation,
- activity testing of fractions,
- LC-MS analysis of active fractions.

Differential analysis of the biological active culture filtrates (or fractions) versus the non-active culture filtrates (or fractions) was an important step, which had

to be achieved during data analysis towards the identification of the compounds of interest. This work was published in several posters and paper #1.

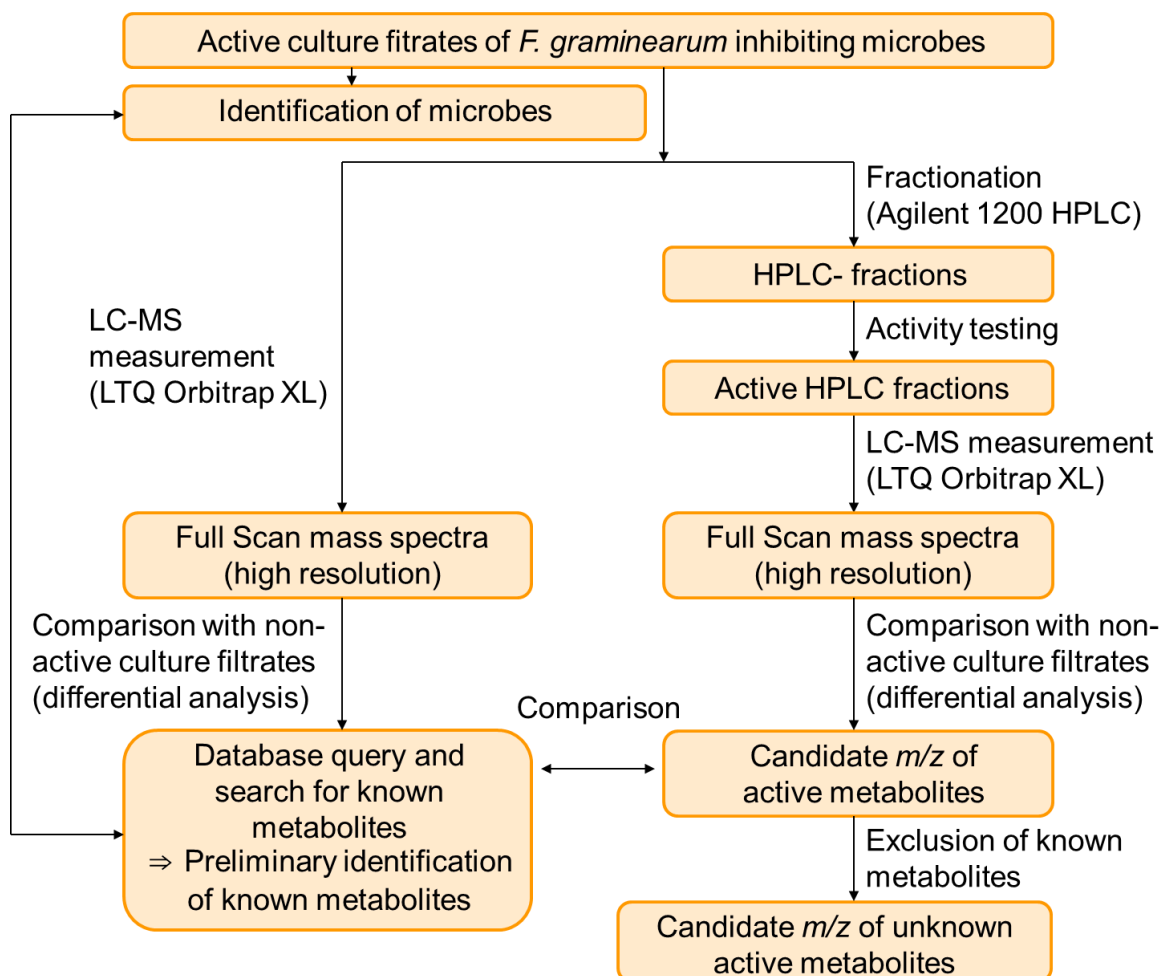


Figure 11 Workflow for the elucidation of bioactive known and/or unknown metabolites (adapted from [97]).

Another study focused on the establishment and application of a method for the quantification of 20 selected mycotoxins in food and feed samples in conjunction with a novel suspects screening for 208 fungal secondary metabolites. This work comprised the evaluation of method performance characteristics and SSE effects as well as an alternative approach for the estimation of the LOD in high-resolution mass spectrometry. The developed suspects screening approach was based on accurate mass, natural isotopic pattern of carbon and peak intensity and was successfully applied to several test materials (paper #2).

Regarding the characterization of fungal iron-containing metabolites (siderophores) a screening workflow was established that included several, specific criteria – amongst others, the natural characteristic isotopic pattern of iron, characteristic UV/VIS absorption of ferri-siderophores and characteristic mass

increments present in MS/MS spectra of hydroxamate-type siderophores. In this respect, a list of common “neutral losses” in MS/MS spectra of fungal siderophores was generated. This list was based on literature data, MS/MS spectra from the measurement of authentic standard compounds and theoretic consideration. Tandem MS spectra of annotated and to date unknown siderophores were searched for this characteristic mass increments. Many *Trichoderma* strains can be used as biocontrol agents, which made them explicitly interesting for this thesis. The developed approach was therefore applied to ten wild type *Trichoderma* strains to capture their siderophore production pattern. Results were published in paper #3.

The established method for the detection of siderophores was additionally applied to mutant strains of *T. virens*. To date it is only hypothesized which NRPS genes are involved in siderophore biosynthesis in *Trichoderma* based on gene homology to related fungi. No experimental study on a functional level has been conducted so far. The investigated strains exhibited knockouts in genes putatively involved in the NRPS synthesis of siderophores (*sidC*, *sidD*, *NPS6*). The effect of these NRPS knockouts was evaluated regarding its influence on siderophore production pattern and will be published in the near future (paper #4).

As structure elucidation of unknown compounds still is the major bottleneck in non-targeted approaches, we carried out a study that focused on the interpretation of MS/MS spectra applying stable isotopic labeling. Authentic standard compounds were measured in their native and labeled form and a software algorithm was implemented to automatically determine the elemental composition of the fragment signals. This software significantly reduces data analysis time for MS/MS spectrum interpretation and constitutes a completely new and automated approach towards structure elucidation of unknowns. The manuscript will be submitted soon to *Rapid Communications in Mass Spectrometry* (paper #5).

CONCLUSIONS AND OUTLOOK

The aims of this thesis were to develop and apply analytical methods for the investigation of biological samples such as fungi and plants in metabolomics research. This was achieved using and evaluating modern approaches such as LC-HRMS. Different aspects were covered and will be summarized in the following.

First of all, an analytical workflow was established for the elucidation of novel fungal bioactive compounds, which show growth inhibition of the plant pathogenic fungus *F. graminearum*. The workflow included alternating steps of activity testing and fractionation towards the localization of the active substance of interest. However, substance identification still is a major challenge in any metabolomics experiment. The established workflow results in a reduced candidate list comprising several mass spectral features – representing the potential bioactive compound of interest. Bioactive substances that could be elucidated are known toxic compounds. Nevertheless, the results prove that the workflow in general is applicable in the search of compounds with a specific biological activity (poster I, poster II, paper #1). Using full *in vivo* stable isotopic labeling shows a great potential for future studies to further support compound elucidation. SIL is a very powerful and promising approach as it is able to greatly facilitate the determination of the elemental composition of unknowns. Additionally, in-depth investigation of the MS/MS spectra by comparison with spectra from databases or *in silico* approaches could further help in the structure elucidation process of unknowns. Furthermore, SIL shows high potential in non-targeted screening approaches as it facilitates automated efficient extraction of metabolite-derived features which truly describe the metabolic composition of biological samples.

Second, the general applicability of LC-HRMS for the quantitative analysis of 20 selected mycotoxins was shown. Evaluation of selected method performance characteristics for regulated mycotoxins for the matrix maize has been included in the study. Regarding the lack of consensus regarding the estimation of the limit of detection (LOD) in HRMS – the common approach is not applicable due to the absence of noise – an alternative for the determination of the LOD was carried out successfully using “full-profile mode”. Resulting LODs were within European Regulation limits [98, 99] for FB₁, FB₂, DON and ZON (with few exceptions). Simultaneously, a suspects screening by retrospective data analysis for 208 fungal metabolites was included based on accurate mass, peak intensity and isotopologue ratio. According to the selected screening criteria, 13 different fungal metabolites were found in proficiency testing materials in addition to the target toxins, showing its potential for suspects screening applications (paper #2). Such screening approaches

show further potential for improvement by adding additional criteria that help to further minimize manual data analysis time and to narrow down the risk of both, false-positives and false-negatives. These criteria could include e.g. automated recognition of highly correlated EIC-peaks origination from the same metabolite (protonated molecule and adducts) or the consideration of MS/MS fragmentation patterns to further gain confidence in the annotation of substances.

The third study made use of LC-HRMS/MS for the screening of iron-containing metabolites (siderophores) investigating ten wild type *Trichoderma* strains (paper #3). The screening was based on typical properties of iron containing compounds: the characteristic isotope pattern of iron, the typical UV/VIS absorption of ferri-siderophores and characteristic MS/MS fragments of siderophore structures. In this respect, an in-house library comprising 422 microbial siderophores was established. Additionally a list of common MS/MS neutral losses of siderophores was created based on literature, MS/MS measurements and theoretical considerations. In total, 18 iron-chelators were detected: four were verified by the measurement of authentic standard compounds and four were annotated based on accurate mass. At least 10 novel hydroxamate-type siderophores were found. This study showed the high potential of LC-HRMS/MS for screening approaches applying special, selected screening criteria. Additionally, the developed screening approach was used to investigate the siderophore production of mutant strains of *T. virens* with deleted genes putatively involved in siderophore biosynthesis (paper #4, in preparation). The effect of these knockouts was investigated on the metabolites' level and revealed the involvement of the *sidC* and *NPS6* genes in NRPS biosynthesis of siderophores. These results therefore showed the high suitability of the developed approach to be successfully used in functional genomics studies. In this respect, they can be used to annotate gene functions by the comprehensive screening for gene products. Further studies could include the investigation of siderophore production of phytopathogenic fungi and of plants in order to assess the natural biological inventory of siderophores and to study possible molecular interactions involved. Another interesting application regarding further investigations include *in planta* studies with the aim to elucidate the role of fungal siderophores regarding the iron nutrition of plants and other fungi. Furthermore, other element specific screening approaches for elements that exhibit a characteristic natural isotope pattern, e.g. magnesium, could be established to monitor compound classes of interest.

Last, the capability for facilitating structure elucidation of compounds using HRMS/MS of unlabeled and ^{13}C labeled compounds was shown. MS/MS measurements were conducted on our LTQ Orbitrap XL system using both, CID and HCD fragmentation (paper #5, in preparation). Data evaluation was greatly facilitated by stable isotopic labeling that helps in the determination of the number of carbon atoms present in MS/MS fragments signals. Additionally, a software was implemented that automatically searches for corresponding fragments in the native and labeled MS/MS spectra, calculates the corresponding number of carbon atoms as well as possible elemental formulas of the detected MS/MS fragment ions. This

tool further speeds up data analysis and provides reasonable suggestions for elemental formulas in MS/MS spectra. Therefore, it shows high potential to be used in future metabolomics studies regarding the structure elucidation of unknown compounds which might play a significant biological role for organisms of interest.

REFERENCES

1. Noble D: **The music of life - Biology beyond the genome**. New York, United States: Oxford University Press Inc.; 2006.
2. Dewick PM: **Medicinal Natural Products - A Biosynthetic Approach**. Chichester, England: John Wiley & Sons Ltd.; 2002.
3. Kliebenstein DJ: **Secondary metabolites and plant/environment interactions: a view through Arabidopsis thaliana tinted glasses**. *Plant, Cell & Environment* 2004, **27**(6):675-684.
4. Karlovsky P: **Soil Biology - Secondary Metabolites in Soil Ecology**, vol. 14. Berlin Heidelberg: Springer-Verlag; 2008.
5. Keller NP, Turner G, Bennett JW: **Fungal secondary metabolism - From biochemistry to genomics**. *Nat Rev Microbiol* 2005, **3**(12):937-947.
6. Osbourn A: **Secondary metabolic gene clusters: Evolutionary toolkits for chemical innovation**. *Trends in Genetics* 2010, **26**(10):449-457.
7. Mukherjee PK, Horwitz BA, Kenerley CM: **Secondary metabolism in Trichoderma - a genomic perspective**. *Microbiology (Reading, U K)* 2012, **158**(Copyright (C) 2012 American Chemical Society (ACS). All Rights Reserved.):35-45.
8. Whitfield PD, German AJ, Noble P-JM: **Metabolomics: an emerging post-genomic tool for nutrition**. *British Journal of Nutrition* 2004, **92**(04):549-555.
9. Fiehn O: **Metabolomics – the link between genotypes and phenotypes**. *Plant Molecular Biology* 2002, **48**(1):155-171.
10. Hoffmeister D, Keller NP: **Natural products of filamentous fungi: Enzymes, genes, and their regulation**. *Nat Prod Rep* 2007, **24**(2):393-416.
11. Newman DJ, Cragg GM: **Natural products as sources of new drugs over the last 25 years**. *J Nat Prod* 2007, **70**(3):461-477.
12. Brakhage AA, Schroeckh V: **Fungal secondary metabolites - Strategies to activate silent gene clusters**. *Fungal Genet Biol* 2011, **48**(1):15-22.
13. Singhanian RR, Sukumaran RK, Patel AK, Larroche C, Pandey A: **Advancement and comparative profiles in the production technologies using solid-state and submerged fermentation for microbial cellulases**. *Enzyme and Microbial Technology* 2010, **46**(7):541-549.

14. Benítez T, Rincón AM, Limón MC, Codón AC: **Biocontrol mechanisms of *Trichoderma* strains.** *Int Microbiol* 2004, **7**(4):249-260.
15. van Egmond HP, Schothorst RC, Jonker MA: **Regulations relating to mycotoxins in food: perspectives in a global and European context.** *Anal Bioanal Chem* 2007, **389**(1):147-157.
16. Bennett JW, Klich M: **Mycotoxins.** *Clin Microbiol Rev* 2003, **16**(3):497-+.
17. Hanson JR: **The Chemistry of Fungi.** Cambridge, UK: RSC Publishing 2008; 2008.
18. Campbell CD, Vederas JC: **Mini Review: Biosynthesis of lovastatin and related metabolites formed by fungal iterative PKS enzymes.** *Biopolymers* 2010, **93**(9):755-763.
19. Fischbach MA, Walsh CT: **Assembly-line enzymology for polyketide and nonribosomal peptide antibiotics: Logic machinery, and mechanisms.** *Chem Rev* 2006, **106**(8):3468-3496.
20. Sieber SA, Marahiel MA: **Molecular mechanisms underlying nonribosomal peptide synthesis: Approaches to new antibiotics.** *Chem Rev* 2005, **105**(2):715-738.
21. Stachelhaus T, Mootz HD, Marahiel MA: **The specificity-conferring code of adenylation domains in nonribosomal peptide synthetases.** *Chemistry and Biology* 1999, **6**(8):493-505.
22. Stachelhaus T, Hüser A, Marahiel MA: **Biochemical characterization of peptidyl carrier protein (PCP), the thiolation domain of multifunctional peptide synthetases.** *Chemistry and Biology* 1996, **3**(11):913-921.
23. Belshaw PJ, Walsh CT, Stachelhaus T: **Aminoacyl-CoAs as probes of condensation domain selectivity in nonribosomal peptide synthesis.** *Science* 1999, **284**(5413):486-489.
24. Clugston SL, Sieber SA, Marahiel MA, Walsh CT: **Chirality of Peptide Bond-Forming Condensation Domains in Nonribosomal Peptide Synthetases: The C5 Domain of Tyrocidine Synthetase is a DCL Catalyst.** *Biochemistry-U* 2003, **42**(41):12095-12104.
25. Stachelhaus T, Walsh CT: **Mutational analysis of the epimerization domain in the initiation module PheATE of gramicidin S synthetase.** *Biochemistry-U* 2000, **39**(19):5775-5787.
26. Hoffmann K, Schneider-Scherzer E, Kleinkauf H, Zocher R: **Purification and characterization of eucaryotic alanine racemase acting as key enzyme in cyclosporin biosynthesis.** *J Biol Chem* 1994, **269**(17):12710-12714.
27. Schauwecker F, Pfennig F, Grammel N, Keller U: **Construction and in vitro analysis of a new bi-modular polypeptide synthetase for synthesis of N-methylated acyl peptides.** *Chemistry and Biology* 2000, **7**(4):287-297.

28. Miller DA, Walsh CT, Luo L: **C-methyltransferase and cyclization domain activity at the intraprotein PK/NRP switch point of yersiniabactin synthetase [2].** *J Am Chem Soc* 2001, **123**(34):8434-8435.
29. O'Brien DP, Kirkpatrick PN, O'Brien SW, Staroske T, Richardson TI, Evans DA, Hopkinson A, Spencer JB, Williams DH: **Expression and assay of an N-methyltransferase involved in the biosynthesis of a vancomycin group antibiotic.** *Chem Commun* 2000(1):103-104.
30. Walsh CT, Chen H, Keating TA, Hubbard BK, Losey HC, Luo L, Marshall CG, Miller DA, Patel HM: **Tailoring enzymes that modify nonribosomal peptides during and after chain elongation on NRPS assembly lines.** *Curr Opin Chem Biol* 2001, **5**(5):525-534.
31. Kessler N, Schuhmann H, Morneweg S, Linne U, Marahiel MA: **The Linear Pentadecapeptide Gramicidin Is Assembled by Four Multimodular Nonribosomal Peptide Synthetases That Comprise 16 Modules with 56 Catalytic Domains.** *J Biol Chem* 2004, **279**(9):7413-7419.
32. Hubbard BK, Walsh CT: **Vancomycin assembly: Nature's way.** *Angewandte Chemie - International Edition* 2003, **42**(7):730-765.
33. Losey HC, Peczuh MW, Chen Z, Eggert US, Dong SD, Pelczer I, Kahne D, Walsh CT: **Tandem action of glycosyltransferases in the maturation of vancomycin and teicoplanin aglycones: Novel glycopeptides.** *Biochemistry-US* 2001, **40**(15):4745-4755.
34. Stoppacher N, Zeilinger S, Omann M, Lassahn PG, Roitinger A, Krska R, Schuhmacher R: **Characterisation of the peptaibiome of the biocontrol fungus *Trichoderma atroviride* by liquid chromatography/tandem mass spectrometry.** *Rapid Commun Mass Sp* 2008, **22**(12):1889-1898.
35. Kleinkauf H, Von Dohren H: **Nonribosomal biosynthesis of peptide antibiotics.** *European Journal of Biochemistry* 1990, **192**(1):1-15.
36. Haas H: **Molecular genetics of fungal siderophore biosynthesis and uptake: the role of siderophores in iron uptake and storage.** *Appl Microbiol Biot* 2003, **62**(4):316-330.
37. Dutta S, Kundu A, Chakraborty MR, Ojha S, Chakrabarti J, Chatterjee NC: **Production and optimization of Fe (III) specific ligand, the siderophore of soil inhabiting and wood rotting fungi as deterrent to plant pathogens.** *Acta Phytopathologica et Entomologica Hungarica* 2006, **41**(3-4):237-248.
38. Lemanceau P, Expert D, Gaymard F, Bakker PAHM, Briat JF: **Role of iron in plant-microbe interactions.** *Adv Bot Res* 2009, **51**(Copyright (C) 2012 American Chemical Society (ACS). All Rights Reserved.):491-549.
39. Renshaw JC, Robson GD, Trinci APJ, Wiebe MG, Livens FR, Collison D, Taylor RJ: **Fungal siderophores: structures, functions and applications.** *Mycol Res* 2002, **106**:1123-1142.

40. Hördt W, Römheld V, Winkelmann G: **Fusarinines and dimerum acid, mono- and dihydroxamate siderophores from *Penicillium chrysogenum*, improve iron utilization by strategy I and strategy II plants.** *Biometals* 2000, **13**(1):37-46.
41. Soliman SSM, Tsao R, Raizada MN: **Chemical inhibitors suggest endophytic fungal paclitaxel is derived from both mevalonate and non-mevalonate-like pathways.** *J Nat Prod* 2011, **74**(12):2497-2504.
42. Kuzuyama T, Seto H: **Diversity of the biosynthesis of the isoprene units.** *Nat Prod Rep* 2003, **20**(2):171-183.
43. Dewick PM: **The biosynthesis of C5-C25 terpenoid compounds.** *Nat Prod Rep* 2002, **19**(2):181-222.
44. Tholl D: **Terpene synthases and the regulation, diversity and biological roles of terpene metabolism.** *Current Opinion in Plant Biology* 2006, **9**(3):297-304.
45. Degenhardt J, Köllner TG, Gershenzon J: **Monoterpene and sesquiterpene synthases and the origin of terpene skeletal diversity in plants.** *Phytochemistry* 2009, **70**(15-16):1621-1637.
46. Wise ML, Savage TJ, Katahira E, Croteau R: **Monoterpene synthases from common sage (*Salvia officinalis*). cDna isolation, characterization, and functional expression of (+)-sabinene synthase, 1,8-cineole synthase, and (+)-bornyl diphosphate synthase.** *J Biol Chem* 1998, **273**(24):14891-14899.
47. Mol HGJ, Plaza-Bolanos P, Zomer P, de Rijk TC, Stolker AAM, Mulder PPJ: **Toward a Generic Extraction Method for Simultaneous Determination of Pesticides, Mycotoxins, Plant Toxins, and Veterinary Drugs in Feed and Food Matrixes.** *Anal Chem* 2008, **80**(24):9450-9459.
48. Vishwanath V, Sulyok M, Labuda R, Bicker W, Krska R: **Simultaneous determination of 186 fungal and bacterial metabolites in indoor matrices by liquid chromatography/tandem mass spectrometry.** *Anal Bioanal Chem* 2009, **395**(5):1355-1372.
49. Weckwerth W: **Metabolomics in Systems Biology.** In., vol. 54; 2003: 669-689.
50. Robertson M: **Biology in the 1980s, plus or minus a decade.** *Nature* 1980, **285**(5764):358-359.
51. Goodacre R: **Metabolomics - The way forward.** *Metabolomics* 2005, **1**(1):1-2.
52. Lottspeich F, Engels JW: **Bioanalytik**, 2. Auflage edn. Munich, Germany: Elsevier GmbH - Spektrum akademischer Verlag; 2006.

53. De Hoffmann E, Stroobant V: **Mass Spectrometry - Principles and Applications**, Third Edition edn. Chichester, England: John Wiley & Sons Ltd.; 2007.
54. Halket JM, Waterman D, Przyborowska AM, Patel RKP, Fraser PD, Bramley PM: **Chemical derivatization and mass spectral libraries in metabolic profiling by GC/MS and LC/MS/MS**. *J Exp Bot* 2005, **56**(410):219-243.
55. Wilm M: **Principles of electrospray ionization**. *Molecular and Cellular Proteomics* 2011, **10**(7).
56. Iribarne JV, Thomson BA: **On the evaporation of small ions from charged droplets**. *The Journal of Chemical Physics* 1976, **64**(6):2287-2294.
57. Thomson BA, Iribarne JV: **Field induced ion evaporation from liquid surfaces at atmospheric pressure**. *The Journal of Chemical Physics* 1979, **71**(11):4451-4463.
58. Dole M, Mack LL, Hines RL, Chemistry DO, Mobley RC, Ferguson LD, Alice MB: **Molecular beams of macroions**. *The Journal of Chemical Physics* 1968, **49**(5):2240-2249.
59. Koppelaar DW, Barinaga CJ, Denton MB, Sperline RP, Hieftje GM, Schilling GD, Andrade FJ, Barnes Iv JH: **MS detectors**. *Anal Chem* 2005, **77**(21):418 A-427 A.
60. **LITQ Orbitrap Operations** In: *European Training Institute - Training Course Manual*. Thermo Scientific.
61. Hernández F, Sancho JV, Ibáñez M, Abad E, Portolés T, Mattioli L: **Current use of high-resolution mass spectrometry in the environmental sciences**. *Anal Bioanal Chem* 2012, **403**(5):1251-1264.
62. Makarov A: **Electrostatic Axially Harmonic Orbital Trapping: A High-Performance Technique of Mass Analysis**. *Anal Chem* 2000, **72**(6):1156-1162.
63. Denisov E, Damoc E, Lange O, Makarov A: **Orbitrap mass spectrometry with resolving powers above 1,000,000**. *Int J Mass Spectrom* 2012.
64. Perry RH, Cooks RG, Noll RJ: **Orbitrap mass spectrometry: Instrumentation, ion motion and applications**. *Mass Spectrom Rev* 2008, **27**(6):661-699.
65. Hu Q, Noll RJ, Li H, Makarov A, Hardman M, Cooks RG: **The Orbitrap: A new mass spectrometer**. *J Mass Spectrom* 2005, **40**(4):430-443.
66. Krauss M, Singer H, Hollender J: **LC-high resolution MS in environmental analysis: from target screening to the identification of unknowns**. *Anal Bioanal Chem* 2010, **397**(3):943-951.

67. Keller BO, Sui J, Young AB, Whittall RM: **Interferences and contaminants encountered in modern mass spectrometry**. *Analytica Chimica Acta* 2008, **627**(1):71-81.
68. Weber RJM, Li E, Bruty J, He S, Viant MR: **MaConDa: a publicly accessible Mass spectrometry Contaminants Database**. *Bioinformatics* 2012.
69. Sumner LW, Amberg A, Barrett D, Beale MH, Beger R, Daykin CA, Fan TWM, Fiehn O, Goodacre R, Griffin JL *et al*: **Proposed minimum reporting standards for chemical analysis: Chemical Analysis Working Group (CAWG) Metabolomics Standards Initiative (MSI)**. *Metabolomics* 2007, **3**(3):211-221.
70. Dunn W, Erban A, Weber R, Creek D, Brown M, Breitling R, Hankemeier T, Goodacre R, Neumann S, Kopka J *et al*: **Mass appeal: metabolite identification in mass spectrometry-focused untargeted metabolomics**. *Metabolomics* 2012:1-23.
71. Neumann S, Böcker S: **Computational mass spectrometry for metabolomics: Identification of metabolites and small molecules**. *Anal Bioanal Chem* 2010, **398**(7):2779-2788.
72. **ISO/IEC 17025:2005, General requirements for the competence of testing and calibration laboratories**.
73. Thompson M, Ellison SLR, Wood R: **Harmonized guidelines for single-laboratory validation of methods of analysis (IUPAC Technical Report)**. *Pure Appl Chem* 2002, **74**(5):835-855.
74. Emons H, Linsinger TPJ, Gawlik BM: **Reference materials: Terminology and use. Can't one see the forest for the trees?** *TrAC - Trends in Analytical Chemistry* 2004, **23**(6):442-449.
75. Kind T, Fiehn O: **Seven Golden Rules for heuristic filtering of molecular formulas obtained by accurate mass spectrometry**. *Bmc Bioinformatics* 2007, **8**:-
76. Kaufmann A: **Strategy for the elucidation of elemental compositions of trace analytes based on a mass resolution of 100 000 full width at half maximum**. *Rapid Commun Mass Sp* 2010, **24**(14):2035-2045.
77. Oberacher H, Pavlic M, Libiseller K, Schubert B, Sulyok M, Schuhmacher R, Csaszar E, Köfeler HC: **On the inter-instrument and inter-laboratory transferability of a tandem mass spectral reference library: 1. Results of an austrian multicenter study**. *J Mass Spectrom* 2009, **44**(4):485-493.
78. Smith CA, O'Maille G, Want EJ, Qin C, Trauger SA, Brandon TR, Custodio DE, Abagyan R, Siuzdak G: **METLIN: A metabolite mass spectral database**. *Ther Drug Monit* 2005, **27**(6):747-751.
79. Sana TR, Roark JC, Li X, Waddell K, Fischer SM: **Molecular formula and METLIN Personal Metabolite Database matching applied to the**

- identification of compounds generated by LC/TOF-MS.** *Journal of biomolecular techniques : JBT* 2008, **19**(4):258-266.
80. Horai H, Arita M, Kanaya S, Nihei Y, Ikeda T, Suwa K, Ojima Y, Tanaka K, Tanaka S, Aoshima K *et al*: **MassBank: A public repository for sharing mass spectral data for life sciences.** *J Mass Spectrom* 2010, **45**(7):703-714.
81. Stein S: **Mass spectral reference libraries: An ever-expanding resource for chemical identification.** *Anal Chem* 2012, **84**(17):7274-7282.
82. Wolf S, Schmidt S, Müller-Hannemann M, Neumann S: **In silico fragmentation for computer assisted identification of metabolite mass spectra.** *Bmc Bioinformatics* 2010, **11**(1):1-12.
83. Böcker S, Letzel MC, Lipták Z, Pervukhin A: **SIRIUS: decomposing isotope patterns for metabolite identification.** *Bioinformatics* 2009, **25**(2):218-224.
84. Rasche F, Svatoš A, Maddula RK, Böttcher C, Böcker S: **Computing Fragmentation Trees from Tandem Mass Spectrometry Data.** *Anal Chem* 2010, **83**(4):1243-1251.
85. Giavalisco P, Hummel J, Lisec J, Inostroza AC, Catchpole G, Willmitzer L: **High-Resolution Direct Infusion-Based Mass Spectrometry in Combination with Whole ¹³C Metabolome Isotope Labeling Allows Unambiguous Assignment of Chemical Sum Formulas.** *Anal Chem* 2008, **80**(24):9417-9425.
86. Giavalisco P, Köhl K, Hummel J, Seiwert B, Willmitzer L: **¹³C Isotope-Labeled Metabolomes Allowing for Improved Compound Annotation and Relative Quantification in Liquid Chromatography-Mass Spectrometry-based Metabolomic Research.** *Anal Chem* 2009, **81**(15):6546-6551.
87. Giavalisco P, Li Y, Matthes A, Eckhardt A, Hubberten H-M, Hesse H, Segu S, Hummel J, Köhl K, Willmitzer L: **Elemental formula annotation of polar and lipophilic metabolites using ¹³C, ¹⁵N and ³⁴S isotope labelling, in combination with high-resolution mass spectrometry.** *The Plant Journal* 2011, **68**(2):364-376.
88. Bueschl C, Kluger B, Berthiller F, Lirk G, Winkler S, Krska R, Schuhmacher R: **MetExtract: A new software tool for the automated comprehensive extraction of metabolite-derived lc/ms signals in metabolomics research.** *Bioinformatics* 2012, **28**(5):736-738.
89. Xu Y, Heilier JF, Madalinski G, Genin E, Ezan E, Tabet JC, Junot C: **Evaluation of Accurate Mass and Relative Isotopic Abundance Measurements in the LTQ-Orbitrap Mass Spectrometer for Further Metabolomics Database Building.** *Anal Chem* 2010, **82**(13):5490-5501.

90. Fiehn O, Robertson D, Griffin J, van der Werf M, Nikolau B, Morrison N, Sumner LW, Goodacre R, Hardy NW, Taylor C *et al*: **The metabolomics standards initiative (MSI)**. *Metabolomics* 2007, **3**(3):175-178.
91. Fiehn O, Wohlgemuth G, Scholz M, Kind T, Lee DY, Lu Y, Moon S, Nikolau B: **Quality control for plant metabolomics: Reporting MSI-compliant studies**. *Plant J* 2008, **53**(4):691-704.
92. Morrison N, Bearden D, Bundy JG, Collette T, Currie F, Davey MP, Haigh NS, Hancock D, Jones OAH, Rochfort S *et al*: **Standard reporting requirements for biological samples in metabolomics experiments: Environmental context**. *Metabolomics* 2007, **3**(3):203-210.
93. Goodacre R, Broadhurst D, Smilde AK, Kristal BS, Baker JD, Beger R, Bessant C, Connor S, Capuani G, Craig A *et al*: **Proposed minimum reporting standards for data analysis in metabolomics**. *Metabolomics* 2007, **3**(3):231-241.
94. Hardy NW, Taylor CF: **A roadmap for the establishment of standard data exchange structures for metabolomics**. *Metabolomics* 2007, **3**(3):243-248.
95. van der Werf MJ, Takors R, Smedsgaard J, Nielsen J, Ferenci T, Portais JC, Wittmann C, Hooks M, Tomassini A, Oldiges M *et al*: **Standard reporting requirements for biological samples in metabolomics experiments: Microbial and in vitro biology experiments**. *Metabolomics* 2007, **3**(3):189-194.
96. Fiehn O, Sumner LW, Rhee SY, Ward J, Dickerson J, Lange BM, Lane G, Roessner U, Last R, Nikolau B: **Minimum reporting standards for plant biology context information in metabolomic studies**. *Metabolomics* 2007, **3**(3):195-201.
97. Lehner SM, Parich A, Koutnik A, Krska R, Lemmens M, Schuhmacher R: **Suche nach neuen natürlichen Substanzen gegen *Fusarium graminearum* (Finding novel natural compounds against *Fusarium graminearum*)**. In: *Mold-Meeting 2010 der ALVA-Fachgruppe Mikrobiologie & Molekularbiologie "Ernährungsrisiko Mykotoxine - Vermeidungsstrategien entlang der Lebensmittelkette": 2010; Linz, Austria*. Arbeitsgemeinschaft für Lebensmittel-, Veterinär- und Agrarwesen (ALVA).
98. European Commission: **Commission regulation (EC) No. 1881/2006 setting maximum levels for certain contaminants in foodstuffs** In: *Official Journal of the European Union*. vol. L364/5; 2006: 5-24.
99. European Commission: **Commission regulation (EC) No. 1126/2007 of 28 September 2007 amending Regulation (EC) No 1881/2006 setting maximum levels for certain contaminants in foodstuffs as regards *Fusarium* toxins in maize and maize products**. In: *Official Journal of the European Union*. vol. L255/14; 2007: 14-17.

ORIGINAL WORKS

Poster I

S.M. Lehner, A. Parich, B. Antlinger, S. Frühauf, A. Koutnik, M. Neureiter, R. Krska, M. Lemmens, R. Schuhmacher. Identification strategy of fungal and bacterial secondary metabolites using accurate mass measurements. *International Metabolomics Austria*. September 2-3, 2012. Vienna, Austria.

Poster II

S.M. Lehner, A. Parich, R. Schuhmacher, B. Antlinger, S. Frühauf, M. Neureiter, A. Koutnik, R. Krska, M. Lemmens. A bioassay guided approach to identify metabolites in culture filtrates of microorganisms that exhibit activity against *Fusarium graminearum*. *Euroanalysis 2009*. September 6-10, 2009. Innsbruck, Austria.

Paper #1

S.M. Lehner, A. Parich, A. Koutnik, R. Krska, M. Lemmens, R. Schuhmacher. Auf der Suche nach aktiven Metaboliten natürlicher Antagonisten gegen *Fusarium graminearum*. *ALVA Mitteilungen* 8:116-120, 2010. ISSN 1811-7317.

Paper #2 (SCI publication)

S.M. Lehner, N.K.N Neumann, M. Sulyok, R. Krska, M. Lemmens, R. Schuhmacher. Evaluation of LC-high-resolution-FT-Orbitrap MS for the quantification of selected mycotoxins and the simultaneous screening of fungal metabolites in food. *Food Additives and Contaminants: Part A* 28:1457-1468, 2011.

Paper #3 (SCI publication)

S.M. Lehner, N.K.N. Neumann, L. Atanasova, R. Krska, M. Lemmens, I.S. Druzhinina, R. Schuhmacher. Isotope-assisted screening for iron-containing metabolites reveals high diversity of known and unknown siderophores produced by *Trichoderma* spp. *Applied and Environmental Microbiology*, published online ahead of print 12 October 2012, doi:10.1128/AEM.02339-12.

Paper #4, in preparation for submission to FEMS Microbiology Letters

J. Hurley, P.K. Mukherjee, **S.M. Lehner**, R. Schuhmacher, I.S. Druzhinina, R.D. Stipanovic, G. Vittone, and C.M. Kenerley. The siderophores and siderophore biosynthesis genes of *Trichoderma virens*

Determination of fungal bioactive compounds using LC-HRMS

Paper #5, in preparation for submission to *Rapid Communications in Mass Spectrometry*

S.M. Lehner*, N.K.N. Neumann*, K. Sedelmaier, M. Lemmens, R. Krska, R. Schuhmacher. Towards structure elucidation of unknown substances: liquid chromatography - tandem mass spectrometry of stable isotopic labelled compounds assists elemental composition determination

* shared first authorship

A Bioassay Guided Approach to Identify Metabolites in Culture Filtrates of Microorganisms that Exhibit Activity against *Fusarium graminearum*



S.M. Lehner, A. Parich, R. Schuhmacher, B. Antlinger, S. Frühauf, M. Neureiter, A. Koutnik, R. Krska, M. Lemmens

University of Natural Resources and Applied Life Sciences, Vienna, Department for Agrobiotechnology (IFA-Tulln), Konrad Lorenz Str. 20, A-3430 Tulln, Austria, sylvia.lehner@boku.ac.at



University of Natural Resources and Applied Life Sciences, Vienna Department for Agrobiotechnology, IFA-Tulln

Introduction

Fusarium graminearum (teleomorph *Giberella zeae*) is a plant pathogen that can cause Fusarium head blight disease (FHB) in wheat. This disease leads to mycotoxin contamination; the most prevalent toxins include trichothecenes and zearalenone, which are harmful for both humans and animals. Therefore, FHB causes enormous economic losses each year. FHB cannot be controlled easily by the application of conventional chemical fungicides; they are able to reduce the affection of *F. graminearum*, but the mycotoxin contamination cannot be diminished reliably in this way. Therefore, it is of special interest to discover natural compounds with specific effects to protect wheat plants against this pathogen. A major goal of our project is to identify microorganisms and their bioactive natural metabolites which exhibit activity against FHB in wheat.



Figure 2 Orbitrap mass analyzer

Figure 3 LTQ Orbitrap XL

Overview of the Analytical Workflow

As illustrated in figure 1, microorganisms that were isolated from natural habitats were cultivated and tested for their growth-inhibiting activity against *F. graminearum* (figure 4). Active microbial culture filtrates were analysed in a bioassay guided approach using SPE (figure 5), obtaining one polar fraction (washing fraction) and one apolar fraction (elute fraction), which were tested for their *F. graminearum*-inhibiting activity. Active fractions were further separated, using either HILIC (washing fraction) or RP (elute fraction) HPLC in respect to confine fractions that exhibit activity (figure 6). After another activity testing step (figure 7), the active fractions obtained were analysed via LC-MS/MS using an LTQ OrbiTrap XL (figure 2 and 3). The full scan raw data (figure 8) were interpreted using XCMS with the method CentWave [1], peak annotation was done using the XCMS package CAMERA [2]. Additional LC-MS/MS experiments were done considering the candidate m/z values obtained by XCMS analysis (figure 9). Subsequently, the Seven Golden Rules Software [3] was used to receive candidate structures for the elemental composition corresponding to the neutralised accurate masses of interest (figure 10). First results of the identification experiments will be presented.

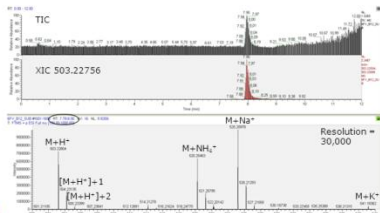


Figure 8 TIC, EIC of m/z 503.22756 ± 5 ppm and spectrum at 7.95 min (percentage refer to the monoisotopic M+H⁺ ion)

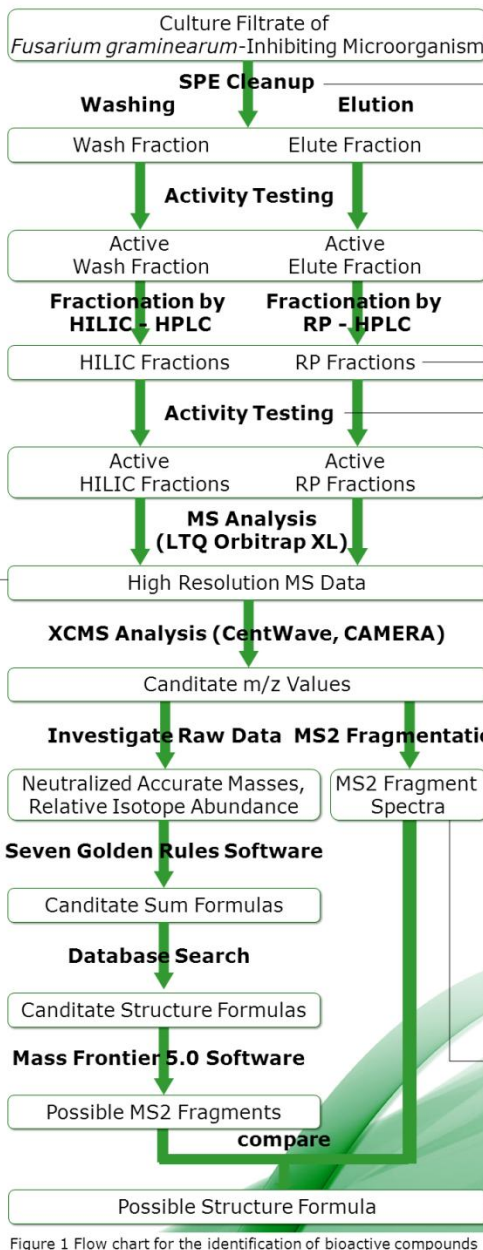


Figure 1 Flow chart for the identification of bioactive compounds



Figure 4 LTQ Culture Broths that show antagonistic activity against *F. graminearum*



Figure 5 Culture Filtrates (bottom left) and SPE Cleanup Station (right)

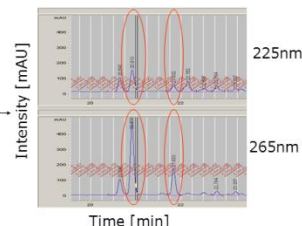


Figure 6 HPLC-Chromatogram (DAD); (active fractions are encircled red)

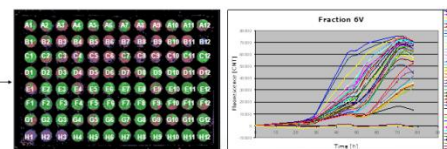


Figure 7 96-well plate bioassay and corresponding fluorescence curves of fraction 6V

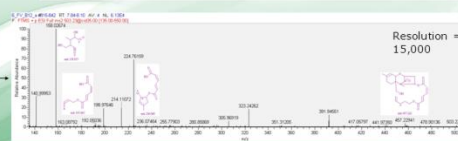


Figure 9 MS2 Spectrum of m/z 503.23 with adduct ions and possible MS2 fragments of verrucarin A

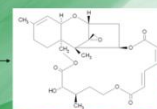


Figure 10 Structure Formula of verrucarin A

Results and Outlook

The proposed flow chart of figure 1 was used for analysing culture broths of *Myrothecium verrucaria*, identifying verrucarin A (figures 7-10) and roridin A, and *Penicillium griseofulvum*, identifying roquefortine C. Additionally standards of these compounds were measured on the LTQ Orbitrap XL, to verify the findings. The workflow shall be used to further analyse culture broths of microorganisms that exhibit biological activity against *Fusarium graminearum* with the goal to identify active compounds produced by these microorganisms.

References

- [1] Tautenhahn, R., Böttcher, C., Neumann, S., Highly sensitive feature detection for high resolution LC/MS, 2008, BMC Bioinformatics 9:504
- [2] Tautenhahn, R., Böttcher, C., Neumann, S., Annotation of LC/ESI MS Mass Signals, BIRD 2007, Proc. of BIRD 2007 1st International Conference on Bioinformatics Research and Development, 2007.
- [3] Kind, T., Fiehn, O., Seven Golden Rules for heuristic filtering of molecular formulas obtained by accurate mass spectrometry, 2007, BMC Bioinformatics 8:105



Correspondence should be addressed to: Sylvia M. Lehner sylvia.lehner@boku.ac.at



Acknowledgements

This project is funded by the Federal Country Lower Austria and co-financed by the European regional development fund (ERDF) of the European Union.



Identification Strategy of Fungal and Bacterial Secondary Metabolites Using Accurate Mass Measurements



Sylvia M. Lehner¹, A. Parich¹, B. Antlinger², S. Frühauf², A. Koutnik³, M. Neureiter², R. Krska¹, M. Lemmens³, R. Schuhmacher¹

University of Natural Resources and Life Sciences, Vienna, Department for Agrobiotechnology, IFA-Tulln,
¹ Center for Analytical Chemistry,
² Institute for Environmental Biotechnology
³ Institute for Biotechnology in Plant Production, Konrad-Lorenz-Str. 20, A-3430 Tulln, Austria, Sylvia.Lehner@boku.ac.at



University of Natural Resources and Life Sciences, Vienna
 Department for Agrobiotechnology, IFA-Tulln

1. Introduction and Aim of the Study

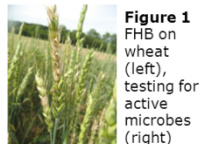
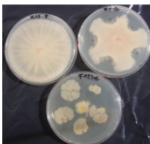


Figure 1 FHB on wheat (left), testing for active microbes (right)



Fusarium Head Blight (FHB; caused by *Fusarium graminearum*) is a severe disease of wheat, causing enormous economic losses each year, due to reduced grain yield and mycotoxin contamination.

Aim of this work is to find active metabolites which are produced by natural antagonistic microbes that can help reducing this disease. Microorganisms are isolated from their natural habitats and tested for their *Fusarium* growth-inhibiting potential. Active culture filtrates are subsequently analysed via LC-MS on an LTQ Orbitrap XL and data is screened for metabolites causing activity.



Figure 2 Culture broths of active microbes (left), LTQ Orbitrap XL (right)

2. Experimental Setup

Penicillium brevicompactum serves as model organism in this study. It was isolated from forest soil (50 m depth) and showed **no activity when grown with 12 h light-darkness-cycle and highest activity when grown with 24 h UV light**. The workflow is shown in figure 3.

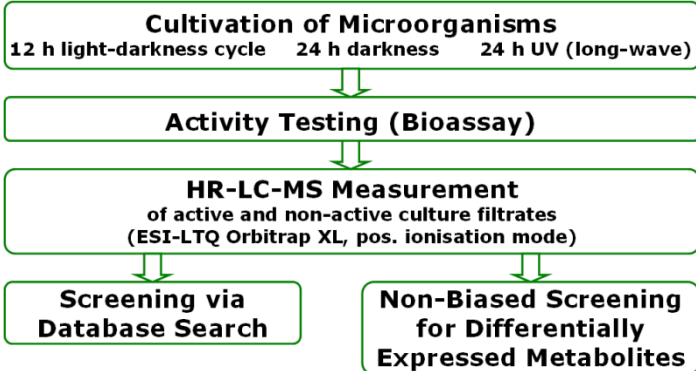


Figure 3 Schematic overview of the identification strategy

4. Screening for Differentially Expressed Metabolites

Full scan data (figure 6, five technical replicates each) was analysed with XCMS [1] for finding **features** (bounded, two-dimensional (m/z and retention time) LC-MS signals) and elucidating **differential expression**. Peak annotation was done manually with the aid of CAMERA [2] (**at least one adduct** had to be found to confirm the protonated molecule). For protonated molecules with **intensities > 10⁶ counts** (for achieving accurate isotope ratio measurements), elemental formulas were searched for with the aid of Seven Golden Rules software [3]. Five of the eleven protonated molecules, that fulfilled all criteria, support findings from the screening for known metabolites, suggesting the appropriate elemental formula to those of the database search (table 1).

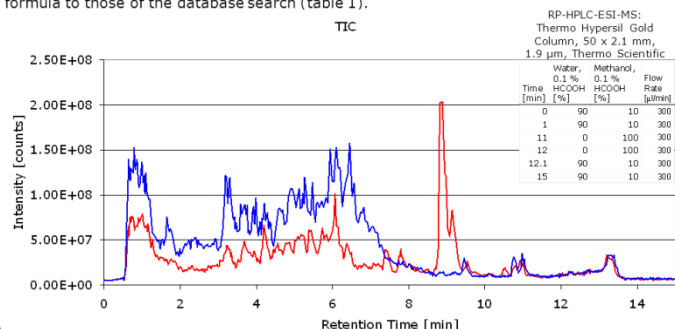


Figure 6 TIC of the LCMS measurements of *P. brevicompactum* culture filtrates; red: growth with 24h UV light (antifungal-activity), blue: growth with 12h light-darkness-cycle (no antifungal activity)

5. Conclusions

The presented strategy aims to identify both, known and unknown metabolites present in culture broths of microorganisms that inhibit the growth of *F. graminearum*. For the **detection of known metabolites**, a database search with subsequent peak detection in the HR-LCMS data was applied. For the **elucidation of unknowns**, data analysis including feature finding, elucidation of differential expression, peak annotation and proposition for elemental formulas were achieved. Some candidates could be found with both the database screening and the screening for differential expression, confirming the ability of both approaches. For structure elucidation of remaining substances, tandem MS experiments will be carried out in near future.

3. Screening via Database Search

Antibase (Wiley-VCH, Weinheim; database containing 33,557 natural compounds from microorganisms and higher fungi) served for searching known metabolites of *P. brevicompactum*. The identification strategy is shown in figure 4. Verification of putatively identified metabolites (figure 5, table 1) via MS/MS experiments and authentic standards is in progress.

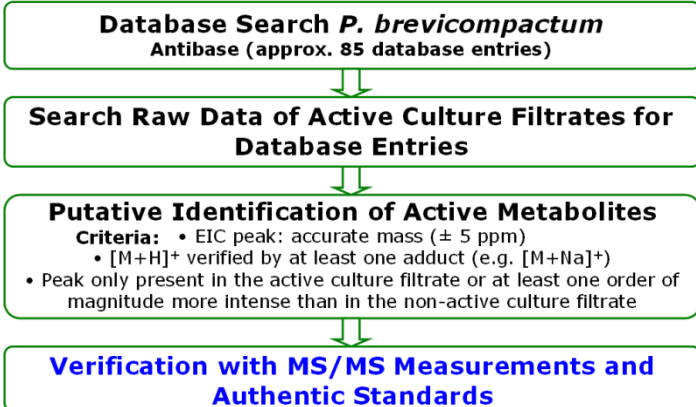


Figure 4 Workflow for the identification of known metabolites

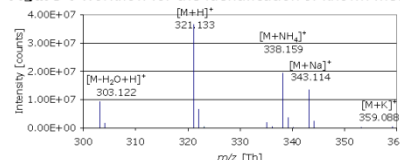


Figure 5 Spectrum of putatively identified mycophenolic acid, found through both approaches (exact mass of [M+H]⁺ of mycophenolic acid: 321.133)

Table 1 Results of both approaches, the screening via database search and the screening for differentially expressed metabolites.

Experimental Data		Hits from Screening via Database Search	Hits from Screening for Differentially Expressed Metabolites
m/z of [M+H] ⁺ [Th]	Retention Time [min]	Putatively Identified Secondary Metabolites	Possible Elemental Formula
227.055	3.9	2,4-Dihydroxy-6-(1-hydroxyacetyl)lbenzoic acid	-
582.291	7.1	-	C ₂₈ H ₃₀ N ₂ O ₉
566.296	7.4	-	C ₂₈ H ₃₀ N ₂ O ₈
596.308	7.7	Brevigellin	-
256.133	7.8	N-Benzoyl-L-phenylalaninol	C ₁₈ H ₁₈ N ₂ O ₂
337.128	7.9	Mycophenolic Acid Diol Lactone	-
319.118	8.0	Mycochromenic Acid	-
270.112	8.1	N-Benzoylphenylalanin	-
467.205	8.3	-	C ₂₇ H ₃₀ O ₇
368.197	8.4	Brevinamide E	-
437.232	8.9	(+)-Brevione D	C ₂₇ H ₃₂ O ₈
321.133	8.9	Mycophenolic Acid	C ₁₇ H ₁₆ O ₆
663.240	8.9	-	C ₂₈ H ₃₀ N ₂ O ₁₀
443.242	9.2	-	C ₂₈ H ₃₄ O ₆
349.165	9.5	Mycophenolic Acid Ethyl Ether	-
354.218	9.6	Brevicomparine C	-
441.262	9.6	-	C ₂₇ H ₃₀ O ₈
421.237	10.2	(+)-Brevione C	-
361.237	10.5	Macrophonin A	-
423.253	10.6	(+)-Brevione A	C ₂₇ H ₃₄ O ₈
425.269	10.8	(+)-Brevione B	C ₂₇ H ₃₄ O ₈
389.196	10.8	Desacetylpebratride	-

6. References

[1] C.A. Smith, E.J. Want, G. O'Maille, R. Abagyan, G. Siuzdak, Anal. Chem.; **78**, 779-787 (2006).
 [2] R. Tautenhahn, C. Böttcher, S. Neumann, Proc. of BIRD 2007, 1st International Conference on Bioinformatics Research and Development, 2007.
 [3] T. Kind, O. Fiehn, BMC Bioinformatics; **8**:105 (2007).



Correspondence should be addressed to:
 Sylvia.Lehner@boku.ac.at

Acknowledgements

This project is funded by the Federal Country Lower Austria and co-financed by the European Regional Development Fund (ERDF) of the European Union.



Auf der Suche nach neuen natürlichen Substanzen gegen *Fusarium graminearum*

Finding novel natural compounds against Fusarium graminearum

S. M. Lehner, A. Parich, A. Koutnik, R. Krska, M. Lemmens, R. Schuhmacher

Summary

Fusarium head blight disease (FHB) is a severe fungal infection on wheat. It can be caused by *Fusarium graminearum* (teleomorph *Gibberella zeae*), resulting in mycotoxin contamination and grain yield reduction. Mycotoxin contamination cannot be reliably reduced by the application of chemical fungicides. Therefore, it is of special interest to discover novel natural compounds with a specific effect to protect wheat plants against pathogen infection and mycotoxin contamination.

Microorganisms were isolated from their natural habitats, cultivated and tested for their biological activity (growth inhibition) against *F. graminearum*. Following a bioassay guided approach (using HPLC) and LC-HR-MS analysis, the study aims at the identification and characterization of active compounds against *F. graminearum* which might be used for the development of novel plant protection agents in the future.

Keywords: *Fusarium graminearum*, Fusarium Head Blight, biological activity, Orbitrap

Zusammenfassung

Ährenfusariose ("Fusarium Head Blight", FHB) ist eine Pflanzenkrankheit auf Getreide, v.a. Weizen, welche von *Fusarium graminearum* (teleomorph *Gibberella zeae*) verursacht wird und zur Kontamination des Getreides mit Mykotoxinen und einem reduziertem Ernteertrag führt. Die Belastung mit Mykotoxinen kann nicht verlässlich durch den Einsatz kommerzieller Pestizide reduziert werden. Daher ist es von Interesse neue, natürliche Substanzen zu entdecken, die die Weizenpflanze vor Pathogenbefall und damit einhergehender Mykotoxinbelastung schützen.

Dazu wurden Mikroorganismen von ihren natürlichen Habitaten isoliert, kultiviert und auf Aktivität (Wachstumshemmung) gegen *F. graminearum* getestet. Das Ziel des Projektes ist es, anhand eines Bioassay-geleiteten Ansatzes (mittels HPLC) und LC-HR-MS Analyse, aktive Substanzen mit Wirksamkeit gegen *Fusarium graminearum*

zu identifizieren und zu charakterisieren, welche in Zukunft als Pflanzenschutzmittel eingesetzt werden können.

Schlüsselwörter: *Fusarium graminearum*, Ährenfusariose, biologische Aktivität, Orbitrap

Experimentielles

Im Zuge des Projektes wurden Mikroorganismen aus unterschiedlichen Lebensräumen (z.B. Weizenpflanzenteile, Boden...) isoliert und deren Kulturüberstände auf die biologische Aktivität gegen *Fusarium graminearum* getestet und bei Aktivität die Mikroorganismus Art bestimmt. Dafür wurde ein Bioassay entwickelt, der zur Austestung der biologischen Aktivität aller Proben herangezogen wurde. Hierbei kommt ein *Fusarium graminearum*-Stamm zur Anwendung der konstitutiv GFP (green fluorescent protein) bildet, welches bei einer Anregungswellenlänge von 488 nm und einer Emissionswellenlänge von 526 nm mittels Fluoreszenzmessung (Typhoon Trio, GE Healthcare Life Sciences) bestimmt werden kann. Die Mikroorganismen wurden bei 25°C für 9 Tage und Schütteln (120 rpm) kultiviert. Die Lichtzufuhr wurde variiert: 24 Stunden Dunkelheit, natürlicher Tag/Nacht-Zyklus (ca. 14 Stunden Licht zum Kultivierungszeitraum) oder 24 Stunden Bestrahlung mit langwelligem UV (366 nm). Aktive, sterilfiltrierte Kulturfiltrate wurden entweder direkt mittels LC-MS analysiert oder zuvor mittels RP (reversed phase)-HPLC fraktioniert und nochmals auf Aktivität untersucht.

Fraktionierung mittels HPLC

Aufkonzentrierte (1 ml abgedampft (unter Stickstoffzufuhr bei 40°C), aufgenommen in 300 µl Methanol/Wasser (2/8)) Kulturfiltrate wurden mittels HPLC-UV-System inklusive Fraktionskollektor (Agilent 1200 Series) über eine RP-HPLC Säule (Hypersil Gold 50 x 2,1 mm, 1,9 µm; Gradient mit Wasser (A) und Methanol (B); Start mit 10 % B, linearer Gradient 40 Minuten auf 100 % B, halten bis Minute 42, Rückspülen auf 10 % B bis Minute 43 und halten bis Minute 60; 0,3 ml/min; 20 µl Injektionsvolumen) fraktioniert (zeitbasierende Fraktionierung, 180 Fraktionen zu je 0,25 Minuten). Pro Probe wurden 5 Injektionen in zwei 96-well Platten sowohl für die Aktivitätsbestimmung als auch für die Analyse mittels LC-MS gesammelt.

Messung mittels LC-MS

Sowohl die aktiven, sterilfiltrierten, unfraktionierten Kulturfiltrate als auch die aktiven RP-HPLC-Fractionen (gelöst mit 300 µl Methanol/Wasser (2/8) je Kavität, geschüttelt bei 60 U/min für 2 Stunden) wurden auf einem ESI (Electrospray)-LTQ Orbitrap XL-System (Thermo Electron Corporation) gekoppelt an eine Accela HPLC (Thermo Electron Corporation) analysiert (Hypersil Gold HPLC Säule, 50 x 2,1 mm, 1,9 µm; Gradient mit Wasser (A) und Methanol (B), jeweils 0,1 % Ameisensäure; Start mit 10 % B, halten bis Minute 1, linearer Gradient bis Minute 11 auf 100 % B, halten bis Minute 12, Rückspülen auf 10 % B bis Minute 12,1 und halten bis Minute 15; 0,3 ml/min; 5 µl Probenschleife). MS-Parameter: positiver Modus, Sheath Gas 40 arbitrary units (arb), Aux Gas 5 arb, Sweep Gas 0 arb, Kapillartemperatur 300°C, Quellspannung 4 kV, Tube Lens 95 V, Full Scan, m/z 200-2000, max. Füllzeit 500 ms, AGC Zielwert $5 \cdot 10^5$.

Dabei wurden zwei unterschiedliche Strategien verfolgt. Zum einen wurde, um bereits bekannte Metaboliten aufzufinden, eine Datenbankabfrage (Laatsch, 2007) nach Mikroorganismen durchgeführt. Anschließend wurde nach den protonierten Molekülen der Datenbank-Treffer in den LC-MS-Chromatogrammen der unfraktionierten Kulturfiltrate gesucht. Dabei galten folgende Kriterien:

- EIC (Extracted Ion Current) Peak vorhanden (exakte Masse m/z $[M+H]^+$ \pm 5ppm).
- $[M+H]^+$ verifiziert durch mindestens ein Addukt (z.B. $[M+Na]^+$).
- EIC Peak im aktiven Kulturfiltrat zumindest um einen Faktor 10 intensiver als im inaktiven Kulturfiltrat.

Zum anderen wurden, zum Auffinden möglicher bislang unbekannter Metaboliten, HPLC Fraktionen mittels LC-MS analysiert. Anschließend wurden aktive Fraktionen der Kulturfiltrate mit nicht-aktiven Fraktionen der Kulturfiltrate bzw. fraktioniertem Kulturmedium verglichen. Dafür kam die frei zugängliche Software xcms (Smith et al., 2006) zur automatisierten Auswertung der Rohdaten unter Verwendung des Peak-Detektions-Algorithmus *centWave* (Tautenhahn et al., 2008) zur Anwendung. Differentiell auftretende m/z Verhältnisse hatten folgende Kriterien zu erfüllen:

- $[M+H]^+$ verifiziert durch mindestens ein Addukt (z.B. $[M+Na]^+$).
- Intensität des $[M+H]^+$ größer 10^6 counts.

Da bei Massen größer 300 Da selbst eine Massengenauigkeit von 1 ppm nicht ausreicht um nur eine einzige Summenformel berechnen zu können (Kind und Fiehn, 2006), wurde zum Berechnen möglicher Summenformeln die „Seven Golden Rules“-Software verwendet (Kind und Fiehn, 2007), die sowohl Isotopenverhältnisse der ^{13}C Peaks relativ zum monoisotopischen Massenpeak, als auch weitere, heuristische, Regeln zur Anwendung kommen lässt. Ein Überblick des Analysenschemas ist in Abbildung 1 dargestellt.

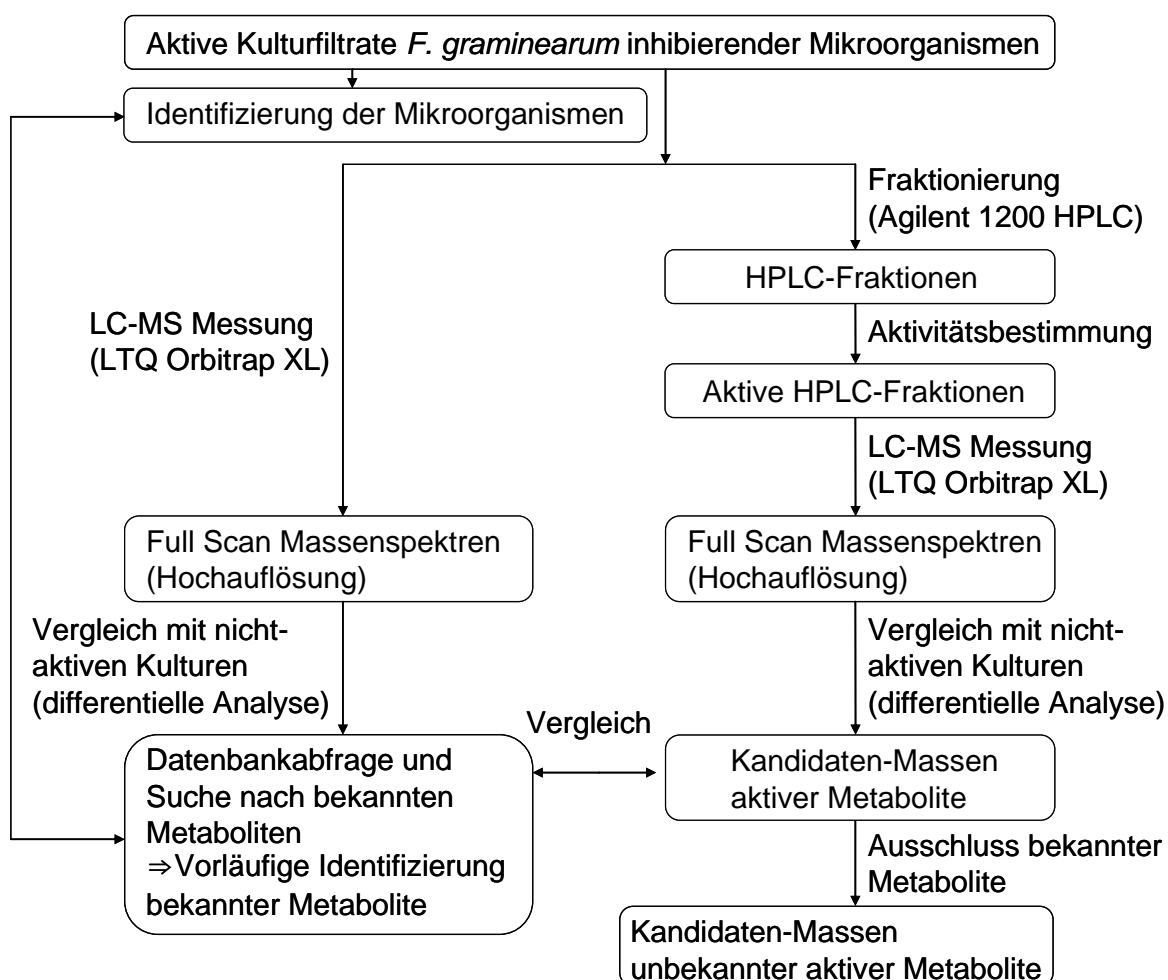


Abbildung 1. Analysenschema zum Auffinden neuer, aktiver Metabolite gegen *Fusarium graminearum*.

Anwendung des Analysenschemas zur Charakterisierung mikrobieller Kulturfiltrate

Mikroorganismen wurden, wie im experimentiellen Teil beschrieben, von ihren natürlichen Habitaten isoliert. Dabei zeigte ein aus 50 cm tiefem Waldboden

kultivierter Organismus hohe Aktivität gegen *F. graminearum*. Dieser wurde als *Penicillium brevicompactum* bestimmt.

Abbildung 2 zeigt den Vergleich zweier TIC (Total Ion Current)-Chromatogramme von Kulturfiltraten von *P. brevicompactum*. Die aktive Kultur wurde 24 Stunden UV-Beleuchtung ausgesetzt, während die nicht-aktive Kultur mit Tag/Nacht-Zyklus kultiviert wurde.

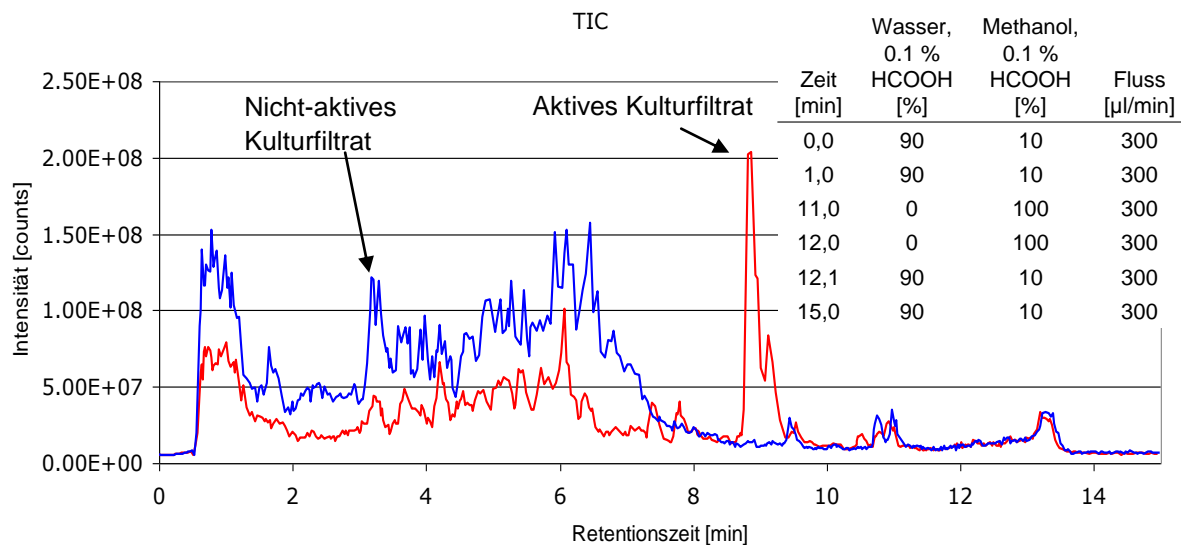


Abbildung 2. Vergleich der TIC (Total Ion Current)-Chromatogramme einer aktiven (Kultivierung bei 24 h UV-Bestrahlung) und einer nicht-aktiven Probe (Kultivierung mit Tag/Nacht-Zyklus) des selben Mikroorganismus.

Über das Verfolgen der ersten Strategie, dem Suchen nach Datenbank-Treffern im aktiven, unfraktionierten Kulturfiltrat, war es möglich folgende Substanzen nachzuweisen: 2,4-Dihydroxy-6-(1-hydroxyacetyl)benzoesäure, Brevigellin, N-Benzoyl-L-phenylalaninol, Mycophenolsäurediolacton, Mycochromensäure, N-Benzoylphenylalanin, Brevinamid E, (+)-Brevion D, Mycophenolsäure, Mycophenolsäureethylester, Brevicompanin C, (+)-Brevion C, Macrophorin A, (+)-Brevion A, (+)-Brevion B und Deacetylpebrolid (geordnet nach Retentionszeit).

Über die zweite verwendete Strategie, der Analyse aktiver HPLC-Fractionen, konnten einige der über die erste Strategie gefundenen Substanzen bestätigt werden. Darüber hinaus konnten differentiell auftretenden Massenspuren, die nicht durch bekannte Metaboliten erklärt werden können, mögliche Summenformeln zugeordnet werden.

Ausblick

Das dargestellte Analysenschema zum Auffinden neuer, gegen *Fusarium graminearum* aktiver Substanzen soll weiter verfolgt und verbessert werden. Dabei soll auch über gezielte MS/MS Experimente weiter an der Aufklärung möglicher Wirkstoffkandidaten gearbeitet werden.

Danksagung

Die Autoren bedanken sich beim Land Niederösterreich und dem Europäischen Fonds für regionale Entwicklung (EFRE) der Europäischen Union für die finanzielle Unterstützung.

Literatur

Kind und Fiehn, 2006. Metabolomic database annotations via query of elemental compositions: Mass accuracy is insufficient even at less than 1 ppm. BMC Bioinformatics, **7**:234.

Kind und Fiehn, 2007. Seven Golden Rules for heuristic filtering of molecular formulas obtained by accurate mass spectrometry. BMC Bioinformatics, **8**:105.

Laatsch Hartmut, 2007. Antibase 2007: The Natural Product Identifier. Wiley-VCH Verlag GmbH, **ISBN-13**: 9783527319756, **ISBN-10**: 3527319751.

Smith C.A., Want E.J., O'Maille G., Abagyan, R., Siuzdak G., 2006. XCMS: processing Mass Spectrometry Data for Metabolite Profiling Using Nonlinear Peak Alignment, Matching, and Identification. Anal. Chem. **78**, 779-787.

Tauthenhahn R., Böttcher C., Neumann S., 2008. Highly sensitive feature detection for high resolution LC/MS. BMC Bioinformatics **9**:504.

Autoren: Sylvia M. Lehner, Alexandra Parich, Rudolf Krska, Rainer Schuhmacher, Analytikzentrum, Andrea Koutnik, Marc Lemmens, Institut für Biotechnologie in der Pflanzenproduktion, Interuniversitäres Department für Agrarbiotechnologie IFA-Tulln, Universität für Bodenkultur Wien, Konrad Lorenz Straße 20, 3430 Tulln

Evaluation of LC-high-resolution FT-Orbitrap MS for the quantification of selected mycotoxins and the simultaneous screening of fungal metabolites in food

S.M. Lehner^a, N.K.N. Neumann^a, M. Sulyok^a, M. Lemmens^b, R. Krska^a and R. Schuhmacher^{a*}

^aCenter for Analytical Chemistry, Department for Agrobiotechnology (IFA-Tulln), University of Natural Resources and Life Sciences, Vienna, Konrad Lorenz Str. 20, 3430 Tulln, Austria; ^bInstitute for Biotechnology in Plant Production, Department for Agrobiotechnology (IFA-Tulln), University of Natural Resources and Life Sciences, Vienna, Konrad Lorenz Str. 20, 3430 Tulln, Austria

(Received 22 April 2011; final version received 20 June 2011)

A liquid chromatography-high-resolution mass spectrometry-based method is reported for the quantification of 20 selected mycotoxins and the simultaneous screening for 200 fungal metabolites in food. For regulated mycotoxins, such as aflatoxins, fumonisins, ochratoxin A, zearalenone and trichothecenes, the evaluation of the method performance characteristics, such as precision, trueness, limit of detection and matrix effects, has been exemplified for the matrix maize. In the case of the limit of detection, an alternative evaluation approach for high-resolution FT-Orbitrap data is proposed. Measurements of the signal-to-noise ratios obtained from 'full-profile mode' data led to detection limits between 8 and 160 ng g⁻¹. Eight naturally contaminated wheat- and maize-based matrix test materials, originating from interlaboratory comparison studies, were used to confirm the trueness of the method for deoxynivalenol, zearalenone, fumonisin B₁ and B₂, HT-2, and T-2 toxin. In addition to accurate quantification of the most relevant mycotoxins, the full-scan chromatograms were used to investigate the potential of the FT-Orbitrap to screen simultaneously for a large number of fungal metabolites. First, a list of 200 metabolites, potentially being present in food samples, was established. Next, specific detection and identification criteria were defined, which are based on accurate mass, peak intensity and isotopologue ratio. The application of these criteria to the suspected metabolites from the list resulted in the putative identification of 13 fungal metabolites in addition to the target toxins.

Keywords: accurate mass; fungal metabolites; liquid chromatography; LC-MS; LOD; mycotoxins; FT-Orbitrap; high-resolution mass spectrometry

Introduction

Mycotoxins are fungal secondary metabolites produced by various mould species. By definition they are toxic to vertebrates and other animal groups in low concentrations (Bennet and Klich 2003). Mycotoxins can enter the food and feed chain by fungal infection of crop plants, either on the field or during storage. The use of contaminated raw cereals or processed commodities therefore constitutes a threat to animal and human health. For this reason regulations or guidelines exist in approximately 100 countries (van Egmond et al. 2007).

The need for monitoring a huge number of regulated compounds in different matrices led to the development of multi-target methods for the simultaneous detection of several analytes in a single method (e.g. Sulyok et al. 2006; Mol et al. 2008). A wide range of physicochemical properties of the analytes makes simultaneous and adequate sample clean-up and

complete HPLC separation for all target compounds impossible. Therefore, highly sensitive, selective and robust MS instruments that allow the injection of crude sample extracts with minimum or no clean-up are necessary. Triple-quadrupole (QqQ) instruments fulfil these requirements when operated in selected reaction monitoring (SRM) mode and are therefore well suited for quantitative target analysis. They show a high sensitivity and a wide linear range, but they also show limitations inherent to their targeted acquisition mode: the number of analytes is limited in one method, time-consuming optimisation of acquisition parameters is needed for each compound (e.g. dwell time, collision energy, acquisition time window) in order to achieve maximum sensitivity, and retrospective data analysis is not possible. Operated in full-scan mode, QqQ instruments produce unit resolution spectra and show low sensitivity, limiting their capabilities for screening applications.

*Corresponding author. Email: rainer.schuhmacher@boku.ac.at

New generations of high-resolution mass spectrometers, such as time-of-flight (TOF), Fourier-transformation-ion-cyclotron resonance (FT-ICR) and FT-Orbitrap instruments are promising alternatives for the simultaneous analysis of multiple compounds. Their particular strength lies in their high mass-resolving power and high mass accuracy. While TOF instruments show lower sensitivity and dynamic range than QqQ instruments in SRM mode, FT-ICR instruments have been rarely used due to their high costs, their slow scan time (1–3 s) and their elaborate mode of operation. FT-Orbitrap instruments offer a better dynamic range and sensitivity close to that of many QqQ instruments (Krauss et al. 2010).

High-resolution mass spectra show high selectivity when generating extracted ion chromatograms (EICs) of the exact mass of the respective compound out of full-scan data with a narrow relative mass extraction window (typically ± 5 ppm). Hence, no pre-selection of compounds and time-consuming set-up of acquisition parameters are necessary. Retrospective analysis of full-scan data makes it possible to assess virtually all compounds present in a sample. This makes liquid chromatography-high-resolution mass spectrometry (LC-HR-MS) on FT-Orbitrap instruments particularly interesting for screening purposes (Krauss et al. 2010).

Guidelines for screening approaches for the monitoring of regulated substances exist (e.g. European Commission 2002, 2009). However, such qualitative screening methods usually aim to avoid only false-negative results since the outcome needs verification by an appropriate confirmatory method (for which standards are needed). Nielen et al. (2007) and Blokland et al. (2008) made suggestions for implementing HR-MS measurements for confirmatory analysis in European Commission (2002).

According to Krauss et al. (2010), screening approaches on LC-HR-MS instruments can be separated into non-target screenings (in the search of unknowns) and suspect screenings (where full-scan data can be examined for a positive list of compounds of interest). Both of these approaches aim to generate a list of highly likely substances present in a sample without the availability of reference standards (which is in contrast to the target analysis). To the best of the authors' knowledge, no detailed guidelines or requirements for non-target or suspects screening applications using LC-HR-MS exist. Besides accurate mass (due to the high resolving power and mass accuracy) with which (de-)protonated molecules or adducts can be searched for, criteria such as the relative isotope abundance (RIA) of naturally occurring isotopic ions (^{13}C) can be included for increasing the confidence in the presence of suspects (conformance with theoretical isotopic pattern). Xu et al. (2010) evaluated the accuracy with which isotope patterns can be determined on FT-Orbitrap instruments. For obtaining

structural information, it is possible to include data dependant MS/MS (e.g. of the most intense ion of a full scan) to facilitate retrospective analysis as well as confirmation of the detected substances.

LC-HR-MS using FT-Orbitrap instruments in full-scan mode has been successfully used for the (semi-)quantitative determination of, for example, small molecules in biological samples (Zhang et al. 2009), veterinary drugs in food matrices (Kaufmann et al. 2011), hormone and veterinary drug residue analysis (van der Heeft et al. 2009), residue analysis in food and feed (Kellmann et al. 2009), mycotoxin analysis in maize, wheat (Herebian et al. 2009) and barley (Zachariasova et al. 2010a), and mycotoxin analysis in beer (Zachariasova et al. 2010b). However, certain methodical aspects when dealing with HR-MS data remain unanswered or are to be further discussed in the scientific community.

One of these aspects is how to estimate the limit of detection (LOD) for HR-MS data. In literature, values for the LOD are often given as the concentration level at a signal-to-noise ratio (S/N) of 3 (e.g. Herebian et al. 2009). This method for the estimation of LODs is frequently used, regardless of the fact, that with narrow relative mass extraction windows (e.g. ± 5 ppm) the corresponding extracted ion chromatograms (EICs) usually do not show any noise, due to the high mass resolving power of these instruments. Owing to this fact, other approaches have been suggested, such as the lowest calibration level (LCL, Zachariasova et al. 2010b) which is 'the lowest concentrations of matrix-matched standards which it was possible to repeatedly determine during a longer time period' and alternative approaches for the calculation of detection limits (Kaufmann 2009). While the LCL is defined as the lowest analyte concentration of a calibration (European Commission 2009) but has no definition regarding its use as performance characteristic (LOD) of an analytical method, calculation approaches are prone to errors caused by model assumptions. So far no standardised procedure for the determination of the LOD in HR-MS has been established and is accepted throughout the scientific community. The present work presents the successful application of an alternative approach for the estimation of LOD values which is based on 'full-profile mode' LC-MS chromatograms that can be used in case of FT-Orbitrap instruments.

The main focus was to explore the capabilities of an LTQ Orbitrap XL system for the establishment of an LC-HR-MS method for the quantitative analysis of the most relevant mycotoxins in food samples in combination with a first explorative approach for the simultaneous screening of a large number of fungal metabolites potentially being present in food. The extraction procedure and LC method is based on previous work of our group in this field (Sulyok et al.

2006). After generating fit-for-purpose calibration functions, we evaluated the limits of detection in pure solvents and in the presence of the matrix maize (including critical assessment regarding European regulations) and matrix effects for maize. Precision and trueness were assessed from spiking experiments as well as the measurement of matrix test materials. A preliminary approach for exploring the general applicability of HR-MS using an LTQ Orbitrap XL for a suspects screening for 200 fungal secondary metabolites in food samples was conducted. Therefore, specific detection and identification criteria were defined and applied to the HR-full-scan chromatograms.

Materials and methods

Chemicals and reagents

Methanol (MeOH, LiChrosolv, LC gradient grade) and glacial acetic acid (HAc) were purchased from Merck (Darmstadt, Germany); acetonitrile (ACN, HiPerSolv Chromanorm, HPLC gradient grade) was purchased from VWR (Vienna, Austria); formic acid (FA, MS grade) was obtained from Sigma-Aldrich (Vienna, Austria). Water was purified successively by reverse osmosis and an ELGA Purelab Ultra-AN-MK2 system (Veolia Water, Vienna, Austria). Mycotoxin standards were purchased from different sources and dissolved in ACN if not stated otherwise. Stock solutions of 3-acetyldeoxynivalenol (3ADON), aflatoxins B₁, B₂, G₁, G₂, M₁ (AFB₁, AFB₂, AFG₁, AFG₂, AFM₁), deoxynivalenol (DON), fumonisins B₁ and B₂ (FB₁, FB₂, in ACN:water 1:1, v/v), HT-2 toxin (HT-2), ochratoxin A (OTA), T-2 toxin (T-2) and zearalenone (ZON) were obtained from Biopure Referenzsubstanzen GmbH (Tulln, Austria). Alternariol, mycophenolic acid (MPA) and tentoxin were purchased from Sigma-Aldrich. Roquefortine C (RFC) was purchased from Iris Biotech GmbH (Marktredwitz, Germany). α-Ergocryptine was obtained from Dr Miroslav Flieger (Academy of Sciences of the Czech Republic, Prague). A stock solution of enniatin B and B₁ (EnnB, EnnB₁) was provided as a gift by Dr Marika Jestoi (National Veterinary and Food Research Institute, Finland). All standards were stored at −20°C, except for FB₁ and FB₂, which were stored at 4°C.

For external calibration, a multi-analyte stock solution of the 20 mycotoxins with concentrations ranging from 100 to 5351 ng g^{−1} was prepared freshly prior to analysis. The stock solutions were diluted with ACN:water 1:1 (v/v) 1:10 to 1:1000 over various levels, ranging from 1 to 535 ng g^{−1}. Since samples are diluted by a factor of 8 during sample preparation (extraction and dilution of raw extract) this corresponds to a concentration range of 8–4281 ng g^{−1} in food samples.

Sample preparation

Sample extraction and further preparation was based on a recently described procedure that allows efficient extraction of fungal metabolites in food samples from various matrices (Sulyok et al. 2006). A total of 20 ml extraction solvent (ACN:water:HAc, 79:20:1 (v/v/v)) were added to 5 g of ground sample. The sample was extracted for 90 min at 170 rpm using a GFL 3017 rotary shaker (GFL, Burgwedel, Germany) and then left for 5 min to allow sedimentation of the solids. An aliquot of 350 μl of the supernatant was diluted with the same volume of a mixture consisting of ACN:water:HAc, 20:79:1 (v/v/v) and homogenised using a vortex mixer (Janke + Kunkel IKA Labortechnik VF2, Müller-Scherr, Vienna, Austria). A total of 5 μl of the diluted extract were injected into the LC-MS system. The final concentration of sample equivalent in the extract was 0.125 g ml^{−1}, corresponding to 0.625 mg of sample injected into the LC-MS system.

LC-MS analysis

The chromatographic separation of the analytes was carried out using an HPLC system (Accela, Thermo Fisher Scientific, San Jose, CA, USA) equipped with a reversed-phase Gemini C₁₈ analytical column, 150 × 2.0 mm i.d., 5 μm particle size, equipped with a C₁₈ 4 × 2 mm i.d. security cartridge (all from Phenomenex, Torrance, CA, USA). The column temperature was maintained at 25°C. Eluent A was water, eluent B was MeOH, both containing 0.1% FA. The chromatographic method held the initial mobile phase composition (90% A) constant for 2 min, followed by a linear gradient to 100% B in 12 min. This final condition was held for 4 min, followed by 5 min column re-equilibration at 90% A. The flow rate was 350 μl min^{−1}.

The HPLC system was coupled to an LTQ Orbitrap XL (Thermo Fisher Scientific) equipped with an electrospray ionisation (ESI) interface which was operated in positive ionisation mode using the following settings: electrospray voltage: 4 kV, sheath gas: 40 arbitrary units, auxiliary gas: 5 arbitrary units, capillary temperature 350°C. All other source parameters were automatically tuned for a maximum MS signal intensity of reserpine (Sigma Aldrich) solution (10 mg l^{−1}). To this end, 10 μl min^{−1} of reserpine solution (dissolved in ACN:water = 8:2 (v/v)) were infused via syringe pump into mobile phase (Eluent A : B, 1 : 1) of a flow rate of 350 μl min^{−1}.

For the FT-Orbitrap, the automatic gain control was set to a target value of 5 × 10⁵ and a maximum injection time of 500 ms was chosen. The mass spectrometer was used with a resolving power setting of 60,000 FWHM (at *m/z* 400) and a scan range of *m/z*

100–1000. Data were generated using Xcalibur 2.1.0 (Thermo Fisher Scientific).

Mass calibration of the LTQ Orbitrap XL system was done using MSCAL5 ProteoMass™ LTQ/FT-Hybrid ESI Pos. Mode CalMix (Sigma Aldrich) at an interval of maximum 1 week. Mass calibration was checked prior to measurements with common background ions (Keller et al. 2008). In case of a relative mass deviation ≥ 3 ppm, mass calibration was carried out using Thermo TunePlus software (Version 2.5.5. SP1, Thermo Fisher Scientific). With external calibration, 95% of the data showed less than 3 ppm relative mass deviation at the peak apex (most intense scan of chromatographic peak; data not shown). Less intense scans at the beginning and end of a chromatographic peak occasionally showed slightly higher mass deviations. Hence, for generating extracted ion chromatograms (EICs) a relative mass extraction window size of exact mass ± 5 ppm was applied during data analysis, resulting in reasonable chromatographic peak shapes.

Data analysis

Data processing was done using Xcalibur 2.1.0 QualBrowser, QuanBrowser (using Genesis peak detection algorithm, relative mass extraction window: ± 5 ppm), and the validation software Validata, a Microsoft Excel macro developed by Wegscheider et al. (1999). For all analytes the protonated molecules (exceptions: HT-2 and T-2 toxins: ammonium adducts) were used for data evaluation.

Estimation of method performance characteristics

Spiking experiments

For the evaluation of matrix-induced signal suppression/enhancement (SSE), the method precision and the determination of the limit of detection in the presence of matrix ($\text{LOD}_{\text{matrix}}$), maize was used as model matrix. Non-contaminated maize was extracted and diluted as described under sample preparation. Subsequently, to 900 μl of diluted blank maize extract, 100 μl of the multi-analyte stock solution were added to obtain the highest spiking level. Further dilution with diluted blank maize extract was carried out to achieve nine defined concentration levels of the toxins (covering the same range as for the external calibration) without diluting the matrix more than 10%. Blank maize was extracted, diluted and spiked at 3 different days for obtaining three independent data sets. These were used for estimation of matrix effects and of the overall precision of the method.

Determination of the limit of detection

For estimation of the LOD, two different approaches were applied. One common approach, according to

Harris (2006), is to assume that the standard deviation of the signal of an analyte in a sample at a concentration level close to its detection limit is similar to the standard deviation of the analyte signal in a blank. For estimation of the LOD according to this approach, linear calibration curves were generated at low concentrations for which linearity of the detector response was assumed. The slopes (m) of linear regression lines and the standard deviations (s) of ten replicate measurements were used for the estimations of the LOD according to:

$$\text{LOD} = \frac{3s}{m} \quad (1)$$

As an alternative approach, the concentration at which $S/N=3$ is achieved when acquiring full-profile mode data was determined.

From the results obtained for low concentrations of standard solutions in pure solvents, the instrument detection limit ($\text{LOD}_{\text{solvent}}$) was estimated. The LOD in the presence of the matrix maize ($\text{LOD}_{\text{matrix}}$) was estimated by measuring spiked, diluted extracts of blank maize. LOD values obtained were multiplied by a factor of 8 in order to obtain LODs in ng g^{-1} sample.

Evaluation of trueness

To evaluate the trueness of the method, several well-defined matrix test materials originating from inter-laboratory comparison studies were used. Wheat flour originated from Biopure Referenzsubstanzen GmbH (Tulln, Austria), two quality control test materials (maize #1 and #2) originated from FAPAS (FERA, York, UK), and other proficiency testing materials (maize #3, breakfast cereal, wheat draff, grinded wheat and animal feed) originated from Bipea (Gennevilliers, France). Table 1 gives the assigned values (X) and expanded uncertainty U_X (confidence level 95%) of the test materials. When available, the uncertainty u_X (confidence level 68%) of the test materials has been directly taken for obtaining U_X . Otherwise, it has been calculated from the robust standard deviation s_X of the results of the participating laboratories, according to equation (2), where n is the number of the participating laboratories of the interlaboratory comparison studies:

$$U_X = 2 * u_X = 2 * \frac{s_X}{\sqrt{n}} \quad (2)$$

Suspects screening

In order to exploit the possibilities HR-MS can offer for the screening of microbial metabolites suspected to be present in the test materials, criteria were defined. These criteria were applied to full-scan data obtained after analysis of the test materials.

Table 1. Assigned values according to material provider and expanded uncertainty (95% confidence level) for test materials in ng g⁻¹. Concentrations <LOD in the presence of matrix maize (LOD_{matrix}; see Table 3) are not provided.

Test material	Provider, number, year	Analyte	Assigned value (ng g ⁻¹)	Expanded uncertainty (ng g ⁻¹)
Animal feed	Bipea, 2-3031-0052, 2010	DON	32.3 × 10 ¹	5.6 × 10 ¹
Grinded wheat	Bipea, 05-0631-0080, 2010	DON	22.7 × 10 ²	2.5 × 10 ²
Maize #1	FAPAS, T2262, 2010	DON	17.1 × 10 ²	1.3 × 10 ²
Maize #3	Bipea, 3-0731-0095, 2010	DON	40.9 × 10 ²	4.6 × 10 ²
Maize #2	FAPAS, T2246, 2008	FB ₁	16.5 × 10 ²	1.1 × 10 ²
Maize #3	Bipea, 3-0731-0095, 2010	FB ₁	21.7 × 10 ¹	9.2 × 10 ¹
Maize #2	FAPAS, T2246, 2008	FB ₂	46.1 × 10 ¹	3.2 × 10 ¹
Wheat draff	Bipea, 2-2831-0055, 2011	HT-2	7.2 × 10 ¹	1.0 × 10 ¹
Wheat flour	Biopure Referenzsubstanzen GmbH, –, –	HT-2	8.9 × 10 ²	2.7 × 10 ²
Wheat draff	Bipea, 2-2831-0055, 2011	T-2	7.6 × 10 ¹	1.8 × 10 ¹
Wheat flour	Biopure Referenzsubstanzen GmbH, –, –	T-2	7.5 × 10 ¹	3.6 × 10 ¹
Breakfast cereal	FAPAS, T2257, 2010	ZON	70 × 10 ⁰	7.0 × 10 ⁰
Maize #3	Bipea, 3-0731-0095, 2010	ZON	39.9 × 10 ²	6.7 × 10 ²

First, a positive list of 208 fungal metabolites was constructed including molecular formula, CAS number (if available) and exact masses of ions likely to be present in HR-mass spectra (see the supplementary data file Table 1). Eight of those have a molecular mass of <100 or >1000 u, so they cannot be covered with the method applied.

Full-scan LC-MS chromatograms were examined for peaks indicating the presence of these 'suspected' metabolites using the following criteria (automated detection). (1) Presence of at least two ion species ([M + H]⁺ and/or [M + NH₄]⁺ and/or [M + Na]⁺) with a maximum relative mass deviation of ±3 ppm of the exact mass of the metabolites from the above mentioned positive list. This mass deviation was chosen due to the accuracy that was determined prior to measurements (see the Materials and methods section). Depending on the mass accuracy achieved, this parameter needs to be adjusted.

(2) For the most intense ion species a minimum intensity of 10,000 counts was required.

(3) Of the most intense ion species (I) the peak corresponding to the first ¹³C isotopologue had to be present (maximum relative mass deviation ±5 ppm). This mass tolerance was chosen to account for the low intensities of the isotopologue ion species, which can lead to slightly higher mass deviations. The ratio of the measured intensity of the I+1 ion to the calculated (theoretically expected) intensity [Int(I+1)_{meas}]/[Int(I+1)_{calc}] had to be 0.65–1.05. This tolerance was chosen in order to take the accuracy with which relative isotope abundances can be determined on FT-Orbitrap instruments (Xu et al. 2010) into account.

(4) Criteria (1) to (3) had to be fulfilled in at least five scans within a period of 25 s to be considered 'putatively identified'.

For the automated data evaluation of these criteria for full-scan FT-Orbitrap data a python script was

implemented (Neumann et al. data not published). Finally, EICs of putatively detected suspects were evaluated manually to ensure reasonable chromatographic peak shapes.

Results and discussion

Chromatographic separation of the analytes

Figure 1 shows a typical chromatogram for the separation and detection of 20 selected mycotoxins. For all analytes the protonated molecules (exceptions: HT-2 and T-2: ammonium adducts) were used for generating EICs. No ammonia was added to the eluents, but is most likely present in the solvents or from previous experiments (Berger et al. 1999) or formed in the source by redox processes in the electrospray (Nielsen and Smeesgaard 2003). Typical chromatographic peak widths of 15–25 s lead to approximately 15–25 spectra across one peak. The most polar metabolites (DON, 3ADON) show broader peaks. This is caused by the injection of 5 µl of the diluted sample extract (containing 50% ACN in water) into an HPLC-flow (mobile phase consisting of 10% ACN in water) of 350 µl min⁻¹.

Generation of calibration curves

To generate external standard calibration curves, nine concentration levels were measured, ten times each (exception: fumonisins: five to ten times each). Using linear calibration over the whole concentration range, highly negative intercepts (y-axis) were observed. Additionally, sensitivity (slopes) increased with increasing analyte concentration. Therefore, quadratic fitted curves were used to describe the detector response as a function of toxin concentrations. This is in agreement with the findings of Kellmann et al.

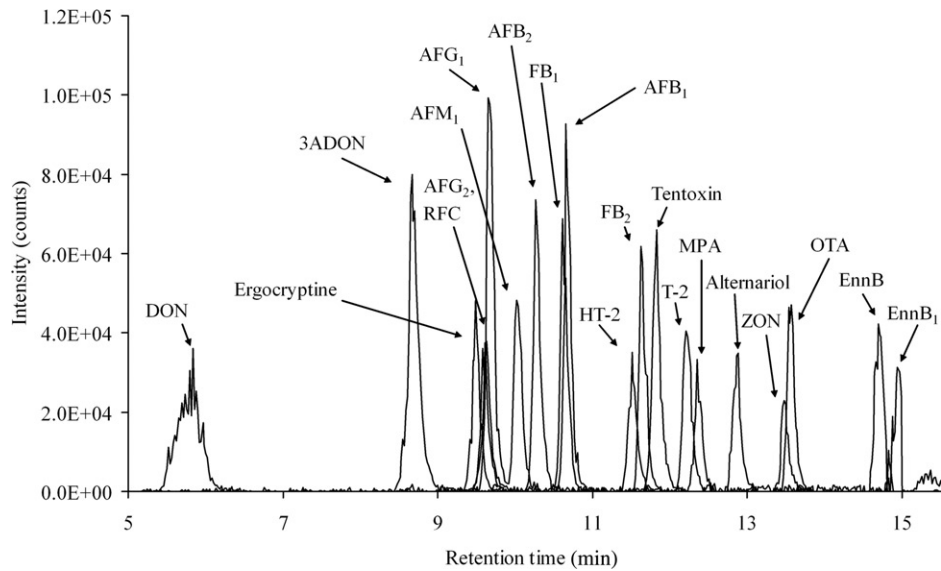


Figure 1. Chromatogram for the separation of 20 selected mycotoxins. EICs were generated from FT-Orbitrap full scan data using a mass extraction window of ± 5 ppm.

Table 2. Retention time, calibration range, number of evaluated levels, relative standard deviation of the lowest calibration level (RSD low) and LODs obtained for standards in pure solvent for the respective analytes.

Analyte	Retention time (min)	Calibration range (ng g^{-1})	Number of evaluated levels	RSD low (%)	LOD _{solvent} (ng g^{-1})
DON	5.9	160–3200	4	15	160
3ADON	8.8	162–3232	4	13	110
Ergocryptine	9.2	10–960	8	16	8
AFG ₂	9.7	13–643	6	14	12
AFM ₁	9.7	30–1536	6	10	32
RFC	9.7	8–162	7	14	8
AFG ₁	10.0	13–643	6	14	12
AFB ₂	10.3	13–637	6	13	12
AFB ₁	10.7	13–212	5	13	12
FB ₁	10.7	86–4281	9	5	8
HT-2	11.6	32–1078	7	17	24
FB ₂	11.7	86–4264	9	6	8
Tentoxin	11.9	16–794	6	17	16
T-2	12.3	16–1066	8	17	16
MPA	12.4	64–3200	6	9	64
Alternariol	12.8	54–1600	5	12	24
ZON	13.5	41–3232	7	15	40
OTA	13.7	26–1318	6	19	24
EnnB	14.8	22–214	4	18	12
EnnB ₁	14.9	87–1728	4	22	16

(2009) who made similar observations when using FT-Orbitrap in full-scan mode for the determination of residues and contaminants in honey and animal feed. Also, signal intensities showed higher absolute standard deviations at high analyte concentrations (heteroskedasticity). Kaufmann et al. (2011), who developed a method for the quantification of veterinary drugs in different food matrices, made similar observations and also used quadratic regression. Table 2 gives the

calibration ranges and precision estimates obtained for standards in pure solvents.

Determination of the limit of detection

The LOD is usually defined as the lowest analyte concentration at which the analyte signal can be reliably differentiated from the blank signal. It is a parameter to prevent the detection of false positives.

Table 3. Performance characteristics in the presence of the matrix maize: calibration range, number of evaluated levels, relative standard deviation of the recovery function (RSD_{matrix}) at a medium concentration of the calibration (ng g^{-1}), signal suppression/enhancement (SSE), LOD in the presence of matrix maize (LOD_{matrix}) and recovery of the extraction step (R_E).

Analyte	Calibration range (ng g^{-1})	Number of evaluated levels	RSD_{matrix} (%) at concentration (ng g^{-1})	SSE (%)	LOD_{matrix} (ng g^{-1})	R_E (%)
DON	160–3200	4	11 (1520)	115	160	98 ^a
3ADON	162–3232	4	12 (1535)	113	150	89 ^a
Ergocryptine	19–960	6	11 (471)	94	16	72 ^b
AFG ₂	32–643	4	12 (306)	77	32	110 ^a
AFM ₁	51–1536	5	9 (743)	96	40	100 ^b
RFC	32–162	4	60 (65)	39	8	^c
AFG ₁	21–643	5	12 (311)	77	20	107 ^a
AFB ₂	32–637	4	18 (303)	69	24	102 ^a
AFB ₁	21–212	4	16 (96)	55	16	95 ^a
FB ₁	121–2414	4	8 (1147)	114	8	57 ^a
HT-2	65–1078	5	11 (507)	77	40	108 ^a
FB ₂	120–2404	4	10 (1142)	124	12	67 ^a
Tentoxin	27–794	5	14 (384)	102	24	110 ^b
T-2	40–1066	6	19 (513)	81	32	105 ^a
MPA	64–3200	6	5 (1568)	105	64	103 ^b
Alternariol	80–1600	4	6 (760)	88	56	107 ^b
ZON	65–3232	6	12 (1584)	99	64	93 ^a
OTA	44–1318	5	7 (637)	96	24	100 ^a
EnnB	22–214	4	5 (96)	109	12	103 ^a
EnnB ₁	87–1728	4	11 (821)	104	20	103 ^a

Notes: Recovery of the extraction step from: ^aSulyok et al. (2006): model matrix maize; ^bSulyok et al. (2007): model matrix breadcrumbs; and ^cnot evaluated for cereals. It has been evaluated for the matrix dust (94%) by Vishwanath et al. (2009).

Applying the approach according to Harris (2006) lead to LODs at which often only a few (zero to three) data points could be found across the chromatographic peaks of the corresponding EICs. Therefore, this approach resulted in estimated LODs that were too optimistic and cannot be used for the reliable estimation of the detection limits (data not shown).

Hence, we suggest an alternative approach for the estimation of the LOD when using FT-Orbitrap in full-scan mode. The most straightforward way to estimate the LOD is to determine the concentration at which $S/N=3$ is achieved. When working with high-resolution mass spectrometers, such as TOF, FT-ICR or FT-Orbitrap instruments, usually no noise is observed, owing to the high mass resolving power of these instruments. EICs generated with relative mass extraction window sizes of ± 5 ppm are highly selective for the molecule of interest. Only in exceptional cases background signals with similar m/z ratios cause the presence of detectable noise in EICs generated out of full-scan data.

Usually, when recording FT-Orbitrap data, most of the noise is removed automatically by the instrument software in the so-called ‘reduced-profile mode’. This is achieved in the following way: the system determines noise during booting of the instrument and subtracts

all mass peaks below a certain threshold automatically during the acquisition of data. This reduces the data file size of a typical LC-MS run in full-scan mode to approximately 130 MB per file for the above-described method. When generating FT-Orbitrap data files in full-profile mode no signals are automatically removed. Therefore, only when acquiring data in full-profile mode, noise can be observed in the corresponding data files when generating EICs with narrow mass extraction windows. By generating EICs of data that was recorded in full-profile mode, the toxin concentrations corresponding to $S/N=3$ was determined for the estimation of LODs. It shall be noted, however, that acquiring full-profile mode data results in very a large file size (approximately 3.2 GB per run for the method in use) and therefore cannot be used for routine measurements. Concentrations for the LODs obtained by this procedure were a factor three to four higher compared with the values achieved according to Harris (2006) and are given in Table 2 (LOD_{solvent}) and Table 3 (LOD_{matrix}). This approach seems to give a more reliable estimation of the LOD for high-resolution data, resulting in reasonable peak shapes with approximately eight to ten data points across a peak. An example EIC of tentoxin (Delaforge et al. 1997) in solution without matrix, recorded in reduced-profile mode and full-profile mode (concentration at $S/N=3$)

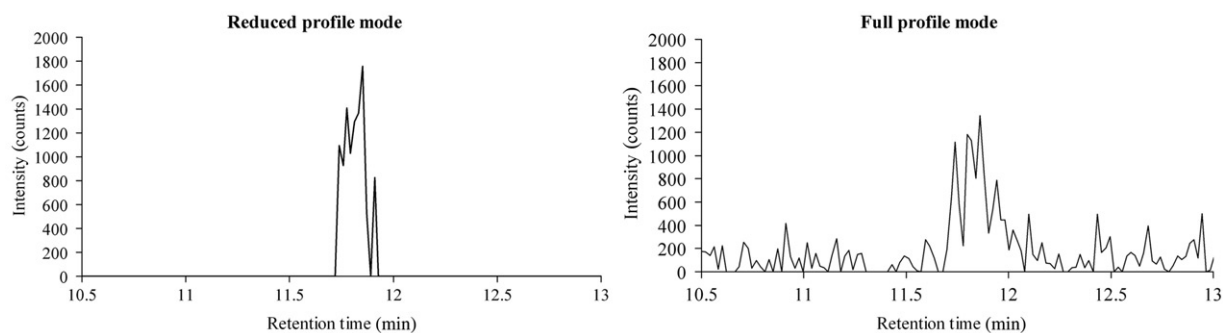


Figure 2. Chromatogram of tentoxin at $\text{LOD}_{\text{solvent}}$ (16 ng g^{-1}) using 'reduced-profile mode' and 'full-profile mode'. EICs were generated using a mass extraction window of ± 5 ppm.

is given in Figure 2. By applying this approach to spiked maize extracts, the limits of the European Regulations could be achieved for FB_1 , FB_2 and DON. For ZON the regulations were achieved, but with the following exceptions: ZON for 'Processed cereal-based food for infants and young children' (20 ng g^{-1}), for 'Bread, pastries and biscuits' (50 ng g^{-1}) and 'Cereal snacks and breakfast cereals' (50 ng g^{-1}). Maximum residue levels for aflatoxins ($0.025\text{--}15 \text{ ng g}^{-1}$) and for OTA ($0.5\text{--}10 \text{ ng g}^{-1}$), however, are at concentrations which cannot be measured with the presented method. For some analytes (e.g. DON, 3ADON and ZON) measurements in negative ionisation mode and/or addition of acetate to the eluents (adduct formation) might be beneficial for achieving lower LODs.

Performance characteristics obtained from matrix-matched calibration (maize)

Maize is a matrix known to be associated with pronounced SSE effects (Sulyok et al. 2006). For this reason it was used for assessing matrix effects. Application of the proposed method to other matrices requires detailed investigations for the matrix in use. Recovery functions were constructed for extracted and diluted blank maize that was spiked with the analytes at several concentration levels. For this, the spiking concentrations of the maize extracts were put on the x -axis; experimentally derived concentrations (external calibration with standards in pure solvents) were put on the y -axis. The resulting calibration functions showed linearity (tested by a Mandel test (Validata; Wegscheider et al. 1999)). RSDs of the recovery functions were used as estimates for the precision of the method. The slope of the recovery function can be used as estimate for matrix induced SSE.

RSDs of the recovery functions was found to be around 10% and generally lower than 20%. The SSE generally showed values of 77–124%, indicating little influence of matrix components on ionisation efficiencies. AFB_1 and AFB_2 show matrix effects of 55% and 69% SSE, respectively. Sulyok et al. (2006) also found

strong matrix effects, namely 18% and 48% SSE for AFB_1 and AFB_2 , respectively. Roquefortine C shows uncommonly large matrix effects (39% SSE) together with low precision (60% RSD at 65 ng g^{-1}). For details of the calibration parameters obtained for spiked maize extracts, see Table 3.

The same extraction procedure (only minor adaptations) as in Sulyok et al. (2006) was used. Therefore, comparison of the results regarding extraction efficiencies as well as matrix effects is possible, the latter giving information about differences of the ion source setup regarding its susceptibility to matrix effects. Matrix effects were similar to those found on the QTrap 4000 triple quadrupole system. SRM measurements show lower LODs for most of the analytes, which is in accordance with the findings of van der Heeft et al. (2009), who investigated hormone and veterinary drug residues using UPLC-HR-MS on an FT-Orbitrap at 60,000 resolving power and compared results with those of an MRM UPLC-QqQ-MS/MS confirmatory method.

Accuracy (trueness and precision) of the method

Measurements of well-defined test materials were performed, showing the principal suitability of this method for wheat and maize-based food commodities. In addition to the food test materials – maize (three), breakfast cereal (one), wheat flour (one), wheat druff (one), grinded wheat (one) – one animal feed test material was included for evaluating the trueness of the method. Results were corrected for matrix effects in case of maize materials. For the other matrices no correction of SSE effects was done, since the extent was not known. For a method to be routinely used, SSE effects should be carefully evaluated and corrected if significant. As estimate for the method precision, the RSDs of the recovery functions were used (Validata; Wegscheider et al. 1999). Values were multiplied by 2 in order to obtain a 95% confidence level. To compare measurement results with assigned concentrations of the inter-laboratory comparison matrix test materials,

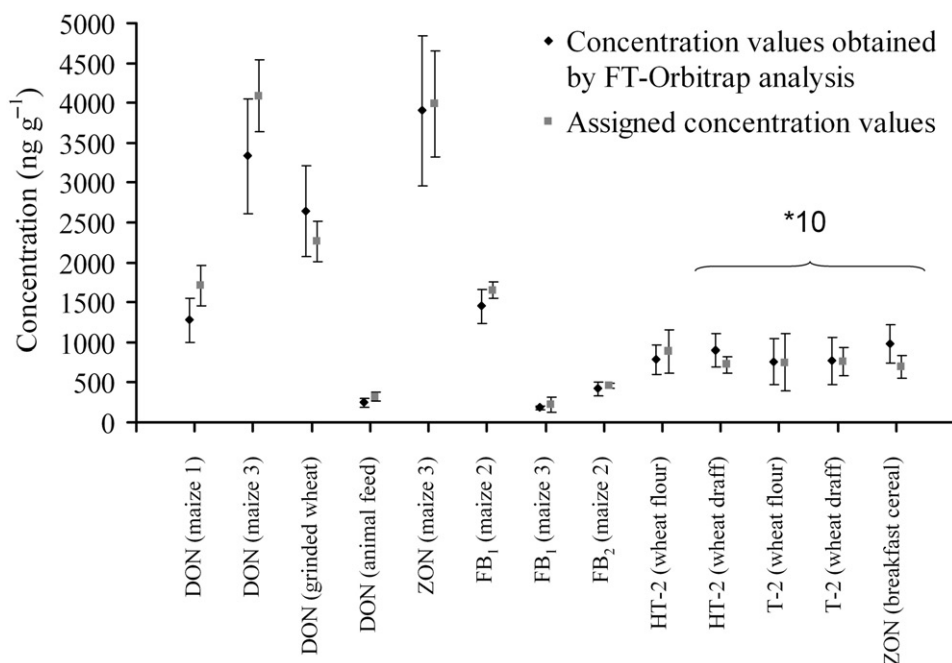


Figure 3. Concentration values obtained by FT-Orbitrap analysis and assigned concentration values (both with 95% confidence intervals). For better visibility, concentration values for HT-2 (wheat draff), T-2 (wheat flour), T-2 (wheat draff) and ZON (breakfast cereal) were multiplied by 10.

the procedure according to European Reference Materials' Application Note 1 of the European Commission (Linsinger 2010) was applied. No significant differences between the measured concentrations and the assigned concentrations were observed, not even for two concentrations that slightly exceeded the highest concentration levels used for instrument calibration (DON and ZON in maize #3). Furthermore, from the results shown in Figure 3 (for test materials, see the Materials and methods section), it can be concluded that for the tested toxin/matrix combination no severe matrix effects occurred. Otherwise, matrices other than maize would not have resulted in an acceptable outcome. In conclusion, the results obtained clearly demonstrate the high potential of LC-HR-MS on FT-Orbitrap instruments for the quantitative determination of mycotoxins and its principal applicability to food samples.

Suspects screening for 200 fungal and bacterial metabolites

In contrast to MS/MS-based quantitative methods such as SRM used with QqQ instruments, HR full-scan measurements offer the opportunity to detect metabolites initially not intended to be monitored. In this respect, we wanted to explore and show the principal suitability of the Orbitrap for the screening of compounds without availability of standards.

In order to estimate the effect of the criteria, those were applied to the full-scan measurements of

standards solutions (in pure solvents and in the presence of matrix maize (non-contaminated)) that lead to signal intensities of approximately 10^4 – 10^6 counts. Searching for the exact masses of the protonated molecules or ammonia/sodium adducts of standard solutions (minimum intensity heights 10^4 counts, mass deviation ± 3 ppm) led to the finding of all 20 standards, but also to 18 (standards in pure solvent) and 41 (standards in the presence of matrix maize) false-positive findings. This indicates that if a screening for the monitoring of regulated substances (e.g. European Commission 2002, 2009) was to be conducted, searching for the exact masses with a certain allowed mass deviation would be sufficient, since a following confirmatory method would have to proof the trueness of these findings. However, for the suspects screening approach, we applied further strict criteria in order to minimise the number of false-positive findings. Applying criteria (1) and (2) led to the reduction to 13 (pure solvent) and 37 (matrix maize) false-positives and zero false-negatives. Application of criteria (1) to (3) led to only three false-positives but also two (pure solvent) and 12 (matrix maize) false-negatives. Applying criteria (1) to (4) to standards in pure solvents and standards in matrix maize led to zero false-positives in both cases and to nine (pure solvents) and 16 (matrix maize) false-negatives.

Applying criteria (1) to (4) to the test materials, several assigned compounds could not be found. The most limiting criterion turned out to be the maximum tolerated deviation from the expected (calculated)

Table 4. Putative compounds detected in test materials found via suspect screening. Only metabolites additionally found along with the target toxins are shown. Compound name, test material, most intense ion species (I), m/z found, retention time, intensity, relative mass deviation and ratio of measured to calculated relative isotope abundance of the first carbon isotopologue (one ^{13}C instead of ^{12}C).

Compound	Test material	Retention time (min)	Most intense ion species (I)	Intensity (counts)	m/z found (Th)	Relative mass deviation (ppm)	$[\text{Int}(I+1)_{\text{meas}}]/[\text{Int}(I+1)_{\text{calc}}]$
Antibiotic Y	Maize 3	12.0	$[\text{M} + \text{H}]^+$	6.5×10^4	319.045	0.05	0.71
Asperlactone	Wheat draff	8.2	$[\text{M} + \text{H}]^+$	1.3×10^5	185.081	-1.62	0.67
Aurofusarin	Maize 3	13.5	$[\text{M} + \text{H}]^+$	6.4×10^5	571.087	-0.01	0.71
Beauvericin	Maize 2	15.0	$[\text{M} + \text{Na}]^+$	3.3×10^5	806.398	-0.25	0.85
Chlamydosporol	Wheat draff	8.5	$[\text{M} + \text{H}]^+$	8.2×10^4	227.091	-1.34	1.02
Cyclopiazonic acid	Maize 1	11.8	$[\text{M} + \text{H}]^+$	8.9×10^5	337.155	0.16	0.91
Cyclopiazonic acid	Maize 2	11.8	$[\text{M} + \text{H}]^+$	8.2×10^5	337.155	0.62	0.82
Cyclopiazonic acid	Maize 3	11.8	$[\text{M} + \text{H}]^+$	1.2×10^6	337.154	-0.56	0.84
Decarestrictine	Maize 1	7.7	$[\text{M} + \text{H}]^+$	3.1×10^4	217.107	0.10	0.68
Decarestrictine	Maize 3	7.8	$[\text{M} + \text{H}]^+$	4.2×10^4	217.107	-0.33	0.86
Enniatin B	Animal feed	14.8	$[\text{M} + \text{Na}]^+$	8.5×10^5	662.397	-2.24	0.70
Enniatin B	Breakfast cereal	14.8	$[\text{M} + \text{Na}]^+$	6.2×10^4	662.398	-1.14	1.02
Enniatin B	Grinded wheat	14.7	$[\text{M} + \text{Na}]^+$	8.7×10^5	662.398	-1.41	0.68
Enniatin B	Maize 3	14.7	$[\text{M} + \text{Na}]^+$	2.4×10^5	662.399	-0.21	0.85
Enniatin B	Wheat draff	14.8	$[\text{M} + \text{Na}]^+$	3.0×10^6	662.397	-2.06	0.86
Enniatin B	Wheat flour	14.7	$[\text{M} + \text{Na}]^+$	3.4×10^5	662.398	-0.40	0.81
Enniatin B1	Animal feed	15.0	$[\text{M} + \text{Na}]^+$	4.7×10^5	676.413	-2.41	0.86
Enniatin B1	Grinded wheat	15.0	$[\text{M} + \text{Na}]^+$	1.8×10^5	676.413	-2.05	0.92
Enniatin B1	Wheat draff	15.0	$[\text{M} + \text{Na}]^+$	2.0×10^6	676.413	-1.69	0.79
Enniatin B1	Wheat flour	14.9	$[\text{M} + \text{Na}]^+$	3.9×10^5	676.414	-0.34	0.74
Ergosine	Maize 3	12.9	$[\text{M} + \text{Na}]^+$	1.8×10^4	570.268	-0.88	0.79
Fusarielin A	Maize 2	13.8	$[\text{M} + \text{Na}]^+$	1.4×10^4	425.265	-2.79	0.76
Macrosporin	Animal feed	11.2	$[\text{M} + \text{H}]^+$	6.5×10^4	285.076	-0.13	0.68
Penicillic acid	Wheat draff	3.5	$[\text{M} + \text{H}]^+$	2.6×10^4	171.065	-1.07	0.82

intensity ratio of the mono-isotopic to the first ^{13}C isotopologue peak of -35% to $+5\%$ (criterion 3). Low-intense mass peaks often show no isotopologue peaks at all (since they show only a fractional amount of the intensity of the mono-isotopic peak). Also, the error of the expected relative intensity with which those can be determined can be considerably large for single spectra. Therefore, criterion (3) had not to be fulfilled in five consecutive scans but rather the occurrence of at least five scans within a time window of 25 s was permitted (criterion 4).

Nevertheless, screening for 200 metabolites in the full-scan chromatograms of the test materials (applying criteria 1–4), further highly likely ‘suspected’ metabolites could be found. A list of the 13 suspects found in addition to the expected target compounds (as specified by distributor of the respective samples) in the data of the test materials is given in Table 4. Those include metabolites, which are known to be produced by the most prevalent food colonising fungi such as *Alternaria* (macrosporin), *Aspergillus* (asperlactone, cyclopiazonic acid), *Fusarium* (antibiotic Y, aurofusarin, beauvericin, chlamydosporol, enniatin B, enniatin B1, fusarielin A), *Penicillium* (decarestrictine,

penicillic acid) and *Claviceps pupurea* (ergosine). All test materials under investigation were naturally contaminated. Since all of them had assigned concentrations for *Fusarium* toxins, it is very likely to find further *Fusarium* metabolites to be present in these samples, supporting the putative identification of seven more *Fusarium* metabolites. It also has to be noted that both ergosine and macrosporin usually are accompanied by related compounds such as other ergot alkaloids and alternaria toxins, respectively, which indicates the need for further measurements in order to confirm the identity of the suspected metabolites. Additional confirmatory measures might include the measurement of authentic standards and the consideration of retention times and MS/MS spectra.

The results obtained clearly show the potential of high-resolution mass spectrometry for the screening of compounds in full-scan data. The positive list of suspects can be adjusted or extended deliberately, according to the expected range of metabolites. Criteria need to be carefully chosen in order to minimise the number of false-positives and -negatives. Further adaptations and improvements as well as the establishment of further criteria (e.g. automated EIC

correlation of signals that belong together; MS/MS fragmentation patterns) are subject of ongoing investigations.

Conclusion

We have established an LC-HR-MS method for the simultaneous quantification of selected mycotoxins and screening of fungal metabolites in food samples. A novel approach for the estimation of LODs of FT-Orbitrap data recorded in 'full-profile mode' was successfully applied, leading to reasonable chromatographic peak shapes and concentrations. LODs were within European Regulation limits (European Commission 2006, 2007) for FB₁, FB₂, DON and ZON (with few exceptions for baby food, 'bread, pastries and biscuits' and processed cereal-based food). The basic applicability of the method could be shown by the quantification of several test materials, also including one animal feed sample. The performance of the method for the analysis of animal feed as a highly complex matrix will be further investigated in the future.

Additionally, the potential of HR-MS for retrospective analysis was shown. Since no common, accepted criteria for the screening/identification by LC-HR-MS exist, defined identification criteria were chosen. According to these criteria, 13 different metabolites were detected in proficiency testing materials in addition to the target toxins for which standards were available. Criteria for the confirmation of suspects need to be carefully chosen in order to minimise the possibilities for both false-positive and -negative findings. Further investigations for the screening and determination of suspect and non-target compounds will be conducted in the future to exploit fully the possibilities which FT-Orbitrap HR-MS can offer.

Acknowledgements

The authors thank the Federal Country Lower Austria and the European Regional Development Fund (ERDF) of the European Union for financial support (Grant Number GZ WST3-T-95/001-2006). Miroslav Fliieger and Marika Jestoi are acknowledged for providing mycotoxin standards. This work contributes to the doctoral thesis of Sylvia M. Lehner.

References

Bennet JW, Klich M. 2003. Mycotoxins. *Clin Microbial Rev.* 16:497–516.

Berger U, Oehme M, Kuhn F. 1999. Quantitative determination and structure elucidation of type A- and B-trichothecenes by HPLC/ion trap multiple mass spectrometry. *J Agric Food Chem.* 47:4240–4245.

Blokland MH, Zoontjes PW, Sterk SS, Stephany RW, Zweigenbaum J, van Ginkel LA. 2008. Confirmatory analysis of trenbolone using accurate mass measurement with LC/TOF-MS. *Anal Chim Acta.* 618:86–93.

Delaforge M, Andre F, Jaouen M, Dolgos H, Benech H, Gomis JM, Noel JP, Cavelier F, Verduci J, Aubagnac JL, et al. 1997. Metabolism of tentoxin by hepatic cytochrome P-450 3 A isozymes. *Eur J Biochem.* 250:150–157.

European Commission. 2002. 2002/657/EC. Commission decision of 12 August 2002 implementing Council Directive 96/23/EC concerning the performance of analytical methods and the interpretation of results. *Off J Eur Commun.* L221:8–36.

European Commission. 2006. Commission regulation (EC) No. 1881/2006 setting maximum levels for certain contaminants in foodstuffs. *Off J Eur Union.* L364:5–24.

European Commission. 2007. Commission regulation (EC) No. 1126/2007 of 28 September 2007 amending Regulation (EC) No 1881/2006 setting maximum levels for certain contaminants in foodstuffs as regards *Fusarium* toxins in maize and maize products. *Off J Eur Union.* L255:14–17.

European Commission. 2009. Method validation and quality control procedures for pesticide residues analysis in food and feed (Document No. SANCO/10684/2009); [cited 2011 June 9]. Available from: http://ec.europa.eu/food/plant/protection/resources/qualcontrol_en.pdf/

Harris DC. 2006. Quantitative chemical analysis. 7th ed. Houndmills (UK): Palgrave Macmillan.

Herebian D, Zühlke S, Lamshöft M, Spittler M. 2009. Multi-mycotoxin analysis in complex biological matrices using LC-ESI/MS: experimental study using triple stage quadrupole and LTQ-Orbitrap. *J Sep Sci.* 32:939–948.

Kaufmann A. 2009. Validation of multiresidue methods for veterinary drug residues; related problems and possible solutions. *Anal Chim Acta.* 637:144–155.

Kaufmann A, Butcher P, Maden K, Walker S, Widmer M. 2011. Development of an improved high-resolution mass spectrometry based multi-residue method for veterinary drugs in various food matrices. *Anal Chim Acta.* 700:86–94.

Keller BO, Sui J, Young AB, Whittall RM. 2008. Interferences and contaminants encountered in modern mass spectrometry. *Anal Chim Acta.* 627:71–81.

Kellmann M, Muenster H, Zomer P, Mol H. 2009. Full-scan MS in comprehensive qualitative and quantitative residue analysis in food and feed matrices: how much resolving power is required? *J Am Soc Mass Spectrom.* 20:1464–1476.

Krauss M, Singer H, Hollender J. 2010. LC-high-resolution MS in environmental analysis: from target screening to the identification of unknowns. *Anal Bioanal Chem.* 397:943–951.

Linsinger T. 2010. Comparison of a measurement result with the certified value. European Reference Materials' Application Note 1 (European Commission); [cited 2011 March 25]. Available from: http://www.erm-crm.org/ERM_products/application_notes/Pages/index.aspx/

Mol HGJ, Plaza-Bolaños P, Zomer P, de Rijk TC, Stolker AAM, Mulder PJP. 2008. Toward a generic extraction method for simultaneous determination of pesticides, mycotoxins, plant toxins, and veterinary

- drugs in feed and food matrixes. *Anal Chem.* 80: 9450–9459.
- Nielen MWF, van Engelen MC, Zuiderent R, Ramaker R. 2007. Screening and confirmation criteria for hormone residue analysis using liquid chromatography accurate mass time-of-flight, Fourier transform ion cyclotron resonance and Orbitrap mass spectrometry techniques. *Anal Chim Acta.* 586:122–129.
- Nielsen KF, Smedsgaard J. 2003. Fungal metabolite screening: database of 474 mycotoxins and fungal metabolites for dereplication by standardized liquid chromatography-UV-mass spectrometry methodology. *J Chromatogr A.* 1002:111–136.
- Sulyok M, Berthiller F, Krska R, Schuhmacher R. 2006. Development and validation of a liquid chromatography/tandem mass spectrometric method for the determination of 39 mycotoxins in wheat and maize. *Rapid Commun Mass Spectrom.* 20:2649–2659.
- Sulyok M, Krska R, Schuhmacher R. 2007. A liquid chromatography/tandem mass spectrometric multi-mycotoxin method for the quantification of 87 analytes and its application to semi-quantitative screening of moldy food samples. *Anal Bioanal Chem.* 389:1505–1523.
- van der Heeft E, Bolck YJC, Beumer B, Nijrolde AWJM, Stolker AAM, Nielen MWF. 2009. Full-scan accurate mass selectivity of ultra-performance liquid chromatography combined with time-of-flight and Orbitrap mass spectrometry in hormone and veterinary drug residue analysis. *J Am Soc Mass Spectrom.* 20:451–463.
- van Egmond HP, Schothorst RC, Jonker MA. 2007. Regulations relating to mycotoxins in food. *Anal Bioanal Chem.* 389:147–157.
- Vishwanath V, Sulyok M, Labuda R, Bicker W, Krska R. 2009. Simultaneous determination of 186 fungal and bacterial metabolites in indoor matrices by liquid chromatography/tandem mass spectrometry. *Anal Bioanal Chem.* 395:1355–1372.
- Wegscheider W, Rohrer C, Neubäck R. 1999. Validata (Excel-Makro zur Methodvalidierung), version 3.02.48.
- Xu Y, Heilier JF, Madalinski G, Genin E, Ezan E, Tabet JC, Junot C. 2010. Evaluation of accurate mass and relative isotopic abundance measurements in the LTQ-Orbitrap Mass Spectrometer for further metabolomics database building. *Anal Chem.* 82:5490–5501.
- Zachariasova M, Lacina O, Malachova A, Kostelanska M, Poustka J, Godula M, Hajslova J. 2010a. Novel approaches in analysis of *Fusarium* mycotoxins in cereals employing ultra performance liquid chromatography coupled with high-resolution mass spectrometry. *Anal Chim Acta.* 662:51–61.
- Zachariasova M, Cajka T, Godula M, Malachova A, Veprikova Z, Hajslova J. 2010b. Analysis of multiple mycotoxins in beer employing (ultra)-high-resolution mass spectrometry. *Rapid Commun Mass Spectrom.* 24:3357–3367.
- Zhang NR, Yu S, Tiller P, Yeh S, Mahan E, Emary WB. 2009. Quantitation of small molecules using high-resolution accurate mass spectrometers—a different approach for analysis of biological samples. *Rapid Commun Mass Spectrom.* 23:1085–1094.

Supplement Table 1. List of fungal metabolites for screening purpose.

Compound	Molecular formula	CAS	Exact monoisotopic mass of M [u]	m/z [M+H] ⁺	m/z [M+NH ₄] ⁺	m/z [M+Na] ⁺	m/z [M-H] ⁻
3-Acetyl-deoxynivalenol	C17H22O7	50722-38-8	338.13655	339.14383	356.17038	361.12577	337.12928
15-Acetyl-deoxynivalenol	C17H22O7	88337-96-6	338.13655	339.14383	356.17038	361.12577	337.12928
15-Monoacetoxyscirpenol	C17H24O6	2623-22-5	324.15729	325.16456	342.19111	347.14651	323.15001
16-Ketoaspergillimide	C20H27N3O4	199784-50-4	373.20016	374.20743	391.23398	396.18938	372.19288
2-Amino-14,16-dimethyloctadecan-3-ol	C20H43ON	540770-33-0	313.33447	314.34174	331.36829	336.32369	312.32719
3-O-Methylviridicatin	C16H13NO2	6152-51-4	251.09463	252.10191	269.12845	274.08385	250.08735
AAL-TA1 Toxin	C25H47NO10	79367-52-5	521.32000	522.32727	539.35382	544.30922	520.31272
Actinomycin D	C62H86N12O16	50-76-0	1254.62847	1255.63575	1272.66230	1277.61770	1253.62120
Aflatoxin B1	C17H12O6	1162-65-8	312.06339	313.07066	330.09721	335.05261	311.05611
Aflatoxin B2	C17H14O6	7220-81-7	314.07904	315.08631	332.11286	337.06826	313.07176
Aflatoxin G1	C17H12O7	1165-39-5	328.05830	329.06558	346.09213	351.04752	327.05103
Aflatoxin G2	C17H14O7	7241-98-7	330.07395	331.08123	348.10778	353.06317	329.06668
Aflatoxin M1	C17H12O7	6795-23-9	328.05830	329.06558	346.09213	351.04752	327.05103
Aflatoxin M2	C17H14O7	6885-57-0	330.07395	331.08123	348.10778	353.06317	329.06668
Agroclavine	C16H18N2	548-42-5	238.14700	239.15428	256.18082	261.13622	237.13972
Alamethicin F30	C92H150N22O25	27061-78-5	1963.11425	1964.12152	1981.14807	1986.10347	1962.10697
alpha-Zearalenol	C18H24O5	36455-72-8	320.16237	321.16965	338.19620	343.15160	319.15510
alpha-Zearalenol-4-O-glucoside	C24H34O10	135626-94-7	482.21520	483.22247	500.24902	505.20442	481.20792
Altenuene	C15H16O6	29752-43-0	292.09469	293.10196	310.12851	315.08391	291.08741
Altenusin	C15H14O6	31186-12-6	290.07904	291.08631	308.11286	313.06826	289.07176
Alternariol	C14H10O5	641-38-3	258.05282	259.06010	276.08665	281.04204	257.04555
Alternariolmethylether	C15H12O5	26894-49-5	272.06847	273.07575	290.10230	295.05769	271.06120
Altersolanol	C16H16O7	22268-16-2	320.08960	321.09688	338.12343	343.07882	319.08233
Altertoxin-I	C20H16O6	56258-32-3	352.09469	353.10196	370.12851	375.08391	351.08741
Antibiotic Y	C15H10O8	102426-44-8	318.03757	319.04484	336.07139	341.02679	317.03029
Apicidin	C34H49N5O6	183506-66-3	623.36828	624.37556	641.40211	646.35751	622.36101
Ascomycin	C43H69NO12	104987-12-4	791.48198	792.48925	809.51580	814.47120	790.47470

Aspercolorin	C25H28N4O5	29123-52-2	464.20597	465.21325	482.23980	487.19519	463.19869
Aspergillimide	C20H29N3O3	195966-93-9	359.22089	360.22817	377.25472	382.21011	358.21362
Asperlactone	C9H12O4	76375-62-7	184.07356	185.08084	202.10738	207.06278	183.06628
Asperloxine A	C21H19N3O5	223130-52-7	393.13247	394.13975	411.16630	416.12169	392.12519
Aspionene	C9H16O4	157676-96-5	188.10486	189.11214	206.13868	211.09408	187.09758
Aspyron	C9H12O4	17398-00-4	184.07356	185.08084	202.10738	207.06278	183.06628
Asterric Acid	C17H16O8	577-64-0	348.08452	349.09179	366.11834	371.07374	347.07724
Atpenin A5	C15H21Cl2NO5	119509-24-9	365.07968	366.08695	383.11350	388.06890	364.07240
Aureobasidin A	C60H92N8O11	127757-30-6	1100.68856	1101.69583	1118.72238	1123.67778	1099.68128
Aurofusarin	C30H18O12	13191-64-5	570.07983	571.08710	588.11365	593.06905	569.07255
Austdiol	C12H12O5	53043-28-0	236.06847	237.07575	254.10230	259.05769	235.06120
Austocystin A	C19H13ClO6	55256-58-1	372.04007	373.04734	390.07389	395.02929	371.03279
Avenacein Y	C15H10O8	102426-44-8	318.03757	319.04484	336.07139	341.02679	317.03029
Beauvericin	C45H57N3O9	26048-05-5	783.40948	784.41676	801.44331	806.39870	782.40220
beta-Zearalenol	C18H24O5	71030-11-0	320.16237	321.16965	338.19620	343.15160	319.15510
beta-Zearalenol-4-O-glucoside	C24H34O10	135626-93-6	482.21520	483.22247	500.24902	505.20442	481.20792
Brefeldin A	C16H24O4	20350-15-6	280.16746	281.17474	298.20128	303.15668	279.16018
Brevicompanine B	C22H29N3O2	215121-47-4	367.22598	368.23325	385.25980	390.21520	366.21870
Calphostin C	C44H38O14	121263-19-2	790.22616	791.23343	808.25998	813.21538	789.21888
Cephalosporin C	C16H21N3O8S	61-24-5	415.10494	416.11221	433.13876	438.09416	414.09766
Chaetocin	C30H28N6O6S4	28097-03-2	696.09532	697.10259	714.12914	719.08454	695.08804
Chaetoglobosin A	C32H36N2O5	50335-03-0	528.26242	529.26970	546.29625	551.25164	527.25515
Chanoclavin	C16H20N2O	2390-99-0	256.15756	257.16484	274.19139	279.14678	255.15029
Chetomin	C31H30O6N6S4	1403-36-7	710.11097	711.11824	728.14479	733.10019	709.10369
Chlamydosporol	C11H14O5	135063-30-8	226.08412	227.09140	244.11795	249.07334	225.07685
Citreoviridin	C23H30O6	25425-12-1	402.20424	403.21152	420.23806	425.19346	401.19696
Citrinin	C13H14O5	518-75-2	250.08412	251.09140	268.11795	273.07334	249.07685
Citromycetin	C14H10O7	478-60-4	290.04265	291.04993	308.07648	313.03187	289.03538
Cochliodinol	C32H30N2O4	11051-88-0	506.22056	507.22783	524.25438	529.20978	505.21328
Curvularin	C16H20O5	10140-70-2	292.13107	293.13835	310.16490	315.12029	291.12380
Cycloaspeptide A	C36H43N5O6	109171-13-3	641.32133	642.32861	659.35516	664.31056	640.31406
Cycloechinulin	C20H21N3O3	143086-29-7	351.15829	352.16557	369.19212	374.14751	350.15102
Cyclopenin	C17H14N2O3	19553-26-5	294.10044	295.10772	312.13427	317.08966	293.09317

Cyclopeptide	C17H16N2O2	50886-63-0	280.12118	281.12845	298.15500	303.11040	279.11390
Cyclopiazonic acid	C20H20N2O3	18172-33-3	336.14739	337.15467	354.18122	359.13661	335.14012
Cyclosporin A	C62H111N11O12	59865-13-3	1201.84137	1202.84864	1219.87519	1224.83059	1200.83409
Cyclosporin C	C62H111N11O13	59787-61-0	1217.83628	1218.84356	1235.87011	1240.82550	1216.82901
Cyclosporin D	C63H113N11O12	63775-96-2	1215.85702	1216.86429	1233.89084	1238.84624	1214.84974
Cyclosporin H	C62H111N11O12	83602-39-5	1201.84137	1202.84864	1219.87519	1224.83059	1200.83409
Cytochalasin A	C29H35O5N	14110-64-6	477.25152	478.25880	495.28535	500.24074	476.24425
Cytochalasin B	C29H37O5N	14930-96-2	479.26717	480.27445	497.30100	502.25639	478.25990
Cytochalasin C	C30H37O6N	22144-76-9	507.26209	508.26936	525.29591	530.25131	506.25481
Cytochalasin D	C30H37O6N	22144-77-0	507.26209	508.26936	525.29591	530.25131	506.25481
Cytochalasin E	C28H33O7N	36011-19-5	495.22570	496.23298	513.25953	518.21492	494.21843
Cytochalasin H	C30H39NO5	53760-19-3	493.28282	494.29010	511.31665	516.27204	492.27555
Cytochalasin J	C28H37NO4	56144-22-0	451.27226	452.27954	469.30608	474.26148	450.26498
Decarestrictine	C10H16O5	127393-89-9	216.09977	217.10705	234.13360	239.08899	215.09250
Dechlorogriseofulvin	C17H18O6	3680-32-8	318.11034	319.11761	336.14416	341.09956	317.10306
Deeopxy-deoxynivalenol	C15H20O5	88054-24-4	280.13107	281.13835	298.16490	303.12029	279.12380
Deoxybrevinamide E	C21H25N3O2	34610-68-9	351.19468	352.20195	369.22850	374.18390	350.18740
Deoxynivalenol	C15H20O6	51481-10-8	296.12599	297.13326	314.15981	319.11521	295.11871
Deoxynivalenol-3-glucoside	C21H30O11	131180-21-7	458.17881	459.18609	476.21264	481.16803	457.17154
Diacetoxyscirpenol	C19H26O7	2270-40-8	366.16785	367.17513	384.20168	389.15707	365.16058
Dihydroergosine	C30H39N5O5	7288-61-1	549.29512	550.30240	567.32894	572.28434	548.28784
Dihydroxyergotamine	C33H37N5O5	511-12-6	583.27947	584.28675	601.31329	606.26869	582.27219
Dihydrolysergol	C16H20N2O	18051-16-6	256.15756	257.16484	274.19139	279.14678	255.15029
Elymoclavine	C16H18N2O	548-43-6	254.14191	255.14919	272.17574	277.13113	253.13464
Elymoclavine fructoside	C22H28N2O6	12379-50-9	416.19474	417.20201	434.22856	439.18396	415.18746
Emodin	C15H10O5	518-82-1	270.05282	271.06010	288.08665	293.04204	269.04555
Enniatin A	C36H63N3O9	144446-20-8	681.45643	682.46371	699.49026	704.44565	680.44915
Enniatin A1	C35H61N3O9	4530-21-6	667.44078	668.44806	685.47461	690.43000	666.43350
Enniatin B	C33H57N3O9	917-13-5	639.40948	640.41676	657.44331	662.39870	638.40220
Enniatin B1	C34H59N3O9	19914-20-6	653.42513	654.43241	671.45896	676.41435	652.41785
Enniatin B2	C32H55N3O9	632-91-7	625.39383	626.40111	643.42766	648.38305	624.38655
Enniatin B3	C31H53N3O9	864-99-3	611.37818	612.38546	629.41201	634.36740	610.37090
Enniatin B4	C34H59N3O9	19893-21-1	653.42513	654.43241	671.45896	676.41435	652.41785

Enniatin J1	C31H53N3O9	19893-15-3	611.37818	612.38546	629.41201	634.36740	610.37090
Enniatin K1	C32H55N3O9	716318-00-2	625.39383	626.40111	643.42766	648.38305	624.38655
Equisetin	C22H31NO4	57749-43-6	373.22531	374.23258	391.25913	396.21453	372.21803
Ergine	C16H17N3O	478-94-4	267.13716	268.14444	285.17099	290.12638	266.12989
Erginine	C16H17N3O		267.13716	268.14444	285.17099	290.12638	266.12989
Ergocornine	C31H39N5O5	564-36-3	561.29512	562.30240	579.32894	584.28434	560.28784
Ergocorninine	C31H39N5O5	564-37-4	561.29512	562.30240	579.32894	584.28434	560.28784
Ergocristine	C35H39N5O5	511-08-0	609.29512	610.30240	627.32894	632.28434	608.28784
Ergocristinine	C35H39N5O5	511-07-9	609.29512	610.30240	627.32894	632.28434	608.28784
Ergocryptine	C32H41N5O5	511-09-1	575.31077	576.31805	593.34460	598.29999	574.30349
Ergocryptinine	C32H41N5O5	511-10-4	575.31077	576.31805	593.34460	598.29999	574.30349
Ergometrine	C19H23N3O2	60-79-7	325.17903	326.18630	343.21285	348.16825	324.17175
Ergometrinine	C19H23N3O2	479-00-5	325.17903	326.18630	343.21285	348.16825	324.17175
Ergosine	C30H37N5O5	561-94-4	547.27947	548.28675	565.31329	570.26869	546.27219
Ergosinine	C30H37N5O5	596-88-3	547.27947	548.28675	565.31329	570.26869	546.27219
Ergotamin	C33H35N5O5	113-15-5	581.26382	582.27110	599.29764	604.25304	580.25654
Ergotaminine	C33H35N5O5	639-81-6	581.26382	582.27110	599.29764	604.25304	580.25654
Ergovaline	C29H35N5O5	2873-38-3	533.26382	534.27110	551.29764	556.25304	532.25654
Ergovalinine	C29H35N5O5	3263-56-7	533.26382	534.27110	551.29764	556.25304	532.25654
Festuclavine	C16H20N2	569-26-6	240.16265	241.16993	258.19647	263.15187	239.15537
Fulvic Acid	C14H12O8	479-66-3	308.05322	309.06049	326.08704	331.04244	307.04594
Fumagillin	C26H34O7	23110-15-8	458.23045	459.23773	476.26428	481.21967	457.22318
Fumigaclavin A	C18H22N2O2	6879-59-0	298.16813	299.17540	316.20195	321.15735	297.16085
Fumitremorgin C	C22H25N3O3	118974-02-0	379.18959	380.19687	397.22342	402.17881	378.18232
Fumonisin B1	C34H59NO15	116355-83-0	721.38847	722.39575	739.42230	744.37769	720.38119
Fumonisin B2	C34H59NO14	116355-84-1	705.39356	706.40083	723.42738	728.38278	704.38628
Fumonisin B3	C34H59NO14	136379-59-4	705.39356	706.40083	723.42738	728.38278	704.38628
Fusaproliferin	C27H40O5	152469-17-5	444.28757	445.29485	462.32140	467.27680	443.28030
Fusarenone X	C17H22O8	23255-69-8	354.13147	355.13874	372.16529	377.12069	353.12419
Fusarielin A	C25H38O4	132341-17-5	402.27701	403.28429	420.31084	425.26623	401.26973
Fusidic Acid	C31H48O6	6990-06-3	516.34509	517.35237	534.37891	539.33431	515.33781
Fusaric acid	C10H13NO2	536-69-6	179.09463	180.10191	197.12845	202.08385	178.08735
Geodin	C17H12Cl2O7	427-63-4	397.99601	399.00328	416.02983	420.98523	396.98873

Gibberellic Acid	C19H22O6	77-06-5	346.14164	347.14891	364.17546	369.13086	345.13436
Glilotoxin	C13H14O4N2S2	67-99-2	326.03950	327.04677	344.07332	349.02872	325.03222
Griseofulvin	C17H17O6Cl	126-07-8	352.07137	353.07864	370.10519	375.06059	351.06409
HC-Toxin	C21H32N4O6	83209-65-8	436.23218	437.23946	454.26601	459.22141	435.22491
HT-2-Toxin	C22H32O8	26934-87-2	424.20972	425.21699	442.24354	447.19894	423.20244
hydrolyzed fumonisin B1	C22H47NO5	145040-09-1	405.34542	406.35270	423.37925	428.33464	404.33815
Kojic Acid	C6H6O4	501-30-4	142.02661	143.03389	160.06043	165.01583	141.01933
Lolitrein B	C42H55NO7	81771-19-9	685.39785	686.40513	703.43168	708.38707	684.39058
Lysergol	C16H18N2O	602-85-7	254.14191	255.14919	272.17574	277.13113	253.13464
Macrosporin	C16H12O5	22225-67-8	284.06847	285.07575	302.10230	307.05769	283.06120
Malformin C	C23H39N5O5S2	59926-78-2	529.23926	530.24654	547.27309	552.22848	528.23198
Marcfortine A	C28H35N3O4	75731-43-0	477.26276	478.27003	495.29658	500.25198	476.25548
Meleagrin	C23H23N5O4	71751-77-4	433.17500	434.18228	451.20883	456.16423	432.16773
Methysergide	C21H27N3O2	361-37-5	353.21033	354.21760	371.24415	376.19955	352.20305
Mevastatin	C23H34O5	73573-88-3	390.24062	391.24790	408.27445	413.22985	389.23335
Mevinolin	C24H36O5	75330-75-5	404.25627	405.26355	422.29010	427.24550	403.24900
Moniliformin	C4H2O3	71376-34-6	98.00039	99.00767	116.03422	120.98962	96.99312
Mycophenolic acid	C17H20O6	24280-93-1	320.12599	321.13326	338.15981	343.11521	319.11871
Neosolaniol	C19H26O8	36519-25-2	382.16277	383.17004	400.19659	405.15199	381.15549
Neoxaline	C23H25N5O4	71812-10-7	435.19065	436.19793	453.22448	458.17988	434.18338
NG012	C32H38O15	141731-76-2	662.22107	663.22835	680.25490	685.21029	661.21379
Nidulin	C20H17Cl3O5	10089-10-8	442.01416	443.02143	460.04798	465.00338	441.00688
Nivalenol	C15H20O7	23282-20-4	312.12090	313.12818	330.15473	335.11012	311.11363
Nornidulin	C19H15Cl3O5	33403-37-1	427.99851	429.00578	446.03233	450.98773	426.99123
Ochratoxin A	C20H18NO6Cl	303-47-9	403.08227	404.08954	421.11609	426.07149	402.07499
Ochratoxin alpha	C11H9ClO5	19165-63-0	256.01385	257.02113	274.04768	279.00307	255.00657
Ochratoxin B	C20H19NO6	4825-86-9	369.12124	370.12851	387.15506	392.11046	368.11396
O-Methylsterigmatocystin	C19H14O6	17878-69-2	338.07904	339.08631	356.11286	361.06826	337.07176
Oxaspirodion	C13H14O5	774538-95-3	250.08412	251.09140	268.11795	273.07334	249.07685
Paraheerquamide A	C28H35N3O5	77392-58-6	493.25767	494.26495	511.29150	516.24689	492.25039
Paspaline	C28H39NO2	11024-56-9	421.29808	422.30536	439.33191	444.28730	420.29080
Paspalinine	C27H31NO4	63722-91-8	433.22531	434.23258	451.25913	456.21453	432.21803
Paspalitrein A	C32H39NO4	63722-90-7	501.28791	502.29519	519.32173	524.27713	500.28063

Paspalitre B	C32H39NO5	63764-58-9	517.28282	518.29010	535.31665	540.27204	516.27555
Patulin	C7H6O4	149-29-1	154.02661	155.03389	172.06043	177.01583	153.01933
Paxilline	C27H33NO4	57186-25-1	435.24096	436.24824	453.27478	458.23018	434.23368
Penicillic acid	C8H10O4	90-65-3	170.05791	171.06519	188.09173	193.04713	169.05063
Penicillin G	C16H18O4N2S	61-33-6	334.09873	335.10600	352.13255	357.08795	333.09145
Penicillin V	C16H18N2O5S	87-08-1	350.09364	351.10092	368.12747	373.08286	349.08637
Penigequinolone A	C27H33NO6	180045-91-4	467.23079	468.23806	485.26461	490.22001	466.22351
Penitrem A	C37H44O6NCl	12627-35-9	633.28572	634.29299	651.31954	656.27494	632.27844
Pentoxifylline	C13H18N4O3	6493-05-6	278.13789	279.14517	296.17172	301.12711	277.13061
Pestalotin	C11H18O4	34565-32-7	214.12051	215.12779	232.15433	237.10973	213.11323
Phomopsin A	C36H45ClN6O12	64925-80-0	788.27840	789.28568	806.31222	811.26762	787.27112
Phycion	C16H12O5	521-61-9	284.06847	285.07575	302.10230	307.05769	283.06120
Pseurotin A	C22H25NO8	58523-30-1	431.15802	432.16529	449.19184	454.14724	430.15074
Pyrenophorol	C16H24O6	22248-41-5	312.15729	313.16456	330.19111	335.14651	311.15001
Pyripyropene A	C31H37NO10	147444-03-9	583.24175	584.24902	601.27557	606.23097	582.23447
Radicicol	C18H17ClO6	12772-57-5	364.07137	365.07864	382.10519	387.06059	363.06409
Roquefortine C	C22H23N5O2	58735-64-1	389.18518	390.19245	407.21900	412.17440	388.17790
Roridin A	C29H40O9	14729-29-4	532.26723	533.27451	550.30106	555.25645	531.25996
Rubellin D	C30H22O10	121325-49-3	542.12130	543.12857	560.15512	565.11052	541.11402
Rugulosin	C30H22O10	23537-16-8	542.12130	543.12857	560.15512	565.11052	541.11402
Satratoxin G	C29H36O10	53126-63-9	544.23085	545.23812	562.26467	567.22007	543.22357
Satratoxin H	C29H36O9	53126-64-0	528.23593	529.24321	546.26976	551.22515	527.22866
Scirpentriol	C15H22O5	2270-41-9	282.14672	283.15400	300.18055	305.13594	281.13945
Secalonic acid	C32H30O14	56283-72-8	638.16356	639.17083	656.19738	661.15278	637.15628
Setosusin	C29H38O8	182926-45-0	514.25667	515.26394	532.29049	537.24589	513.24939
Stachybotrylactam	C23H31NO4	163391-76-2	385.22531	386.23258	403.25913	408.21453	384.21803
Sterigmatocystin	C18H12O6	10048-13-2	324.06339	325.07066	342.09721	347.05261	323.05611
Sulochrin	C17H16O7	519-57-3	332.08960	333.09688	350.12343	355.07882	331.08233
T-2 Tetraol	C15H22O6	34114-99-3	298.14164	299.14891	316.17546	321.13086	297.13436
T-2 Toxin	C24H34O9	21259-20-1	466.22028	467.22756	484.25411	489.20950	465.21301
T-2 Triol	C20H30O7	34114-98-2	382.19915	383.20643	400.23298	405.18837	381.19188
Tentoxin	C22H30N4O4	28540-82-1	414.22671	415.23398	432.26053	437.21593	413.21943
Tenuazonic Acid	C10H15O3N	610-88-8	197.10519	198.11247	215.13902	220.09441	196.09792

Terphenyllin	C20H18O5	52452-60-5	338.11542	339.12270	356.14925	361.10464	337.10815
Territrein B	C29H34O9	70407-20-4	526.22028	527.22756	544.25411	549.20950	525.21301
Trichodermin	C17H24O4	4682-50-2	292.16746	293.17474	310.20128	315.15668	291.16018
Ustiloxin A	C28H43N5O12S	143557-93-1	673.26289	674.27017	691.29672	696.25211	672.25562
Ustiloxin B	C26H39N5O12S	151841-41-7	645.23159	646.23887	663.26542	668.22081	644.22432
Ustiloxin D	C23H34N4O8	158243-18-6	494.23766	495.24494	512.27149	517.22689	493.23039
Verrucaric acid	C27H34O9	3148-09-2	502.22028	503.22756	520.25411	525.20950	501.21301
Verrucarol	C15H22O4	2198-92-7	266.15181	267.15909	284.18563	289.14103	265.14453
Verrucofortin	C24H31N3O3	113706-21-1	409.23654	410.24382	427.27037	432.22576	408.22927
Verruculogen	C27H33O7N3	12771-72-1	511.23185	512.23913	529.26568	534.22107	510.22457
Viomellein	C30H24O11	55625-78-0	560.13186	561.13914	578.16569	583.12108	559.12459
Viridicatin	C15H11NO2	129-24-8	237.07898	238.08626	255.11280	260.06820	236.07170
Wortmannin	C23H24O8	19545-26-7	428.14712	429.15439	446.18094	451.13634	427.13984
Zearalenone	C18H22O5	17924-92-4	318.14672	319.15400	336.18055	341.13594	317.13945
Zearalenone-4-glucoside	C24H32O10	105088-14-0	480.19955	481.20682	498.23337	503.18877	479.19227
Zearalenone-4-sulfate	C18H22O8S	132505-04-5	398.10354	399.11081	416.13736	421.09276	397.09626

Note: M, intact molecule; u, unified atomic mass unit.

Determination of fungal bioactive compounds using LC-HRMS

Isotope-Assisted Screening for Iron-Containing Metabolites Reveals a High Degree of Diversity among Known and Unknown Siderophores Produced by *Trichoderma* spp.

Sylvia M. Lehner,^a Lea Atanasova,^b Nora K. N. Neumann,^a Rudolf Krska,^a Marc Lemmens,^c Irina S. Druzhinina,^b Rainer Schuhmacher^a

Center for Analytical Chemistry, Department for Agrobiotechnology (IFA-Tulln), University of Natural Resources and Life Sciences (BOKU), Vienna, Austria^a; Research Group Microbiology, Institute of Chemical Engineering, Vienna University of Technology, Vienna, Austria^b; Institute for Biotechnology in Plant Production, Department for Agrobiotechnology (IFA-Tulln), University of Natural Resources and Life Sciences (BOKU), Vienna, Austria^c

Due to low iron availability under environmental conditions, many microorganisms excrete iron-chelating agents (siderophores) to cover their iron demands. A novel screening approach for the detection of siderophores using liquid chromatography coupled to high-resolution tandem mass spectrometry was developed to study the production of extracellular siderophores of 10 wild-type *Trichoderma* strains. For annotation of siderophores, an in-house library comprising 422 known microbial siderophores was established. After 96 h of cultivation, 18 different iron chelators were detected. Four of those (dimerum acid, fusigen, coprogen, and ferricrocin) were identified by measuring authentic standards. *cis*-Fusarinine, fusarinine A and B, and des-diserylglycylferrirhodin were annotated based on high-accuracy mass spectral analysis. In total, at least 10 novel iron-containing metabolites of the hydroxamate type were found. On average *Trichoderma* spp. produced 12 to 14 siderophores, with 6 common to all species tested. The highest number (15) of siderophores was detected for the most common environmental opportunistic and strongly fungicidal species, *Trichoderma harzianum*, which, however, did not have any unique compounds. The tropical species *T. reesei* had the most distinctive pattern, producing one unique siderophore (*cis*-fusarinine) and three others that were present only in *T. harzianum* and not in other species. The diversity of siderophores did not directly correlate with the antifungal potential of the species tested. Our data suggest that the high diversity of siderophores produced by *Trichoderma* spp. might be the result of further modifications of the nonribosomal peptide synthetase (NRPS) products and not due to diverse NRPS-encoding genes.

Iron is the fourth most abundant element in earth's crust (1). It is an essential trace mineral required for a healthy diet by almost all organisms and is involved in electron transport in metabolic processes, such as respiration and photosynthesis (2). Despite its abundance in nature, the amount of bioavailable iron is limited, as atmospheric oxygen rapidly oxidizes iron to ferric oxyhydroxides (3) that are poorly soluble under neutral to alkaline pH (4). In the case of fungi, the minimum iron requirement for optimal growth was reported to be 10^{-5} to 10^{-7} M (corresponding to approximately 6 to 600 $\mu\text{g/liter}$) (5). One strategy of plants and microbes for accessing iron is the production and excretion of siderophores. Siderophores (from the Greek *sideros*, "iron," and *phorein*, "to carry something") are ferric-iron-chelating, low-molecular-mass compounds (500 to 1,500 Da) (6) that are produced under iron depletion (7). Microbial siderophores show a very high binding constant for iron ($>10^{30}$ M, depending on the pH), enabling them to extract iron even from stainless steel (8).

Interestingly, it has been shown that monohydroxamate and dihydroxamate siderophores of fungal origin increase iron uptake by plants. It was suggested that (hydrolysis products of) fungal siderophores can play an important role in increasing iron availability for plants in soils with small amounts of accessible iron (9). Most fungal siderophores belong to the group of hydroxamate siderophores. Hydroxamate siderophores share the structural unit *N*⁵-acyl-*N*⁵-hydroxyornithine (2) and can be divided into three distinct groups: fusarinines, coprogens, and ferrichromes. They differ in the types of building blocks (*N*⁵-acyl groups or amino acids) and how these building blocks are connected (ester/peptide bonds and/or head-to-head or head-to-tail order) (2, 10).

Most of the fungal siderophores contain three hydroxamate groups and form hexadentate octahedral complexes with Fe^{3+} (6). Moreover, they are usually synthesized with the aid of nonribosomal peptide synthetases (NRPSs) and are mostly derived from L-ornithine (2). The first step in the biosynthetic pathway is hydroxylation of L-ornithine by ornithine-*N*⁵-monooxygenases to *N*⁵-hydroxy-L-ornithine. Second, the hydroxamate group is formed by transfer of an acyl group from acyl-coenzyme A (CoA) derivatives to *N*⁵-hydroxyornithine. This results in *N*⁵-acyl-*N*⁵-hydroxy-L-ornithine with different possible acyl groups (Fig. 1). In a third step, NRPSs covalently link these units via ester or peptide bonds to linear or cyclic oligomeric iron chelators. Last, the NRPS products can be further modified by non-NRPS enzymes to yield a diversity of different siderophores originating from a single NRPS (8).

Many species of the filamentous mycotrophic fungus *Trichoderma* (teleomorph *Hypocrea*, Ascomycota, Dikarya) can be used

Received 26 July 2012 Accepted 28 September 2012

Published ahead of print 12 October 2012

Address correspondence to Rainer Schuhmacher, rainer.schuhmacher@boku.ac.at.

L.A. and N.K.N.N. contributed equally to the research.

Supplemental material for this article may be found at <http://dx.doi.org/10.1128/AEM.02339-12>.

Copyright © 2013, American Society for Microbiology. All Rights Reserved.
doi:10.1128/AEM.02339-12

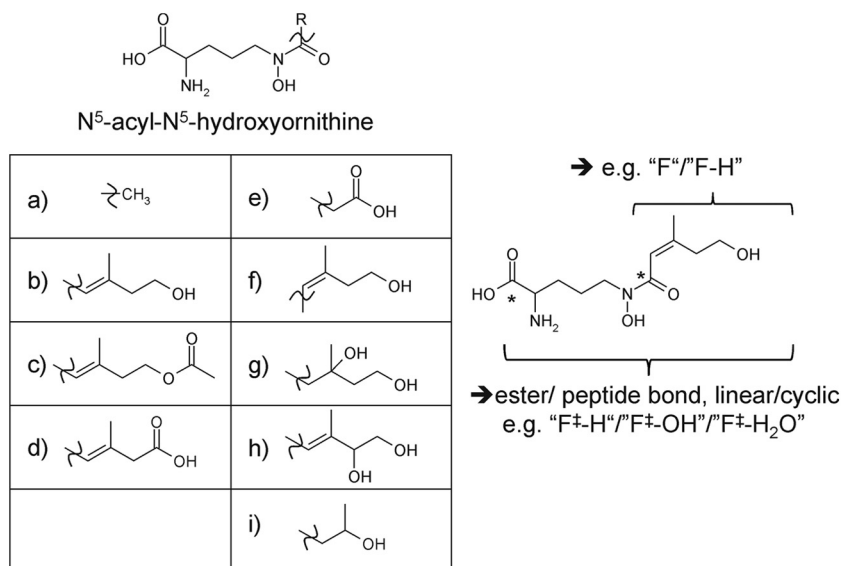


FIG 1 N^5 -Acyl- N^5 -hydroxyornithine units observed for known fungal siderophores; R can be any of the known residues shown in diagrams a to i (10). An example structure (by adding the moiety f to the N^5 -hydroxyornithine unit) is shown on the right. The asterisk indicates the polar acyl or ester/peptide bond, the cleavage of which results in either the moiety shown in capital letters and "±." The cleavage of these moieties results in characteristic siderophore fragments found in tandem mass spectrometry (see Table S2 in the supplemental material).

as agents of biological control of plant-pathogenic fungi (biocontrol) and are known siderophore producers (11). It has been shown that competition for iron plays a key role in the biocontrol exerted by *Trichoderma asperellum* strain T34 against *Fusarium oxysporum* f. sp. *lycopersici* (12). Dutta et al. (4) found that *Botrydiodia theobromae* and *Fusarium* spp. produced only small amounts of siderophores compared to *Trichoderma* spp., indicating a more efficient way for *Trichoderma* to access the available iron. However, our knowledge on the diversity of siderophores produced by the different *Trichoderma* species is slight. Anke et al. (13) investigated the siderophore production of nine morphologically defined *Trichoderma* strains and detected the siderophores coprogen, coprogen B, ferricrocin, and fusigen type in the culture broths and coprogen, ferricrocin, and palmitoylcoprogen from the mycelia. Other studies additionally reported on the occurrence of *cis*- and *trans*-fusarinine, dimerum acid, ferrichrome C, fusarinine B, fusigen (fusarinine C), and N^α -dimethylisonicoconoprogen II in various *Trichoderma* spp. (2, 14, 15).

Recent developments in mass spectrometry (MS) instrumentation give rise to new possibilities for the analysis of small molecules (e.g., metabolites present in biological samples) and exhibit both high mass resolution and good sensitivity. The acquisition of high-resolution full-scan mass spectral data allows for novel screening strategies by retrospective data analysis (16). Therefore, it can lead to novel insights into both the metabolic inventory of living systems and the underlying biological processes. These approaches are most powerful when combined with comprehensive database queries (17). Also, the diversity of *Trichoderma* species is well understood (reference 18 and references therein), and the genome sequences of three species (*T. atroviride*, *T. reesei*, and *T. virens*) are available (19, 20), enabling the interpretation of metabolites on the basis of the genes present.

In this study, liquid chromatography coupled with high-resolution mass spectrometry (LC-HRMS) was used to screen automatically for iron chelators/siderophores. The established method

was applied to culture broths of 10 different *Trichoderma* strains belonging to eight phylogenetic species in order to evaluate siderophore production. Moreover, interpretation of siderophore diversity and its relationship to the genetic inventory (NRPS genes) and taxonomy has been carried out for the first time.

MATERIALS AND METHODS

In-house siderophore library and tandem-MS (MS/MS) neutral-loss list of fungal siderophores. An in-house library of published siderophores was established. Therefore, elemental formulas and the most common ion species observed in electrospray ionization (ESI)-MS (protonated molecule, ammonium and sodium adduct) were calculated. The structures of many siderophores are available at Siderophore Base (http://bertrandsamuel.free.fr/siderophore_base/siderophores.php) and in an excellent review article by Hider and Kong (6).

To facilitate the interpretation of MS/MS spectra, common fragments of siderophore MS/MS spectra were collected from the literature, measurements of standard compounds, and theoretical considerations. Mass increments between two typical fragments in the MS/MS spectrum correspond to characteristic structural units of the intact siderophores (neutral losses [Fig. 1]) and were collected to form an MS/MS neutral-loss list.

Strains and reagents. The species and strains used in this study were selected based on their known mycoparasitic activity (I. S. Druzhinina and L. Espino de Ramer, unpublished data) (Table 1). We used the strongly opportunistic species *Hypocrea atroviridis*/*T. atroviride*, *T. asperellum*, *T. gamsii*, and *T. hamatum* from the section *Trichoderma*; *Hypocrea virens*/*T. virens*, *T. harzianum*, and the weak antagonist *T. pachybasioides*/*T. polysporum* from the section *Pachybasium*; and the moderate mycoparasite *H. jecorina*/*T. reesei* strain QM6a from the section *Longibrachiatum*. The strains are maintained at the Collection of Industrially Important Microorganisms (TUCIM) at Vienna University of Technology, Vienna, Austria. The origins of the respective strains and the GenBank accession numbers for their DNA barcodes are listed in Table 1.

Methanol (MeOH) (LiChrosolv; LC gradient grade), iron standard solution [1 g/liter Fe, Fe(NO₃)₃ in 0.5 mol/l HNO₃], Mg(NO₃)₂ · 6H₂O, MnSO₄ · 4H₂O, and CaCl₂ · 2H₂O were purchased from Merck (Darmstadt, Germany); acetonitrile (ACN) (HiPerSolv Chromanorm; high-performance liquid chromatography [HPLC] gradient grade), Tween 80, and

TABLE 1 Strains used in the study

Taxon	Code	TUCIM no.	Other collection code(s)	Origin	Ecology	Distribution	Mycoparasitic activity	DNA barcode marker
Section <i>Trichoderma</i>								
<i>Hypocrea atroviridis</i> / <i>Trichoderma atroviride</i>	at1680	1680	IMI 206040	Slovenia	Soil, dead wood	Cosmopolitan in temperate zones	Strong	http://genome.jgi-psf.org/Triat2/Triat2_home.html
	at2108 atP1	2108 4241	P1	Hungary	Soil Hybrid strain		Strong Strong	ITS1 and -2 rRNA, TUCIM unpublished ITS1 and -2 rRNA, GU197852
<i>T. asperellum</i>	asp	2128		Russia	Soil	Cosmopolitan	Strong	<i>tef1</i> ^c , TUCIM unpublished
<i>T. gamsii</i>	gam	2323		Italy	Soil	Cosmopolitan	Strong	<i>tef1</i> , EF488129
<i>T. hamatum</i>	ham	2689		Ethiopia	Rhizosphere of <i>Coffea arabica</i>	Cosmopolitan	Strong	ITS1 and -2 rRNA, TUCIM unpublished
Section <i>Pachybasium</i>								
<i>H. virens</i> / <i>T. virens</i>	vir	3530	CBS 249.59, Gv29-8 ^a	USA	Soil	Cosmopolitan	Strong	http://genome.jgi-psf.org/TriviGv29_8_2/TriviGv29_8_2_home.html
<i>H. pachybasioides</i> / <i>T. polysporum</i>	poly	462		Australia	Bark	Cosmopolitan, rare	Weak ^b	ITS1 and -2 rRNA, AY240169
<i>T. harzianum</i>	harz	916	CBS 226.95 ^a	UK	Soil	Cosmopolitan in temperate zones	Strong	<i>tef1</i> , AY605833
Section <i>Longibrachiatum</i>								
<i>H. jecorina</i> / <i>T. reesei</i>	rees	917	QM6a ^a	Solomon Islands	Military tents	Rare, tropical	Moderate	http://genome.jgi-psf.org/Trire2/Trire2_home.html

^a Type strain for the species.

^b I. S. Druzhinina and L. Espino de Rammer, unpublished data.

^c *tef1*, translation elongation factor 1 alpha gene.

ethanol were purchased from VWR (Vienna, Austria); formic acid (FA) (MS grade), nitric acid TraceSelect (69%), chloramphenicol, MgSO₄ · 7H₂O, ZnSO₄ · 7H₂O, K₂HPO₄, KNO₃, L-asparagine, D-glucose, CuSO₄ · 5H₂O, and reserpine were obtained from Sigma-Aldrich (Vienna, Austria). Ultrapure water (18.2 MΩcm) was prepared successively by reverse osmosis with an ELGA Purelab Ultra-AN-MK2 system (Veolia Water, Vienna, Austria) and used throughout the study. Nitric acid was diluted 1:200 with water (0.5% [vol/vol] HNO₃). Hydrochloric acid (HCl) (*pro analysis*; J. T. Baker) was purchased from Bartelt (Vienna, Austria).

Standards for siderophores (HPLC Calibration Kit Coprogens and Fusarinines and HPLC Calibration Kit Ferrichromes) were purchased from EMC (Tübingen, Germany).

Graphite furnace atomic absorption spectroscopy (GF-AAS). Fe determination of the cultivation medium was performed on a PerkinElmer 4100 ZL atomic absorption spectrometer equipped with a THGA graphite furnace and an AS-70 autosampler. Background correction was performed by longitudinal Zeeman effect. Platform atomization from a transversally heated pyrolytically coated graphite tube was applied. Argon was used as the purge gas, and Mg(NO₃)₂ (1.5 g/liter in 0.5% HNO₃ [vol/vol]) was used as the matrix modifier. Twenty microliters of sample and 10 μl modifier were injected (direct injection without further pretreatment). The temperature program consisted of 100°C for 6 s, 110°C for 30 s, 130°C for 45 s, 1,300°C for 30 s, 2,100°C for 4 s, and 2,400°C for 4 s. The working range was 5 μg/liter to 50 μg/liter Fe, and the limit of detection was estimated to be 2 μg/liter Fe by measuring blanks (0.5% [vol/vol] HNO₃) and low-Fe-matrix samples. Standard addition revealed no significant sensitivity change due to the matrix.

Cultivation conditions and sampling. All glassware was rinsed twice with 6 M HCl, followed by five times with ultrapure water prior to use in order to remove traces of iron.

The cultivation medium consisted of glucose (0.5% [mass/vol]), L-asparagine (0.5% [mass/vol]), K₂HPO₄ (0.08% [mass/vol]), KNO₃ (0.07% [mass/vol]), MgSO₄ · 7H₂O (0.05% [mass/vol]), CaCl₂ · 2H₂O (0.02% [mass/vol]), MnSO₄ · 4H₂O (0.001% [mass/vol]), ZnSO₄ · 7H₂O (0.001% [mass/vol]), and CuSO₄ · 5H₂O (0.0005% [mass/vol]). Chloramphenicol was prepared as a 30-mg/ml stock solution in 70% (vol/vol) ethanol and added to the liquid medium to a final concentration of 30 μg/ml to prevent bacterial contamination.

The fungal strains were pregrown on 2% (mass/vol) malt extract agar at 25°C with a 12-h light cycle. The inoculum was prepared after conidial maturation (2 to 3 days) by rolling a sterile, wetted cotton swab over conidiating areas. Conidia were suspended in sterile ultrapure water containing 0.03% (vol/vol) Tween 80 in disposable borosilicate test tubes. The concentration of the spore suspension was adjusted to a transmission of 0.31 using a Biolog turbidimeter (Biolog Inc., Hayward, CA) at an optical density at 590 nm (OD₅₉₀) corresponding to 6 × 10⁶ conidia per ml. Then, 100 μl of the conidial suspension was dispensed into each well of 24-well plates (each well contained 2 ml of liquid medium). The microplates (Greiner, Germany) were incubated under controlled conditions (25°C, 12-h light/dark cycle). Mycelial growth was measured at OD₇₅₀ after 24, 48, 72, and 96 h.

Culture broth from the wells was harvested after 48, 72, and 96 h and filtered through disposable syringe filters (0.45-μm cellulose; Asahi Glass Co., Ltd., Japan). Four technical replicates (inoculated from the same spore suspension) were taken for all strains. The three strains for which genome sequences are available (*T. atroviride* IMI 206040, *T. virens* Gv29-8, and *T. reesei* QM6a) were tested in three independent biological replicates.

Liquid chromatography–high-resolution (tandem) mass spectrometry analysis. To detect the ferriforms of the siderophores, 980 μl of filtered broth sample was mixed with 10 μl of aqueous FeCl₃ solution (2% [mass/vol] FeCl₃, 10% [vol/vol] FA) prior to LC-MS measurements.

Ten microliters and 20 μl of sample (full-scan MS and MS/MS measurements, respectively) were injected into the HPLC system (Accela; Thermo Fisher Scientific, San Jose, CA) equipped with a reversed-phase Atlantis dC₁₈ analytical column, 150- by 2.1-mm inside diameter (i.d.), 3-μm particle size (Waters, Vienna, Austria), and a C₁₈ 4- by 3-mm i.d. security cartridge (Phenomenex, Torrance, CA). The column temperature was maintained at 25°C. Eluent A was ultrapure water and eluent B was MeOH, both containing 0.1% (vol/vol) FA. For chromatographic separation, the initial mobile-phase composition (100% eluent A) was held constant for 1 min, followed by a linear gradient to 100% eluent B in 35 min. This final condition was held for 4.5 min, followed by 4-min column reequilibration at 100% eluent A. The flow rate was 200 μl/min.

The HPLC system was coupled to an Accela PDA (scan wavelength, 200 to 600 nm; bandwidth, 1 nm; scan rate, 20 Hz) and subsequently to an

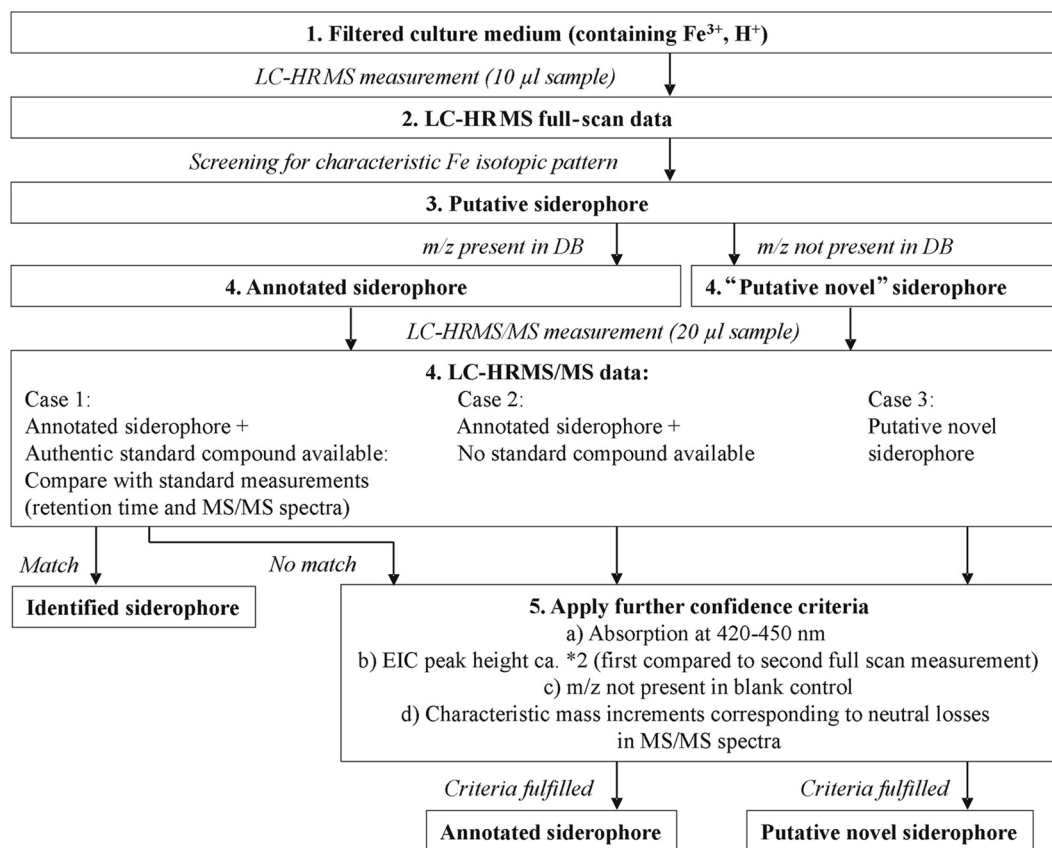


FIG 2 Work flow for the screening of siderophores by LC-HRMS(/MS).

LTQ Orbitrap XL (both Thermo Fisher Scientific) equipped with an ESI interface, which was operated in positive ionization mode using the following settings: electrospray voltage, 4 kV; sheath gas, 40 arbitrary units; auxiliary gas, 5 arbitrary units; capillary temperature, 300°C. All other source parameters were automatically tuned for a maximum MS signal intensity of reserpine solution. To this end, 10 µl/min of reserpine solution (10 mg/liter, dissolved in 8:2 [vol/vol] ACN-ultrapure water) was infused via syringe pump into the mobile phase (1:1 eluent A-eluent B) at a flow rate of 200 µl/min.

For the FT-Orbitrap full-scan and MS/MS measurements, the automatic gain control was set to a target value of 5×10^5 , and a maximum injection time of 500 ms was chosen.

For the initial full-scan measurements, the mass spectrometer was used with a resolving power setting of 100,000 full width at half-maximum (FWHM) (at a mass-to-charge ratio [*m/z*] of 400) and a scan range of *m/z* 200 to 2,000. For subsequent MS/MS measurements, a survey full scan was followed by two data-dependent MS/MS measurements of the 1st and 2nd most intense ions from a parent mass list (obtained by initial screening of full-scan MS measurements at a parent mass width of 20 ppm and an isolation width of 2), all with a resolving power setting of 30,000 FWHM (at *m/z* 400). One MS/MS measurement was done using collision-induced dissociation (CID) (35% normalized collision energy), and another MS/MS measurement was done using higher-energy collision dissociation (HCD) (38% normalized collision energy). Data were generated using Xcalibur 2.1.0 (Thermo Fisher Scientific). Samples were measured in a randomized manner.

Evaluation of LC-MS(/MS) data. The analytical workflow is shown in Fig. 2. In the first step, raw data were automatically screened for the natural iron isotopic pattern in order to detect (putative novel) iron chelators. Therefore, the mass spectra were investigated; to be regarded as a

possible iron chelator, a principal ion containing ⁵⁶Fe had to be accompanied by the corresponding ⁵⁴Fe isotopic signal at -1.99533 *m/z* with a maximum relative mass deviation of ± 5 ppm (from the calculated mass of the ⁵⁴Fe signal) in the same spectrum. Also, the relative intensity of the ⁵⁴Fe-containing ion species had to be between 4 and 7% compared to the peak originating from the ⁵⁶Fe-containing ion. A minimum intensity of 10,000 counts was required for the monoisotopic ion.

The extracted ion chromatograms (EICs) of possible identified iron chelators (⁵⁶Fe- and ⁵⁴Fe-containing ion species) were extracted from raw data, and the Pearson's correlation coefficients of those EICs were calculated; as a threshold, a correlation coefficient of 0.75 had to be exceeded. To achieve peak annotation, the *m/z* values obtained were compared with the calculated *m/z* values of the protonated molecule, the ammonium and the sodium adduct of siderophores present in the in-house siderophore library (maximum relative mass deviation, ± 5 ppm). In order to relate the peaks found to each other, for all putative iron chelators, the exact masses of ammonium and sodium adducts of each putative ion chelator were calculated and searched for in the spectra (maximum relative mass deviation, ± 5 ppm). Additionally, manual curation and annotation of uncommon adducts and in-source fragments were performed.

For *m/z* values of iron chelators found via the screening approach, an Xcalibur processing method (Genesis peak detection algorithm) was generated to determine peak areas in the Xcalibur Quan Browser (Thermo Fisher Scientific). In this way, it was also possible to find some of the iron chelators in samples where the automated screening originally had failed to detect them (strict criteria).

The putative siderophore *m/z* values that were detected in all replicates were included in a parent mass list for further MS/MS investigation. If available, MS/MS spectra were compared with the MS/MS spectra of authentic standard compounds in order to identify known siderophores. If

they were not available, further confidence criteria were applied to annotated siderophores (an m/z value was present in the in-house library, but no commercial standard was available) and “putative novel siderophores” (an m/z was not present in the in-house library). UV/visible (UV/Vis) chromatograms were evaluated at 420 to 450 nm, since most siderophores show absorption maxima between 420 nm and 450 nm (21). Between two full-scan measurements (first time, 10- μ l injection volume; second time, 20- μ l injection volume), the peak heights had to increase by approximately a factor of 2 in order to ensure that it was a reliable signal. Additionally, m/z values that also occurred in the blank control (culture medium plus ultrapure water, Tween 80, and aqueous FeCl₃ solution) were eliminated and not further considered. Finally, MS/MS spectra were searched for characteristic mass increments from the MS/MS neutral-loss list of fungal siderophores (see Table S2 in the supplemental material). First, the parent masses that were selected for further MS/MS investigation were tested if they exhibited the natural iron isotopic pattern. Base peaks of MS/MS spectra had to show a minimum intensity of 100 counts. Only fragment ions with a minimum relative intensity of 15% relative to the base peak were considered. For each fragment ion observed in an MS/MS spectrum, potential masses of related fragments were calculated based on the MS/MS neutral-loss list. The corresponding calculated m/z values were compared to the observed ions in a spectrum. To be correctly assigned, a maximum relative mass deviation of ± 10 ppm had to be achieved.

Fungal siderophores mostly possess a mass of ≥ 500 Da. Therefore, iron chelators found with our screening approach exhibiting a molecular mass below 500 Da were excluded from this study, since they might be the result of degradation processes.

Genome-wide screening for siderophore synthetase genes in *Trichoderma*. The publicly available genome databases (JGI; <http://genome.jgi-psf.org>) for *T. atroviride*, *T. reesei*, and *T. virens* were screened for NRPS genes that might be involved in the biosynthesis of siderophores. A similarity search (BLASTP) of all NRPS protein sequences found in *Trichoderma* genomes (19) as queries against all available fungal genomes revealed 353 homolog NRPS protein sequences. The multiple-sequence alignment was assembled in ClustalX (22), and the maximum-parsimony phylograms were constructed as implemented in PAUP*4.0b10 (heuristic search with 1,000 replicates; Maxtrees in effect). The resulting tree was screened for annotated siderophore synthetases. All orthologous NRPSs that are putatively involved in siderophore biosynthesis, as well as other orthologous genes found in the literature that contribute to siderophore synthesis, were independently analyzed by similarity searches (BLASTP) of their protein sequences in the NCBI database (<http://blast.ncbi.nlm.nih.gov/Blast.cgi>).

RESULTS

In-house siderophore library and MS/MS neutral-loss list of fungal siderophores. An in-house library of microbial siderophores was generated (as a Microsoft Excel spreadsheet), including siderophores described in the literature (6, 10, 23–40). The library contains the elemental formulas and theoretical masses of the protonated molecules and the ammonium and sodium adducts of ferriforms of published siderophores. In bi- and tetradentate iron chelators, the protonated molecule corresponds to the dimer $[\text{Fe}^{3+}\text{SID}_2\text{-3H}^+ + \text{H}]^+$ and in tetradentate and hexadentate chelators to $[\text{Fe}^{3+}\text{SID-3H}^+ + \text{H}]^+$. Currently, the in-house library consists of 422 entries of bacterial (ca. 90%) and fungal (ca. 10%) siderophores and is freely available on request from the laboratory of the corresponding author.

A list of m/z values originating from neutral losses caused by MS/MS fragmentation of known fungal siderophores was generated based on the literature (41–44) and MS/MS measurements of authentic siderophore standards (see Table S2 in the supplemental material). Additionally, the potential mass increments originating

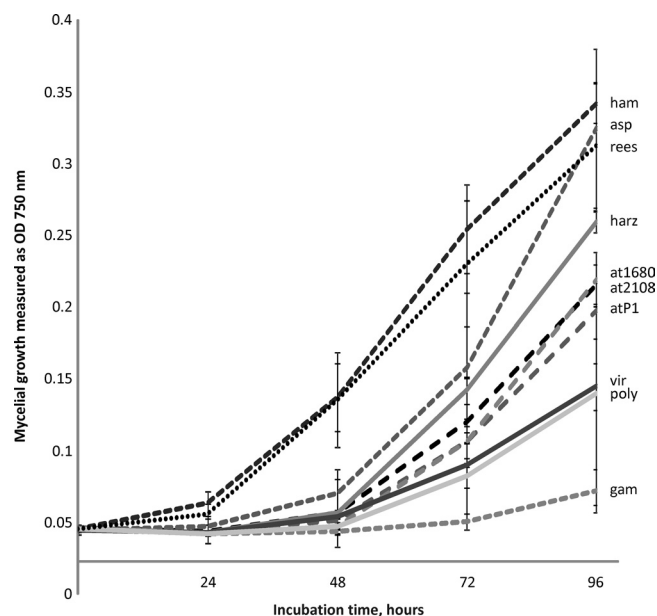


FIG 3 Growth of *Trichoderma* strains used in this study measured as mycelial density at OD₇₅₀. The strains were cultivated with supplementation by asparagine and zinc sulfate. The error bars show standard deviations; $n = 4$. ham, *T. hamatum*; asp, *T. asperellum*; rees, *T. reesei*; at1680, *T. atroviride* IMI 206040; at2108, *T. atroviride* TUCIM 2108; atP1, *T. atroviride* P1; harz, *T. harzianum*; poly, *T. polysporum*; gam, *T. gamsii*.

from neutral losses after rupture of the acyl bonds of N^5 -acyl- N^5 -hydroxyornithine units or the ester/peptide bonds between such building blocks (for known acyl groups a to i [10]) (Fig. 1) were added to the list of neutral losses. Not all of those neutral losses have been reported in the literature. Nevertheless, in analogy to earlier reports, fragmentation at these bonds can be expected due to the high polarity of the acyl bond (resulting in mass increments indicated as capital letters in Fig. 1). Moreover, the cleavage of an ester/peptide bond results in mass increments that are indicated as capital letters and “‡” in Fig. 1.

***Trichoderma* spp. are able to grow under conditions of Fe depletion.** We used a medium with neutral pH containing extra asparagine and zinc sulfate, because these conditions have been reported to be optimal for siderophore production (4, 13, 45). Chloramphenicol was added to the cultivation medium to prevent false-positive findings due to bacterial growth and thereby formation of bacterial siderophores. Prior to cultivation, growth media were measured by GF-AAS; the iron concentration was below 3 $\mu\text{g/liter}$ Fe (corresponding to approximately 5×10^{-8} M Fe, conditions of iron depletion). Under these low-iron conditions, no significant differences were detected in growth when medium with or without iron or asparagine was used; however, siderophore production was increased by asparagine and zinc sulfate supplementation (data not shown). *Trichoderma* strains were in the exponential growth phase at all time points when the samples were taken (Fig. 3). No conidiation was observed during the experiment.

Interestingly, under the conditions of the experiment, the 10 strains showed different growth rates, with *T. hamatum*, *T. asperellum*, and *T. reesei* producing the highest biomass after 96 h. *T. gamsii*, which is a fast-growing fungus on complex media (46), had an extended lag phase up to 72 h and started to develop my-

celial growth only close to the end of experiment. At the first sampling point (48 h), only *T. hamatum* and *T. reesei* had produced considerable biomass, while all other species had only begun to grow. However, nearly equal amounts and numbers of siderophores were detected at this time point for at least six tested strains: *T. hamatum*, *T. asperellum*, and *T. harzianum*, eight; *T. reesei*, *T. atroviride* IMI 206040, and *T. virens*, seven.

Trichoderma spp. produce a high diversity of extracellular iron chelators. Figure 4 shows that in total, 18 siderophores were detected for the tested *Trichoderma* species when following the established workflow (Fig. 2). Examples of EIC and UV/Vis chromatograms are shown in Fig. S1 in the supplemental material. Based on absolute measured signal intensities in the supernatants, the highest concentration of most extracellular (putative) siderophores was observed after a cultivation duration of 96 h. Therefore, these supernatants were used for MS/MS measurements. Under the tested conditions, characteristic neutral losses for hydroxamate siderophores (see Table S2 in the supplemental material) were found in the MS/MS spectra (Table 2) of all Fe-containing metabolites. For identified siderophores, the m/z in Table 2 corresponds to the protonated molecules. In cases of annotated/putative novel siderophores, the protonated molecule was annotated based on the presence of the most common adduct ions (if present in the mass spectra).

The highest number of iron chelators, 15, was found for *T. harzianum*, followed by 14 in cultures of two strains of *T. atroviride* (IMI 206040 and P1). *T. gamsii* and *T. reesei* displayed the lowest number, with only 12 iron chelators detected, while all other strains/species exhibited 13 siderophores (Fig. 4). Dimerum acid, coprogen, and fusigen (identified) were produced by all *Trichoderma* strains; ferricrocin (identified) was produced by all *Trichoderma* strains but *T. gamsii* and *T. polysporum* and was detected at relatively low abundance compared to the other siderophores. Also, fusarinine A was produced by all strains (annotated), although it was significantly more abundant in *T. harzianum* and *T. reesei* than in all other strains. *T. reesei* was the only strain that produced *cis*-fusarinine (annotated), which occurred as both a monomer and a dimer, the latter being more abundant. The EIC at m/z 798.309 showed three distinct characteristic peaks at different retention times: 11.7 min (*T. reesei* and *T. harzianum*), 12.7 min, and 13.2 min (all strains but *T. reesei*). This mass signal corresponds to the protonated molecules of the known isomeric siderophores fusarinine B and des-diserylglycylferrirhodin (DDF). The MS/MS spectra of all three of these iron chelators exhibit characteristic mass increments for hydroxamate siderophores. Both, fusarinine B and DDF consist of the same structural subunits (three N^5 -acyl- N^5 -hydroxyornithine units with three “F” residues [Fig. 1]) and corresponding neutral losses ($\Delta m/z$, 242.127, corresponding to $F\ddagger-H_2O$ [see Table S2 in the supplemental material]) were found in the MS/MS spectra of all three compounds. The chromatographic peak at 11.7 min exhibited extensive in-source fragmentation. Nevertheless, unambiguous assignment of the three MS/MS spectra to the two known siderophores was not possible. Moreover, seven putative novel siderophores were produced by *T. atroviride* strains IMI 206040 and P1 (similar patterns) and *T. harzianum*; six by *T. asperellum*, *T. atroviride* TUCIM 2108, *T. gamsii*, *T. hamatum*, *T. polysporum*, and *T. virens* (similar patterns); and two by *T. reesei* (m/z 798.309 was not considered a novel siderophore). The most distinctive profile of siderophores was found in *T. reesei*, which produces one

unique compound (*cis*-fusarinine) and three other iron-chelating metabolites present only in *T. harzianum* (Fig. 4). The siderophore production patterns of all other strains were relatively similar, with *T. harzianum* displaying the highest siderophore diversity. To see whether siderophore production and diversity correspond to the phylogeny of the genus, we constructed a cladogram, which shows the reasonable groupings within the genus (Fig. 4).

The three biological replicates of the sequenced *Trichoderma* strains revealed consistent qualitative siderophore profiles and only minor differences in relative siderophore abundances (see Table S1 in the supplemental material).

Although the three *T. atroviride* strains were isolated from different ecosystems and locations, they show similar siderophore production patterns. IMI 206040 and P1 produced 14 and TUCIM 2108 13 (putative) siderophores. They produced the same siderophores, the only exception being m/z 902.333 (18.9 min), which was not found in TUCIM 2108 (Fig. 4). The signal with m/z 902.333 showed very low intensity, which might explain why it was not found in the other strain.

Siderophore production in relation to genomic inventory. In order to understand the diversity of *Trichoderma* siderophores found in this study, we performed a phylogenetic analysis of all NRPS protein sequences found in the genomes of *T. atroviride*, *T. reesei*, and *T. virens*, as well as all their fungal orthologues obtained from the JGI genome database. Furthermore, we screened the literature for genes involved in siderophore production in other fungal genera and searched for homologs in *Trichoderma* genomes (Table 3).

Our phylogenetic analysis resulted in three clades containing orthologous genes related to siderophore biosynthesis (data not shown). (i) *T. atroviride* (gene ID 318290), *T. reesei* (gene ID 69946), and *T. virens* (gene ID 85582) orthologues coding for putative protein-containing domains consistent with *A. fumigatus* SidA (JGI genome annotation of *T. reesei*, gene ID 69946 [<http://genome.jgi-psf.org>]); (ii) *T. reesei* and *T. virens* orthologues (gene ID 71005 and 70206, respectively) related to nonribosomal peptide synthetase SidD in *A. fumigatus* and *A. clavatus*; (iii) a *Trichoderma* homolog of nonribosomal peptide synthetase, related to NPS6 (siderophore) of *Cochliobolus heterostrophus* (*T. atroviride*, *T. reesei*, and *T. virens*; gene ID 44273, 67189, and 39887, respectively), putatively involved in fusarinine synthesis in *Aspergillus nidulans*, *Aspergillus oryzae*, and *Fusarium graminearum* (47, 48). Furthermore, homologs of *sidL* and *sidC* genes involved in *A. fumigatus* biosynthesis of ferricrocin (49) and all homologs of *sidI*, *sidH*, and *sidF* genes, together with orthologues NPS6 and *sidD* stepwise involved in the biosynthesis of fusarinine C (49–51), were found in all three *Trichoderma* spp. (Table 3). However, the homolog of acetyltransferase SidG (51), which is required for conversion of fusarinine C (fusigen) into triacetylfusarinine C in *A. fumigatus*, was found only in *T. virens*.

DISCUSSION

In this study, we established an LC-HRMS/MS screening approach to study the production of extracellular iron-containing metabolites in microbial samples.

To facilitate the analysis of siderophores in microbial cultures, an in-house siderophore library was established containing 422 entries for bacterial (ca. 90%) and fungal (ca. 10%) siderophores. Fungal siderophores show higher structural similarity than bacte-



FIG 4 Siderophore production in *Trichoderma* species detected using full-scan and MS/MS measurements (signal intensities were normalized to mycelial production): *T. atroviride* (at2108, at1680, and atP1 for TUCIM 2108, IMI 206040, and P1, respectively), *T. hamatum* (ham), *T. virens* (vir), *T. harzianum* (harz), *T. polysporum* (poly), *T. asperellum* (asp), *T. gamsii* (gam), and *T. reesei* (rees). Dimerum acid, coprogen, fusigen, and ferricrocin were identified; fusarinine A, fusarinine B/DDF, and *cis*-fusarinine were annotated (no unambiguous annotation of fusarinine B/DDF was possible). The strains with sequenced genomes are marked with asterisks. The different colors represent different concentration ranges. The vertical cladogram was obtained based on a complete linkage rule using 1 – Pearson’s *R* distance. The vertical lines indicate standard deviations; *n* = 4.

rial siderophores, which allowed the generation of an MS/MS neutral-loss list of fungal siderophores. Subsequently, a novel screening method for siderophores was established using LC-HRMS/MS. The screening approach was applied to investigate the

production of extracellular siderophores of 10 wild-type *Trichoderma* strains attributed to eight species covering the three major sections of the genus. A number of strict screening criteria were defined in order to ensure that compounds were indeed iron

Lehner et al.

TABLE 2 Characteristic neutral losses of MS/MS spectra found for observed (putative novel) siderophores^r

Name (annotated)	<i>m/z</i> (retention time [min])	Elemental formula(s) corresponding to experimentally determined neutral losses in spectra ^a	
		CID	HCD
Fusarinine A	556.183 ^p (8.5)	C ₆ H ₈ O ₂ ^{a,b,c} , C ₆ H ₁₀ O ₃ ^c	C ₄ H ₄ ^d , C ₅ H ₆ ^d , C ₆ H ₈ O ₂ ^{a,b,c} , C ₁₁ H ₁₉ N ₂ O ₅ ^e
<i>cis</i> -Fusarinine (dimer)	574.193 ^q (10.0)	C ₆ H ₈ O ₂ ^{a,b,c} , C ₆ H ₁₀ O ₃ ^c (2×)	C ₃ H ₅ NO ₃ ^d , C ₅ H ₁₀ N ₂ O ₂ ^a , C ₅ H ₈ N ₄ O ₃ ^f , C ₁₁ H ₁₉ N ₂ O ₅ ^e , C ₁₁ H ₂₀ N ₂ O ₅ ^e , C ₁₁ H ₂₁ N ₂ O ₆ ^e
Fusarinine B/DDF ^o	798.309 ^d (11.7)	C ₆ H ₈ O ₂ ^{a,b,c} (3×), C ₆ H ₁₀ O ₃ ^c , C ₅ H ₁₀ N ₂ O ₂ ^a , C ₁₁ H ₁₈ N ₂ O ₄ ^g , C ₁₁ H ₂₀ N ₂ O ₅ ^e (2×)	
Fusarinine B/DDF ^o	798.309 ^d (12.7)	C ₄ H ₄ ^d (2×), C ₆ H ₁₀ O ₃ ^c , C ₅ H ₁₀ N ₂ O ₂ ^a , C ₇ H ₁₂ N ₂ O ₃ ^{a,g} (2×), C ₁₁ H ₁₈ N ₂ O ₄ ^g (3×), C ₁₁ H ₂₀ N ₂ O ₅ ^e	C ₆ H ₈ O ₂ ^{a,b,c} , C ₇ H ₁₂ N ₂ O ₃ ^{a,g} , C ₁₁ H ₁₈ N ₂ O ₄ ^g , C ₁₁ H ₂₀ N ₂ O ₅ ^e , C ₁₃ H ₂₀ N ₂ O ₅ ^{a,e,h}
Fusarinine B/DDF ^o	798.309 ^d (13.2)	C ₄ H ₄ ^d , C ₆ H ₁₀ O ₃ ^c , C ₁₁ H ₁₈ N ₂ O ₄ ^g , C ₁₁ H ₂₀ N ₂ O ₅ ^e	C ₂ H ₂ O ^{c,i} , C ₉ H ₁₆ N ₂ O ₄ ^c
Unknown	510.175 ^p (10.7)	C ₆ H ₈ O ₂ ^{a,b,c} (2×), C ₁₂ H ₁₉ NO ₄ ^b	C ₁₁ H ₁₇ N ₂ O ₅ ^e , C ₁₁ H ₁₉ N ₂ O ₅ ^e
Unknown	555.151 ^p (11.5)	C ₆ H ₈ O ₂ ^{a,b,c}	C ₅ H ₆ ^d
Unknown	651.220 ^p (11.8)	C ₂ H ₄ O ^b , C ₄ H ₄ ^d , C ₃ H ₅ O ⁱ , C ₅ H ₆ ^d , C ₆ H ₈ O ₂ ^{a,b,c} (2×), C ₄ H ₂ NO ₃ ^d , C ₅ H ₁₀ N ₂ O ₂ ^a , C ₅ H ₆ NO ₃ ^j , C ₉ H ₁₇ N ₂ O ₃ ^{j,k} (2×), C ₈ H ₁₂ N ₂ O ₅ ^e , C ₉ H ₁₇ N ₂ O ₄ ^e , C ₁₁ H ₁₇ N ₂ O ₄ ^e , C ₁₁ H ₁₈ N ₂ O ₄ ^g (2×), C ₁₁ H ₁₆ N ₂ O ₅ ^e , C ₁₁ H ₁₇ N ₂ O ₅ ^e (2×), C ₁₁ H ₁₈ N ₂ O ₅ ^e , C ₁₁ H ₁₉ N ₂ O ₅ ^e (3×), C ₁₁ H ₂₀ N ₂ O ₅ ^e (2×), C ₁₁ H ₂₁ N ₂ O ₅ ^e (2×), C ₁₁ H ₁₇ N ₂ O ₆ ^e , C ₁₁ H ₁₉ N ₂ O ₆ ^e , C ₁₁ H ₂₁ N ₂ O ₆ ^e	
Unknown	651.220 ^p (12.1)	C ₂ H ₂ O ^{c,i} (2×), C ₄ H ₄ ^d , C ₅ H ₆ ^d (2×), C ₆ H ₈ O ₂ ^{a,b,c} (2×), C ₆ H ₁₁ N ₂ O ₄ ^{a,i} , C ₉ H ₁₇ N ₂ O ₃ ^{j,k} (2×), C ₁₁ H ₁₇ N ₂ O ₄ ^e (2×), C ₁₁ H ₁₈ N ₂ O ₄ ^g (2×), C ₁₁ H ₁₉ N ₂ O ₄ ^e (2×), C ₁₁ H ₁₆ N ₂ O ₅ ^e , C ₁₁ H ₁₇ N ₂ O ₅ ^e (2×), C ₁₁ H ₁₈ N ₂ O ₅ ^e (2×), C ₁₁ H ₁₉ N ₂ O ₅ ^e (3×), C ₁₁ H ₂₀ N ₂ O ₅ ^e (2×), C ₁₁ H ₂₁ N ₂ O ₅ ^e , C ₁₁ H ₁₉ N ₂ O ₆ ^e , C ₁₁ H ₂₁ N ₂ O ₆ ^e	
Unknown	878.370 ^d (25.2)	C ₆ H ₈ O ₂ ^{a,b,c} , C ₆ H ₉ O ₃ ^c , C ₆ H ₁₀ O ₃ ^c (4×), C ₁₂ H ₁₉ NO ₄ ^b	C ₅ H ₆ ^d , C ₆ H ₈ O ₂ ^{a,b,c} , C ₆ H ₁₀ O ₃ ^c
Unknown	892.387 ^d (27.3)	C ₆ H ₈ O ₂ ^{a,b,c} (2×), C ₆ H ₈ O ₃ ^c , C ₆ H ₁₀ O ₃ ^c (3×), C ₁₂ H ₁₉ NO ₄ ^b	C ₂ H ₄ O ^b , C ₄ H ₄ ^d , C ₅ H ₆ ^d (2×), C ₆ H ₈ O ₂ ^{a,b,c} (3×), C ₆ H ₈ O ₃ ^c , C ₇ H ₁₆ N ₂ O ₂ ^k
Unknown	902.333 ^d (18.9)	C ₃ H ₅ O ⁱ , C ₄ H ₇ O ₂ ^c , C ₆ H ₈ O ₂ ^{a,b,c} , C ₁₁ H ₁₈ N ₂ O ₄ ^g , C ₉ H ₁₆ N ₂ O ₄ ^e , C ₅ H ₁₂ N ₂ O ⁱ , C ₅ H ₁₀ N ₂ O ₂ ^a	
Unknown	906.403 ^d (29.3)	C ₆ H ₈ O ₂ ^{a,b,c} , C ₆ H ₁₀ O ₃ ^c (3×), C ₁₂ H ₁₉ NO ₄ ^b	
Unknown	934.397 ^d (24.3)	C ₆ H ₈ O ₂ ^{a,b,c} , C ₅ H ₁₄ N ₂ O ^k , C ₆ H ₁₀ O ₃ ^c (4×), C ₈ H ₁₆ O ₃ ^m , C ₈ H ₁₃ N ₂ O ₅ ^e , C ₉ H ₁₇ N ₂ O ₄ ^e , C ₉ H ₁₇ N ₂ O ₅ ^e , C ₁₂ H ₁₉ NO ₄ ^b	C ₄ H ₄ ^d , C ₅ H ₆ ^d , C ₆ H ₈ O ₂ ^{a,b,c} , C ₆ H ₁₁ O ₃ ^c

^a Reported for fusarinines (20).

^b Reported for coprogens (20).

^c Expected/typical for acyl loss (e.g., F-H).

^d Reported for cyclic ferrioxamines (20).

^e Expected, typical for loss of N⁵-acyl-N⁵-hydroxyornithine unit (e.g., F[±]-H).

^f Reported for ferrichromes (41).

^g Reported for ferrichromes (20).

^h Observed for MS/MS measurement of triacetylfulsigen standard.

ⁱ Reported for Fe-rhodotoluate (20).

^j Expected, in analogy to observed neutral losses (20).

^k Reported for desferrioxamine B (42).

^l Observed for MS/MS measurement of fusigen standard.

^m Reported for dimerum acid (44) and observed for MS/MS measurement of dimerum acid standard.

ⁿ 2×/3×, neutral loss two/three times that observable in the MS/MS spectrum.

^o Unambiguous annotation not possible.

^p Ion species not identified.

^q Protonated molecule.

^r Siderophores for which standards were available are not included.

chelators produced by the fungi under investigation. They included verification of low-iron conditions by GF-AAS, addition of chloramphenicol to the culture medium in order to exclude bacterial contamination (production of bacterial siderophores), a realistic mass range allowing putative novel siderophores known

from former publications, a characteristic iron isotopic pattern present in the full-scan mass spectra, characteristic UV/Vis absorption of ferrisiderophores at 420 to 450 nm, increasing peak heights of putative novel siderophores in different measurements due to increased sample injection, measurement of a blank con-

TABLE 3 Identified and annotated siderophores detected in this study and the genes putatively involved in their synthesis

Siderophore name (<i>m/z</i> ; retention time [min])	Type	<i>T. virens</i>			<i>T. atroviride</i>			<i>T. reesei</i>			Reference(s)
		Gene name(s)	GenBank no.	E value ^b	GenBank no.	E value	GenBank no.	E value	Annotation		
All	All	<i>sidA</i>	EHK26838	2E-162	EHK44669	2E-144	EGR44632	1E-161	The initial biosynthetic step, shared by pathways of both intra- and extracellular siderophore biosynthesis, is catalyzed by the ornithine- <i>N</i> ^ε -monooxygenase SidA (in <i>A. fumigatus</i> XP_755103).	50	
Ferricrocin (771.248; 14.6)	Ferriochrome	<i>sidL</i>	EHK18514	5E-145	EHK46975	2E-144	EGR46972	9E-135	Biosynthesis of ferricrocin and hydroxyferricrocin involves acetylation of <i>N</i> ^ε -hydroxyornithine to <i>N</i> ^ε -acetyl- <i>N</i> ^ε -hydroxyornithine by SidL in <i>A. fumigatus</i> (XP_750195). In <i>A. fumigatus</i> , NRPS SidC (XP_753088; Sid2 in <i>U. maydis</i>) couples 3-acetylhydroxyornithine molecules to 1 serine and 2 glycine residues to yield cyclic ferricrocin.	49	
Coprogen (822.309; 18.2) Fusigen (780.299; 14.3) <i>cis</i> -fusarin (574.193; 10.0) Fusarinine A ^a (556.183; 8.5) Fusarinine B ^a (798.309; 12.7) Dimerum acid (538.172; 10.7)	Fusarinine/coprogen	<i>sidI</i>	EHK26839 NPS2	0E+00	EHK44670	0E+00	EGR44663	0E+00	Acyl-CoA ligase SidI in <i>A. fumigatus</i> (XP_753087) converts mevalonate to mevalonyl-CoA. Enoyl-CoA hydratase SidH in <i>A. fumigatus</i> (XP_748661) converts mevalonyl-CoA to anhydromevalonyl-CoA. In <i>A. fumigatus</i> , anhydromevalonyl-CoA is transferred to <i>N</i> ^ε -hydroxyornithine by the transacylase SidF (XP_748660) that is required for biosynthesis of fusarinine C and triacetyl-fusarinine C. NRPS related to NPS6 siderophore of <i>Cochliobolus heterostrophus</i> (AAX09988); NPS6 might produce a siderophore corresponding to fusarinine of <i>A. nidulans</i> , <i>A. oryzae</i> , and <i>F. graminearum</i> and coprogen in <i>Neurospora crassa</i> based on the domain structure of the predicted protein and sequence homology.	51	
		<i>sidH</i>	EHK21207, EHK20720, EHK20161	2E-102, 3E-89, 8E-85	EHK46085	3E-87	EGR44125, EGR44857, EGR49665	4E-98, 2E-91, 3E-84		51	
		<i>sidF</i>	EHK21208	0E+00	EHK45575	3E-129	EGR44134	0E+00		50	
		NPS6	EHK18682	0E+00	EHK46196	0E+00	EGR46022	0E+00		48 ^c	

<i>sidD</i>	ID 70206/EHK21211	0E+00	ID 71005/EGR44132	0E+00	50 ^c
					Siderophore synthetase SidD, homologous to NRPS of <i>Trichoderma</i> sp. NRPS SidD in <i>A. fumigatus</i> (XP_748662), transfers N ⁵ -α-anhydrovaleryl-N ⁵ -hydroxy-L-ornithine to fusarinine C.
<i>sidG</i>	EHK22271	2E-62			50, 51
					Acetyltransferase SidG is required for conversion of fusigen (fusarinine C) into triacetyl-fusarinine C in <i>A. fumigatus</i> (XP_748685).

^a Unambiguous annotation not possible.

^b E values refer to the query accession number listed in annotation.

^c Also *Trichoderma* genome annotation (<http://genome.jgi-psf.org/pages/home.jsf?query=Trichoderma&searchType=Keyword>).

trol to exclude false positives, and characteristic mass increments corresponding to neutral losses in MS/MS spectra of putative novel siderophores (Fig. 1).

Minor differences between the three biological replicates of the sequenced *Trichoderma* strains occurred and are explicable due to the already low intensity values (peak area, ca. 10⁴ counts · s) in the replicates where they were found; their absence in the other replicates is most likely due to concentration variations (see Table S1 in the supplemental material). Three iron chelators were found in two of three biological replicates in *T. reesei*; they were removed only from the *T. reesei* results (Fig. 4 and Table 2), since they were consistently found in *T. atroviride* IMI 206040 and *T. virens*.

The putative siderophore with *m/z* 1121.344 was consistently found in all *Trichoderma* samples. Since it showed perfect coelution with dimerum acid, it was excluded from the results because it was likely being generated during the ionization process in the ESI ion source.

The screening approach applied suggested high diversity in siderophore production by *Trichoderma* spp. In total, 18 different siderophores were detected in the culture filtrates. Ferricrocin plays an important role in intracellular iron storage (52) and is usually described as an intracellular siderophore. Nevertheless, it has been previously reported to be found as a minor component in *Trichoderma* culture filtrates (13). Possibly, small amounts of ferricrocin are washed out from the mycelium during filtration of the culture broths. Dimerum acid has so far been described only for *T. virens* (15). The possibility that its presence, as well as the presence of fusarinine A, in all samples is due to hydrolysis of larger siderophores cannot be ruled out, since they constitute subunits of many other, larger siderophores. In total, at least 10 putative novel siderophores were found using our screening approach.

Our findings demonstrate the potential of LC-HRMS(/MS) screening methods using selected criteria for the elucidation of (putative novel) metabolites of special interest, e.g., siderophores, relevant to the molecular mechanisms regarding their beneficial use, e.g., their use as biocontrol agents.

Examples of the characterization of novel siderophores. The putative siderophore with *m/z* 878.371 was produced by all *Trichoderma* strains but *T. reesei* (Fig. 4). Figure 5 shows the EIC, the MS spectrum, and the MS/MS spectrum of *m/z* 878.371. Investigation of the MS/MS spectra revealed the mass increment between two signals in the MS/MS spectrum corresponding to the neutral losses (calculated values) Δ130.063, which is typical for the loss of C₆H₁₀O₃ caused by cleavage of the acyl bond of the N⁵-acyl-N⁵-hydroxyornithine unit (corresponding to “G-H” in Fig. 1 and Table S2 in the supplemental material); Δ112.052, indicating a loss of C₆H₈O₂ caused by either the rupture of the acyl bond of the N⁵-acyl-N⁵-hydroxyornithine unit (corresponding to “B-H”/“F-H” in Fig. 1 and in Table S2 in the supplemental material), but also described by Mawji et al. (43) for fusarinines and coprogens; and Δ241.131 (C₁₂H₁₉NO₄), described by Mawji et al. (43) for coprogens. Interestingly, there were two more similar (putative) siderophores that eluted one after another with a mass difference of ca. Δ14.016 (CH₂), namely, *m/z* 892.387 and 906.403 (also present in all *Trichoderma* strains but *T. reesei*), and showing similar characteristic mass increments in the MS/MS spectra that might indicate that they correspond to a homologous siderophore differing in a single CH₂ group.

The diversity of siderophores corresponds to the ecology of *Trichoderma* species. In this study, we tested one relatively (in

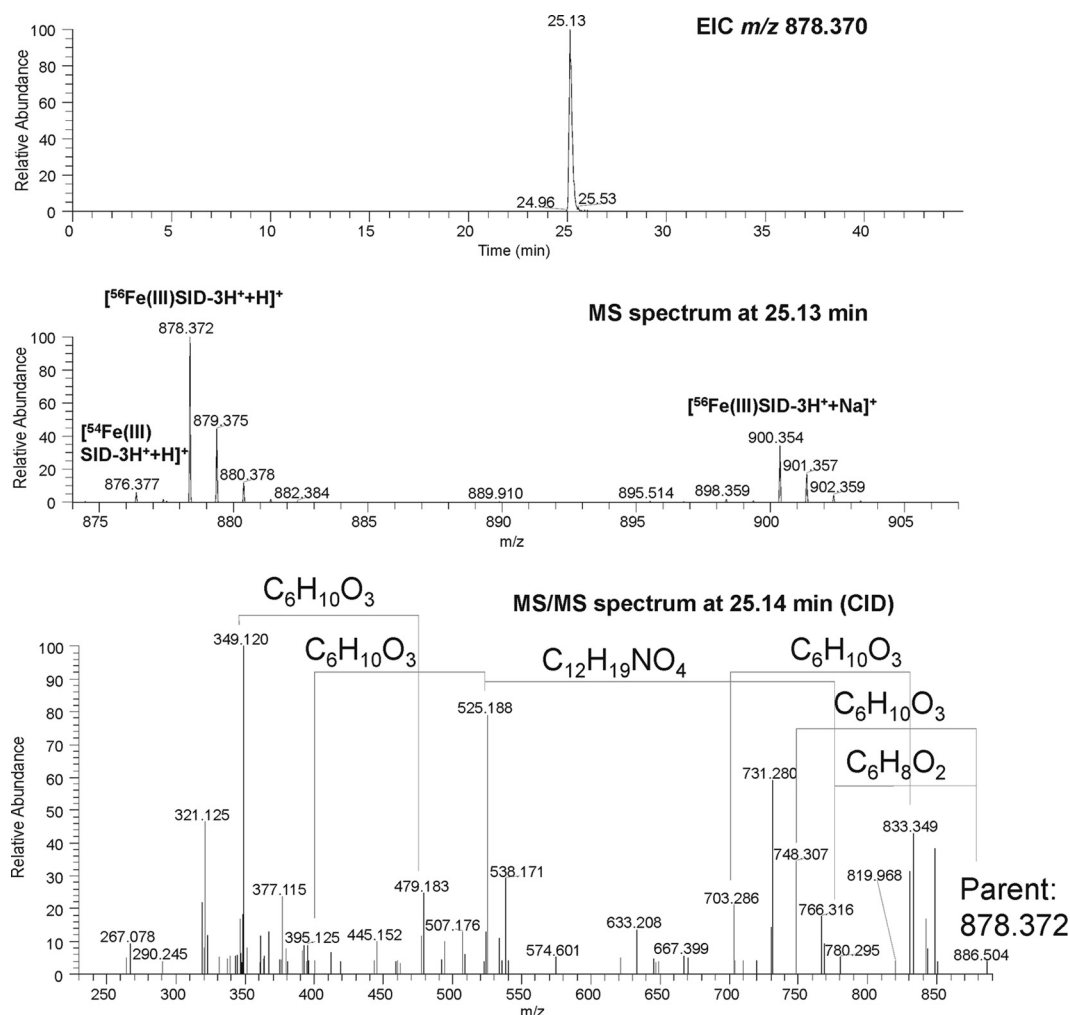


FIG 5 EIC of m/z 878.370 (± 5 ppm), MS spectrum at a retention time of 25.13 min, and MS/MS spectrum (using CID) of m/z 878.372 at 25.14 min in *T. polysporum*. Elemental formulas corresponding to characteristic neutral losses of siderophores are indicated in the MS/MS spectrum.

relation to the average for the genus [I. S. Druzhinina and L. Espino de Rammer, unpublished data]) weak mycoparasitic species (*T. polysporum*) and one moderate (*T. reesei*, [53]) and six strong antifungal agents. The results show that the diversity of siderophores is not reflected in the degree of antagonistic activity of *Trichoderma* spp., as *T. polysporum* and the strongly mycoparasitic *T. gamsii* both had 12 siderophores detected. However, comparison of the ecologies of the tested species suggests a habitat bias: *T. reesei*, the species with the most distinctive siderophore profile, is a rare tropical species that is known only from several specimens isolated from wood from low levels of tropical rain forests. Unlike all other *Trichoderma* species, *T. reesei* has never been isolated from soil. Moreover, the species has an outstanding capacity to secrete cellulose-degrading enzymes. All other species are powerful environmental opportunists that are cosmopolitan and frequently isolated from soil, the rhizosphere, dead wood, and other fungi. Analysis of opportunistic species related to *T. reesei* (e.g., *T. longibrachiatum*) will be necessary to verify this hypothesis.

Low diversity of genes coding for siderophore synthetases in *Trichoderma* might indicate post-synthetic modifications as a reason for high compound diversity. As in other filamentous as-

comycetes, *Trichoderma* siderophores are mostly produced nonribosomally by large multifunctional peptide synthetases, which are organized into repetitive synthase units. Each of the repetitive synthase units has functions required to complete a different single amino acid elongation step in the synthesis of the peptide product (15). The siderophores of *Trichoderma* spp. belong to the fusigen, ferrichrome, and coprogen families (54), and their orthologous NRPS gene clusters involved in siderophore synthesis (SidD and NPS6) have been identified in *T. atroviride*, *T. reesei*, and *T. virens* (19, 54).

Our phylogenetic analyses identified three clades involved in siderophore biosynthesis in three *Trichoderma* species: a putative ornithine- N^5 -monooxygenase, SidA; an NPS6 siderophore synthetase; and a putative nonribosomal peptide synthetase, SidD. The last two are orthologous enzymes, yet *T. atroviride* contains the SidD homolog, which is more closely related to NPS6 of *C. heterostrophus*, whereas the other two species share orthologues closely related to both SidD and NPS6.

The ornithine- N^5 -monooxygenase SidA is known to catalyze the initial step in siderophore biosynthesis in both intra- and extracellular siderophores (50). Genetic analysis of orthologues of *sidA* from *A. nidulans* (45, 55) and *A. fumigatus* (56), *dffA* from *A.*

oryzae (57), and *sid1* from *F. graminearum* (58) revealed that the expression of the gene is repressed by iron, whereas gene disruption blocks the synthesis of all the hydroxamate siderophores each fungus can synthesize (49).

Numerous publications on *Aspergillus* spp. and other siderophore-producing fungi have reported several other genes that might be involved in siderophore production. Recently, it was reported that the biosynthesis of ferricrocin and hydroxyferricrocin involves acetylation of N^5 -hydroxyornithine to N^5 -acetyl- N^5 -hydroxyornithine by the *sidL* gene (49). *sidL* was not found to be genomically clustered with other siderophore-biosynthetic genes, and it is not regulated by iron availability (49). We found that all three *Trichoderma* spp. possess a *sidL*-homologous gene that has 47 to 49% identity to *A. fumigatus*, with significant E values (Table 3).

Furthermore, Tobiasen et al. (47) recently reported that NPS2 encodes an NRPS with a composition analogous to the structure of SidC from *A. nidulans* (45) and Sid2 from *Ustilago maydis* (59), whose genes are known to produce the siderophores ferricrocin and ferrichrome, respectively. Schwecke et al. (60) concluded that NPS2 produces ferricrocin, based on the domain structure and architecture of the predicted enzyme. Additionally, it was shown that NPS2 in *F. graminearum* produces a siderophore corresponding to ferricrocin from *A. nidulans* (47). Corresponding to our detection of ferricrocin in *T. virens*, *T. atroviride*, and *T. reesei*, we found the highly similar orthologous genes *sidL* and *sidC* in the genomes of all three species (Table 3).

Moreover, it was recently shown that the biosynthesis of fusarinine- and coprogen-type siderophores in *A. fumigatus* requires five genes corresponding to *sidI*, *sidH*, *sidF*, *sidD*, and *sidF* (49–51), starting with the hydroxylation of ornithine, catalyzed by the monooxygenase SidA. Based on finding highly similar orthologues for all the genes involved in fusarinine C synthesis in *Trichoderma* spp. (Table 3), we propose that the production of fusarinine-type siderophores is similar to the well-understood process in *Aspergillus* spp. However, the nonribosomal siderophore synthetase SidD, which is involved in the last step of fusarinine C synthesis in *A. fumigatus* (51) (Table 3), or its orthologue NPS6 was present in all three *Trichoderma* spp., suggesting their important roles in fusarinine C production in *Trichoderma*.

We detected dimerum acid in all three *Trichoderma* spp., but until now, its production has been reported only for *T. virens* (15). Wilhite et al. (15) found that Psy1 disruptants produced normal amounts of gliotoxin in *T. virens* but grew poorly under low-iron conditions, suggesting that Psy1 plays a role in siderophore production. The disruptants could not produce the major *T. virens* siderophore dimerum acid, a dipetide of acylated N^5 -hydroxyornithine (15). However, Wiest et al. (61) described Psy1 as a fragment of peptaibol synthase, which is unrelated to siderophore biosynthesis, and furthermore, stressed that it is unlikely that it is involved in dimerum acid biosynthesis because of the numerous dimerum acid/coprogen-type siderophore producers that lack Psy1 orthologues (61).

However, the diversity of siderophores excreted by *Trichoderma* spp. is much higher than the number of NRPS genes present in their genomes (Table 3). Nevertheless, the siderophore production pattern is not reflected in the phylogenetic diversity of NRPS siderophore synthetases. However, further biosynthetic modification of NRPS products by non-NRPS enzymes, such as transacetylases and oxygenases, has been reported (8). Our data suggest that the great diversity of siderophores found in this study

might be the result of even more enzymes involved in the modification of siderophores. Modification by external enzymes (in *trans*-modifications) or enzymes that work postassembly could also support the diversity of siderophores found in our study (62). Such known modifications include glycosylation, halogenation, and oxidation/reduction.

Since the competition for iron can play a key role in the biological control exerted by *Trichoderma* spp., the new insights into the productivity and diversity of extracellular iron-containing metabolites that have been gained in our studies demonstrate the great value of the LC-HRMS/MS method developed for this research area.

ACKNOWLEDGMENTS

The Federal Country Lower Austria and the European Regional Development Fund (ERDF) of the European Union are acknowledged for financial support (grant number GZ WST3-T-95/001-2006) which also enabled the Ph.D. studies of Sylvia M. Lehner.

We thank Wolfgang Kandler for facilitation and support of the GF-AAS measurements. We are thankful to Christian P. Kubicek for the critical discussion of results. The assistance of Jasmin Dopplinger and Lukas Purgstaller in the establishment of the in-house siderophore library is gratefully acknowledged.

REFERENCES

- Riedel E. 1994. Anorganische Chemie, 3rd ed. De Gruyter, Berlin, Germany.
- Renshaw JC, Robson GD, Trinci APJ, Wiebe MG, Livens FR, Collison D, Taylor RJ. 2002. Fungal siderophores: structures, functions and applications. *Mycol. Res.* 106:1123–1142.
- Haas H. 2003. Molecular genetics of fungal siderophore biosynthesis and uptake: the role of siderophores in iron uptake and storage. *Appl. Microbiol. Biotechnol.* 62:316–330.
- Dutta S, Kundu A, Chakraborty MR, Ojha S, Chakrabarti J, Chatterjee NC. 2006. Production and optimization of Fe(III) specific ligand, the siderophore of soil inhabiting and wood rotting fungi as deterrent to plant pathogens. *Acta Phytopathol. Entomol. Hung.* 41:237–248.
- Loper JE, Buyer JS. 1991. Siderophores in microbial interactions on plant surfaces. *Mol. Plant Microbe Interact.* 4:5–13.
- Hider RC, Kong XL. 2010. Chemistry and biology of siderophores. *Nat. Prod. Rep.* 27:637–657.
- Lemanceau P, Expert D, Gaymard F, Bakker PAHM, Briat JF. 2009. Role of iron in plant-microbe interactions. *Adv. Bot. Res.* 51:491–549.
- Haas H, Eisendle M, Turgeon BG. 2008. Siderophores in fungal physiology and virulence. *Annu. Rev. Phytopathol.* 46:149–187.
- Hördt W, Römheld V, Winkelmann G. 2000. Fusarinines and dimerum acid, mono- and dihydroxamate siderophores from *Penicillium chrysogenum*, improve iron utilization by strategy I and strategy II plants. *Bio-metals* 13:37–46.
- Jalal MAF, van der Helm D. 1991. Isolation and spectroscopic identification of fungal siderophores. CRC Press, Boca Raton, FL.
- Benítez T, Rincón AM, Limón MC, Codón AC. 2004. Biocontrol mechanisms of *Trichoderma* strains. *Int. Microbiol.* 7:249–260.
- Segarra G, Casanova E, Aviles M, Trillas I. 2010. *Trichoderma asperellum* strain T34 controls Fusarium wilt disease in tomato plants in soilless culture through competition for iron. *Microb. Ecol.* 59:141–149.
- Anke H, Kinn J, Bergquist KE, Sterner O. 1991. Production of siderophores by strains of the genus *Trichoderma*: isolation and characterization of the new lipophilic coprogen derivative, palmitoylcoprogen. *Biol. Metals* 4:176–180.
- Jalal MA, Love SK, van der Helm D. 1986. Siderophore mediated iron(III) uptake in *Gliocladium virens*. 1. Properties of cis-fusarinine, trans-fusarinine, dimerum acid, and their ferric complexes. *J. Inorg. Biochem.* 28:417–430.
- Wilhite SE, Lumsden RD, Straney DC. 2001. Peptide synthetase gene in *Trichoderma virens*. *Appl. Environ. Microbiol.* 67:5055–5062.
- Krauss M, Singer H, Hollender J. 2010. LC-high resolution MS in environmental analysis: from target screening to the identification of unknowns. *Anal. Bioanal. Chem.* 397:943–951.

Lehner et al.

- H, Akita O. 2003. *dffA* gene from *Aspergillus oryzae* encodes L-ornithine N⁵ oxygenase and is indispensable for deferriferrichrysin biosynthesis. *J. Biosci. Bioeng.* 95:82–88.
58. Greenshields DL, Liu G, Feng J, Selvaraj G, Wei Y. 2007. The siderophore biosynthetic gene *SID1*, but not the ferroxidase gene *FET3*, is required for full *Fusarium graminearum* virulence. *Mol. Plant Pathol.* 8:411–421.
59. Yuan WM, Gentil GD, Budde AD, Leong SA. 2001. Characterization of the *Ustilago maydis* *sid2* gene, encoding a multidomain peptide synthetase in the ferrichrome biosynthetic gene cluster. *J. Bacteriol.* 183:4040–4051.
60. Schwecke T, Gottling K, Durek P, Duenas I, Kaufer NF, Zock-Emmenthal S, Staub E, Neuhof T, Dieckmann R, von Dohren H. 2006. Nonribosomal peptide synthesis in *Schizosaccharomyces pombe* and the architectures of ferrichrome-type siderophore synthetases in fungi. *Chembiochem* 7:612–622.
61. Wiest A, Grzegorski D, Xu BW, Goulard C, Rebuffat S, Ebbolle DJ, Bodo B, Kenerley C. 2002. Identification of peptaibols from *Trichoderma virens* and cloning of a peptaibol synthetase. *J. Biol. Chem.* 277:20862–20868.
62. Walsh CT, Chen H, Keating TA, Hubbard BK, Losey HC, Luo L, Marshall CG, Miller DA, Patel HM. 2001. Tailoring enzymes that modify nonribosomal peptides during and after chain elongation on NRPS assembly lines. *Curr. Opin. Chem. Biol.* 5:525–534.

SUPPLEMENTAL MATERIAL

Figure S1. Extracted ion chromatogram (EIC) of coprogen (a) and the putative new siderophore with m/z 892.387 (b) and corresponding UV/VIS chromatogram at 420-450 nm (c for coprogen, d for m/z 892.387) which is characteristic for ferri-siderophores. Note that the peak in the UV/VIS spectrum can be seen at a slightly earlier retention time since the detector is passed by the LC flow prior to the ESI ion source.

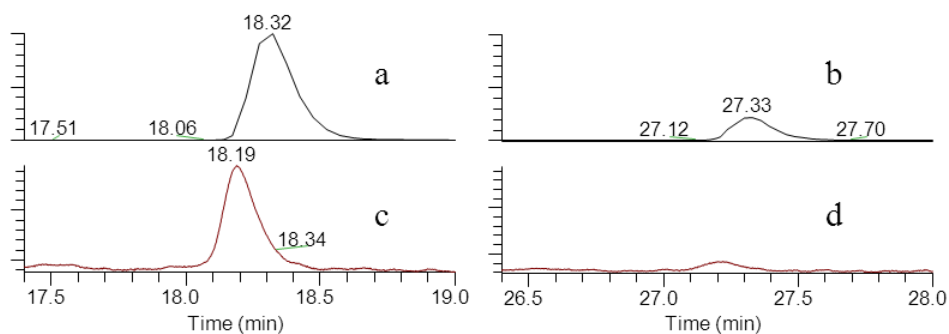


Table S1. Average area of biological replicates (four technical replicates each) after 96 hours of cultivation of *T. atroviride* IMI 206040, *T. virens* Gv29-8 and *T. reesei* QM6a. Differences between the biological replicates are indicated with grey background colour (n.d., not detected; * unambiguous annotation not possible); for the abbreviation of the strains see Table 1.

Siderophore	<i>m/z</i> (retention time [min])	at1680			vir			rees		
		Peak Area [counts*s]	Peak Area [counts*s]	Peak Area [counts*s]	Peak Area [counts*s]	Peak Area [counts*s]	Peak Area [counts*s]	Peak Area [counts*s]	Peak Area [counts*s]	Peak Area [counts*s]
Dimerum Acid	538.172 (10.7)	1.55E+08	1.44E+08	1.74E+08	1.37E+08	1.43E+08	1.69E+08	5.04E+07	5.43E+07	6.20E+07
Coprogen	822.309 (18.2)	6.56E+06	6.36E+06	7.38E+06	5.87E+06	9.03E+06	8.29E+06	1.67E+04	5.50E+03	3.37E+03
Fusigen	780.299 (14.3)	3.41E+08	5.20E+08	5.77E+08	1.80E+08	2.88E+08	2.20E+08	6.27E+07	8.53E+07	8.56E+07
Ferricrocin	771.248 (14.6)	4.40E+04	8.14E+04	1.27E+05	1.63E+04	1.52E+05	8.62E+04	1.48E+04	3.03E+04	3.57E+04
annotated: Fusarinine A	556.183 (8.5)	1.13E+05	1.96E+05	2.30E+05	2.86E+05	4.45E+05	6.01E+05	1.15E+07	1.12E+07	1.43E+07
annotated: Cis-fusarinine (Dimer)	574.193 (10.0)	n.d.	n.d.	n.d.	n.d.	n.d.	n.d.	3.15E+05	3.97E+05	6.89E+05
annotated: Fusarinine B/DDF*	798.309 (11.7)	n.d.	n.d.	n.d.	n.d.	n.d.	n.d.	3.94E+06	3.31E+06	4.11E+06
annotated: Fusarinine B/DDF*	798.309 (12.7)	3.82E+05	1.24E+06	1.42E+06	2.08E+05	1.17E+06	5.82E+05	n.d.	3.16E+04	3.71E+04
annotated: Fusarinine B/DDF*	798.309 (13.2)	1.06E+05	2.39E+05	3.72E+05	2.83E+05	5.58E+05	4.11E+05	n.d.	1.16E+04	1.29E+04
Unknown	510.175 (10.7)	n.d.	n.d.	n.d.	n.d.	n.d.	n.d.	1.74E+05	1.23E+06	1.36E+06
Unknown	555.151 (11.5)	n.d.	n.d.	n.d.	n.d.	n.d.	n.d.	2.17E+05	4.73E+05	6.12E+05
Unknown	651.220 (11.8)	3.89E+04	8.31E+03	1.24E+04	5.17E+04	1.58E+04	7.81E+04	n.d.	1.77E+04	2.24E+04
Unknown	651.220 (12.1)	1.03E+05	2.12E+04	2.85E+04	1.34E+05	3.11E+04	2.38E+05	n.d.	n.d.	n.d.
Unknown	878.370 (25.2)	8.07E+04	8.22E+04	1.02E+05	1.21E+05	4.52E+05	2.96E+05	n.d.	n.d.	n.d.
Unknown	892.387 (27.3)	5.07E+05	2.51E+04	8.17E+04	6.33E+05	4.37E+05	2.29E+05	n.d.	n.d.	n.d.
Unknown	902.333 (18.9)	1.01E+04	1.10E+04	3.07E+04	n.d.	n.d.	n.d.	n.d.	n.d.	n.d.
Unknown	906.403 (29.3)	8.79E+05	9.25E+05	1.46E+06	1.91E+06	6.74E+06	4.98E+06	n.d.	n.d.	n.d.
Unknown	934.397 (24.3)	4.88E+05	2.89E+04	3.69E+04	4.06E+05	2.00E+04	2.31E+04	n.d.	n.d.	n.d.

Table S2. List of mass increments between two typical fragments in the MS/MS spectrum corresponding to (characteristic) elemental formulas/ neutral losses for siderophores (observed and theoretical); asterisk indicates that the increment is more than once in the list (isomer of different structural subunits). Capital letters indicate the rupture of the acyl bond, capital letters[‡] indicate rupture of the ester/peptide bond of the respective N⁵-acyl-N⁵-hydroxyornithine units (see also Fig. 1).

Optional structural description	Neutral loss	$\Delta m/z$	Reference/ derived from
	C ₅ H ₁₂ N ₂ * [‡]	100.10005	(3), observed for linear ferrioxamines
	C ₅ H ₁₂ N ₂ O	116.09496	(1), observed for linear ferrioxamines
	C ₄ H ₄ O ₂ +O	100.01605	(3), observed for linear ferrioxamines
	C ₄ H ₇ NO ₃	117.04259	(3); contains a moiety similar to d and e (Fig 1., loss of hydroxamate)
	C ₅ H ₉ NO ₃	131.05824	expected, analog to C ₄ H ₇ NO ₃ for d (Fig. 1, loss of hydroxamate)
	C ₃ H ₅ NO ₃	103.02694	expected, analog to C ₄ H ₇ NO ₃ for e (Fig., 1, loss of hydroxamate)
	C ₄ H ₄	52.03130	(3), observed for cyclic ferrioxamines
	C ₅ H ₆	66.04695	(3), observed for cyclic ferrioxamines
“A [‡] -H ₂ O”	C ₇ H ₁₂ N ₂ O ₃ * [‡]	172.08479	(3), observed for ferrichromes
“B [‡] -H ₂ O”	C ₁₁ H ₁₈ N ₂ O ₄ * [‡]	242.12666	(3), observed for ferrichromes, also observed for dimerum acid (MS/MS of authentic standard)
“C [‡] -H ₂ O”	C ₁₃ H ₂₀ N ₂ O ₅ * [‡]	284.13722	expected, analog to “A [‡] -H ₂ O”, “B [‡] -H ₂ O” and “F [‡] -H ₂ O”
“D [‡] -H ₂ O”	C ₁₁ H ₁₆ N ₂ O ₅	256.10592	expected, analog to “A [‡] -H ₂ O”, “B [‡] -H ₂ O” and “F [‡] -H ₂ O”
“E [‡] -H ₂ O”	C ₈ H ₁₂ N ₂ O ₅	216.07462	expected, analog to “A [‡] -H ₂ O”, “B [‡] -H ₂ O” and “F [‡] -H ₂ O”
“F [‡] -H ₂ O”	C ₁₁ H ₁₈ N ₂ O ₄ * [‡]	242.12666	(3), observed for ferrichromes
“G [‡] -H ₂ O”	C ₁₁ H ₂₀ N ₂ O ₅	260.13722	expected, analog to “A [‡] -H ₂ O”, “B [‡] -H ₂ O” and “F [‡] -H ₂ O”
“H [‡] -H ₂ O”	C ₁₁ H ₁₈ N ₂ O ₅ * [‡]	258.12157	expected, analog to “A [‡] -H ₂ O”, “B [‡] -H ₂ O” and “F [‡] -H ₂ O”
“I [‡] -H ₂ O”	C ₉ H ₁₆ N ₂ O ₄	216.11101	expected, analog to “A [‡] -H ₂ O”, “B [‡] -H ₂ O” and “F [‡] -H ₂ O”
“Gly-H ₂ O”	C ₂ H ₃ NO	57.02146	(3), observed for ferrichromes

“Ser-H ₂ O”	C ₃ H ₅ NO ₂	87.03203	(3), observed for ferrichromes
“Ala-H ₂ O”	C ₃ H ₅ NO	71.03711	expected, analog to “A [‡] -H ₂ O”, “B [‡] -H ₂ O” and “F [‡] -H ₂ O”
“A [‡] -H”	C ₇ H ₁₃ N ₂ O ₄	189.08753	expected, analog to “A [‡] -H ₂ O”, “B [‡] -H ₂ O” and “F [‡] -H ₂ O”
“B [‡] -H”	C ₁₁ H ₁₉ N ₂ O ₅ *	259.12940	expected, analog to “A [‡] -H ₂ O”, “B [‡] -H ₂ O” and “F [‡] -H ₂ O”
“C [‡] -H”	C ₁₃ H ₂₁ N ₂ O ₆ *	301.13996	expected, analog to “A [‡] -H ₂ O”, “B [‡] -H ₂ O” and “F [‡] -H ₂ O”
“D [‡] -H”	C ₁₁ H ₁₇ N ₂ O ₆	273.10866	expected, analog to “A [‡] -H ₂ O”, “B [‡] -H ₂ O” and “F [‡] -H ₂ O”
“E [‡] -H”	C ₈ H ₁₃ N ₂ O ₆	233.07736	expected, analog to “A [‡] -H ₂ O”, “B [‡] -H ₂ O” and “F [‡] -H ₂ O”
“F [‡] -H”	C ₁₁ H ₁₉ N ₂ O ₅ *	259.12940	expected, analog to “A [‡] -H ₂ O”, “B [‡] -H ₂ O” and “F [‡] -H ₂ O”
“G [‡] -H”	C ₁₁ H ₂₁ N ₂ O ₆	277.13996	expected, analog to “A [‡] -H ₂ O”, “B [‡] -H ₂ O” and “F [‡] -H ₂ O”
“H [‡] -H”	C ₁₁ H ₁₉ N ₂ O ₆	275.12431	expected, analog to “A [‡] -H ₂ O”, “B [‡] -H ₂ O” and “F [‡] -H ₂ O”
“I [‡] -H”	C ₉ H ₁₇ N ₂ O ₅	233.11375	expected, analog to “A [‡] -H ₂ O”, “B [‡] -H ₂ O” and “F [‡] -H ₂ O”
“A [‡] -OH”	C ₇ H ₁₃ N ₂ O ₃	173.09262	expected, analog to “A [‡] -H ₂ O”, “B [‡] -H ₂ O” and “F [‡] -H ₂ O”
“B [‡] -OH”	C ₁₁ H ₁₉ N ₂ O ₄ *	243.13448	expected, analog to “A [‡] -H ₂ O”, “B [‡] -H ₂ O” and “F [‡] -H ₂ O”
“C [‡] -OH”	C ₁₃ H ₂₁ N ₂ O ₅ *	285.14505	expected, analog to “A [‡] -H ₂ O”, “B [‡] -H ₂ O” and “F [‡] -H ₂ O”
“D [‡] -OH”	C ₁₁ H ₁₇ N ₂ O ₅	257.11375	expected, analog to “A [‡] -H ₂ O”, “B [‡] -H ₂ O” and “F [‡] -H ₂ O”
“E [‡] -OH”	C ₈ H ₁₃ N ₂ O ₅	217.08245	expected, analog to “A [‡] -H ₂ O”, “B [‡] -H ₂ O” and “F [‡] -H ₂ O”
“F [‡] -OH”	C ₁₁ H ₁₉ N ₂ O ₄ *	243.13448	expected, analog to “A [‡] -H ₂ O”, “B [‡] -H ₂ O” and “F [‡] -H ₂ O”
“G [‡] -OH”	C ₁₁ H ₂₁ N ₂ O ₅	261.14505	expected, analog to “A [‡] -H ₂ O”, “B [‡] -H ₂ O” and “F [‡] -H ₂ O”
“H [‡] -OH”	C ₁₁ H ₁₉ N ₂ O ₅ *	259.12940	expected, analog to “A [‡] -H ₂ O”, “B [‡] -H ₂ O” and “F [‡] -H ₂ O”
“I [‡] -OH”	C ₉ H ₁₇ N ₂ O ₄	217.11883	expected, analog to “A [‡] -H ₂ O”, “B [‡] -H ₂ O” and “F [‡] -H ₂ O”
	C ₅ H ₈ N ₄ O ₃	172.05964	(1), observed for ferrichromes
“F [‡] -H + COCH ₃ ”	C ₁₃ H ₂₁ N ₂ O ₆ *	301.13996	expected, analog to “A [‡] -H ₂ O”, “B [‡] -H ₂ O” and “F [‡] -H ₂ O”
“F [‡] -OH + COCH ₃ ”	C ₁₃ H ₂₁ N ₂ O ₅ *	285.14505	expected, analog to “A [‡] -H ₂ O”, “B [‡] -H ₂ O” and “F [‡] -H ₂ O”
“F [‡] -H ₂ O + COCH ₃ ”	C ₁₃ H ₂₀ N ₂ O ₅ *	284.13722	expected, analog to “A [‡] -H ₂ O”, “B [‡] -H ₂ O” and “F [‡] -H ₂ O”, observed for triacetylfuligin (MS/MS of authentic standard)
”I [‡] -H ₂ O + COCH ₃ ”	C ₁₁ H ₁₈ N ₂ O ₅ *	258.12157	expected, analog to “A [‡] -H ₂ O”, “B [‡] -H ₂ O” and “F [‡] -H ₂ O”
”NH ₂ COCH ₃ ”	C ₂ H ₅ NO	59.03711	(3), observed for fusarinines
	C ₅ H ₁₀ N ₂ O ₂	130.07423	(3), observed for fusarinines
	C ₅ H ₁₁ N ₂ O ₃	147.07697	observed for fusigen (MS/MS of authentic standard)
	C ₆ H ₁₁ N ₂ O ₄	175.07188	observed for fusigen (MS/MS of authentic standard)
	C ₇ H ₁₂ N ₂ O ₃ *	172.08479	(3), observed for fusarinines

“F-H + O”	C ₆ H ₈ O ₂ *	112.05243	(3), observed for fusarinines
“B [‡] -H ₂ O-H”	C ₁₁ H ₁₇ N ₂ O ₄	241.11883	expected, analog to “A [‡] -H ₂ O”, “B [‡] -H ₂ O” and “F [‡] -H ₂ O”
“B [‡] -OH + COCH ₃ ”	C ₁₃ H ₂₁ N ₂ O ₅ *	285.14505	expected, analog to “A [‡] -H ₂ O”, “B [‡] -H ₂ O” and “F [‡] -H ₂ O”
“A [‡] -OH + COCH ₃ ”	C ₉ H ₁₅ N ₂ O ₄	215.10318	expected, analog to “A [‡] -H ₂ O”, “B [‡] -H ₂ O” and “F [‡] -H ₂ O”
“B [‡] -OH + 2x CH ₃ ”	C ₁₃ H ₂₃ N ₂ O ₄	271.16578	expected, analog to “A [‡] -H ₂ O”, “B [‡] -H ₂ O” and “F [‡] -H ₂ O”
“A [‡] -OH + 2x CH ₃ ”	C ₉ H ₁₇ N ₂ O ₃	201.12392	expected, analog to “A [‡] -H ₂ O”, “B [‡] -H ₂ O” and “F [‡] -H ₂ O”
“H [‡] -OH + COCH ₃ ”	C ₁₃ H ₂₁ N ₂ O ₆ *	301.13996	expected, analog to “A [‡] -H ₂ O”, “B [‡] -H ₂ O” and “F [‡] -H ₂ O”
	C ₂ H ₄ O	44.02622	(3), observed for coprogens
“B-H”	C ₆ H ₈ O ₂ *	112.05243	(3), observed for coprogens
	C ₁₂ H ₁₉ NO ₄	241.13141	(3), observed for coprogens
	C ₁₃ H ₂₀ N ₂ O ₅ *	284.13722	(4), observed for coprogens (negative ionization mode)
	C ₂₂ H ₃₁ N ₄ O ₇ Fe	519.15422	(4), observed for coprogens (negative ionization mode)
”B [‡] -OH + palmitic acid”	C ₂₇ H ₄₉ N ₂ O ₅	481.36415	expected, analog to “A [‡] -H ₂ O”, “B [‡] -H ₂ O” and “F [‡] -H ₂ O”
“C ₆ H ₁₀ O ₂ + C ₂ H ₆ O”	C ₈ H ₁₆ O ₃	160.10995	observed for dimerum acid (MS/MS of authentic standard)
	C ₂ H ₂ O	42.01057	(1), observed for coprogens
	C ₃ H ₅ O	55.04220	(1), observed for coprogens
	C ₇ H ₁₆ N ₂ O ₂	160.12118	(2), observed for desferrioxamine B
	C ₁₁ H ₂₂ O ₄ N ₂	242.17428	(2), observed for desferrioxamine B
	C ₁₁ H ₂₃ N ₄ O ₃ Fe	315.11196	(2), observed for desferrioxamine B
	C ₁₄ H ₃₀ N ₄ O ₄	318.22671	(2), observed for desferrioxamine B
	C ₁₄ H ₂₇ N ₄ O ₃	299.20832	(2), observed for desferrioxamine B
	C ₉ H ₁₇ N ₂ O ₃	201.12392	(2), observed for desferrioxamine B
	C ₉ H ₁₉ N ₃ O ₃	217.14264	(2), observed for desferrioxamine B
	C ₁₆ H ₃₄ N ₅ O ₄	360.26108	(2), observed for desferrioxamine B
	C ₁₆ H ₃₁ N ₅ O ₄ Fe	413.17254	(2), observed for desferrioxamine B
	C ₅ H ₁₄ N ₂ O	118.11061	(2), observed for desferrioxamine B
	C ₅ H ₁₂ N ₂ *	100.10005	(2), observed for desferrioxamine B
	C ₆ H ₁₄ N ₂ O ₂	146.10553	(2), observed for desferrioxamine B
“A”	C ₂ H ₃ O	43.01839	expected, analog to “B-H”
“A-H”	C ₂ H ₂ O	42.01057	expected, analog to “B-H”
“B-H”=“F-H”	C ₆ H ₈ O ₂ *	112.05243	(3), observed in fusarinines and coprogens

“C”	C ₈ H ₁₁ O ₃	155.07082	expected, analog to “B-H”
“C-H”	C ₇ H ₁₀ O ₃	154.06300	expected, analog to “B-H”
“D”=”H-2H”	C ₆ H ₇ O ₃	127.03952	expected, analog to “B-H”
“H-H”	C ₆ H ₆ O ₃	126.03170	expected, analog to “B-H”
“E”	C ₃ H ₃ O ₃	87.00822	expected, analog to “B-H”
“E-H”	C ₃ H ₂ O ₃	86.00040	expected, analog to “B-H”
“G”	C ₆ H ₁₁ O ₃	131.07082	expected, analog to “B-H”
“G-H”	C ₆ H ₁₀ O ₃	130.06300	expected, analog to “B-H”
“G-2H”=”H”	C ₆ H ₉ O ₃	129.05517	expected, analog to “B-H”
“H-H”	C ₆ H ₈ O ₃	128.04735	expected, analog to “B-H”
“I”	C ₄ H ₇ O ₂	87.04461	expected, analog to “B-H”
“I-H”	C ₄ H ₆ O ₂	86.03678	expected, analog to “B-H”

References

1. **Gledhill, M.** 2001. Electrospray ionisation-mass spectrometry of hydroxamate siderophores. *Analyst* **126**:1359-1362.
2. **Groenewold, G. S., M. J. Van Stipdonk, G. L. Gresham, W. Chien, K. Bulleigh, and A. Howard.** 2004. Collision-induced dissociation tandem mass spectrometry of desferrioxamine siderophore complexes from electrospray ionization of UO₂²⁺, Fe³⁺ and Ca²⁺ solutions. *Journal of Mass Spectrometry* **39**:752-761.
3. **Mawji, E., M. Gledhill, P. J. Worsfold, and E. P. Achterberg.** 2008. Collision-induced dissociation of three groups of hydroxamate siderophores: ferrioxamines, ferrichromes and coprogens/fusigens. *Rapid Communications in Mass Spectrometry* **22**:2195-2202.
4. **Simionato, A. V. C., G. D. de Souza, E. Rodrigues, J. Glick, P. Vouros, and E. Carrilho.** 2006. Tandem mass spectrometry of coprogen and deferoxamine hydroxamic siderophores. *Rapid Communications in Mass Spectrometry* **20**:193-199.

The siderophores and siderophore biosynthesis genes of *Trichoderma virens*

James Hurley¹, Prasun K. Mukherjee², Sylvia M. Lehner³, Rainer Schuhmacher³, Irina S. Druzhinina⁴, Robert D. Stipanovic⁵, Gloria Vittone¹, and Charles M. Kenerley¹

¹Department of Plant Pathology & Microbiology, Texas A&M University, College Station, Texas 77843

²Crop Protection Division, Central Institute for Cotton Research, Shankar Nagar, Nagpur 440010, India

³Center for Analytical Chemistry, Department of Agrobiotechnology (IFA-Tulln), University of Natural Resources and Applied Life Sciences (BOKU) Vienna, Konrad Lorenz Strasse 20, A-3430 Tulln, Austria

⁴Research Group Microbiology, Institute of Chemical Engineering, Vienna University of Technology, Gumpendorfer Strasse 1a, A-1060 Vienna, Austria

⁵USDA, ARS, Southern Plains Agricultural Research Center, Cotton Pathology Research Unit, College Station, Texas 77845

Abstract:

The genomes of three *Trichoderma* spp. have been analyzed for the presence of genes for siderophore biosynthesis NRPSs (non-ribosomal peptide synthetases). All the three species (*reesei*, *virens* and *atroviride*) have a conserved NRPS (SidC) for predicted ferrichrome (intracellular siderophore) biosynthesis. *T. reesei* and *T. virens* harbour two genes for predicted extracellular siderophore biosynthesis (orthologues of NPS6 and SidD) while *T. atroviride* has only one (NPS6). The functions of the three siderophore biosynthesis genes have been analyzed by gene knockout in *T. virens*. An analytical method based on selected screening criteria, such as the characteristic UV/VIS absorption of ferri-siderophores and the characteristic iron isotopic pattern was applied to detect the siderophores produced by these strains. This chemical analysis showed that *T. virens* produces the intracellular siderophore ferricrocin and 12 (six unknown) extracellular siderophores belonging to the fusigen and coprogen type. Gene knockout experiments confirmed that the ferrichrome biosynthesis NRPS SidC is involved in biosynthesis of ferricrocin while the deletion of an orthologue of NPS6 abolished the production of ten of twelve extracellular siderophores. The deletion of SidD did not have any effect on siderophore

production. This is the first study on the genetics of siderophore production in any *Trichoderma* spp.

Introduction:

Fungal siderophores are known to be involved in iron acquisition and storage, as well as in pathogenicity on plants and animals (Lee et al. 2005; Oide et al. 2006; Renshaw et al. 2002; Winkelmann 2007; Hof et al. 2009; Schrettl et al. 2007). *Trichoderma* spp., as biocontrol agents, have the ability to attack other fungi in the soil/rhizosphere, and also can colonize roots that leads to the induction of host resistance in many crops (Mukherjee et al. 2012; Harmosa et al. 2012; Microbiology Special issue). Microbial competition is indeed a crucial component in the biocontrol process for *Trichoderma* spp. These fungi produce a large number of secondary metabolites that are involved in aid the establishment of them in the soil/rhizosphere as well as negating the deleterious effects of the oxidative burst that results from root colonization (Djonovic et al. 2006). Siderophores play a crucial role in microbial competition as iron is an essential and limiting component. The intracellular siderophore ferricrocin, involved in storage of iron in cells, is a virulence factor in the pathogenicity of *Aspergillus fumigatus* in mammals and *Cochliobolus heterostrophus*, *Gibberella zeae* and *Magnaporthe grisea* in their respective host plants (Hof et al. 2007; Oide et al. 2007; Schrettl et al. 2007; Wallner et al. 2009). Some recent studies have indicated the involvement of extracellular siderophores in biocontrol efficacy of *Trichoderma* spp. (Segarra et al. 2010). We have, in this study, attempted to establish the role of putative siderophore -NRPSs in the biosynthesis of intracellular ferrichrome and the extracellular siderophores in *Trichoderma virens* using a reverse genetics approach. In addition, culture filtrates of the wild type and the mutant strains were analysed regarding their siderophore production using a recently described method using liquid chromatography coupled to high resolution mass spectrometry (Lehner et al., 2013).

Materials and Methods:

Strains and culture conditions:

The wild-type strain of *T. virens* Gv29-8 (wild-type) was grown on potato dextrose agar (PDA) at 27°C, and the deletion mutants were grown on PDA supplemented

with 100 mg/mL hygromycinB. For siderophore extraction experiments, iron-free glass ware was prepared according to Oide et al. (2007). Conidial suspensions (10^6 /ml) of *T. virens* were inoculated into 100 ml Vogel's minimal medium supplemented with 1.5% sucrose (VMS) without any iron supplement (iron depleted) or supplemented with of 10 μ M FeSO₄ (iron replete) and placed on an incubator shaker at 125 rpm maintained at 27^o C.

Identification of genes putatively involved in siderophores biosynthesis:

The *sidC* gene was identified by TBASTN search on the JGI genome portal (http://genome.jgi-psf.org/TriviGv29_8_2/TriviGv29_8_2.home.html) using *C. heterostrophus* (Acc. No. AY884187) sequence as an input. Similarly, using the *C. heterostrophus* NPS6 as an input, we identified two putative orthologs in the *T. virens* genome (designated as NPS6 and SidD, as the second one is identical with the *A. fumigatus* SidD). Both the orthologs are present in *T. reesei* genome, but only NPS6 is present in the *T. atroviride* genome. The genes in the neighborhood of *sidC*, *NPS6* and *sidD* were identified from the same genome portals as those of *T. virens*, *T. reesei* and *T. atroviride* (<http://genome.jgi-psf.org/programs/fungi>), and putative clusters from other fungi were included for comparison. The phylogenetic relationships using CLUSTALW software (www.ebi.ac.uk/clustalw/), and the domain architecture of the proteins were determined online (<http://pfam.sanger.ac.uk/search>).

Generation of loss-of-function mutants:

Loss-of-function mutants in *sidC* and *NPS6* were generated by single cross-over homologous recombination as described earlier for *T. virens* NRPSs (Mukherjee et al. 2012 Microbiol Spl. Issue). For *sidC*, part of the ORF (+4.5 kb to +6.5 kb) was amplified using the primer pair FeSals (CAG GGA GCA GTC GAC GAA G) and FeKpnas (GCA TGG CAG GTACCTGAA CTG), digested with Sall and KpnI and integrated into pATBS (harboring the hygromycin resistance cassette under the TrpC promoter; Mukherjee et al. 2003) that was pre-digested with the same set of enzymes. The resulting plasmid (pFeSCO) was used to transform *T. virens* protoplasts (Thomas and Kenerley, 1989), and the colonies screened by PCR with FeOuts (CAA TAC ATG CTG CAG TAA CCA C), a primer located upstream of FeSals, and M13F (a primer located on pBlueScript). This strategy identified

Determination of fungal bioactive compounds using LC-HRMS

homologous recombination events in the *sidC* locus. The putative recombinants were further purified by repeated single-spore isolation, and the purity of the mutants confirmed by PCR using FeOuts and FeOutas (CTG CGA TCT GAG CCG ATA TCT C, located downstream of FeKpnas). The conditions used for this PCR reaction (Taq polymerase and 3 min extension) do not yield any product for homologous recombinants, but amplifies a 2 kb band in wild- type strain. The mutation was further confirmed by Southern hybridization. The *NPS6* ortholog was disrupted using the same strategy as described for *sidC*. The *sidD* gene deletion was performed by a double cross-over homologous recombination strategy using the Gv10-4 strain (auxotroph for arginine). The gene deletion was confirmed by Southern analysis.

Cultivation of *Trichoderma* strains for siderophore profiling:

Wild-type and mutant strains were cultivated in liquid minimal medium. For each strain three independent biological replicate cultivations with four technical replicates (each inoculated from the same spore suspension) were conducted. The medium was composed as follows: glucose (0.5% ,m/V), L-asparagine (0.5% ,m/V), K₂HPO₄ (0.08%, m/V), KNO₃ (0.07%, m/V), MgSO₄·7H₂O (0.05%, m/V), CaCl₂·2H₂O (0.02%, m/V), MnSO₄·4H₂O (0.001%, m/V), ZnSO₄·7H₂O (0.001%, m/V), CuSO₄·5H₂O (0.0005%, m/V) and chloramphenicol (30 ppb, m/V). Fungal strains were pre-grown (2-3 days) on malt extract agar plates (2%, m/V). Then, a sterile, wetted cotton swab was rolled over conidiating areas. Conidia were suspended in water containing 0.03% (v/v) Tween 80. The spore suspension (borosilicate test tubes) was adjusted to a transmission of 0.31 using BIOLOG (Biolog Inc. Hayward, CA, USA) turbidimeter at O.D. 590 nm. Cultivation (25 °C, 12 h light/darkness cycle) was done using 24-well plates (Greiner, Germany) containing 2 mL liquid minimal medium and 100 µL of a conidial suspension. O.D. 750 nm (mycelial growth) was measured after 24, 48, 72 and 96 hours. Samples were harvested after 96 hours by filtration through disposable syringe filters (0.45 µm cellulose, Asahi Glass co., LTD., Japan) and samples were immediately prepared for LC-HRMS analysis.

Analysis of siderophore production using liquid chromatography – high resolution mass spectrometry (LC-HRMS):

A detailed protocol of the ⁵⁴Fe/⁵⁶Fe isotope pattern assisted screening approach for siderophores has been published elsewhere (Lehner et al., 2013). In brief, 10 µL of

aqueous FeCl₃ solution (2% (m/V) FeCl₃, 10% (v/v) formic acid) were added to 990 µL of culture filtrate prior to full scan LC-HRMS measurements. Ten µl of this sample solution were injected into the HPLC system (Accela, Thermo Fisher Scientific, San Jose, CA, USA) equipped with a reversed-phase Atlantis dC18 analytical column, 150 x 2.1 mm i.d., 3 µm particle size (Waters, Vienna, Austria) and a C18 4 x 3 mm i.d. security cartridge (Phenomenex, Torrance, CA, USA). The column temperature was held at 25 °C. Eluent A was ultrapure water, eluent B was methanol, both containing 0.1% (v/v) formic acid. For chromatographic separation (flow rate 200 µL min⁻¹), 100% A was held constant for 1 min, followed by a linear gradient to 100% B in 35 min. This final condition was held for 4.5 min, followed by 4 min column re-equilibration at 100% A. The HPLC system was coupled to an Accela PDA (scan wavelength 200-600 nm, bandwidth 1 nm, scan rate 20 Hz) and subsequently to an LTQ Orbitrap XL (both Thermo Fisher Scientific) equipped with an electrospray ionization (ESI) interface (operated in positive ionization mode). The full scan data was then automatically screened for the characteristic iron isotopic pattern by the aid of a recently developed in-house software programme. Subsequently, Pearson's correlation coefficient was calculated for the extracted ion current (EIC) chromatograms of the putative iron chelators (⁵⁶Fe and ⁵⁴Fe containing ion species) and had to exceed a value of 0.75 in order to be further considered as a potential siderophore. As siderophore reference standards, HPLC calibration kit coprogens & fusarinines and HPLC calibration kit ferrichromes were purchased from EMC Microcollections (Tuebingen, Germany).

Results:

The putative siderophore biosynthesis genes:

The *T. virens* *sidC* gene (protein ID 85582) is present as a single copy in the genome, consisting structurally as a 14616 bp ORF interrupted by two introns (a 57-bp intron close to the 5' end and a 79-bp intron close to the 3' end). An analysis of the genes in the proximity of *sidC* revealed the presence of ferricrocin synthesis related genes such as a transcription factor, L-ornithine-N5-oxygenase, an oxidoreductase and an aldehyde dehydrogenase (Fig. 1A). The organization of this putative cluster was fully conserved in the other two species of *Trichoderma*- *T. reesei* and *T. atroviride*, and fairly conserved in other fungal genomes examined. In the phylogenetic analysis of the whole *sidC* amino acid sequences, the *G. zeae* *sidC*

clustered with the *sidC* orthologs from *Trichoderma* spp. (Fig 1B). Interestingly, the *A. fumigatus* cluster aligned with the basidiomycete *Ustilago maydis*, and was distinctly different from the other ascomycete sequences (Fig. 1B). The modular organization of the *sidC* NRPSs from *Trichoderma* spp. revealed another interesting feature. The *T. reesei* and *T. atroviride* *sidC* have an identical modular organization (ATCATCTCATCTCT), that was different from *T. virens* (ATCATCTATCTCT), which seems to have suffered a loss of the third condensation domain during evolution (Fig. 1C). Similarly, the putative extracellular siderophore NRPSs were also part of large gene clusters (Fig. 2). A phylogenetic analysis of extracellular siderophore biosynthesis NRPSs, and their modular structure are presented in Fig. 3. As can be seen, the phylogenetic analysis clearly divides the fungal extracellular siderophore biosynthesis NRPSs into two groups- one represented by fusigen formed from SidD and the second siderophore coprogen formed by NPS6s (Fig. 3). The *Trichoderma* NPS6 orthologs belong to the second group while the extra genes (*sidD*) of *T. virens* and *T. reesei* belong to the former. Since *T. atroviride* is ancestor of the closely related *T. virens* and *T. reesei*, this additional gene/cluster may have been acquired by the common ancestor of *T. reesei/virens* by horizontal gene transfer.

Loss-of-function mutants:

Using the single cross-over homologous recombination strategy, we obtained two mutants each for *sidC* (Fig 4). The same strategy was used for deletion of *NPS6* resulting in the formation of two mutants. *sidD* was deleted using double cross-over homologous integration using arginine auxotrophy as a marker. The mutants showed a slightly lower germination rate. However, after 96 hours of cultivation, all tested strains formed approximately the same amount of biomass in liquid culture (Fig. 5).

Detection of siderophores in WT and mutants:

Table 1 provides an overview of the siderophores detected in the cultures of the wild-type and mutant strains. According to the applied screening criteria, the wild-type strain exhibited 13 distinguishable siderophores at different retention times with a mass range from m/z 500-1000. Some siderophores showed the same m/z value, but eluted at clearly different retention times, thus representing isomers of the same elemental composition but different molecular structure. Retention time and MS/MS spectrum were compared with those of authentic standard compounds to achieve

substance identification (dimerum acid, fusigen, ferricrocin, coprogen). If no standard compounds were available, annotation was performed by querying the observed m/z values against an in-house siderophore library (calculated m/z values of the protonated molecule, the ammonium and the sodium adduct, ± 5 ppm). Fusarinine A, fusarinine B and des-diserylglycylferrirhodin (DDF) were annotated. If no entry in the in-house siderophore library correlated to the observed m/z value, they were considered as “putative new”. Further confidence criteria (including the characteristic UV/VIS absorption at 420-450 nm, investigation of tandem MS spectra) were applied in order to ensure that those compounds indeed are siderophores.

Figure 6 shows typical EIC chromatograms (target $m/z \pm 5$ ppm) of the detected siderophores for the wild-type, *sidC* and *NPS6* mutant strains. The *sidD* mutant showed no qualitative differences regarding its siderophore production compared to the wild-type strain (no chromatogram shown). However, compared to the wild-type strain, the mutant strain *sidC* lacked ferricrocin production. The *NPS6* mutant produced only dimerum acid, fusigen and ferricrocin at detectable levels. For each of the tested *T. virens* strains, all twelve LC-HRMS analyses (three biological replicates, each consisting of four technical replicates) yielded consistent results with respect to both, type and pattern of the detected siderophores.

Discussion:

Trichoderma spp. are important fungi being widely used in industry and agriculture. Some isolates are also human pathogens. The understanding of the biology of these fungi has implications regarding their widespread applications. Since siderophores are known to be involved in interactions of fungi with plants and animals, and also involved in microbial interactions, knowledge of the genes involved for siderophore biosynthesis is important for strain development in these economically important fungi. So far, the siderophores coprogen, coprogen B, ferricrocin, coprogen, ferricrocin, *cis*- and *trans*-fusarinine, dimerum acid, ferrichrome C, fusarinine B, fusigen (fusarinine C), N^{α} -dimethylisoneocoprogen II and palmitoylcoprogen (associated with the mycelium) have been reported in various *Trichoderma* spp. (Anke et al., 1991; Jalal et al., 1986; Renshaw et al., 2002; Wilhite et al., 2001). We found dimerum acid, fusigen, ferricrocin, coprogen (all identified), fusarinine A, fusarinine B and DDF (annotated) as well as six unknown siderophores to be present in the culture filtrates of *T. virens* Gv29-8. In the present study, taking the advantage

of the genome sequence, we have identified putative siderophore NRPSs in *T. virens*, *T. atroviride* and *T. reesei*. Two of these fungi (*T. virens* and *T. reesei*) have two NRPSs (*sidD* and *NPS6*) for extracellular siderophores, while the third examined (*T. atroviride*) has only one (*NPS6*). The additional gene cluster in *T. virens* and *T. reesei* is non-functional as far as biosynthesis of siderophores is concerned. Gene knockout of *NPS6* affects biosynthesis of the annotated siderophores fusarinine A, fusarinine B, des-diserylglycyferrirhodin (DDF), the identified siderophore coprogen and all six unknown siderophores. All three species contain a highly conserved gene cluster for ferricrocin biosynthesis (*sidC*). We have thus, for the first time identified and established the role of siderophore gene clusters in *Trichoderma* spp. and investigated the effects of the gene knockouts on the metabolites level.

References

- Anke, H., Kinn, J., Bergquist, K.E., Sterner, O. 1991. Production of siderophores by strains of the genus *Trichoderma*. *Biometals* 4, 176-180.
- Baek, J.M., Kenerley, C.M. 1998. The *ARG2* gene of *Trichoderma virens*: Cloning and development of a homologous transformation system. *Fungal Genetics and Biology* 23, 34-44.
- Benitez, T., Rinco, A.M., Limon, M.C., Codon, A.C. 2004. Biocontrol mechanisms of *Trichoderma* strains. *International Microbiology* 7, 249-260.
- Eisendle, M., Oberegger, H., Zadra, I., Haas, H. 2003. The siderophore system is essential for viability of *Aspergillus nidulans*: functional analysis of two genes encoding L-ornithine N⁵-monooxygenase (*sidA*) and a nonribosomal peptide synthetase (*sidC*). *Molecular Microbiology* 49, 359-375.
- Haas, H., 2003. Molecular genetics of fungal siderophore biosynthesis and uptake: the role of siderophores in iron uptake and storage. *Applied Microbiological Biotechnology* 62, 316-330.
- Haas, H., Eisendle, M., Turgeon, B.G. 2008. Siderophores and fungal physiology and virulence. *Annual Review Phytopathology* 46, 149-187.
- Hof, C., Einfeld, K., Antelo, L., Foster, A.J., Anke, H. 2009. Siderophore synthesis in *Magnaporthe grisea* is essential for vegetative growth, conidiation, and resistance to oxidative stress. *Fungal Genetics & Biology* 46, 321-332.
- Howard, D.H., 1999. Acquisition, Transport and Storage of Iron by Pathogenic Fungi. *Clinical Microbiology Reviews* 12, 394-404.
- Howell, C.R. 2003. Mechanisms employed by *Trichoderma* species in the biological

- control of plant diseases: the history and evolution of current concepts. *Plant Disease* 87, 4-10.
- Jalal MA, Love SK, van der Helm D. 1986. Siderophore mediated iron (III) uptake in *Gliocladium virens*. 1. Properties of cis-fusarinine, trans-fusarinine, dimerum acid, and their ferric complexes. *J. Inorg. Biochem.* 28:417– 430.
- Lee, B.N., Kroken, S., Chou, D.Y., Robbertse, B., Yoder, O.C., Turgeon, G.C. 2005. Functional analysis of all nonribosomal peptide synthetases in *Cochliobolus heterostrophus* reveals a factor, NPS6, involved in virulence and resistance to oxidative stress. *Eukaryotic Cell* 4, 545-555.
- Lehner S.M., Atanasova L., Neumann N.K.N., Krska R., Lemmens M., Druzhinina I.S., Schuhmacher R. 2013. Isotope-assisted screening for iron-containing metabolites reveals a high degree of diversity among known and unknown siderophores produced by *Trichoderma* spp. *Applied and Environmental Microbiology* 79, doi:10.1128/AEM.02339-12. In press.
- Mei, B., Budde, A.D., Leong, S.A. 1993. *Sid1*, a gene initiating siderophore biosynthesis in *Ustilago maydis*: molecular characterization, regulation by iron, and role in pathogenicity. *Proceedings National Academy Science USA* 90, 903-907.
- Mukherjee, M., Hadar, R., Mukherjee, P.K., Horwitz, B.A. 2003. Homologous expression of a mutated beta-tubulin gene does not confer benomyl resistance on *Trichoderma virens*. *Journal of Applied Microbiology* 95, 861-867.
- Mukherjee, M., Mukherjee, P. K., Horwitz, B. A., Zachow, C., Berg, G., & Zeilinger, S. 2012. *Trichoderma*–Plant–Pathogen Interactions: Advances in Genetics of Biological Control. *Indian Journal of Microbiology*, 1-8. In press.
- Oide, S., Moeder, W., Haas, H., Krasnoff, S., Gibson, D., Yoshioka, K., Turgeon, B.G. 2006. NPS6, encoding a nonribosomal peptide synthetase involved in siderophore-mediated iron metabolism, is a conserved virulence determinant of plant pathogenic ascomycetes. *The Plant Cell* 18, 2839-2853.
- Renshaw, J.C., Robson, G.D., Trinci, A.P.J., Wiebe, M.G., Livens, F.R., Collison, D., Taylor, R.J. 2002. Fungal siderophores: structures, functions, and applications. *Mycological Research* 106, 1123-1142.
- Schrettl, M., Bignell, E., Kragl, C., Joechl C., Rogers, T., Arnst Jr., H.N., Haynes, K., Haas, H. 2004. Siderophore biosynthesis but not reductive iron assimilation is essential for *Aspergillus fumigatus* virulence. *Journal of Experimental Medicine* 200, 1213-1219.
- Schrettl, M., Bignell, E., Kragl, C., Sabiha, Y., Loss, O., Eisendle, M., Wallner, A., Arnst Jr., H.N., Haynes, K., Haas, H. 2007. Distinct roles for intra- and extracellular siderophores during *Aspergillus fumigatus* infection. *PLoS Pathogens* 3, 1195-1207.

Determination of fungal bioactive compounds using LC-HRMS

Segarra, G., Casanova, E., Aviles, M., & Trillas, I. 2010. *Trichoderma asperellum* strain T34 controls *Fusarium* wilt disease in tomato plants in soilless culture through Competition for iron. *Microbial Ecology* 59, 141-149.

Wilhite SE, Lumsden RD, Straney DC. 2001. Peptide synthetase gene in *Trichoderma virens*. *Appl. Environ. Microbiol.* **67**:5055–5062.

Winkelmann, G. 2007. Ecology of siderophores with special reference to the fungi. *Biometals* 20, 379-392.

Fig. 1: The ferrichrome siderophore gene clusters, phylogeny and modular organization.

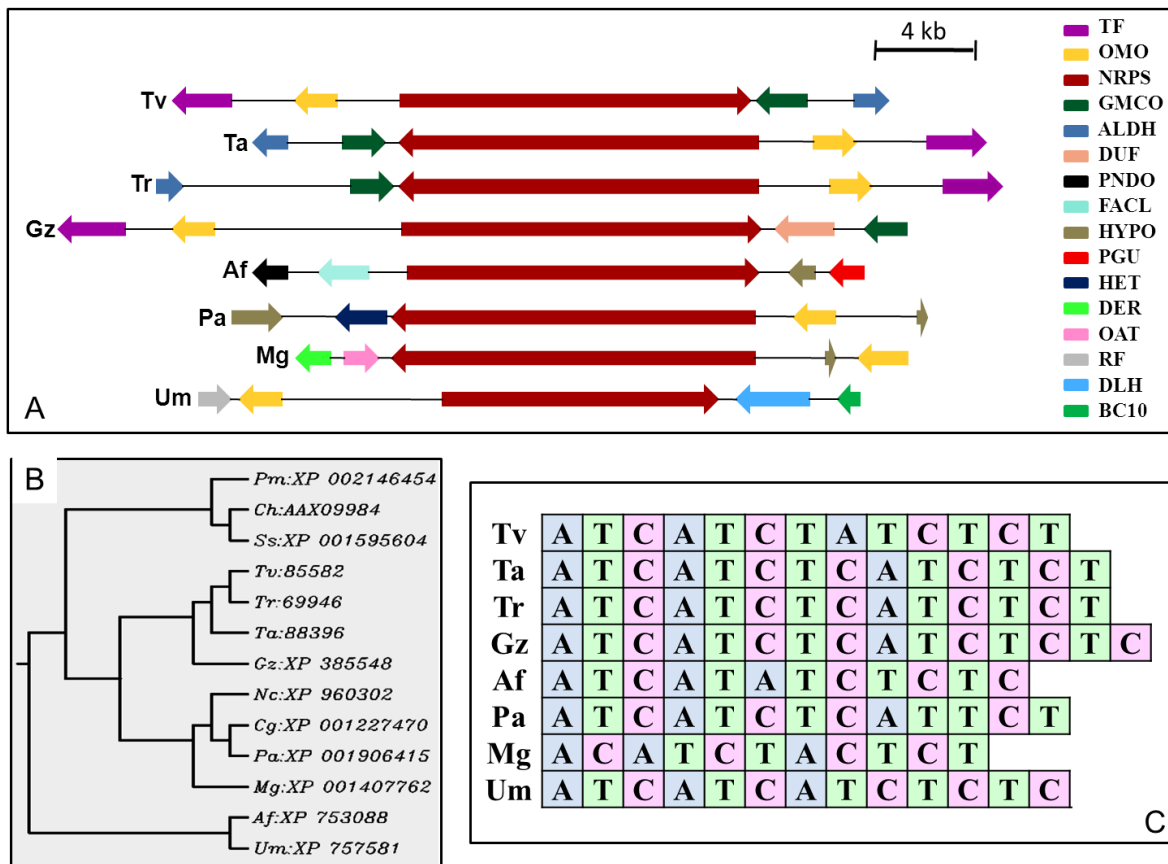


Fig. 2: The extracellular siderophore gene clusters.

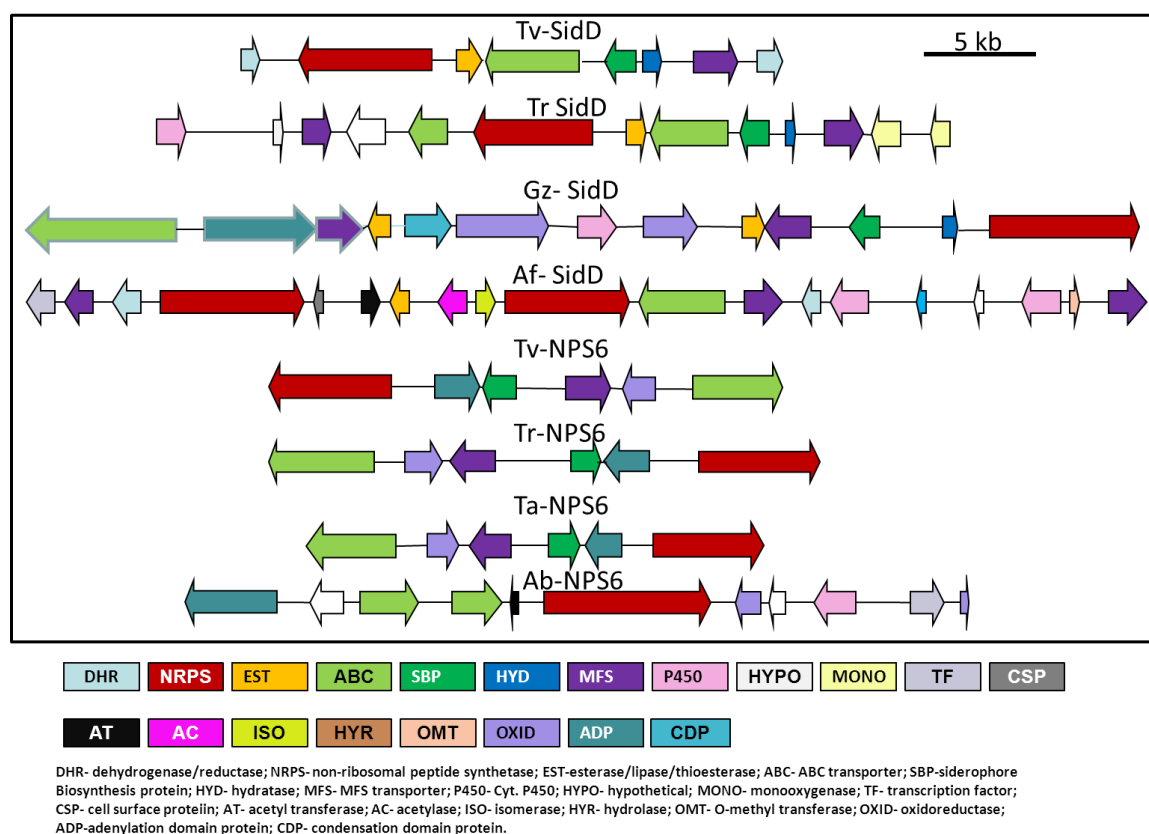


Fig 3: The phylogeny and modular organization of extracellular siderophore- NRPSs.

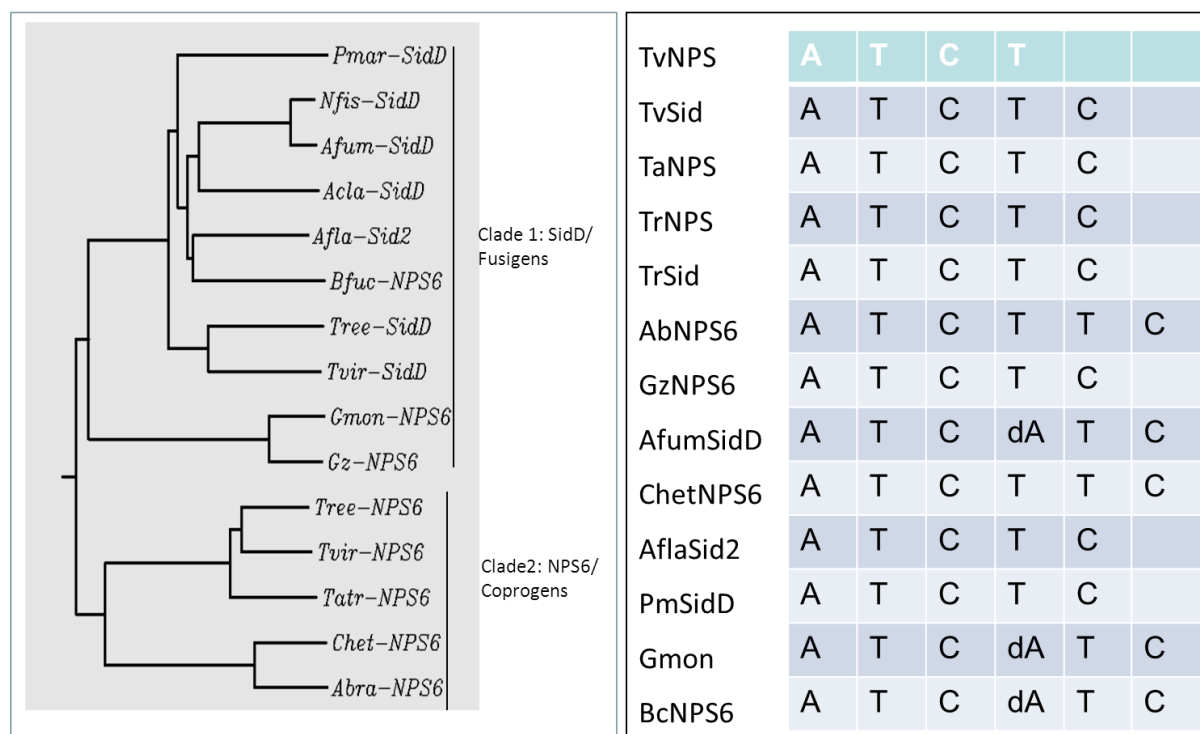


Fig 4. Knockout strategy for *sidC*. The same strategy was followed for *NPS6* while for *sidD* double cross-over strategy was used using arginine auxotrophy marker.

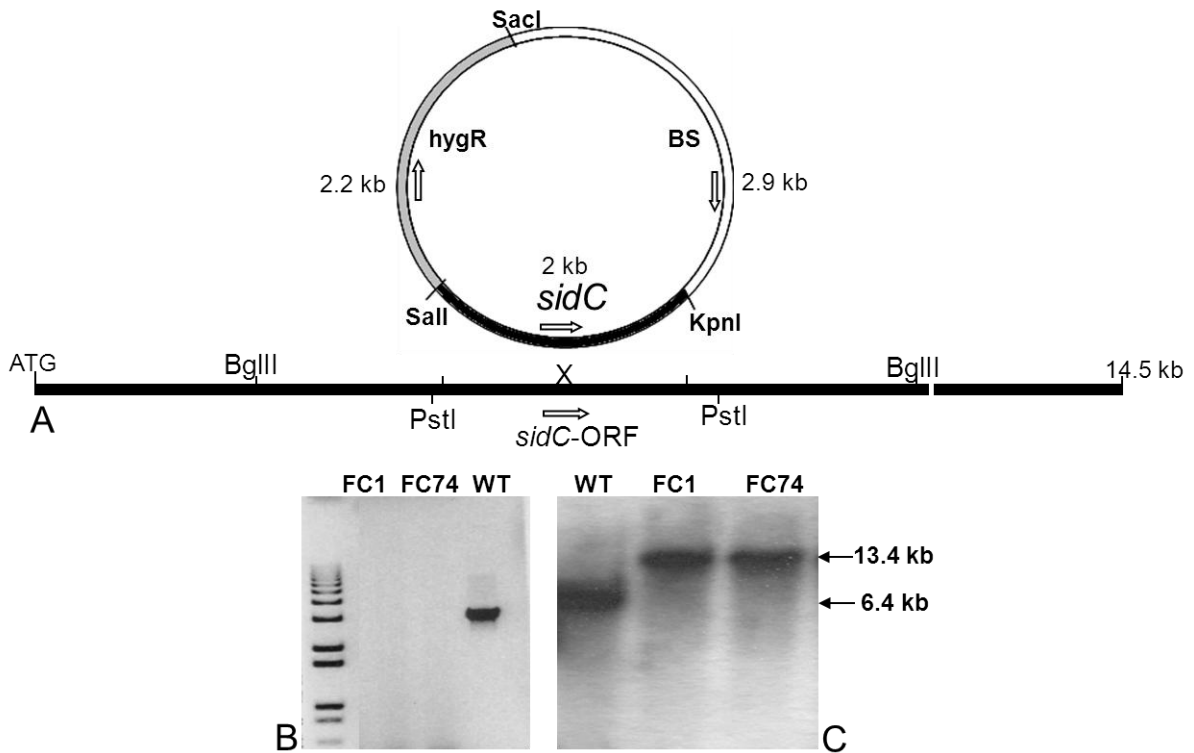
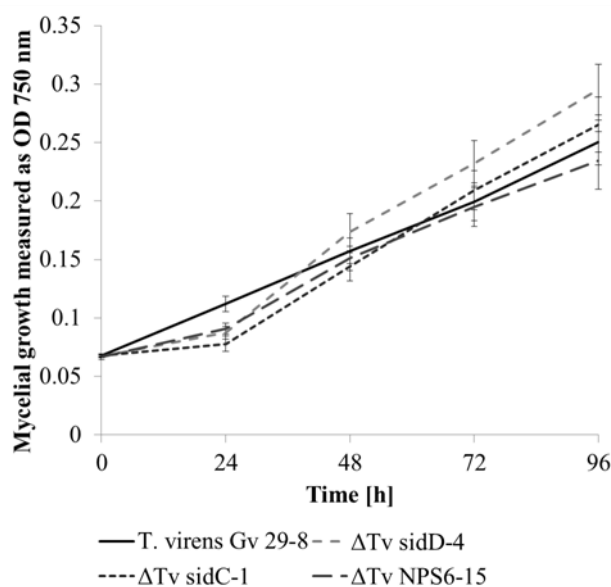
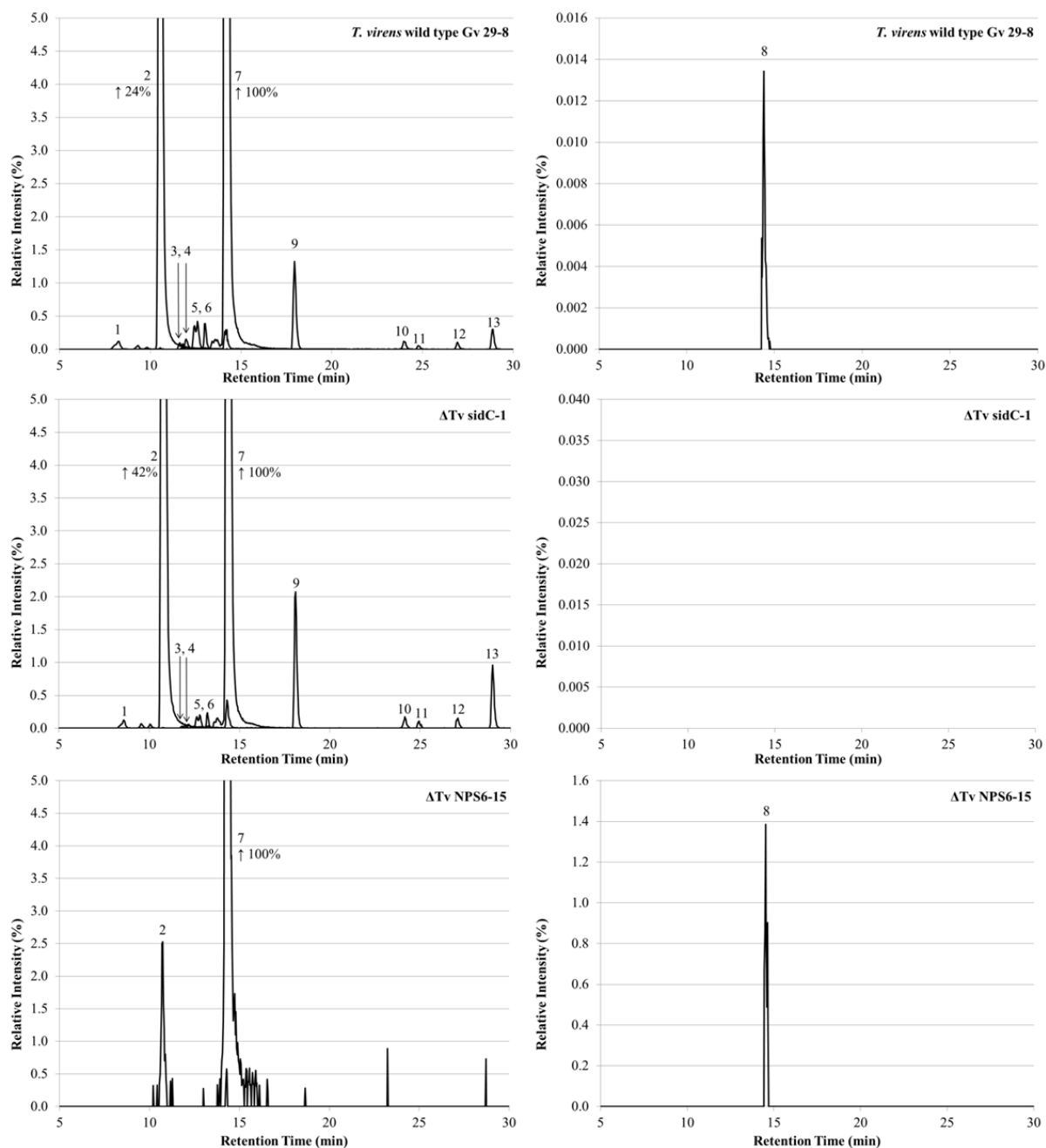


Figure 5. Growth of strains measured as mycelial density at OD at 750 nm. Vertical bars show standard deviation, n=12.



Determination of fungal bioactive compounds using LC-HRMS

Figure 6. Siderophore production pattern (EIC chromatograms of siderophores $m/z \pm 5$ ppm) of the *Trichoderma virens* Gv 29-8 wild type and ΔTv sidC-1 and ΔTv NPS6-15 mutant strains (96 hours of cultivation). Numbering of the chromatographic peaks is according to Table 1. Data obtained by LC-HRMS analysis. Peak heights were normalized to the most intense peak (fusigen) of each sample.



Scientific Publications

Table 1. Siderophore production of the wild type and mutant strains after 96 hours of cultivation (¹: identified; ²: annotated; +: present; n.d.: not detected).

No.	Siderophore	Retention Time (min)	<i>m/z</i>	Ion Species	Siderophore Type	<i>T. virens</i> wild type Gv 29-8	Δ Tv <i>sidD-4</i>	Δ Tv <i>sidC-1</i>	Δ Tv <i>NPS6-15</i>
1	Fusarinine A ²	8.6	556.183	[Fe ³⁺ SID-2H ⁺] ⁺	Fusarinine	+	+	+	n.d.
2	Dimerum Acid ¹	10.7	538.172	[Fe ³⁺ SID-2H ⁺] ⁺	Coprogen	+	+	+	+
3	Unknown SID-1	11.8	651.220	Unknown	Unknown	+	+	+	n.d.
4	Unknown SID-2	12.1	651.220	Unknown	Unknown	+	+	+	n.d.
5	Fusarinine B/DDF ²	12.6	798.309	[Fe ³⁺ SID-2H ⁺] ⁺	Fusarinine/ Ferrichrome	+	+	+	n.d.
6	Fusarinine B/DDF ²	13.2	798.309	[Fe ³⁺ SID-2H ⁺] ⁺	Fusarinine/ Ferrichrome	+	+	+	n.d.
7	Fusigen ¹	14.4	780.299	[Fe ³⁺ SID-2H ⁺] ⁺	Fusarinine	+	+	+	+
8	Ferricrocin ¹	14.6	771.248	[Fe ³⁺ SID-2H ⁺] ⁺	Ferrichrome	+	+	n.d.	+
9	Coprogen ¹	18.2	822.309	[Fe ³⁺ SID-2H ⁺] ⁺	Coprogen	+	+	+	n.d.
10	Unknown SID-3	24.3	934.397	Unknown	Unknown	+	+	+	n.d.
11	Unknown SID-4	25.1	878.370	Unknown	Unknown	+	+	+	n.d.
12	Unknown SID-5	27.2	892.387	Unknown	Unknown	+	+	+	n.d.
13	Unknown SID-6	29.1	906.403	Unknown	Unknown	+	+	+	n.d.

Towards structure elucidation of unknown substances: liquid chromatography - tandem mass spectrometry of stable isotopic labelled compounds assists elemental composition determination

Short title (max. 70 characters): LC-MS/MS using SIL for facilitating structure elucidation of unknowns

Sylvia M. Lehner^{1*}, Nora K.N. Neumann^{1*}, Karoline Sedelmaier¹, Marc Lemmens², Rudolf Krska¹, Rainer Schuhmacher^{1#}

¹Center for Analytical Chemistry, Department for Agrobiotechnology (IFA-Tulln), University of Natural Resources and Life Sciences (BOKU), Vienna, Konrad Lorenz Strasse 20, 3430 Tulln, Austria.

²Institute for Biotechnology in Plant Production, Department for Agrobiotechnology (IFA-Tulln), University of Natural Resources and Life Sciences (BOKU), Vienna, Konrad Lorenz Strasse 20, 3430 Tulln, Austria.

corresponding author: Tel.: +43-2272-66280-407, Fax: +43-2272-66280-403, rainer.schuhmacher@boku.ac.at

* these authors contributed equally to the research

Keywords (max. 5): LC-HRMS/MS, LTQ Orbitrap XL, substance identification, stable isotopic labelling, tandem mass spectrometry

ABSTRACT:

Structure elucidation is still the major bottleneck in non-targeted metabolomics approaches. We used stable isotopic labelling (SIL) to assist in the elucidation of the elemental formula of fragments in tandem MS (MS/MS) experiments. In this respect, a software tool using Python Programming Language was developed and exemplified with high resolution MS/MS data of both, native and fully ¹³C labelled

Detection and characterization of fungal secondary metabolites using LC-HRMS

mycotoxins. The program efficiently detects corresponding peak pairs in the MS/MS spectra of the native and the labelled compounds. This software tool significantly reduces data processing time of MS/MS spectra as it calculates the number of carbon atoms present in a fragment ion and suggests reasonable corresponding elemental compositions. This is a first important step regarding structure elucidation of unknowns. Therefore, this work is a significant contribution towards the structure elucidation of compounds in future SIL-assisted metabolomics studies.

RATIONALE:

The aim of this work was to facilitate structure elucidation of compounds using stable isotopic labelling (SIL) and MS/MS. A software tool for the automated data processing to speed up the process of elemental composition determination of the MS/MS fragments was implemented. The tool shall be used in the structure elucidation process of unknowns in future studies and is available upon request from the laboratory of the corresponding author.

METHODS:

Liquid chromatography coupled to high resolution tandem mass spectrometry on an LTQ Orbitrap XL was used to measure native and ^{13}C labelled standard compounds in the same analytical run. Full scan and MS/MS measurements (CID and HCD) of these samples were carried out. Regarding structure elucidation, an automated algorithm was implemented in Python that finds corresponding peak pairs present in the MS/MS spectra of the native and the labelled compound. Additionally, the number of carbon atoms present in fragment signals as well as corresponding elemental formulas are automatically calculated.

RESULTS:

The software tool generates meaningful suggestions for elemental formulas of the parent and fragment ions. Therefore, the algorithm effectively reduces the time needed for data processing of the MS/MS spectra regarding the elucidation process of the corresponding elemental composition. This in turn helps in determining the elemental composition of the precursor ion. Additionally, stable isotopic labelling increases confidence in the annotation of the elemental composition since the actual number of carbon atoms can be directly derived from the MS data.

CONCLUSIONS:

SIL in combination with high resolution tandem mass spectrometry is a very versatile tool towards the characterization of the elemental composition of unknown compounds. In combination with automated data processing, it provides a powerful and fast approach for the determination of elemental formulas of fragment signals in MS/MS spectra. Additionally, it shows the potential to assist in structural elucidation of unknowns in non-targeted studies, especially if characteristic mass increments are obtained and considered.

INTRODUCTION

Elucidation of the elemental composition or even the structure of unknown compounds in biological samples remains one of the most challenging tasks in non-targeted metabolomics studies. Many metabolomics studies nowadays couple chromatography with mass spectrometry since it is a very versatile and sensitive technique. Novel high resolution mass spectrometers at affordable costs give rise to many LC-MS applications that aim at providing a holistic picture of the metabolic state of an organism at a certain condition/treatment. The first goal of data analysis

Detection and characterization of fungal secondary metabolites using LC-HRMS

in non-targeted approaches is to determine as many compounds as possible. A first step in this respect is data annotation of the detected mass spectral features that can be done by querying (organism-specific) databases (e.g. AntiBase^[1]). Another possibility to annotate compounds is by applying (heuristic) rules to obtain elemental formula prediction^[2]. The second approach is especially important for truly novel compounds that are not present in databases.

Definitive substance identification, which would be the next step after compound annotation, can only be achieved by comparing two or more orthogonal properties with the measurement of an authentic standard compound under identical experimental conditions^[3]. However, most detectable features in mass spectra cannot be identified or even annotated due to various reasons. First of all, one needs to identify relevant signals in mass spectra and verify that they are of biological origin and not merely artefacts, background signals or contaminants. One particular elegant and sophisticated approach in this respect is full *in vivo* stable isotopic labelling (SIL) of whole organisms, by e.g. applying growth media that contain a labelled carbon source. For example, organisms can be in parallel cultivated *in vivo* with the native and the labelled carbon source. Samples (e.g. the diluted culture filtrates) can then be mixed 1+1 prior to measurements. This approach allows for the elucidation of substances of biological relevance, since peak pairs that are present under both, the native and the uniformly labelled condition are (intermediate) products of metabolism. Additionally, elemental formula determination is facilitated as the peak pairs show a distinct distance in the mass spectra that is traceable to the number of carbon atoms present in the substance. A sophisticated software tool has been developed to determine the number of carbon atoms of full *in vivo* SIL experimental data automatically^[4]. Nitrogen labelling could be additionally conducted

in order to determine the presence and number of nitrogen atoms of a compound. Knowledge of the elemental formula can lead to putative annotation; however, usually many structural isomers correlate to one elemental formula.

Further approaches towards the elucidation of the structure of a compound involve tandem MS (MS/MS). Different strategies for the interpretation of MS/MS spectra have been suggested. The probably most straightforward approach (if no authentic standard compound is available in-house) is to try to match the measured fragments against a tandem MS databases, e.g. METLIN^[5, 6] (<http://metlin.scripps.edu/>) or MassBank^[7] (www.massbank.jp). However, the major limitation is the size and the range of the database in use as many compounds and compound classes usually are not covered. Moreover, no programmatic access is available to MassBank outside the MassBank consortium, which means only single spectra are available for download and further comparison.

Other software tools aim at the *in silico* fragmentation of substances. For example, MassFrontier (HighChem, Ltd., Bratislava, Slovakia, <http://www.highchem.com/>), a commercial software, provides automated generation of possible fragments starting from chemical structure formulas according to defined fragmentation rules based on known reaction mechanisms and fragmentation rules derived from curated literature data. Metfrag^[8], a freely available software tool (<http://msbi.ipb-halle.de/MetFrag/>), aims at finding structural similarities to substances present in public databases. It first creates a candidate list from database entries (based on the precursor mass), generates *in silico* fragments of the found entries and compares these with the measured fragment list. Sirius^[9, 10], a java-based software framework (<http://bio.informatik.uni-jena.de/sirius2/>), tries to suggest the elemental formula of a

precursor based on the isotope pattern and then generates fragmentation trees from the measured fragment list.

The aim of the present study was to combine the approach of stable isotopic labelling and tandem mass spectrometry towards the structure characterization of compounds. Using the MetExtract^[4] algorithm, the number of carbon atoms present in an intact compound (precursor mass for MS/MS) can be derived. Based on this knowledge, we developed an automated approach to find corresponding fragment peaks in the MS/MS spectra of the native and the uniformly ¹³C labelled precursor ion in order to determine the number of carbon atoms of the fragments. Subsequently the corresponding elemental formulas are calculated based on heuristic rules. These elemental formulas can help in determining the elemental composition of the parent ion and additionally, if characteristic, can be of further relevance in the structure elucidation process. Automated elucidation of the elemental composition of MS/MS fragments therefore is a first step towards more efficient structure characterization of unknowns in future metabolomics studies.

EXPERIMENTAL

Chemicals and reagents

Methanol (MeOH, LiChrosolv, LC gradient grade) was purchased from Merck (Darmstadt, Germany); acetonitrile (ACN, HiPerSolv Chromanorm, HPLC gradient grade) was purchased from VWR (Vienna, Austria); formic acid (FA, MS grade) was obtained from Sigma-Aldrich (Vienna, Austria). Water was purified successively by reverse osmosis and an ELGA Purelab Ultra-AN-MK2 system (Veolia Water, Vienna, Austria).

Analytical standards (both with natural isotopic composition and uniformly ^{13}C labelled) of 3-acetyldeoxynivalenol (3AcDON), diacetoxyscirpenol (DIAS), fumonisin B₁, B₂ and B₃ (FB₁, FB₂, FB₃), griseofulvin (GRIS), HT-2 and T-2 toxin, sterigmatocystin (STER), tetracycline (TETR) and zearalenone (ZEN) were obtained from Biopure Referenzsubstanzen GmbH (Tulln, Austria).

Measurement of standard solutions

Analytical standard solutions were mixed to obtain two multi-analyte stock solutions. Those contained both, the analytes with natural isotopic composition and the uniformly ^{13}C labelled ones in the same concentration. The multi-analyte stock solutions were diluted with water to achieve a solvent composition of ACN:water = 1:1 (v/v). The first final multi-analyte solution comprised 3-AcDON, DIAS, FB₃, HT-2, T-2, ZEN (each isotopologue at a concentration of 1.1 mg.L⁻¹). The second final multi-analyte solution consisted of 0.9 mg.L⁻¹ of both, FB₁ and FB₂, 1.4 mg.L⁻¹ GRIS, 1.7 mg.L⁻¹ STER and 1.5 mg.L⁻¹ TETR.

LC-MS/MS analysis

Five μL of multi-analyte standard solutions were introduced into an Accela HPLC system (Thermo Fisher Scientific, San Jose, CA, USA) equipped with a reversed-phase XBridge C₁₈ analytical column, 150 x 2.1 mm i.d., 3.5 μm particle size (Waters, Vienna, Austria), equipped with a C₁₈ 4 x 2 mm i.d. security cartridge (Phenomenex, Torrance, CA, USA). The column temperature was maintained at 25°C. Eluent A was water, eluent B was MeOH, both containing 0.1% FA. The chromatographic method held the initial mobile phase composition (90% A) constant for 2 min, followed by a linear gradient to 100% B in 30 min. This final condition was

Detection and characterization of fungal secondary metabolites using LC-HRMS

held for 5 min, followed by 8 min column re-equilibration at 90% A. The flow rate was 250 $\mu\text{L}\cdot\text{min}^{-1}$.

The HPLC system was coupled to an LTQ Orbitrap XL (Thermo Fisher Scientific) equipped with an electrospray ionization (ESI) interface which was operated in positive ionization mode using the following settings: electrospray voltage: 4 kV, sheath gas: 60 arbitrary units, auxiliary gas: 15 arbitrary units, sweep gas: 5 arbitrary units, capillary temperature: 300°C. All other source parameters were automatically tuned for a maximum MS signal intensity of reserpine (Sigma Aldrich (Vienna, Austria)) solution (10 $\text{mg}\cdot\text{L}^{-1}$). To this end, 10 $\mu\text{L}\cdot\text{min}^{-1}$ of reserpine solution (dissolved in ACN:water = 8:2 (v/v)) were infused via syringe pump into mobile phase (Eluent A:B, 1:1) of a flow rate of 250 $\mu\text{L}\cdot\text{min}^{-1}$.

As the multi-analyte solution contained a 1+1 mixture of the native and labelled compounds, the MS method contained three scan events. First, a survey full scan (resolving power setting 30,000 FWHM at m/z 400, scan range of m/z 100-1000) was followed by two tandem MS measurements (resolving power setting 7,500 FWHM at m/z 400, varying m/z range adapted to the analyte mass, starting from m/z 50) of the analyte with natural isotopic composition followed by the ^{13}C labelled analyte. The isolation width for the precursor isolation was set to 2. Two measurement methods were generated: one using collision induced dissociation (CID) and one using higher energy collision dissociation (HCD). For all compounds the protonated molecule was chosen for fragmentation with the exception of DIAS, HT-2 and T-2 toxin for which the sodium adducts were used. The normalized collision energies (%) were optimized by direct infusion measurements resulting for 3AcDON in 24% (CID)/ 30% (HCD), for DIAS in 37% (CID)/ 53% (HCD), for FB_1 in 25% (CID)/ 35% (HCD), for FB_2 in 23% (CID)/ 34% (HCD), for FB_3 in 23% (CID)/

34% (HCD), for GRIS in 30% (CID)/ 37% (HCD), for HT-2 in 29% (CID)/ 43%(HCD), for STER in 40% (CID)/ 60% (HCD), for T-2 in 32% (CID)/ 40% (HCD), for TETR in 25% (CID, HCD) for ZEN in 34% (CID)/ 46% (HCD). For the FT-Orbitrap, the automatic gain control was set to a target value of $5 \cdot 10^5$ and a maximum injection time of 500 ms was chosen for both full scan and tandem MS measurements. Data was generated using Xcalibur 2.1.0 (Thermo Fisher Scientific).

Manual data analysis

Manual interpretation of the tandem MS spectra was achieved by comparing the fragmentation pattern of the analyte with natural isotopic composition with the fragmentation pattern of the ^{13}C labelled analyte. By calculating the mass differences of corresponding mass signals it was possible to determine the number of carbon atoms of the respective signals. Further composition (number/presence of hydrogen and heteroatoms) of the signals was determined by carefully evaluating the well-known analyte structure and eliciting chemical meaningful fragmentation sites.

Automated data processing

The developed algorithm msIdentify uses a brute force approach for the MS/MS fragment identification and calculation of the number of carbon atoms. It was developed in Python using the QtSDK for the graphical user interface and is available for Windows and MacOSX. The program is capable of processing high-resolution LC-MS/MS data and comprises a set of steps which will be described in the following.

The software uses the mzML data format which is a common data format and was suggested by the Metabolomics Standards Initiative (MSI). Therefore, raw LC-

Detection and characterization of fungal secondary metabolites using LC-HRMS

MS/MS data files have to be converted first to mzML. First of all, the user has to define a positive list of precursor masses. Additionally, the number of carbon atoms of the precursor is known from investigating the full scan data and is provided to the software. The user also specifies a retention time window.

MS/MS spectrum selection: The program searches the full scan data to find the most intense mass peak of the target precursor mass within a user defined retention time window. The subsequent two tandem MS spectra after the full scan signal exhibiting the highest intensity (one MS/MS spectrum for the native and one for the ^{13}C labelled compound) were then selected. As additional quality criterion, the intensity of the most intense peak (base peak) of the MS/MS spectrum of the native compound had to exhibit a minimum intensity of 100 counts.

Fragment peak identification and calculation of carbon atoms: As MS/MS spectra can exhibit very complex fragmentation patterns (including m/z signals with very low intensities), only the 20 most intense fragment peaks are selected for further identification. The mass peaks in both corresponding MS/MS spectra are compared to calculate the number of carbon atoms of the respective fragment ions. This results in a list containing selected fragment signals and their calculated number of carbon atoms. Further evaluation of the preselected fragment signals is done by investigating the intensity pattern (ratio of the intensities Int. A : Int. B of the corresponding fragment signals A and B in both spectra of the native and labelled compound) of m/z values in each MS/MS spectrum (Figure 1). As the native and the labelled compound shows the same fragmentation behaviour (same fragmentation sites, formation of the same fragments), the intensity patterns of m/z peak pairs in both MS/MS spectra have to exhibit similar relative intensity ratios to be further selected for elemental composition calculations of the detected fragments.

Elemental composition calculation: Molecular formulas for fragment peaks are then calculated based on a publication of Kind and Fiehn^[2]. First, the mass of the neutral fragment molecule was calculated by adding the mass of an electron. This step was chosen regarding future applications of the algorithm with potentially unknown compounds, for which the ion species of the parent m/z might be e.g. a sodium adduct or not be known. This led to a selection of rule #1 (restriction for element numbers), #4 (Hydrogen/Carbon element ratio check), #5 (heteroatom ratio check) and #6 (element probability check) of the publication of Kind and Fiehn^[2] for molecular formula calculation. For the resulting elemental compositions, the corresponding exact monoisotopic masses were calculated and the mass difference (in ppm) compared to the neutralized fragment mass (measured m/z of the respective fragment plus the mass of one electron in positive ionization mode) was computed with maximum allowed mass deviation of 10 ppm.

Results of the algorithm: For a given LC-MS/MS data file, msIdentify offers a final list of fragments sorted by MS/MS spectrum. In the results file all fragment m/z pairs, the number of atoms of the specified labelled element (e.g. carbon) for each m/z value as well as the calculated molecular formulas and their respective mass deviation (in ppm) are listed.

RESULTS AND DISCUSSION

MS/MS spectra of the native and the labelled compounds essentially exhibit the same fragmentation pattern and these are only shifted by the natural weight difference between ^{12}C and ^{13}C times the number of carbon atoms present in the compound or respective fragment ion. Based on this, an automated direct spectral comparison of the two MS/MS spectra is not possible. An algorithm based on several parameters and criteria to determine the corresponding signals in the MS/MS spectra of the native and the labelled compound was developed. The program relies on a user defined positive list that includes the m/z values of the ^{12}C and ^{13}C precursor mass, a defined retention time window as well as the amount of carbon atoms of the precursor ion, which can be derived from the full scan data. The algorithm then searches for the scan with the most intense precursor intensity. The next two adjacent scan events (MS/MS of the native and the labelled compound) are used for further analysis – the minimum base peak intensity of the spectrum of the native compound has to exceed 100 counts. As the native and the labelled compounds show the same chromatographic behaviour (and therefore show their most intense scans at comparable retention times), this criterion was only applied to the MS/MS spectrum of the native compound. Only the 20 most intense fragments are considered for MS/MS interpretation. For each of these fragment signals in the spectrum of the native compound, possible corresponding ^{13}C labelled fragment signals are calculated and searched for in the MS/MS spectrum of the ^{13}C labelled compound (maximum mass deviation: 10 ppm) – this way the number of carbon atoms of fragments is calculated. Then, the ratio of relative intensities of peak pairs in MS/MS spectra between the native and the labelled compounds are used to further determine meaningful fragments and to verify their corresponding labelled

fragment signal. This criterion is explicitly useful as relative intensity ratios are largely independent of absolute precursor intensities. The last step is the calculation of corresponding elemental formulas for the MS/MS fragments. The algorithm is applicable to both, CID and HCD spectra. Both types of MS/MS spectra have been used within this study as CID and HCD are complementary techniques and HCD leads to a higher fragmentation. Additionally, which fragmentation method works better for a given compound is also dependant on its chemical structure.

Application of the algorithm

First, full scan data were searched for features with the characteristic ^{13}C isotopic pattern of native/labelled compounds. This led to the verification of the presence of all standard compounds including the correct calculated number of carbon atoms. Table 1 gives the rank of the correct elemental formula using the same heuristic rules for elemental composition calculation as described in the materials and methods section. Restricting the number of carbon atoms leads to less possibilities regarding elemental compositions and ranks the software-derived elemental formula much better (based on mass deviation). Often, the correct elemental formula exhibits the lowest mass deviation. In case of TETR, an elemental formula containing chlorine shows a smaller mass deviation – however, presence of chlorine can be very easily verified or excluded based on its characteristic isotopic pattern in the full scan MS spectrum. For T-2 toxin, the correct elemental formula is in 2nd place. One elemental formula containing three phosphorus and two sulphur atoms were ranked better. For FB₁, FB₂ and FB₃, two, five and four elemental formulas, respectively, that are better ranked than the correct elemental composition contain chlorine. The others contain high numbers of N, S and/or P. Isotopic fine structure can help in elucidation the correct elemental composition. On the other hand, the MS/MS

Detection and characterization of fungal secondary metabolites using LC-HRMS

fragments can also assist in determining the correct elemental composition. As the MS/MS fragments exhibit lower masses than the intact molecular ions, less possible elemental compositions correspond to the accurate masses with less than 10 ppm mass deviation. With a proper mass calibration, higher mass deviations than 10 ppm are highly unusual even at very small signal intensities as are encountered in MS/MS fragment spectra.

The results table from the automated data processing of MS/MS spectra gives the possible elemental composition of the fragments, sorted by mass deviation. Mostly, the elemental composition that was also assigned manually is ranked in the first place. For few fragments, however, elemental formulas are suggested that mostly exhibit a very unlikely stoichiometry. In addition, if only one of many fragments exhibits e.g. sulfur, this result is also highly improbable. Evaluation of the fragments can therefore a) help to determine the elemental composition of the intact ion and b) structural elucidation of compounds can be facilitated by characteristic mass increments. Therefore, data analysis requires some manual inspection in order to obtain meaningful results. However, the implemented software tool significantly speeds up data processing time and represents therefore a valuable first step towards structural elucidation of unknowns.

Exemplification of application of the algorithm to 3AcDON

The MS/MS interpretation will be shown exemplary for 3AcDON. Figure 2 shows the MS/MS spectra of the native and the labelled compound together with annotation of the fragment elemental formulas. Table 2 gives the elemental formulas to the fragment signals (derived from both, manual and automated data analysis) and the rank of the manually annotated formula among the automated generated possible

elemental formulas based on the heuristic rules described in the materials and methods section. Again, it shows that restricting the number of carbon atoms to the actual amount significantly reduces the number of possible elemental formulas. In case of 3AcDON, the data processing of the CID spectra ranks the manually assigned formula always at first place (smallest mass deviation). Only four of sixteen fragments exhibit more than one possible elemental composition with a mass deviation smaller than 10 ppm: The signal at m/z 297 ($C_{15}H_{21}O_6$, Δ 2.5 ppm) could also be explained by $C_{15}H_{24}ONSP$ (Δ 5.3 ppm), m/z 291 ($C_{16}H_{19}O_5$, Δ 0.3 ppm) by $C_{16}H_{22}NSP$ (Δ 7.2 ppm), m/z 279 ($C_{15}H_{19}O_5$, Δ 2.7 ppm) by $C_{15}H_{22}NSP$ (Δ 5.2 ppm) and m/z 233 ($C_{14}H_{17}O_3$, Δ 1.5 ppm) by $C_7H_{17}ON_6S$ (Δ 4.4 ppm)/ $C_7H_{16}N_7Cl$ (Δ 8.0 ppm)/ $C_7H_{22}O_6P$ (Δ 8.7 ppm). For m/z 233 the algorithm finds two corresponding signals in the MS/MS spectrum of the labelled compound – therefore, seven and fourteen carbon atoms are allowed for calculation of the elemental composition. All the other twelve detected fragments contain only the elements C, H, O and only one possible combination of these elements. In the HCD MS/MS fragmentation spectra, the algorithm is able to identify four fragments – only one of them with two suggestions regarding its elemental composition: m/z 279 with $C_{15}H_{19}O_5$ (Δ 0.9 ppm) and $C_{15}H_{22}NSP$ (Δ 6.9 ppm).

By looking at the possible elemental formulas of all fragment ions it is possible to exclude highly unlikely elements or compositions (e.g. if only one/few of approx. 10 fragments include N). Therefore, the user can decide which elements/elemental compositions to allow or exclude. Additionally, the isotopic fine structure in the full scan data can be used to further help determine the correct elemental composition as has been suggested by Kaufmann^[11].

Exemplification of application of the algorithm to FB₁

The fumonisins show molecular masses of approx. 700 Da. Therefore, FB₁ was used as model compound for metabolites > 500 Da. As bigger fragments can potentially be explained by a higher variety of elemental compositions, MS/MS spectra of FB₁ will be discussed in this part of the manuscript. The algorithm elucidated nine and sixteen meaningful fragment ions (CID and HCD, respectively) and calculated corresponding number of carbon atoms and potential elemental compositions. In CID, for four fragments only one elemental composition was found: C₂₂H₄₄O₃N for *m/z* 370, C₂₂H₄₂O₂N for *m/z* 352, C₂₂H₄₀ON for *m/z* 334 and C₂₂H₃₈N for *m/z* 316. One of the remaining five fragments ranked the manually derived elemental composition in first place (C₂₈H₄₈O₇N for *m/z* 510), for the other four, elemental compositions containing both, chlorine and sulfur were ranked in first place. Again, chlorine could easily be excluded due to its characteristic isotopic pattern. Other elements can be excluded due to the isotopic fine structure as has been shown by Kaufmann^[11].

Using HCD, only one elemental composition per fragment is suggested for all sixteen fragments considered. This is due to the higher fragmentation, leading to fragments ranging from *m/z* 70 – *m/z* 370.

Typical for the structures of fumonisins, many water losses can be observed in their fragment spectra. Additionally, cleavage at the ester bonds of the side chains occur and can be seen in the spectra. As HCD yields higher fragmentation, degradation of the remaining backbone is visible in the corresponding MS/MS spectra (see Figure 3).

Application to a “real world sample”: Aurofusarin in a *Fusarium graminearum* culture filtrate

The established automated algorithm was subsequently applied to a culture filtrate of a (genetically modified) *Fusarium graminearum* strain that was grown on liquid minimal medium containing either native or ^{13}C fully-labelled glucose. Detailed results on the biological relevance and results will be published elsewhere. One very dominant signal in the full scan MS data was the one of aurofusarin ($\text{C}_{30}\text{H}_{18}\text{O}_{12}$, monoisotopic mass: 570.0798 Da), which was further characterized and will be discussed in more detail. MS/MS experiments (both CID and HCD) led to meaningful fragments only $> m/z$ 450. In this respect, MS^3 experiments would help in further elucidation the structure of this compound. Nevertheless, the general applicability of the algorithm is shown and discussed in the following. A CID MS/MS spectrum is shown in Figure 4. The developed algorithm lists the possible elemental formula to the fragment signals, listed by mass deviation in ppm. Mostly, the elemental formula that was also assigned by manual data evaluation is assigned in the first place (lowest mass deviation). However, for some fragments elemental formulas containing an unlikely combination of elements exhibit a lower mass deviation. Nevertheless, by excluding formulas that do not fit to the average element occurrence and number can be excluded. Of course, this decision needs to be made case by case, needs careful evaluation by a person with experience in MS/MS spectral interpretation and cannot be done automatically. Our approach significantly reduces the effort involved in MS/MS interpretation as it automatically calculates the number of carbon atoms present in a fragment (based on the comparison of the MS/MS spectra of the native and fully ^{13}C -labelled compound) and suggests corresponding elemental formulas based on several heuristic rules. Many of the

neutral losses and the respective fragments are typical for certain structural units which help in the identification process – in the case of aurofusarin e.g. ΔCH_3 for methyl, $\Delta \text{CH}_2\text{O}$ for methoxy, $\Delta \text{CH}_3\text{CO}$ for methyl & CO in the ring structure.

CONCLUSIONS

Structure elucidation of unknown compounds still is the major bottleneck in non-targeted approaches. Stable isotopic labelling shows high potential for elemental formula determination as the atom count of the labelled element can be derived from HRMS data. In conjunction with tandem MS, SIL has the possibility to further help in the determination of chemical structures of unknowns. We developed an automated software tool that significantly improves data processing time and elemental formula assignment of fragment signals in MS/MS spectra. The developed software tool additionally allows for the investigation of a high number of spectra (and hence, many compounds). Typical fragmentation behaviour of functional groups, as described by Holčápek and co-workers^[12], can be taken into account to further help in the structure elucidation process. This tool shows high potential to be used in future studies towards the elucidation of unknown compounds.

Acknowledgements

The Federal Country Lower Austria and the European Regional Development Fund (ERDF) of the European Union is acknowledged for financial support (Grant Number GZ WST3-T-95/001-2006) which also enabled the Ph.D. studies of Sylvia M. Lehner (analytical chemistry). The authors thank the Austrian Science Fund (project SFB Fusarium 3706-B11) for financial support, which enabled the Ph.D. studies of Nora K.N. Neumann (bioinformatics).

REFERENCES

- [1] H. Laatsch, Wiley-VCH, **2007**.
- [2] T. Kind, O. Fiehn, *Bmc Bioinformatics* **2007**, *8*.
- [3] L. W. Sumner, A. Amberg, D. Barrett, M. H. Beale, R. Beger, C. A. Daykin, T. W. M. Fan, O. Fiehn, R. Goodacre, J. L. Griffin, T. Hankemeier, N. Hardy, J. Harnly, R. Higashi, J. Kopka, A. N. Lane, J. C. Lindon, P. Marriott, A. W. Nicholls, M. D. Reily, J. J. Thaden, M. R. Viant, *Metabolomics* **2007**, *3*, 211.
- [4] C. Bueschl, B. Kluger, F. Berthiller, G. Lirk, S. Winkler, R. Krska, R. Schuhmacher, *Bioinformatics* **2012**, *28*, 736.
- [5] C. A. Smith, G. O'Maille, E. J. Want, C. Qin, S. A. Trauger, T. R. Brandon, D. E. Custodio, R. Abagyan, G. Siuzdak, *Therapeutic Drug Monitoring* **2005**, *27*, 747.
- [6] T. R. Sana, J. C. Roark, X. Li, K. Waddell, S. M. Fischer, *Journal of biomolecular techniques : JBT* **2008**, *19*, 258.
- [7] H. Horai, M. Arita, S. Kanaya, Y. Nihei, T. Ikeda, K. Suwa, Y. Ojima, K. Tanaka, S. Tanaka, K. Aoshima, Y. Oda, Y. Kakazu, M. Kusano, T. Tohge, F. Matsuda, Y. Sawada, M. Y. Hirai, H. Nakanishi, K. Ikeda, N. Akimoto, T. Maoka, H. Takahashi, T. Ara, N. Sakurai, H. Suzuki, D. Shibata, S. Neumann, T. Iida, K. Funatsu, F. Matsuura, T. Soga, R. Taguchi, K. Saito, T. Nishioka, *Journal of Mass Spectrometry* **2010**, *45*, 703.
- [8] S. Wolf, S. Schmidt, M. Müller-Hannemann, S. Neumann, *Bmc Bioinformatics* **2010**, *11*, 1.
- [9] S. Böcker, M. C. Letzel, Z. Lipták, A. Pervukhin, *Bioinformatics* **2009**, *25*, 218.

- [10] F. Rasche, A. Svatoš, R. K. Maddula, C. Böttcher, S. Böcker, *Analytical Chemistry* **2010**, 83, 1243.
- [11] A. Kaufmann, *Rapid Communications in Mass Spectrometry* **2010**, 24, 2035.
- [12] M. Holčapek, R. Jirásko, M. Lísa, *Journal of Chromatography A* **2010**, 1217, 3908.

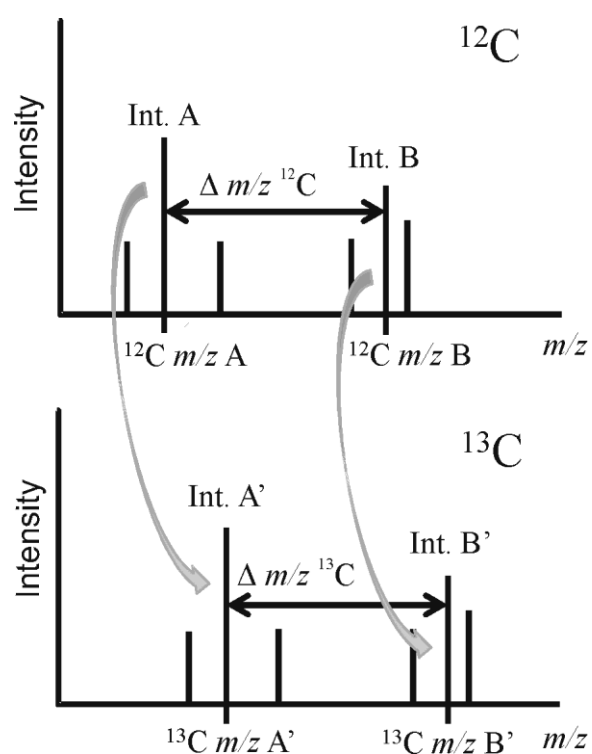


Figure 1. Schematic illustration of the comparison of relative intensities during automated fragment signal detection. Corresponding signals of the native and the labelled compound have to exhibit comparable signal ratios. The number of carbon atoms present in a fragment ion can be directly derived from the mass difference between the signals A and B compared to A' to B'.

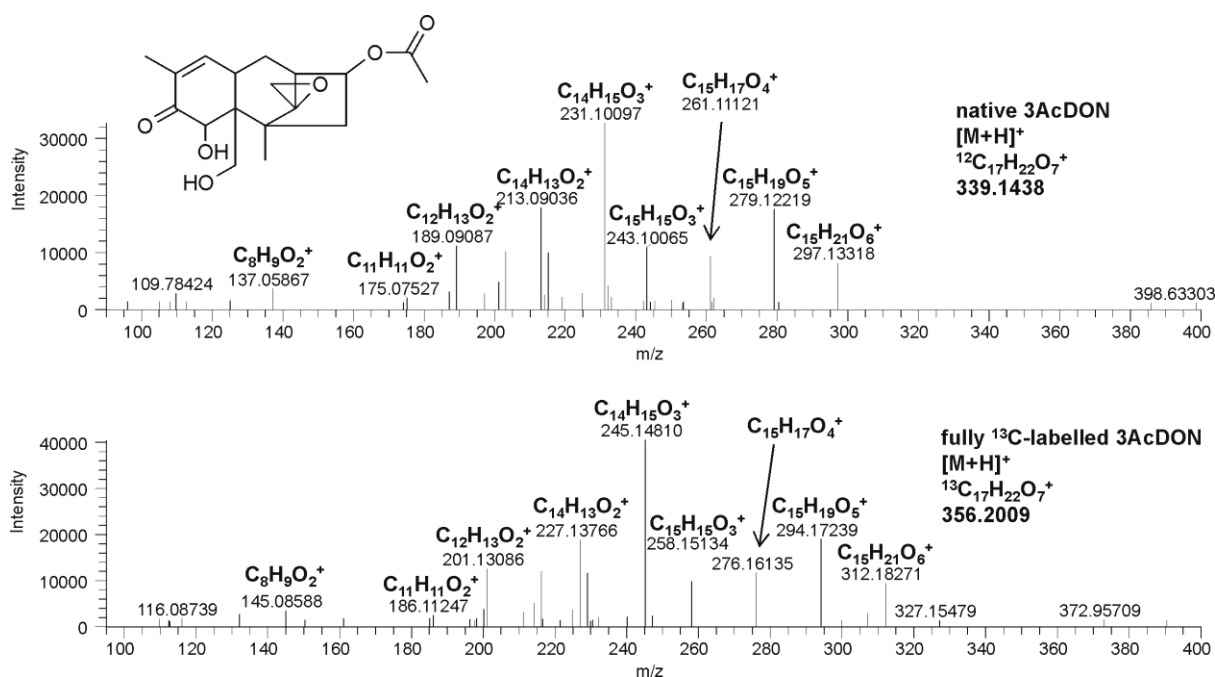


Figure 2. MS/MS spectra (CID) of the native 3AcDON and the fully ^{13}C -labelled 3AcDON standard. Elemental formulas to selected fragment peaks are given. Structure formula of 3AcDON is shown in the upper left corner.

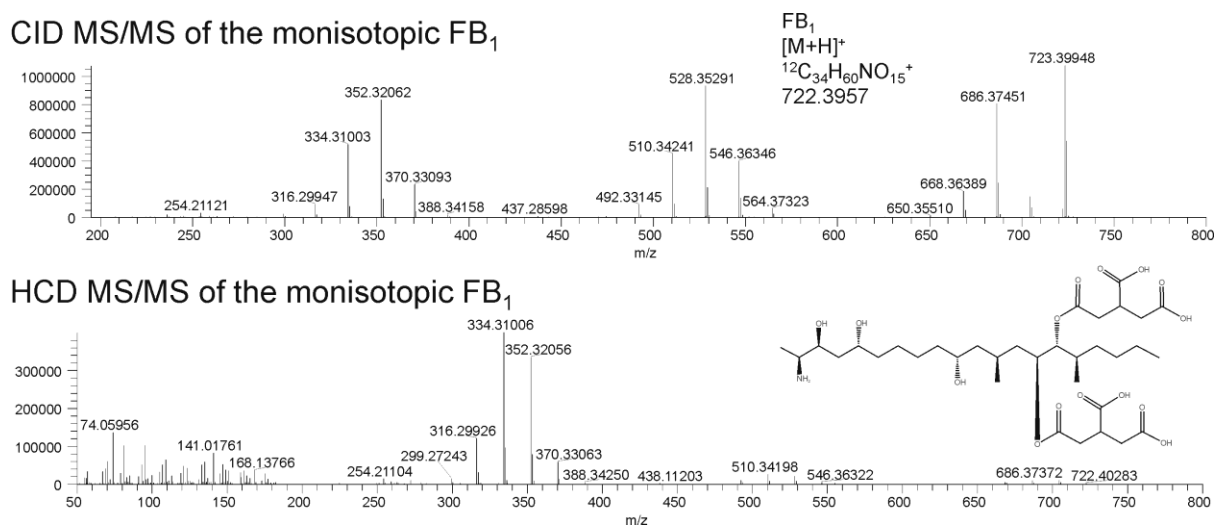


Figure 3. CID and HCD MS/MS spectrum of FB₁ and corresponding elemental structure.

Detection and characterization of fungal secondary metabolites using LC-HRMS

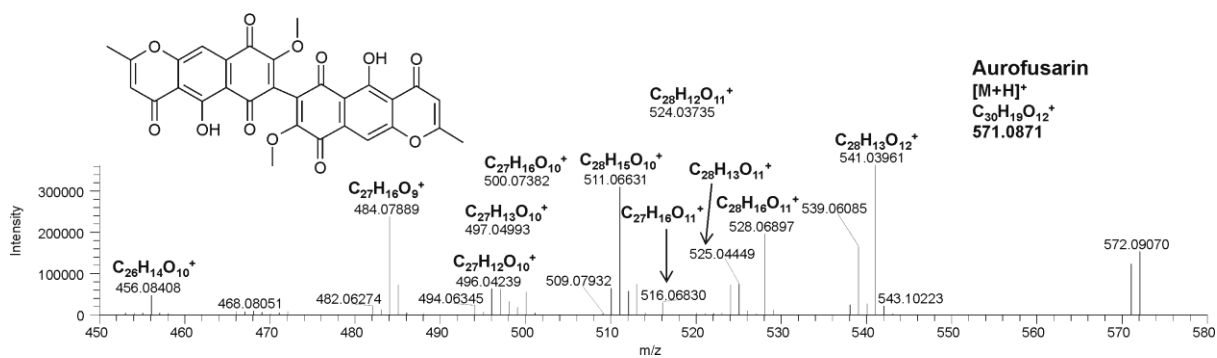


Figure 4. MS/MS spectrum of the native aurofusarin precursor $[M+H]^+$ of m/z 571.09 from a culture supernatant of a *Fusarium graminearum* mutant strain. The structure of aurofusarin is depicted in the upper left corner. Elemental formulas of the protonated molecule and the fragments are shown.

Table 1. Elemental formulas and masses of the measured standards. The mass deviation in ppm for the measured protonated molecule $[M+H]^+$ in relation to the calculated $[M+H]^+$ of the monoisotopic signal is given. Additionally the rank of the right elemental formula (sorted by mass deviation in ppm) when calculated based on allowed elements only: I: CHNOCISPF, without restriction of carbon atom count, II: CHNOCISPF, with restriction of carbon atom count. I: range of carbon atom count derived from full scan (mass difference between native and fully ^{13}C labelled compound), II: only actual number of carbon atom derived from full scan measurement (native vs. labelled compound) allowed. Atom count of allowed element derived from Kind and Fiehn (2007)^[2] for $M < 500$ Da (max. 39 C, 72 H, 20 N, 20 O, 9 P, 10 S, 16 F, 10 Cl atoms) and $M < 1000$ Da (max. 78 C, 126 H, 25 N, 27 O, 9 P, 14 S, 34 F, 12 Cl atoms), respectively. For DIAS, HT-2 and T-2, additionally one Na atom was allowed as the sodium adduct was used. This information can usually easily be derived from the full-scan spectra.

Compound	Elemental Formula of M	Retention Time [min]	Ion Species	m/z $[M+H]^+_{\text{calc}}$	m/z $[M+H]^+_{\text{meas}}$	Δ ppm	Rank of manually assigned elemental formula	
							I	II
3AcDON	$\text{C}_{17}\text{H}_{22}\text{O}_7$	14.6	$[M+H]^+$	339.1438	339.1436	0.81	4	1
DIAS	$\text{C}_{19}\text{H}_{26}\text{O}_7$	19.4	$[M+\text{Na}]^+$	389.1571	389.1571	-0.01	1	1
HT-2	$\text{C}_{22}\text{H}_{32}\text{O}_8$	22.5	$[M+\text{Na}]^+$	447.1989	447.1989	0.04	1	1
T-2	$\text{C}_{24}\text{H}_{34}\text{O}_9$	24.1	$[M+\text{Na}]^+$	489.2095	489.2093	0.36	5	2
ZON	$\text{C}_{18}\text{H}_{22}\text{O}_5$	25.7	$[M+H]^+$	319.1540	319.1538	0.68	5	1
FB3	$\text{C}_{34}\text{H}_{59}\text{NO}_{14}$	24.7	$[M+H]^+$	706.4008	706.4014	-0.78	152	7
TETR	$\text{C}_{22}\text{H}_{24}\text{N}_2\text{O}_8$	11.0	$[M+H]^+$	445.1605	445.1602	0.84	27	2
GRIS	$\text{C}_{17}\text{H}_{17}\text{O}_6\text{Cl}$	22.3	$[M+H]^+$	353.0786	353.0782	1.27	19	1
STER	$\text{C}_{18}\text{H}_{12}\text{O}_6$	26.1	$[M+H]^+$	325.0707	325.0703	1.08	11	1
FB1	$\text{C}_{34}\text{H}_{59}\text{NO}_{15}$	23.1	$[M+H]^+$	722.3957	722.3960	-0.37	74	4
FB2	$\text{C}_{34}\text{H}_{59}\text{NO}_{14}$	25.7	$[M+H]^+$	706.4008	706.4015	-0.95	180	10

Detection and characterization of fungal secondary metabolites using LC-HRMS

Table 2. MS/MS fragment spectra of 3AcDON (C₁₇H₂₂O₇). Fragments and corresponding elemental compositions are derived from automated and manual data evaluation. Rank of manually assigned elemental formula with no restrictions but the number of elements calculated with Xcalibur QualBrowser. M⁺_{calc}: *m/z* of calculated elemental formula, M⁺_{meas}: measured *m/z*, I: CHNOCISPF, without restriction of carbon atom count, II: CHNOCISPF, with restriction of carbon atom count. Maximum atom count of elements derived from Kind and Fiehn^[2] for for M < 500 Da (max. 39 C, 72 H, 20 N, 20 O, 9 P, 10S, 16 F, 10 Cl atoms).

Elemental Formula F	Relative Intensity [%]	<i>m/z</i> M ⁺ _{calc}	<i>m/z</i> M ⁺ _{meas}	Δ ppm	Rank of manually assigned elemental formula	
					I	II
CID spectrum						
C ₁₅ H ₂₁ O ₆	23	297.1333	297.1325	2.5	8	1
C ₁₆ H ₁₉ O ₅	8	291.1227	291.1226	0.3	3	1
C ₁₅ H ₁₉ O ₅	48	279.1227	279.1220	2.7	7	1
C ₁₅ H ₁₇ O ₄	32	261.1121	261.1115	2.4	3	1
C ₁₅ H ₁₅ O ₃	23	243.1016	243.1009	2.7	7	1
C ₁₄ H ₁₇ O ₃	9	233.1172	233.1169	1.5	1	1
C ₁₄ H ₁₅ O ₃	100 (4*10 ⁴ counts)	231.1016	231.1009	3.0	4	1
C ₁₅ H ₁₃ O ₂	7	225.0910	225.0916	-2.6	7	1
C ₁₄ H ₁₅ O ₂	31	215.1067	215.1056	5.2	4	1
C ₁₄ H ₁₃ O ₂	46	213.0910	213.0901	4.4	5	1
C ₁₃ H ₁₅ O ₂	28	203.1067	203.1054	6.2	4	1
C ₁₄ H ₁₃ O	8	197.0961	197.0957	2.2	1	1
C ₁₂ H ₁₃ O ₂	32	189.0910	189.0905	2.7	2	1
C ₁₃ H ₁₅ O	10	187.1117	187.1109	4.5	3	1
C ₁₁ H ₁₁ O ₂	9	175.0754	175.0754	-0.2	1	1
C ₈ H ₉ O ₂	8	137.0597	137.0593	2.9	1	1
HCD spectrum						
C ₁₅ H ₁₉ O ₅	100 (4*10 ³ counts)	279.1227	279.1224	0.9	2	1
C ₁₂ H ₁₃ O ₂	73	189.0910	189.0901	5.0	4	1
C ₁₁ H ₁₁ O ₂	75	175.0754	175.0752	0.7	1	1
C ₈ H ₉ O ₂	94	137.0597	137.0585	8.6	2	1
C ₇ H ₉ O ₂	64	125.0597	125.0593	3.3	1	1
C ₇ H ₉ O	76	109.0648	109.0645	2.4	1	1

CURRICULUM VITAE

Sylvia M. Lehner

Neubaugasse 45, 3462 Absdorf
 sylvia.lehner@hotmail.com, Mobile: +43 688 862 87 49
 Date of Birth: November 24, 1984; Place of Birth: Vienna
 Nationality: Austria

Education

- 11/2008 – 12/2012 **Vienna University of Technology**
PhD in Technical Chemistry
 “Detection and characterization of fungal secondary metabolites using LC-HRMS/MS”
 Center for Analytical Chemistry, Department for Agrobiotechnology (IFA-Tulln), University of Natural Resources and Life Sciences (BOKU), Vienna
- 05/2007 – 10/2008 **Vienna University of Technology**
Master Degree Technical Chemistry – Biotechnology and Bioanalytics, awarded distinction
 ”Characterization of the *Trichoderma atroviride gpr1* gene encoding a G-Protein coupled receptor”
- 10/2003 – 05/2007 **Vienna University of Technology**
Diploma study Technical Chemistry
 1st and 2nd segment, change in the curriculum:
Bachelor Degree Technical Chemistry
- 06/2003 **Academic high school, Vienna**
School leaving exam passed with distinction
 Specialized paper in chemistry “Structure and properties of food additives on the basis of selected examples“

International Experience

- 11/2007 **ATHENS program at the Universidad Politécnica de Madrid (Spain)**
 Lecture, ”Industrial Utilization of Aromatic and Medicinal Plants”
- 08/2007 – 09/2007 **IAESTE internship at the Pontifícia Universidade Católica de Campinas (Brazil), Faculty of Chemistry**

Professional Experience

- 10/2006 – 10/2007 **Voluntary work at IAESTE Austria**
- 02/2006 – 06/2006 **Laboratory employee at Ashland Austria GmbH**
Routine analysis of water samples: photometry, titration
- 02/2006 **Internship at the Institute of Applied Synthetic Chemistry, Vienna University of Technology**
Research division "Organic Synthesis"
- 08/2005 **Internship at the Institute of Chemical Technologies and Analytics, Vienna University of Technology**
Research division "Bio and Polymer Analysis"

Grants Awarded

- 2010 Performance scholarship of the Windhag Scholarship Foundation of Lower Austria
- 2008 Foundation scholarship of the Vienna University of Technology
- 2007 Advancement scholarship of the Vienna University of Technology, Faculty of Technical Chemistry
- 2007 Performance scholarship of the Vienna University of Technology, Faculty of Technical Chemistry
- 2007 Foundation scholarship of the Vienna University of Technology

Language Skills

- German: Mother tongue
- English: fluent (spoken and written)
- Spanish: Intermediate
- Portuguese: Basic knowledge
- French: Basic knowledge

EDV Kenntnisse

- MS Office (Microsoft Word, Microsoft Excel, Microsoft PowerPoint)
- Manufacturer-specific instrument software (Thermo Xcalibur, Agilent ChemStation)
- Basic knowledge in R, XCMS, SIEVE, Mass Frontier, MetWorks

Extracurricular Activities

- Volleyball: in a hobby team
- Music: playing the guitar, singing (in the past in a choir)